Aalborg Universitet

AALBORG UNIVERSITY
DENMARK

Process Integration

Core processes and utility systems

Grue, Jeppe

Publication date:
2005

Document Version
Accepted author manuscript, peer reviewed version

Link to publication from Aalborg University

Citation for published version (APA):
Grue, J. (2005). *Process Integration: Core processes and utility systems*. Institut for Energiteknik, Aalborg Universitet.

General rights
Copyright and moral rights for the publications made accessible in the public portal are retained by the authors and/or other copyright owners and it is a condition of accessing publications that users recognise and abide by the legal requirements associated with these rights.

- Users may download and print one copy of any publication from the public portal for the purpose of private study or research.
- You may not further distribute the material or use it for any profit-making activity or commercial gain
- You may freely distribute the URL identifying the publication in the public portal -

Take down policy
If you believe that this document breaches copyright please contact us at vbn@aub.aau.dk providing details, and we will remove access to the work immediately and investigate your claim.

Downloaded from vbn.aau.dk on: May 05, 2023

Process Integration

Core processes and utility systems

Ph.D. thesis

M.Sc. Jeppe Grue

Institute of Energy Technology, Aalborg University

ISBN: 87-89179-58-7

PREFACE

This thesis is submitted for partial fulfilment of the requirements for the degree of Doctor of Philosophy in Energy Engineering at Aalborg University. The work has been carried out in the period May 1999 to November 2005, though with leaves of absence January 2000 to March 2001, and November 2003 to October 2005. The work has been supervised by Associate professor Inger Bach at the Institute of Energy Technology, who quit her job at the university in 2003 and afterwards by associate professor Jan Dimon Bendtsen at the Institute of Control Engineering.

I am especially grateful that Jan Dimon Bendtsen agreed to become a supervisor so late in the project, accepting to spend lots of time to become acquainted with a project he had until then not known at all.

I am also very much indebted to the Nordic Energy Research Programme, who has funded part of my work; and also provided a set of excellent world class courses on process integration. The knowledge gained and personal networks created during these meetings have been of tremendous value, not to mention very funny and enjoyable!

A thanks also to Professor Tapio Westerlund at Åbo Akademi in Finland, where I spend a very beautiful summer, learning much of chemical engineering and optimisation. Again my friends and colleagues from the Nordic Programme made this stay enjoyable.

At the University of Iceland my thanks goes to Professor Páll Valdimarsson, I spent only a month there, being forced to return to Denmark earlier than expected. Nevertheless the stay in Iceland was very enjoyable. To this end the very warm welcome and good friendship from Jon Agust Thorsteinson has made a lasting memory.

A very special thanks go to my fellow ph.d. student Jens Møller Andersen, for all the inspiring discussions and good friendship, without him I would probably never have become a ph.d. student. At the Institute of Energy Technology ph.d. students, Mads Pagh Nielsen, Henrik Sørensen, Lotte Sørensen, Mads Bang and Søren Knudsen Kær also deserve my thanks.

Finally my thanks go to my family and friends for support during all the hard work, and especially to Trine for a tremendous patience and support during all the busy days and weekends.

ABSTRACT

The present thesis deals with process integration of core processes and utility systems. It is generally recognised that sequential design procedures leads to sub optimal design, however only limited effort has been put into integrating the utility system with the rest of the process. Therefore this topic is addressed by this work, at first and overview of process design is given.

Afterwards follows a description of mathematical programming, and disjunctive programming. Since no commercial disjunctive solver is available today, a disjunctive solver based on the branch-and-bound algorithm is implemented.

The method for integrated design between process and utility is presented next. Even though it could be desirable to formulate the entire synthesis problem as a single large problem, it is considered to be unrealistic. Instead it is proposed that a pre-screening stage will limit the reactor and separation network before the integrated design is applied. Hence the integrated design will select among a limited number of reactors and separation techniques, and optimise the temperature and pressure of these units. This is to be done simultaneously with the design of the utility system. Linking the utility system with the process is done through extensive heat integration and mechanical driver interfaces. The economic model used for the objective function is also presented.

Next the method for optimising the utility system in the integrated context is described. First of all it is recognised that the utility system must be able to receive and supply heat on equal terms with the process, thus the traditional distinction between utility and process streams in pinch analysis vanishes. Furthermore the importance of selecting the correct steam pressure in the utility system is addressed by formulating a new set of simplified steam property correlations. That allows for simultaneous design and pressure level optimisation. A number of unit operation models for boilers, steam turbines, gas turbines and heat recovery generators are presented. The heat integration model is described and it is chosen to use a method where each stream contributes with a temperature difference to the pinch analysis. Finally the driver interface between the utility system and the process is presented.

To test the proposed method for synthesis of utility systems a number of small test cases are used. The first case highlights the strength of the model as the found solution is improved compared to earlier work. Furthermore the disjunctive solver is compared to commercial MINLP-solvers, from which it is clear that the disjunctive solver is far more robust, and finds a better optimum.

The next test case is a methanol process, which is optimised both sequentially and simultaneously. The process is limited to a single reformer technology and a simplified methanol purification step. Then in this restricted case, the integrated design finds a better solution than the sequential design, improving the net present worth with approx. 10%. The

results clearly indicate the pressure and temperature levels in both the process and the utility system are changed when the interaction between the two are taken into account.

The integrated design is also tested on the well-known HDA-test case. Once again the proposed method manage to find a superior design, improving the net present worth with approximately 13% compared to the sequential design procedure. In addition this case also illustrates that the method can find plants with higher marginal efficiencies than the sequential method.

SYNOPSIS

Denne afhandling omhandler procesintegration mellem kerneprocesser og forsyningssystemer. På trods af at det er almindeligt anerkendt at en sekventiel design procedure giver sub-optimalt design har der kun været begrænset fokus på at integrere forsyningssystemet med resten af processen. Indledningsvis introduceres den aktuelle status for proces design.

Det næste kapitel omhandler matematisk programmering og disjunktiv programmering. Der findes ikke nogen kommerciel disjunktive optimeringspakke og derfor er der i forbindelse med afhandlingen implementeret en løsningsalgoritme baseret på "branch-and-bound".

Dernæst præsenteres metoden for integreret design mellem proces og forsyningssystem. Principielt kunne det være ønskeligt at formulere hele procesdesignproblemet som et stort problem, men det betragtes pt. som urealistisk. I stedet formuleres en metode, hvor det forventes at en forundersøgelse har reduceret antallet af reaktor og separationsteknologier til et begrænset antal. Den integrerede design metode kan derefter anvendes på det begrænsede sæt og samtidigt med designet af forsyningssystem kan reaktor og separationsteknik vælges, samt tryk- og temperaturniveauer optimeres. Koblingen mellem forsyningssystem og proces sker gennem varmeintegration samt et drev-interface, hvor mekanisk arbejde og elektricitet udveksles.

På baggrund heraf præsenteres en metode til design af forsyningssystemer i integreret design. Modellen udarbejdes så forsyningssystemet både kan afgive og modtage varme fra processen, og således indgår alle strømme i forsyningssystemet på samme niveau som strømmene i processen. Det betyder at den traditionelle forskel på proces og forsyningssystem i pinch-analysen forsvinder. Da fastsættelsen af trykniveauer for dampen i forsyningssystemet kan have stor indflydelse på resultatet kan de optimeres frit. Det sætter krav til de termodynamiske data for vand/damp, og derfor er et nyt sæt simplificerede dampdata udarbejdet til dette formål. Et antal enhedsoperationer, som kedler, damp- og gasturbiner etc. er modelleret og indgår i en superstruktur. Varmeintegrationsmodellen tager hensyn til at hver strøm kan bidrage med forskellige temperaturdifferens afhængig af konvektionskoefficienten for den enkelte strøm. Derudover præsenteres drev-interfacet.

For at afprøve forsyningssystemmodellen anvendes den på et antal mindre test cases. Den først case viser tydeligt styrken ved metoden og finder et bedre optimum end tidligere rapporteret. Derudover anvendes casen til sammenligning mellem den disjunktive løsningsalgoritme og traditionelle MINLP-algoritmer. Det kan konkluderes at den disjunktive løser er mere robust og dermed ofte finder et bedre optimum. Den anden case illustrere i høj grad hvor vigtigt det er at tryk niveauerne i dampkredsen frit kan vælges, og der findes en væsentlig forbedring af tidligere resultater.

Dernæst afprøves den integrerede design metode på to forskellige store test cases. Den første er et eksempel på metanol syntese, processen optimeres både med den traditionelle

sekventielle procedure og den nye integrerede procedure. Det viser sig at den integrerede metode finder en proces som har 10% større nuværdi. Optimeringen viser også tydeligt at tryk- og temperaturniveauer ændres ved anvendelsen af den integrerede metode, og dermed at interaktionen mellem proces og forsyningssystem er taget med i betragtning. Den næste case er den meget veletablerede HDA-case, der findes også her tilsvarende trends form for metanol casen, og nuværdien forbedres med ca. 13%. Derudover viser det sig at den integrerede metode også designer et anlæg som har en større marginalvirkningsgrad for el-produktion.

TABLE OF CONTENT

LIST OF FIGURES

LIST OF TABLES

1

INTRODUCTION

The overall subject of this thesis is systematic methods for conceptual design of chemical processes. In this chapter the aim of this thesis is stated, and a brief background for chemical process design is provided. Finally the scientific contributions of this work are summarised.

Chemical process design is often a large and complex activity, indicating that systematic methods are absolutely necessary. In addition the chemical industry utilises large amounts of energy and raw materials, which considerable influences the overall economy of a process plant. This means that a plant often is more feasible if energy and resource consumption is reduced by use of an integrated design. A systematic approach to this is *Process Integration*, which is a common term for all the methods available to the engineer in process design (Gundersen 97). Process Integration can be used in several phases of a project, e.g. both conceptual design and detailed design. In this work the focus is on the conceptual design.

Much research has already been contributed to the area, e.g. in individual parts of the plant, like design of reactions, separation networks, and synthesis of heat exchanger networks. In process synthesis the problem is often divided into a sequential procedure (Douglas 88). The idea is that the designer makes the most important decisions first, leaving the less important for a later stage. E.g. the core process is synthesised first, as it is the most important; secondary systems like separation systems afterwards and so on.[1] In the end the heat recovery system and utility[2] supply is synthesised.

[1] We define the core process as the part of the overall process where the essential part of the production takes place. E.g. in methanol production the conversion of syngas to methanol is the core process, while the distillation system for purification of the methanol is a secondary process.

[2] The utility system is primarily the energy supply system, including electricity, steam, hot water, and cooling. Note that in some cases water supply is also included in the utilities.

It is widely recognised that the sequential approach might lead to sub-optimal systems, as the full interaction between all parts of the plant is not accounted for, e.g. shown by (Duran and Grossmann 86b; Yee *et al.* 90b). To overcome these weaknesses several suggestions for more integrated design procedures have been set forth. Nevertheless only few authors have investigated the interaction between core processes and utility systems; therefore this is the aim of this work. Specifically:

> *The aim of this thesis is to provide a framework for simultaneous synthesis of the entire process including utilities. Through a number of test cases it will be investigated whether this method leads to different designs and more efficient processes.*

It must be stressed that this will not be "the theory of everything" nor a completely automated procedure. It should be considered a contribution towards more integrated design procedures than the ones that already exist today.

Before moving on, a background on the current state of research in process synthesis is provided.

1.1 Background on process design

In this section the background for process synthesis is provided. Process synthesis covers both the area of flowsheet design (macroscale) and design of reactions (microscale), both are very important but only the macro scale has been considered here. Even this is a very large field, and it will not be attempted to cover every single detail in this review; rather the focus will be on the topics relevant for this thesis and make a brief outline. For more information (Biegler *et al.* 97) is an excellent textbook on the topic.

First a general overview of the area is given and afterwards a brief introduction to some of the commonly treated sub problems, including

- Reactor
- Separation system
- Heat exchanger networks
- Utility systems

And finally integrated design among these areas is discussed.

1.1.1 Overview of process design

The course from an idea to an operating process plant usually moves though several phases, as outlined in fig. 1-1. Starting out with the very fundamentals of specifying requirements and generating the fundamental ideas, this leads on to the concept development in which the process is synthesized typical through a screening of alternatives. Afterwards additional levels of details are added in order to actually build, start-up, and operate the plant.

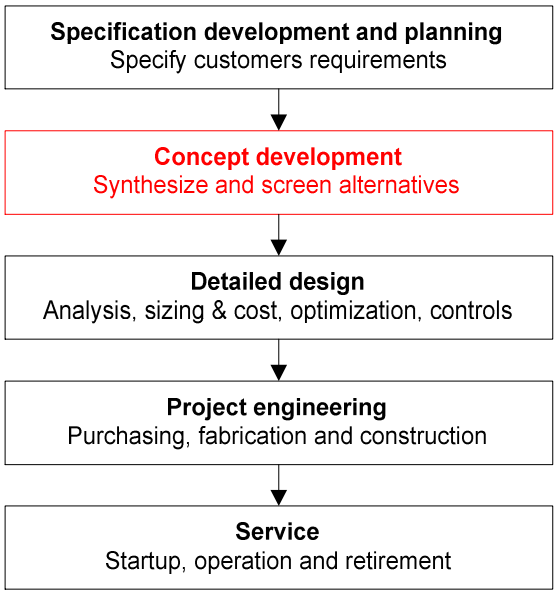

fig. 1-1 Typical project life-cycle. Adapted from (Bejan et al. 96)

Typically 80% of the capital cost will be fixed by the decisions of the conceptual design[3] (Bejan *et al.* 96; Biegler *et al.* 97).This observation makes the concept development phase one of the most crucial in the project. Changes in the subsequent phases will only be able to save a maximum of 20% of the total capital cost. Therefore it is important to acknowledge the interaction between all the process units during the concept development.

Process flow diagrams

The task in process synthesis is to develop a process flow diagram (PFD) – or in short a flowsheet[4]. This encapsulates the overall structure of the plant, including components and their interconnections - see fig. 1-2. Normally it also includes a steady state heat and mass balance at the design point.

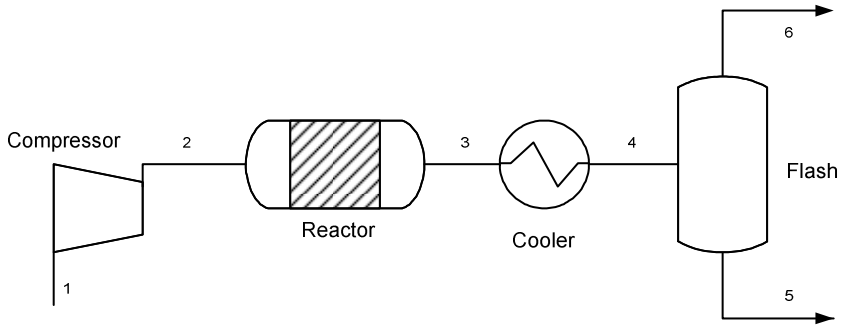

fig. 1-2 example of a simple process flow diagram (or flowsheet). The flowsheet illustrate the different unit operations and their interconnections. The connections are typically numbered.

[3] This is the well known 80-20 rule, as 80% of the cost is fixed during the first 20% of the project time.

[4] We will use the term flowsheet for process flow diagrams.

Each connecting stream in a flowsheet is described by the chemical composition of the stream, flow rates, thermodynamic state etc. The connections are assumed not to have any physical size. Physical equipment is modelled by the unit operations, where the composition, flow rate and thermodynamic state of the inlet stream are transformed, to the state of the outlet stream. The operation of the units are typically described through simplified unit operation models that model the overall operation without going into details; typically only one-dimensional, steady-state models are used for concept generation.

The flowsheet and the mass and energy balance provides the basis for estimating both the capital and operational cost for the plant, using simplified correlations for capital cost.

Systematic process synthesis in general

For process plants a set of systematic design tools and methods have emerged, known as process integration methods. The International Energy Agency (IEA) defines process integration to be (Gundersen 97):

> *Process Integration is the common term used for the application of methodologies developed for system-oriented and integrated approaches to industrial process plant design for both new and retrofit applications.*

The main development of the methods has been within chemical engineering. This is largely because of the energy and resource-consumption in the chemical industry. (Gundersen 97) defines the methods to include

> *Such methodologies can be mathematical, thermodynamic and economic models, methods and techniques. Examples of these methods include: Artificial Intelligence (AI), Hierarchical Analysis, Pinch Analysis and Mathematical Programming.*

During process synthesis a large number of designs are usually evaluated, and therefore a clear objective is needed to decide whether one design is better than the other. The objective is typically an economical function (Biegler *et al.* 97), though in some cases it might also be of interest to use a more "environmental objective", e.g. maximum efficiency or minimum fuel consumption. In this work the net present worth is used as objective, but from time to time optimal designs with different objective functions will be compared.

Process synthesis problems can become very large, due to the large number of possible combinations, and therefore almost impossible to handle. Especially before the introduction of modern computers it has been of great importance to divide the synthesis task into a number of hierarchical steps. Here the goal is to settle the most important decisions first, and then move on to more and more detailed decisions. (Douglas 88) described a very thorough hierarchical approach, where the synthesis is divided into the following steps

- Batch or continuous
- Input – output structure of the flowsheet
- Reactor and recycle structure
- Separation system
- Heat exchanger networks

It seems reasonable that the first two steps are so general and important that they can be decided upon very early in the project. But for the last three points it is recognised that when the interaction between the subsystems are neglected the synthesis might lead to a sub optimal design, as e.g. shown by (Duran and Grossmann 86b).

Often each step has been solved using heuristic rules. But with the appearance of cheap and powerful computers the use of mathematical programming has been made possible. Mathematical programming can be used to formulate a superstructure, that consists of several process flowsheets and through the use of binary variables different units in the flowsheet are either included or omitted (fig. 1-3).

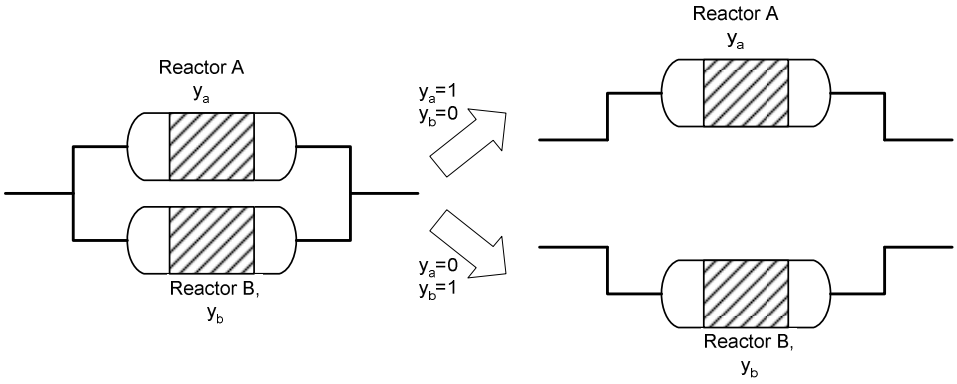

fig. 1-3 A superstructure for selection between to reactors, each reactor is assigned a binary variable. Depending on the value of the variable different flowsheets will be generated.

If the unit models are formulated linearly the problem is a MILP, otherwise it becomes a MINLP problem[5]. The problem with this approach is that an exhaustive superstructure can include a huge amount of options, and thereby creating a combinatorial problem of prohibitively large size. To overcome the problem of a "combinatorial explosion" different decomposition strategies can be applied e.g. (Daichendt and Grossmann 97) or (Kocis and Grossmann 89).

1.1.2 Reaction

This step covers the design of the reaction network, which (Biegler *et al.* 97) formulates as:

> *Given the reaction stoichiometry and rate laws, initial feeds, a desired objective, and system constraints, what is the optimal reactor network structure? In particular: What is the flow pattern of this network? Where should mixing occur in this network? Where should heating and cooling be applied in this network?*

Despite the importance of this problem and the amount of research in reaction engineering, only a limited amount of research has been carried out for reactor network synthesis (Biegler *et al.* 97). This probably reflects that the modelling after all is more difficult than for

[5] Further description of optimisation problems are found in chapter 2.1

e.g. energy systems, because knowledge of the reaction kinetics is often quite limited. Still the research that has actually been carried out can be divided into three main categories:

- Heuristics
- Superstructure optimisation
- Attainable regions

Heuristics are applied by e.g. (Douglas 88; Levenspiel 99), the approach is somewhat limited and only applicable to relatively simple systems.

For the more systematic approaches a set of basic building blocks are used to formulate the superstructure, as shown in fig. 1-4.

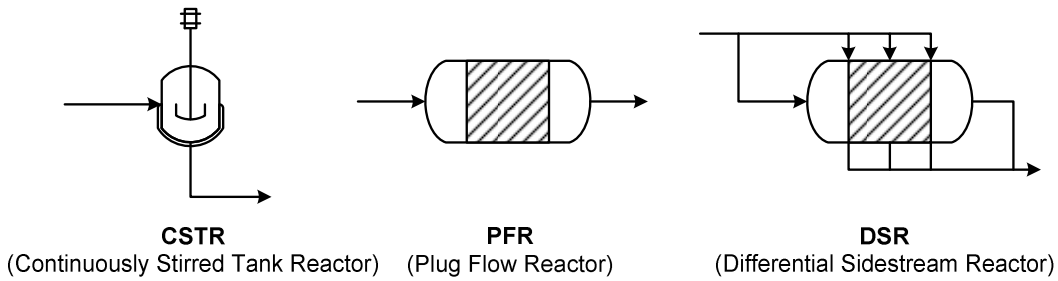

fig. 1-4 Typically basic building blocks in reactor network design

The CSTR is assumed to be perfectly mixed and oppositely no mixing is assumed in the PFR. The DSR can be considered a more general formulation of the PFR. Generally the modelling of the CSTR can be formulated by algebraic equations, whereas the PFR and the DSR are modelled by differential equations.

A superstructure formulation for design of an isothermal reaction network was proposed by (Kokossis and Floudas 90; Kokossis and Floudas 94), and a more general approach for non-isothermal operation was formulated by (Kokossis and Floudas 94). Both approaches used a superstructure consisting of CSTRs and PFRs, though the PFRs were modelled as a series of CSTRs. A more general concept for selection of combinations of CSTR and PFRs have recently been reported by (Hillestad 04; Hillestad 05). The method is able to handle any number of components and reactions, but at the expense of making the model non-convex.

The attainable region is a geometric concept, where a convex region containing all the possible reaction paths can be constructed, while disregarding the actual equipment. Afterwards the result can be interpreted in terms of reactor configurations; this is outlined in fig. 1-5. With the construction of the convex region it is easy to find e.g. the maximum concentration of B, i.e. the top of the red curve.

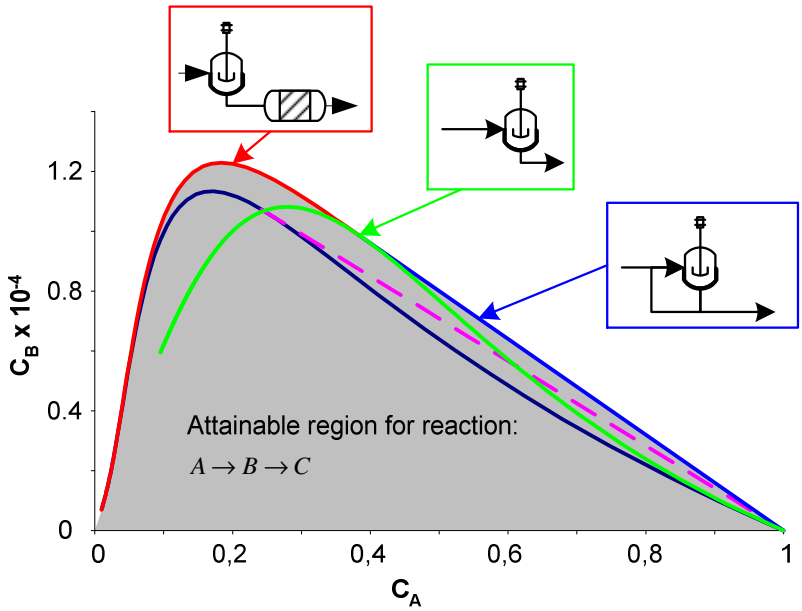

fig. 1-5 Attainable region for a simple reaction, example from (Biegler et al. 97). Different parts of the region corresponds to different reactor combinations.

The attainable region is somewhat limited, as it can only be used in two dimensional space, i.e. two reactions. In addition it is difficult to use the method in flowsheet synthesis (Biegler *et al.* 97). To overcome these problems a combination of the attainable region with mathematical programming was suggested by (Balakrishna and Biegler 92a; Balakrishna and Biegler 92b).

The combination of the attainable region and the superstructure optimisation was proposed by (Lakshmanan and Biegler 96), where the properties of the attainable region were used to ensure that the superstructure was sufficiently rich to include the optimal network. The superstructure was extended by (Schweiger and Floudas 99), and especially different methods for solving the differential equations modelling the PFR and DSR were investigated.

The problem with the mathematical programming approach is that reactor models can be very non-linear, and the models are normally non-convex. In addition reactors can have multiple steady states. Altogether this makes it difficult to ensure that the solution is close to the global optimum.

1.1.3 Separation systems

Practically all chemical processes involve a step where a mixture needs to be separated into products and by-products. The task is often complicated as a large number of parameters must be decided upon; these include mixture properties, separation techniques and operational parameters. In general (Jaksland *et al.* 95) formulates the synthesis problem as

> *Given a multicomponent mixture, determine the separation techniques (and corresponding separation tasks), sequence the selected separation techniques into a process flowsheet and determine estimates for the corresponding condition of operation.*

Also for separation systems the research appears in three areas

- Heuristics
- Thermodynamic insight
- Superstructure optimisation

Often the areas overlap, but nevertheless the impression is that these are three main methods. Investigating the separation of a four component mixture, assuming ideal separation a number of different paths can be proposed, as summarised in fig. 1-6.

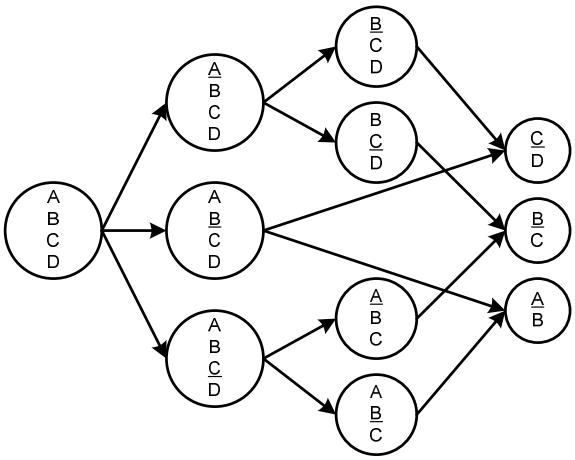

fig. 1-6 The combinations of separation sequences for a four component mixture separated by sharp distillation.

It is obvious that the task of designing a separation system can be combinatorially explosive, as shown by the Thomson and King formula (e.g. (Biegler *et al.* 97)), where the number of potential separation sequences, N for n different components and S different separation methods can be calculated from

$$N = \frac{\big(2(n-1)\big)!}{n!(n-1)!} S^{n-1} \tag{1.1}$$

The calculation is limited to sharp separators, but even with this limitation the number of combinations can become very large as illustrated in fig. 1-7.

Therefore it is often necessary to use some simplifications to solve the separation problem. Heuristic rules appears in plenty of papers, and are also applied in the hierarchical decomposition proposed by (Douglas 88). Here the separation synthesis is divided into vapour and liquid recovery, and a set of heuristic rules helps the designer to select the separation techniques, as well as the sequencing of the separation. The resulting separation system is not guaranteed to be optimal, but only to form a "good" solution, that will actually work.

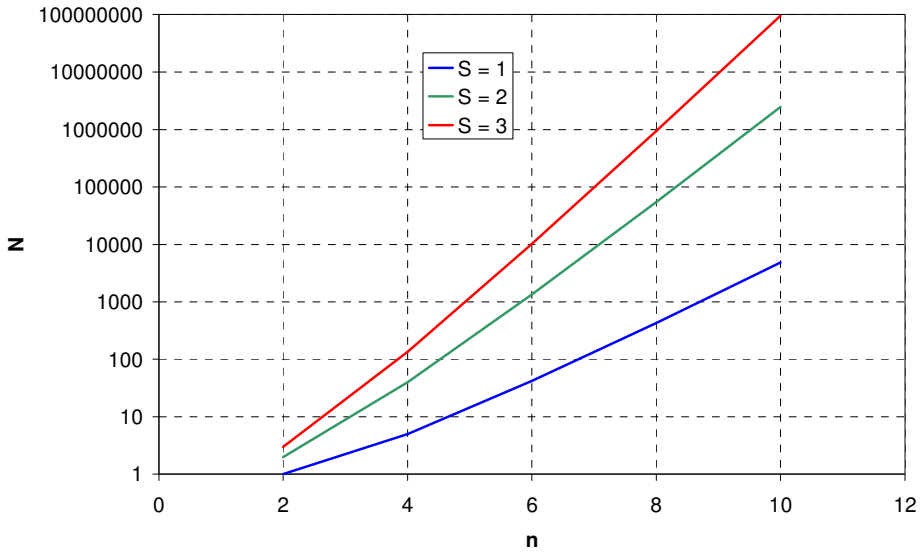

fig. 1-7 Plot of equation (1.1)

Thermodynamic insight is used by (Jaksland *et al.* 95). The physiochemical properties of the components is combined with a large number of separation technologies, and by screening all the technologies available, the feasible space is identified. Afterwards a more detailed analysis is made, and a flowsheet of the separation train is proposed, along with any solvents needed for the separation.

Mathematical programming using superstructures have been proposed by several authors. (Biegler *et al.* 97) provides an overview of several MILP models for the design of a distillation using ideal separation.

If the systems are non-ideal or the distillations columns are modelled using rigorous equations, the models give rise to both non-linear and non-convex problems. The thermodynamics of separation is also often quite complicated, and therefore commercial simulation tools are often preferable to predict the correct separation. To overcome these problems (Leboreiro and Acevedo 04) proposed to couple a genetic algorithm with a commercial process simulation. The results were interesting, albeit computational expensive. The difficult problem of separating azeotropic mixtures[6], has been addressed by several authors, more recently by (Thong *et al.* 04). Most of the methods so far assume that every distillation column has a condenser and reboiler, but there is a significant potential for integrating the columns, thus reducing the need for the condenser and reboilers. This has been investigated by (Caballero and Grossmann 04).

Recent work by (Seuranen *et al.* 05) use "case-base-reasoning" which is a mix of the above methods, where a large database of existing processes are used to extract information for generation of new processes. The method seems to work well for overall identification of the

[6] If there exists a point where the vapour phase and the liquid phase have the same composition a substance is said to be azeotropic. One of the most commonly known azeotrops is ethanol-water.

possible separation path, but still requires a large effort from the engineer in the synthesis of the actual separation sequence. The possibility to base the design on a large database of existing knowledge is very interesting, however.

Altogether the generation of optimal separation sequences is a difficult task, both in terms of modelling very non-linear equations and large number of combinations.

1.1.4 Heat integration

Heat integration deals with recovering waste heat in a process and thereby reducing the need for external utilities. In some way heat integration can be considered far easier than topics discussed so far, since no chemical reaction or separation is involved, thus the thermodynamic part is simpler. A systematic approach for heat integration was proposed by (Hohmann 71; Linnhoff *et al.* 82), who discovered that the minimum utility consumption can be predicted, by combining all stream data into hot and cold composite curves in a T,Q-diagram (fig. 1-8)

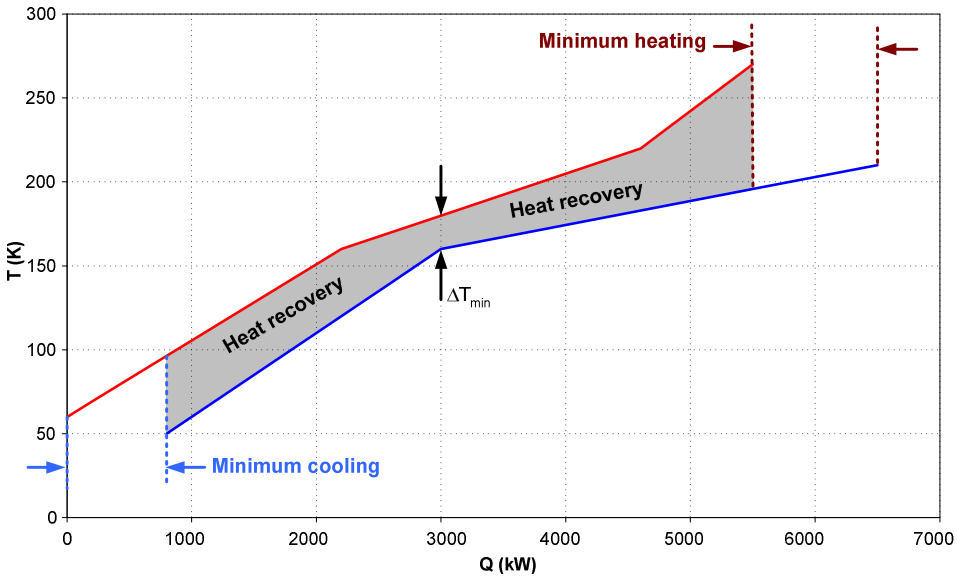

fig. 1-8 An example of graphical representation of hot and cold stream data for a process plant. Once the value of ΔT_{min} is defined, the maximum heat recovery and minimum utility consumption can be obtained from the diagram. Adapted from (Franck et al. 98)

It must be observed that the pinch-method only provides an upper bound at a fixed ΔT_{min}, but does not tell how the heat recovery can be realised.

To obtain the heat exchanger network (Papoulias and Grossmann 83b) proposed a sequential model. First the minimum utility requirements are found for a set ΔT_{min}, and afterwards a MILP problem is used to derive the network structure.

However, this approach does not ensure that the global optimum is found, since ΔT_{min} is fixed a priori. To overcome this (Yee *et al.* 90a) formulated a superstructure in which the

ΔT_{min} was to be found simultaneously with the derivation of the network, the superstructure is outlined in fig. 1-9.

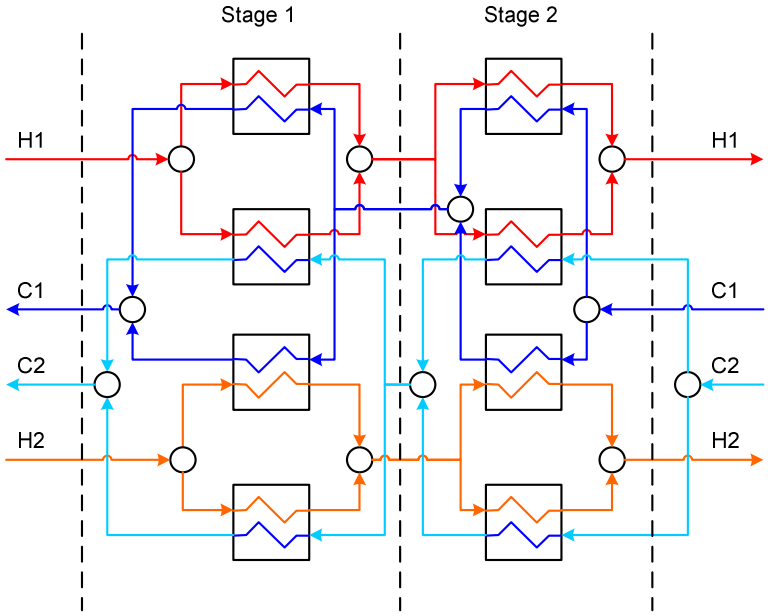

fig. 1-9 The superstructure proposed by (Yee et al. 90a), the number of stages can be extended to whatever seems appropriate for the network in question. Here two hot streams and two cold streams exchange heat in two stages.

The modelling of the superstructure results in a non-convex MINLP-problem and to reduce the non-convexities isothermal mixing was assumed. (Björk and Westerlund 02) has recently proposed a global optimisation method to overcome the isothermal mixing constraints, and even better networks have thus been found. The global optimisation approach increases the calculation time significantly, and has therefore only been applied to networks with no more than six streams.

Another issue that is neither accounted for by the pinch-analysis nor the super structure is the pressure drop in the heat exchanger network. The pressure drop leads to additional pump or compressor work that can be an important factor. (Zhu and Nie 02) derived a sequential model to deal with this issue, whereas (Fausto-Hernández *et al.* 03) extended the superstructure in fig. 1-9 to include the pressure drop, thereby being able to simultaneously optimise the heat exchanger area and the pressure drop. Another important issue is variations in operating conditions which is discussed by (Aaltola 02).

The main drawback of the superstructure is that it can only solve problems of limited size, since it becomes combinatorially prohibitive for large problems. Therefore (Petterson 05) has proposed a sequential LP and MILP formulation. The LP and MILP formulation guarantees that the global optimum is found in each stage, but due to the sequential nature there is no guarantee the overall global optimum is found. Nevertheless the method is reported to perform better than other methods when large scale networks are considered.

1.1.5 Utility system design

The design of utility system is typically based on knowledge from the power generation industry. A large effort has been devoted to the design of new power plants, supplying heat and power for the community.

The current best available technology for ultra super critical fossil fired steam plants is represented by the 400 MW Nordjyllandsvaerket plant in Denmark. The plant operates at a net-efficiency of 47% LHV[7], burning coal (Sondreal *et al.* 01). For natural gas fired combined cycle plants the net efficiency becomes even higher, 59% LHV is reported in (Najjar 01). These plants represent the upper bound which can be achieved with the technology commercial available today.

Utility systems at process plants usually have a lower net efficiency, as process steam is needed. When the plant has to produce steam, the electricity production and thereby the electric efficiency decreases, though the overall efficiency might be higher if less heat is rejected to the cooling water. In addition the plants are usually smaller.

In process plants there is often a need for mechanical drives e.g. steam turbines, and therefore the design of the utility system for a process system is somewhat different from a power plant. The synthesis of optimal utility system has been addressed by (Bruno *et al.* 98), who formulated a superstructure, however the insights that can be gained from thermodynamics are not fully used in this work. (Manninen and Zhu 99a) did include exergy analysis with superstructure optimisation, and devised a method to iteratively improve the superstructure with new options.

The optimisation of the steam turbine network for covering work demands in the process has been addressed by (Mavromatis and Kokossis 98a; Mavromatis and Kokossis 98c). The approach is a comprehensive design procedure, but does not consider integration with the rest of the system. Nevertheless the methods can be incorporated into a more overall integration method, e.g. shown by (Manninen and Zhu 99a).

The methods so far have all considered the steam pressure level fixed, but this was addressed by (Shang and Kokossis 04), where each pressure level could be selected among a given set of candidates. The method was extended to optimise cost effective CO_2 reduction in the work by (Varbanov *et al.* 05).

The integration of gas turbines into utility systems where included in the superstructure by (Bruno *et al.* 98), though much more comprehensively addressed by (Manninen and Zhu 99b).

Since the modelling of the utility system often involves complex models, the models in the previous work have been somewhat limited, especially with regard to the prediction of steam properties. The prediction of steam properties is important for calculation of estimates for turbine expansion etc. To use more complex models while at the same time limiting the

[7] Lower Heating Value

complexity of the optimisation problem, (Tveit 05) used rigorous process simulation to define a set of regression functions or response surfaces, which where afterwards used for optimisation. However, this work purely focused on the utility system.

1.1.6 Integrated design

The integration of the separate tasks described above has also been investigated by several authors. One of the earliest attempts to simultaneous synthesis the process and the utility system was performed by (Papoulias and Grossmann 83c). The problem was formulated as an MILP problem, by fixing a number of process parameters a priori. Nevertheless an increase in the annual profit for the total plant of 15-20% compared to sequential design was reported.

(Duran and Grossmann 86b) combined the heat integration with optimisation of pressure and temperature in a process flowsheet. They only included pinch analysis and not actual design of the heat exchanger network, the problem was formulated as an MINLP-problem. An impressive 90% increase in the annual operating profit for the plant in question was reported, by the use of simultaneous process optimisation and heat integration[8]. The utility system was not addressed in this work. A more rigorous approach was published by (Yee *et al.* 90b), which included the superstructure of the heat exchanger network (mentioned in 1.1.4) in the process formulated by (Duran and Grossmann 86b) but the problem is still too large for practical use in process synthesis.

Based on previous work a general process synthesis tool for reaction, separation and heat exchanger network was developed by (Kravanja and Grossmann 90). This approach used here has been extended several times, most recently in the work of (Bedenik *et al.* 04). Here a hierarchical approach for synthesis of the process system. Initially a pre-screening step for the reactor network is performed and afterwards more detailed steps are applied to optimise separation and heat integration. The method does not allow complete interaction between all the elements, since the pre-screening cut away a number of options.

Several authors have proposed an procedure for integrated design of reactor-recycle-separation systems, e.g. (Kokossis and Floudas 91) though this approach is limited to isothermal reactors and sharp distillation. A more rigorous approach was suggested by (Smith and Pantelides 95), even though it was only applied to a relatively small problem.

In all the cases mentioned above the reactor network has been fixed, only allowing adjustment of reactor temperature and pressure. To overcome these limitations the design of the reactor network was included in the formulation by (Balakrishna and Biegler 93). Still the utility system was not addressed at all.

[8] Note that in the base case they assumed that all heating and cooling was provided by external utilities, i.e. no heat integration. Therefore the cost of external utilities is unrealistic large in the base case, explaining how some of the 90% improvement where reached.

The work by (Lavric *et al.* 05) suggests a method for heat integration of reactors, but the application range is limited to two reactors, and the separation system is not addressed.

On the other hand the simultaneous design of the heat exchanger network and the utility system has been reported by (Maréchal and Kalitventzeff 98). In this case the reaction and separation systems are left almost fixed.

The integration of turbine expanders to recover the work from hot high pressure reactor outlet streams has been investigated by (Greeff *et al.* 02; Greeff *et al.* 04). The work is somewhat limited in scope focusing on the use of gas expanders, and discusses neither process optimisation nor heat integration further. The objective of the work was to reduce energy consumption, and significant savings where reported in a number of case studies. The recovery of work from process waste heat has also been reported by (Gorsek and Glavic 03), who used an extension of the pinch method to integrate a steam turbine into the process.

In general heat integration has been utilised in combination with process design, but the integration of the entire utility system apparently have only received little attention since the early work of (Papoulias and Grossmann 83c). Much of the work mentioned above treat important parts of the integration, and can serve a base of inspiration for proposing a new method.

1.1.7 Summary

(Li and Kraslawski 04) provides a recent overview of the process synthesis in general and addressed both micro- and macroscale, ending with four suggestions for future research:

> *The emerging need to design chemical processes with the simultaneous consideration of many criteria of technical, economical, social and environmental nature.*
>
> *The requirement for further insight into the fundamental principles at the molecular level to enable the integration of the product and process design.*
>
> *Process integration by elimination of the boundaries between unit operations—combining unit operations into hybrid systems (process integration).*
>
> *The improvement of optimisation and simulation techniques as well as of information management tools in order to handle more information and knowledge from various sources.*

Of these four suggestion, the objective of this work fits into the first.

1.2 Outline of the thesis

The first part of the thesis deals with proposing the method for integrated design, along with a method for design of utility systems in this context. In the second part of the thesis the methods are used for a number of test cases to demonstrate the usefulness.

Chapter 2: Preliminaries

Tools and basic methods for process integration are introduced, especially with focus on mathematical programming. Disjunctive programming is also introduced, and the

disjunctive solver used in this work is presented. Exergy analysis and pinch analysis are also briefly described.

Chapter 3: Methodology

Based on the hypothesis that integrated design leads to better process plants a novel methodology for integrated design is proposed. The method relies on a limited superstructure for reaction and separation tasks, combined with a complete heat and work integration with the utility system. In addition economic modelling is briefly discussed.

Chapter 4: Design of utility systems

The synthesis of utility system is a major part of the overall methodology, here the detailed models for the utility system is described. The models are based on existing work, but improved in a number of ways. A new set of steam property correlations is developed to ensure that pressure can be selected freely during optimisation. Models for steam- and gas turbines are also developed. The entire superstructure for the utility system is completely connected to the heat integration method. Furthermore the heat integration model is presented, followed by the model for the driver selection.

Chapter 5: Optimisation of utility systems

In this chapter a number of small cases for optimisation of utility systems and heat integration are presented. They serve to test the models developed in the previous chapter, and in addition a test of different optimisation algorithms are carried out for the first test case. Generally the proposed superstructure and disjunctive approach is able to find solutions superior to those found earlier.

Chapter 6: Optimisation of the methanol process

The conversion of natural gas to methanol is used as a test case for integrated design, though only some of the steps in integrated design are addressed by this example, e.g. no effort is put into improving the process superstructure. The methanol process described along with the relevant unit operation models, and the process is optimised. Relatively complex model are used for modelling the reactors. It turns out that the integrated design finds a better solution than the traditional sequential design.

Chapter 7: Optimisation of the HDA process

The well-known HDA-test case is used here for demonstration of the integrated design method. Initially the process is described, the process superstructure proposed and the unit operation models are formulated. The base case by (Douglas 88) is used for an exergy analysis and discussion of the process and the superstructure. The optimisation of the superstructure both with traditional hierarchical design and integrated design are carried out. Comparison of the results shows an increased net present worth for the plant designed with integrated design.

Chapter 8: Conclusion.

A summary of the thesis, chapter by chapter, the main conclusion, scientific contributions and suggestions for future work.

1.3 Original contributions to science

The contribution of the thesis is summarised here, but for a more complete discussion please read chapter 8. The findings have partly been reported in (Grue and Bendtsen 03a; Grue and Bendtsen 03b; Grue and Bendtsen 05), and the remaining findings will be published in the near future.

In general it has been necessary to create a robust solution framework for the optimisation the entire method relies on disjunctive formulation of the problem. To this end a disjunctive branch-and-bound algorithm has been implemented. Even on small systems this algorithms has proven superior to commercial solvers.

1.3.1 Integrated design method

A methodology that simultaneously optimises the process, utility system and heat integrates both has been proposed. The method is formulated in general terms, but relies on the utility system optimisation method described below. The method provides the mean of interfacing the utility model seamlessly with the process model for simultaneous optimisation.

To ensure optimal heat integration between the process and the utility system, the traditional separation of process streams and utility streams in the pinch analysis have been removed, and allowing a complete integration across process to utility.

Two large test cases, for integrated design have been used to test the method, and improved results are found compared to the sequential approach. (Grue and Bendtsen 03a; Grue and Bendtsen 03b).

1.3.2 Utility systems

A superstructure for synthesis of utility systems both for sequential design and integrated design has been formulated using disjunctive programming. Unlike most other work within the field, the superstructure allows for simultaneous selection of pressure levels in the utility system.

- To this end a new formulation for steam properties is proposed, which is more detailed than the one usually used for optimisation, yet far simpler than the standard IF-97 formulation. The properties show good agreement for pressures below 150 bar.
- A number of different heat integration methods have been tried out, but all of the MINLP formulations become too combinatorially large for practical use.
- The unit operation models for steam turbines now have much better prediction of the isentropic expansion enthalpy, thus making the models much more reliable.
- Gas turbine models have been improved based on manufacturer data for more than 150 different gas turbines and models are developed for industrial and aero-derivative turbines.

1.4 Summary

In this chapter the subject of the thesis were stated. A brief background on process synthesis where provided. Much research has already been carried out in the individual fields of process synthesis but the integration of the fields are more limited. It is, however widely recognised that the sequential design procedure by (Douglas 88) leads to suboptimal designs, since the interaction of the systems are not taken into account. Especially the integration between process and utility system has only been addressed in a very limited manner. This motivates the subject of this thesis.

Finally the outline of the thesis and the original contributions to science were summarised. A brief note on the outline, here it is apparent that no industrial case studies were used in this work. Unfortunately it was not possible to find an industrial case study within the framework of the project, instead the development of the methods are emphasised through typically test cases found in literature.

2 PRELIMINARIES

Tools and basic methods for process integration are introduced, especially with focus on mathematical programming. Disjunctive programming is also introduced, and the disjunctive solver used in this work is presented. Exergy analysis and pinch analysis are also briefly described.

The main objective of this chapter is to provide a short review mathematical programming and exergy analysis. As pinch analysis has already been described in chapter 1.1.4 it will not be treated any further here.

2.1 Mathematical programming

The field of mathematical programming or optimisation[9] is by no means particular to process integration, but rather a very broad range of mathematical methods that have found use within everything from airplane scheduling to protein folding, and also in the field of process integration.

Optimisation deals with the maximisation or minimisation of a function by changing a set of design variables. In the basic form this is unconstrained optimisation. If the change of the variables is limited or interlinked through a set of equations or inequalities the problem turns into a constrained optimisation problem. In general this can be formulated as

$$\begin{aligned} & \min_{\mathbf{x},\mathbf{y}} \quad f(\mathbf{x},\mathbf{y}) \\ \text{subject to} \quad & \\ & \mathbf{g}(\mathbf{x},\mathbf{y}) \leq 0 \\ & \mathbf{h}(\mathbf{x},\mathbf{y}) = 0 \\ & \mathbf{x} \in \mathbb{R}^n, \mathbf{y} \in \mathbb{Z}^m \end{aligned} \tag{2.1}$$

[9] Please note that the terms *mathematical programming* and *optimisation* are used interchangeably.

The objective function can represent anything that one wants to maximise or minimise from annual profit to environmental impact. Usually the result is heavily dependent on the objective function.

The constraints usually models physical limits of the process, e.g. mass or energy balances.

The design variables are the parameters of the current problem that can be changed, e.g. feed composition, reaction temperature etc. The design variables may be either continuous or discrete; e.g. a temperature can often be set continuously, but it is only possible to have a discrete set of boilers in a plant (1, 2 etc – but certainly not 1.5!).

Problems are usually classified in different classes. If the any of the constraints or the objective function are non linear, then the problem becomes a non-linear optimisation problem. Combining this with the different type of variables, the problems are divided as illustrated in fig. 2-1

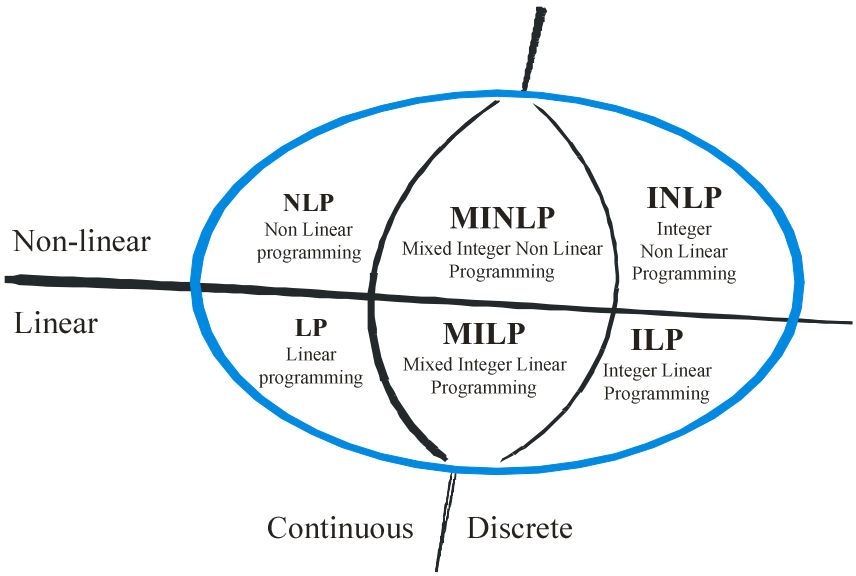

fig. 2-1 different classes of optimisation problems, adapted from(Franck et al. 98).

LP is by far the easiest class to solve and the solution is guaranteed to be the global optimum. The same applies to MILP and ILP, but in this case the computational demand rises significantly with the number of integer variables, as the problem turns into a combinatorial problem.

NLP problems can be significantly harder to solve, depending on the non linear nature of the functions, and it can only be assured that the optimum found is global, when all the non-linear functions are convex; in fig. 2-2 this is illustrated for non-linear objective functions.

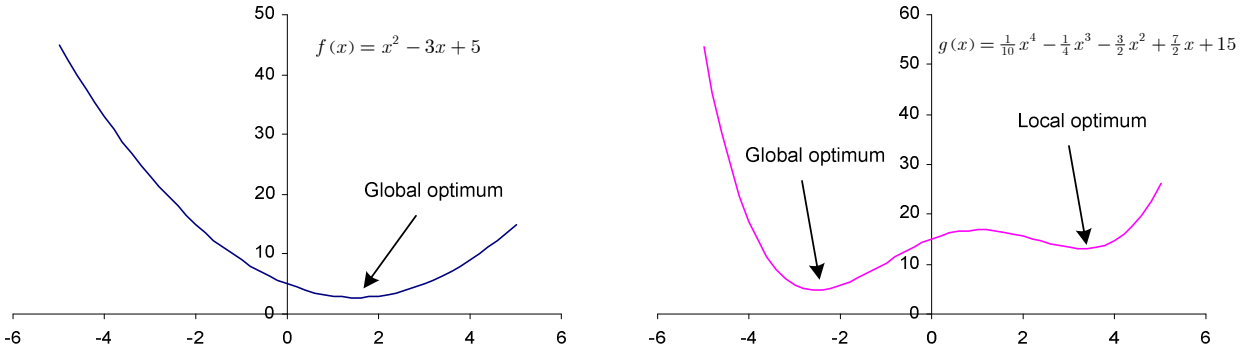

fig. 2-2 The convex function f only has one minimum, the global, while the non-convex function g both have a local and a global minimum.

The constraints can also make the problem non-convex, as shown in fig. 2-3.

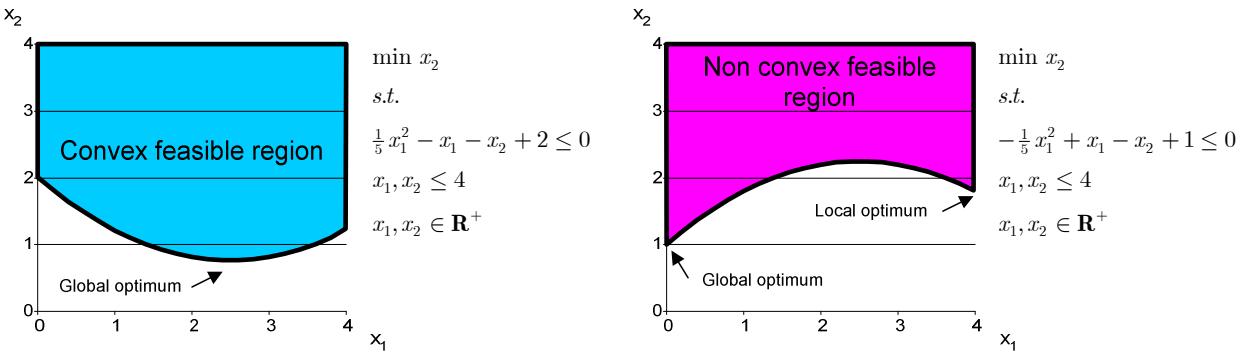

fig. 2-3 The optimisation problem to the left is convex and only have one optimum (the global), while the problem to the right have both a local and a global optimum. In both cases the objective function is linear, while the convexity is determined by the inequality constraint.

It ought to be noted that for some classes of problems a number of non-convexities can be eliminated through clever formulation.

2.1.1 Algorithms

Optimisation algorithms are usually divided into deterministic and stochastic algorithms. The first use a search technique that always search "downhill"[10], while still fulfilling the constraints. If a deterministic algorithm becomes trapped in a local optimum it will never find the global optimum, since this will require an "uphill" search. The latter type uses a somewhat randomized search direction, thereby making it less likely to become trapped in a local optimum.

A recent overview of both the past and future of optimisation is given by (Biegler and Grossmann 04; Grossmann and Biegler 04).

[10] Downhill means that the algorithms searches in the direction of decreasing objective function values

Solution algorithms differ depending on the problem type. For LP problems the solvers are typically based on the SIMPLEX algorithm. MILP and ILP can be solved using a combination of SIMPLEX and Bound & Branch strategies. As there is only the global optimum for these problem types, there is no use for stochastic methods. See (Edgar *et al.* 01) for more information on the algorithms.

For NLP problems it seems that two major deterministic algorithms are dominating, the Generalised Reduced Gradient (GRG) and the Successive Quadratic Programming (SQP). Both exist in several commercial software packages. An excellent overview is given by (Conn *et al.* 00).

The most recent advances in optimisation are within algorithms for MINLP-problems, (Grossmann and Kravanja 95) provides an excellent overview of the field. In short the OA alternates between solving a MILP-master problem and a NLP subproblem. Several other algorithms have been developed, e.g. "Generalized Benders Decomposition" and "The Extended Cutting Plane Algorithm". The latter is developed by (Westerlund *et al.* 98), and can solve pseudo-convex problems to global optimum.

Much work has been put into making deterministic algorithms for NLP-problems able to find the global optimum. Some of the latter work includes convexification of the important class of functions signomials (Björk *et al.* 03; Pörn *et al.* 99):

$$S(x) = \sum_{j=1}^{N} \left[a_j \prod_{k=1}^{M} x_k^{b_{j,k}} \right] \quad a,b \in \mathbb{R} \tag{2.2}$$

The convexification technique introduces piecewise convex functions that underestimates the actual signomial. By successively applying more and more detailed piecewise approximations the method can converge to a global optimum, though this requires the solution of a sequence of convex MINLP-problems. The method is thus only suited for relatively small problems at the moment. Still the development is important since the ability to avoid local optima is one of the big challenges in process synthesis.

Disjunctive programming

The formulation based on continuous and discrete variables are in many practical applications not very intuitive. Instead it is more convenient to think in terms of boolean operators, i.e. in the modelling of a heat exchanger as illustrated in fig. 2-4.

The benefit of the disjunctive formulation is not only the more intuitive formulation of the problem, but also in terms of solution. One of the typical problems with standard algorithms is that the constraints for deselected equipment are still part of the optimisation problem, and often this leads to badly conditioned systems or even errors in the evaluation of the constraints. This problem is almost completely avoided with the use of disjunctive programming, though the relaxed solution formulation still requires considerable work in order to avoid badly conditioned equations for zero-flow.

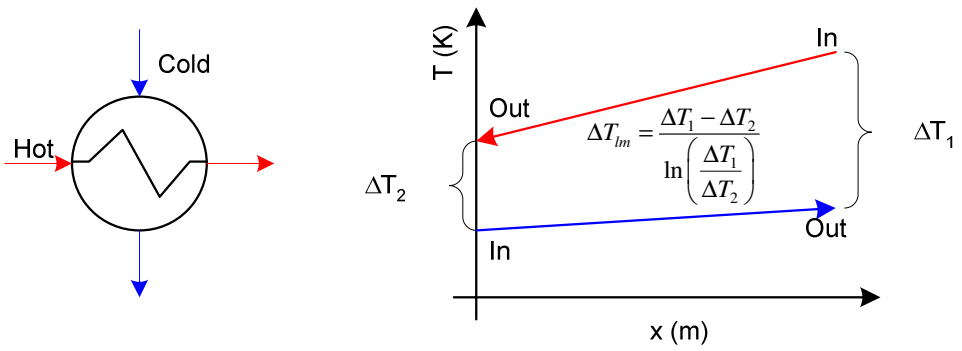

fig. 2-4 Heat exchanger and temperature curves.

The model can in terms of boolean variables briefly be formulated as follows

$$\begin{bmatrix} Y_{HX} \\ \dot{m}_{cold}\left(h_{cold}^{in} - h_{cold}^{out}\right) + \dot{m}_{hot}\left(h_{hot}^{in} - h_{hot}^{out}\right) = 0 \\ \dot{m}_{hot}\left(h_{hot}^{in} - h_{hot}^{out}\right) = UA\Delta T_{lm} \end{bmatrix} \vee \begin{bmatrix} \neg Y_{HX} \\ \dot{m}_{cold} = 0 \\ \dot{m}_{hot} = 0 \\ h_{cold}^{in} = h_{cold}^{out} \\ h_{hot}^{in} = h_{hot}^{out} \end{bmatrix} \tag{2.3}$$

Here the boolean variable Y_{HX} determines whether the heat exchanger exists, and a different set of equations apply if the heat exchanger is deselected in the superstructure. Disjunctive programming is still very much in development and no commercial tools exist today.

Nevertheless it is necessary to convert the problem into a formulation of continuous and integer variables before it can be solved. This is caused by the nature of most MILP/MINLP methods, where the relaxed problem is solved first and then by successively fixing integer variables the integer solution is found. In the case of disjunctive programming this means that a relaxed formulation for the heat exchanger is required for the step before branching on the boolean variable, but after the branching of the boolean variable the equations in (2.3) apply, as illustrated in fig. 2-5.

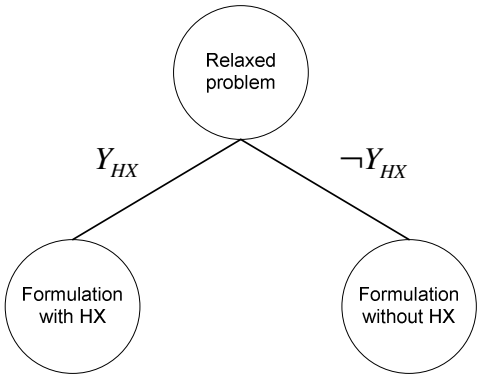

fig. 2-5 Problem formulations needed in different parts for the search tree

Several methods exists to convert the disjunctive formulation into a relaxed formulation, e.g. proposed by (Lee and Grossmann 00; Turkay and Grossmann 98).

2.1.2 Software for optimisation

Several commercial available software packages for optimisation exist. GAMS (General Algebraic Modelling System)by (Brooke *et al.* 98) is a general interface for formulating algebraic equations and inequalities. A number of third-party vendors have developed optimisation packages that interface with GAMS. The key benefit is that the user only needs to think about the modelling, but do not have to consider implementing the model for different solver-suites. GAMS is widely used, and the solvers provided for the system is thoroughly tested.

For MINLP there are two commercial available algorithms DICOPT++ for GAMS implements the Outer Approximation algorithm, and the SBB (Simplified Branch & Bound), also for GAMS, implements a branch-and-bound algorithm, that solves a NLP problem in each node.

In both solvers the NLP-problem needs independent NLP-solver, and for GAMS several options are available. CONOPT for GAMS (Drud 02) implements a combination of the GRG and the SQP algorithm and have been reported to solve with more than 10000 constraints routinely, and as much as 1 million constraint in special cases. It is beyond the scope of this work to go into more details of the inner working of the algorithms. A brief test of the different methods has been performed in chapter 5.1.2.

As of today no commercial solver exists for solving disjunctive programming problems, though several academic codes have been developed, e.g. the LOGMIP algorithm by (Türkay and Grossmann 96), which is actually based on the Outer Approximation. A branch-and-bound algorithm was formulated by (Lee and Grossmann 00).

It is obvious that other software exists; in particular, a number of academic codes are available, and often these include some of the newest development in the algorithms. On the other hand the commercial systems are usually more reliable and robust.

2.1.3 Numerical methods for solving ODEs in optimisation problems

Normally process models are described by algebraic equations in steady state operation, though exceptions do occur. One is the plug flow reactor which requires the solution of a set of ODEs that cannot be solved analytically. At the same time the NLP-solvers only handles algebraic equations, and therefore discretisation of the ODEs into algebraic equations is needed.

Several methods are available, e.g. the well-known Runge-Kutta method. When the ODEs need to be part of an optimisation problem, there exists basically two ways to handle them.

- Solution of the ODEs outside the optimisation algorithm.
- Discretisation of the ODEs into algebraic equations.

The first option solves the ODEs over and over again, thus making the ODEs seem like a black-box to the optimisation. In the latter the discretised ODE are directly a part of the optimisation problem, and as such the solution of the ODE are simultaneous with the

solution of the optimisation problem. There are benefits and drawbacks for both approaches; the first is clearly superior in solving the ODEs since adaptive stepsize algorithms etc. can be used to ensure convergence, this is more difficult with the latter since the number of elements needs to be determined beforehand. On the other hand it is clear that it is far more effective to solve the discretised ODEs simultaneous with the optimisation problem.

One of the most common methods is "orthogonal collocation points on finite elements", which has been successfully applied in a number of studies, e.g. (Biegler *et al.* 02). A brief description of the method is provided here. For the solution of the ODE,

$$\frac{dy}{dt} = f(y) \tag{2.4}$$

y is approximated with a LaGrange interpolation polynomial over N finite elements with M internal collocation points.

$$\begin{aligned} y(t) &\approx \sum_{k=0}^{M} y_{i,k} L_k(t) \quad for\ t_{i,0} < t < t_{i+1,0} \quad ; \quad i = [1 \ldots N] \\ L_k(t) &= \prod_{l=0; l \neq k}^{M} \left(\frac{t - t_{i,l}}{t_{i,k} - t_{i,l}} \right) \quad ; \quad k = [1 \ldots M] \end{aligned} \tag{2.5}$$

The collocation points must be *orthogonal*, for details see (Rice and Do 95). Normally the roots of the Jacobi-polynomial are chosen, though other options do exist. If the elements are normalised to unit length the differential equation can be transformed into a number of algebraic equations, one for each interior collocation point.

$$\frac{1}{\Delta\alpha_i} \sum_{k=0}^{M} y_{i,k} \frac{dL_k(\tau_j)}{dt} = f(y_{i,j}) \quad ; \quad i = [1 \ldots N] \quad ; \quad j = [1 \ldots M] \tag{2.6}$$

The benefit of this equation is that the derivative of the Lagrange polynomial can be calculated in advance. At the interface between the finite elements, continuity must be ensured:

$$\sum_{k=0}^{M} y_{i,k} L_k(\tau = 1.0) = y_{i+1,0} \quad ; \quad i = [1 \ldots N] \tag{2.7}$$

Again, the value of the Lagrange polynomial can be calculated in advance, turning this equation into a simple linear equation. Altogether equation (2.6), and (2.7) provides a system of algebraic equations that approximates the solution of the ODE. An appropriate number of interior collocation points and finite elements must be chosen, normally the same number of collocation points are used throughout the model, and increased detail are obtained by decreasing element length.

For estimation of the error (Vasantharajan and Biegler 90) has proposed the following method:

$$e_i = \sum_{k=0}^{M} y_{i,k} \frac{dL_k(\tau=1)}{dt} - \Delta\alpha_i \sum_{k=0}^{M} f\left(y_{i,k}\right) L_k(\tau=1) \quad ; \quad i=1,N \tag{2.8}$$

If the error is bounded by a small number ε, e.g. $-\varepsilon < e_i < \varepsilon$, and letting the element length be variable, the algorithm becomes one with adaptive step length, which will be infeasible if too few elements or collocation points are used.

2.1.4 Disjunctive MINLP solver

In this work a disjunctive MINLP has been developed. As mentioned above there is a lack of commercially available disjunctive solvers, but at the same time the disjunctive formulation are considered very interesting in terms of model formulation. The solver has been implemented as a branch-and-bound solver, where a relaxed NLP-problem is solved at each node. The NLP-problem in each node is different, as the constraints depend on the boolean (or binary) variables. The algorithm is outlined in fig. 2-6.

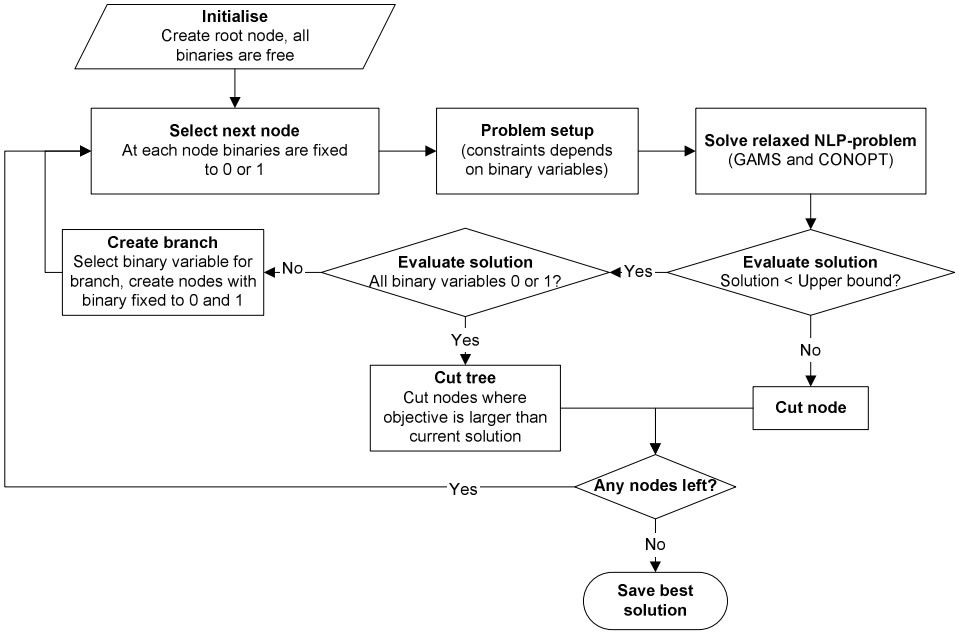

fig. 2-6 Working principle for the disjunctive Branch-and-bound algorithm

Most of the algorithm are common to all other branch-and-bound algorithms, and it is only the *problem setup phase* that differs, since the logic selections in the current node is used to define which constraint to include in the NLP-problem. The actual implementation is a wrapper around GAMS, which is used to solve the NLP-problems. The solution process can be monitored in the wrapper application, see fig. 2-7.

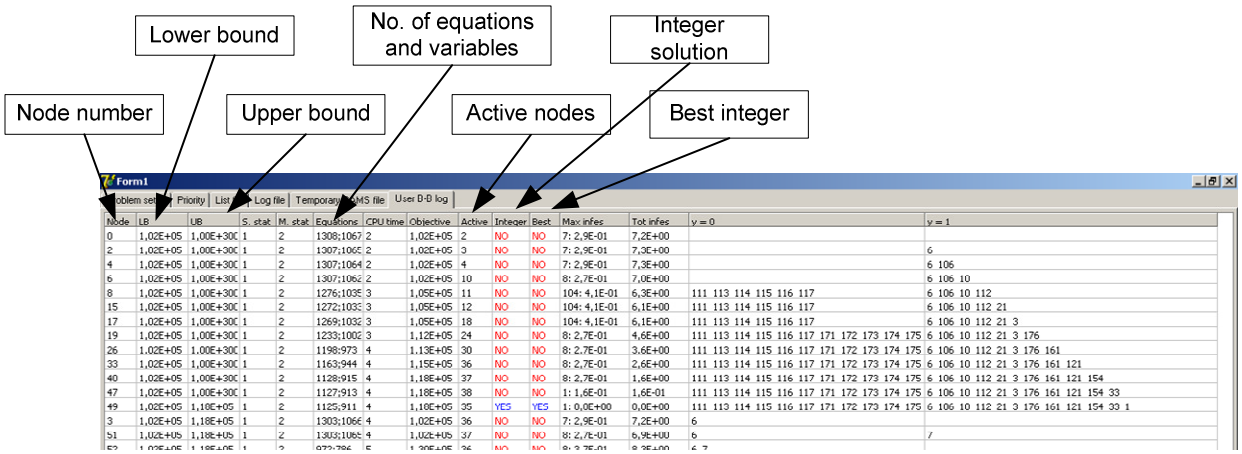

fig. 2-7 Screenshot from the disjunctive B&B-solver

One of the crucial steps in a branch-and-bound solver is the selection of binary variables when branches are created and selection of the next node to solve. Several strategies exists, and some of the simpler have been tried out with the solver. The following strategy has been applied as default.

- Initially nodes are selected with depth first search[11], and the branches are created by fixing the binary with smallest integer infeasibility in last solution.
- When the first integer solution is found, a best-bound search is used[12]. The binary variable for branching is selected as the one with the largest integer infeasibility.

The benefit of doing a *depth first search* initially is that an upper bound is established. This reduces the number of nodes to be evaluated, as nodes with solutions larger than the upper bound are not considered any further. With the upper bound established it is however much better to use the *best-bound* strategy, since this ensures that the minimum number of nodes are evaluated, since the node with the current best objective is always used. This works very well as long as the solver continues until there is no nodes left to evaluate. However, for large problems it might be desirable to stop the iteration whenever the lower and upper bound are within a predefined margin, e.g. 5% difference between the two. In this case it is very important to quickly improve the upper bound, even at the expense of evaluating nodes that the *best-bound* strategy would never consider. One way to select promising nodes and select the best variable for branching is the pseudo-costs described by (Linderoth and Savelsbergh 99). In all the examples of this thesis it has been possible to solve the B&B-problem until no nodes were left, and thus the pseudo-costs have not really been helpful.

[11] In *depth first search* the node furthest down in the search tree are selected as the next to be evaluated.

[12] In *best bound search* the node whose parent has the lowest (best) objective value is selected as the next to be evaluated.

2.2 Pinch analysis

The pinch analysis is perhaps one of the most well-established methods in process integration, even if it only covers heat integration. The method has already been discussed in chapter 1, and therefore it will not be addressed any further here.

2.3 Exergy Analysis

Traditionally flowsheets are evaluated by the 1st law of thermodynamics, as the energy balance for the flowsheet is calculated. This approach is important for identifying energy flows, and the need for heating, cooling and power. On the other hand this analysis does not take the quality of the energy into account, which is why the 2nd law of thermodynamics is to be used. This is known as exergy analysis. (Bejan *et al.* 96) defines exergy as

> *An opportunity for doing useful work exists whenever two systems at different states are placed in communication, for in principle work can be developed as the two are allowed to come into equilibrium. Exergy is the maximum theoretical useful work obtainable as the systems interact to equilibrium.*

While energy is conserved, exergy is not and can be destroyed. For calculation of the maximum theoretical work, one needs to establish a reference environment. Several definitions for the reference environments exist, but it is beyond this work to go into it.

Normally exergy is divided into four components

$$\mathbf{e} = \mathbf{e}^{ph} + e^{kin} + e^{pot} + e^{ch} \tag{2.9}$$

The kinetic and potential energy of a system is (at least in theory) fully convertible to work as it corresponds directly to kinetic and potential exergy. Chemical exergy reflects the maximum work that can be obtained when a chemical component is transformed into the components of the reference environment. The chemical exergy for a number of substances is found in (Bejan *et al.* 96), and in addition the chemical exergy for any hydro-carbon might be evaluated by considering the reaction of hydro-carbon into known substances of the reference environment.

$$C_a H_b + \left(a + \frac{b}{4}\right) O_2 \rightarrow aCO_2 + \frac{b}{2} H_2O(l) \tag{2.10}$$

Note that it is assumed that the water is in liquid form. The chemical exergy of the hydro-carbon can be evaluated from the gibbs-molar-energies.

$$\begin{aligned} \overline{e}_{ch,F} = &\left[\overline{g}_F + \left(a + \frac{b}{4}\right)\overline{g}_{o_2} - a\overline{g}_{CO_2} - \frac{b}{2}\overline{g}_{H_2O(l)}\right]_{(T_0,p_0)} \\ &+ a\overline{e}_{ch,CO_2} + \frac{b}{2}\overline{e}_{ch,H_2O(l)} - \left(a + \frac{b}{4}\right)\overline{e}_{ch,O_2} \end{aligned} \tag{2.11}$$

Note that the reaction is assumed to take place at the temperature and pressure of the reference environment.

The physical exergy is associated with the generation of entropy and is defined as:

$$\mathbf{e}^{ph} = (h - h_0) - T_0(s - s_0) \tag{2.12}$$

Exergy is an extensive property that can be transferred between different systems. For an open system the exergy balance can be summarised as

$$\mathbf{e_{in}} = \mathbf{e_{out}} + \mathbf{e_{loss}} \tag{2.13}$$

And from this the exergetic efficiency of a process can be defined as

$$\eta_e = \frac{\mathbf{e_{out}}}{\mathbf{e_{in}}} = 1 - \frac{\mathbf{e_{loss}}}{\mathbf{e_{in}}} \tag{2.14}$$

In this way it is possible to evaluate where a system can be optimised, from a thermodynamic viewpoint.

Exergy analysis has been combined with pinch analysis, e.g. (Franck *et al.* 98) for an overview. In this context the temperature scale of the composite curve is replaced with the Carnot-efficiency.

$$\eta_c = 1 - \frac{T_0}{T} \tag{2.15}$$

Thus the exergy loss due to heat exchange is visualised on the composite curves, since the exergy loss corresponds to the area between the curves. This can of course lead to information about heat exchanges where work potential is lost. Nevertheless the method is still centred on heat exchange, and is as such not able to take any other equipment into consideration. This was addressed by (Feng and Zhu 97) who extended the analysis to include expansion and compression work. Furthermore they divided exergy loss into avoidable and inevitable losses; the first can be avoided provided the best available technology is used, whereas the latter cannot be avoided because even the best available technology is not perfect.

Still the major disadvantage of the exergy method is the focus upon thermodynamic efficiency, and a thermodynamically optimal system might be different from an economically optimal system. To address this subject several authors have proposed the concept of thermoeconomics, in which an economic value is associated with each exergy loss. See (Bejan *et al.* 96) for more.

In general exergy analysis is best used for evaluating existing systems or a proposed base case, but is generally not useful for generation of the initial design.

2.4 Summary

In this chapter mathematical programming was introduced, formulations were divided into different classes, and algorithms for solving the problems were briefly described. The intuitive and easy formulation of problems using disjunctions was introduced, and the branch-and-bound solver that handles the disjunctions was described. The solver relies on a

depth-first-search to establish the initial upper bound, and afterwards searches the tree with a *best-bound-search*. The method of pseudo-costs by (Linderoth and Savelsbergh 99) was implemented, but it is only beneficial for cases where the solver is stopped when the lower and upper bound are within a given tolerance. As all problems in this work have been solved to completion, this option has not been used extensively.

Afterwards the notion of exergy analysis was briefly described, and the evaluation of chemical exergy for hydro carbons was introduced. In addition evaluation of exergetic efficiencies was described.

The pinch method was described in section 1.1.4, and not treated any further here.

3 METHODOLOGY

Based on the hypothesis that integrated design leads to better process plants the methodology for integrated design is proposed. The method relies on a limited superstructure for reaction and separation tasks, combined with a complete heat and work integration with the utility system. In addition economic modelling is briefly discussed.

In this chapter the main methodology and contribution is described in detail. Based on the hierarchical design procedure a number of general considerations for an integrated design of the core process and the utility system are described.

This leads to the proposal of a method for integrated design in section 3.2, which is followed by a discussion on the interaction between process systems and utility systems. Afterwards the methods are described step-by-step, with discussions about limitations for each step in the method.

3.1 Integrated design – core process to utility

First the hierarchical method (Douglas 88) is revisited, here in a slightly revised version.

1. Batch or continuous
2. Input – output structure of the flowsheet
3. Reactor and recycle structure
4. Separation system
5. Heat exchanger networks
6. *Design of utility systems*

The last task is not included in the original work by (Douglas 88), but in the end the utility system needs to be designed. Usually a process will need heating, cooling and work, thus it is obvious that the utility system must be designed, and in accordance with the hierarchical progress of the method this must necessarily be the last task.

A fully integrated method will of course take all the steps into consideration in one simultaneous synthesis task, but this is unlikely to be very realistic. Recalling the outline of reaction, and separation network subsystems in chapter 1, these tasks are by themselves very difficult to solve, and combinatorially very large by themselves. It is therefore unrealistic to believe that a completely integrated method can be formulated at present. Instead the focus will be somewhat limited, in order to pose a problem that can be considered realistic to solve. An important issue in the integrated design is that it can handle the introduction of new non-convexities in the optimisation problem in an efficient manner, compared to hierarchical design. This is simply because in hierarchical design a number of variables are fixed as boundary conditions, but in integrated design these are often free.

With the focus on integration of the utility system in mind the major scope limitations of the method can be summarised as follows:

- The method will only address the latter stages of the design (task 3 to 6). Thus it will not be a completely integrated and simultaneous design of all steps.
- The detailed synthesis of both reactor networks and separation systems are not included in this methodology. Thus task 3 and 4 will only be partly included into the integrated approach.
- The method will not be completely automated. The engineer is still very much needed for formulating superstructures and evaluating designs.

The reaction and separation network subsystems are excluded in recognition of the difficulty involved in solving these problems by themselves. Therefore the method for integrated design will assume that the superstructure for both reaction- and separation network is reduced to a level where the total problem size becomes reasonable. This could e.g. be obtained with the pre-screening procedure proposed by (Bedenik *et al.* 04).

3.2 *Method for integrated design*

The overall hypothesis of this work is that integrated design between process and utility system generates better plants[13]. Based on this hypothesis the methodology will be proposed. The following method for integrated design is proposed.

1. Batch or continuous
2. Input – output structure of the flowsheet
3. *Reduced* reaction and recycle *super structure*
4. *Reduced* separation system *super structure*
5. *Integrated optimisation of*
    a. Reaction and recycle structure
    b. Separation system

[13] The term *better* can be understood as with respect to any chosen objective function

c. Heat integration

d. Utility system

Comparing with the hierarchical method, the first three tasks remain unchanged. It has been considered outside the scope of this work to discuss the initial design of the process. Still, this does not mean that the reactor network and separation sequence should be fixed; as mentioned, a reduced superstructure of both is assumed to be within the limits of the integrated design. The size of the reduced superstructure cannot be specifically defined, but will change on a case to case basis.

The main topic of this work is the integrated design of the process and the utility system (task 6). In here the reduced super structure for reactor and separation are optimised simultaneous with the heat integration and utility system design.

With these limitations in mind, the details of the interactions of the subsystems are now discussed, to establish how they are linked together.

3.2.1 Interaction of the subsystems

In fig. 3-1 gives an overview of the interaction between the process system, the heat integration and the utility system. The figure also indicates that the different subtasks from (Douglas 88) are still more or less intact, but the interaction between the different parts are accounted for.

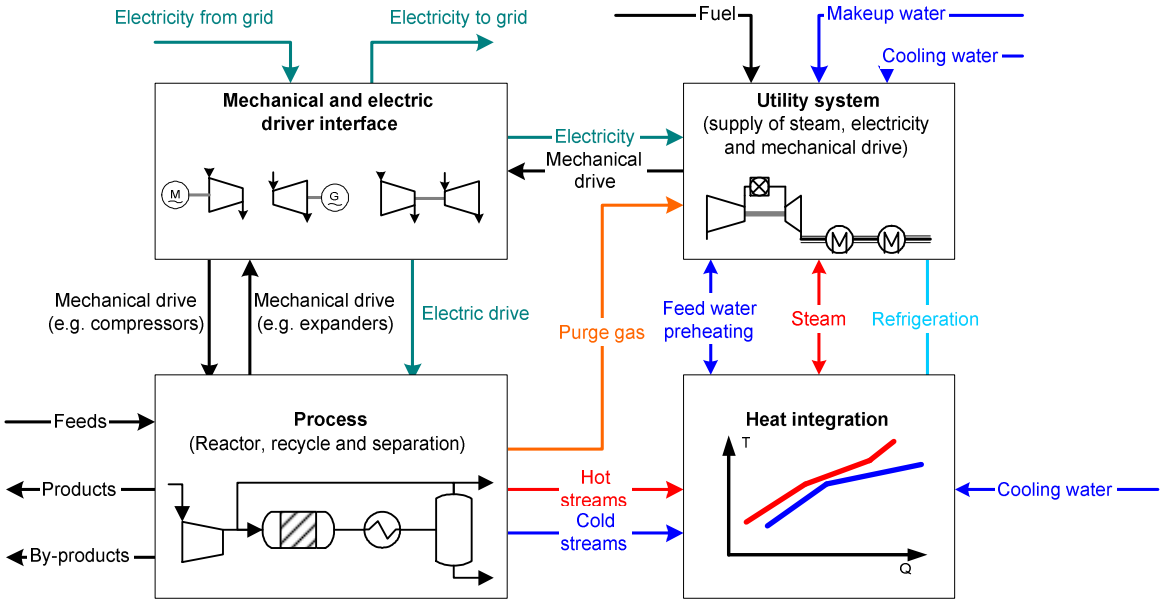

fig. 3-1 The interaction between process system, heat integration and utility system

The process requires one or more feed streams of the raw materials, which are then converted into a number of products and by-products. In some plants, a particular by-product might be gas, which is purged in order to avoid build up in the system; if the gas has a fuel value it can be burned in a furnace to raise steam. Therefore the gas purges must

be connected to the utility system. The process usually needs both heating and cooling of a number of streams; these streams can be interfaced to the heat integration method.

The heat integration ensures an energy balance between heat and cooling, as well as suitable heat recovery. The utilities include steam and cooling water, and optionally refrigeration for sub zero processes. Cooling water is assumed to obtained from the surrounding, e.g. rivers, lakes or cooling towers. The steam and the refrigeration must be produced at the utility plant.

The utility system provides electricity and mechanical work for the process (through the driver interface), along with steam and refrigeration for the heat integration. The system consumes fuel, cooling water for the condenser and make-up water for the steam/water circuit. The utility plant usually also requires electricity, e.g. for feed water pumps. For water/steam plants feed water pre-heating is often used to increase the efficiency of the plant, and in order to ensure full integration this is considered as a set of cold streams to be included in the heat integration.

An interface for mechanical and electrical energy has been included. The process typically needs mechanical work for compressors, pumps etc. For large components it might be desirable to have a steam turbine directly coupled to the shaft. For smaller components electric drives are usually selected. The utility system will provide mechanical energy to the interface and electric energy is returned to the utility plant. During conceptual design it is often only the major components of the process plant that are included. A process plant might also include gas expanders that produce mechanical energy; this can either be used for generation of electricity or coupled to work-requiring devices, e.g. compressors. The driver interface matches mechanical and electrical requirements of the process with the production of mechanical and electrical energy at the utility system. Electricity can alternatively be bought from the electricity grid or in the event of an excess of electricity it can be sold to the grid. The latter depends typically on local legislations for production of electricity.

Hereby the interaction between the process and the utility system has been outlined. In summary, the utility system and the process are as such considered two systems, which interact through the heat integration and the driver interface.

3.2.2 Details of the method

Here more details on the method are described, using this “roadmap” in order to set up the optimisation problem.

1. Process economics
    a. Determine cost of raw material, income from products and by-products (this is normally available from previous steps in the design)
    b. Determine fuel availability and prices, electricity prices (both for buying and if possible for selling) and cooling water prices
2. Formulation of process superstructure

   a. Create short-cut models for all reaction and separation tasks.
   b. Find correlations for investment cost for major process equipment
3. Enhancement of process superstructure
   a. Identification of large exergy losses in the base case
   b. Addition of relevant options to overcome the exergy losses
4. Integrated optimisation of combined superstructure
5. Verification of results, e.g. comparison with rigorous simulation tools

The individual steps will now be discussed in detail.

Step 1: Process economics

Estimated prices for raw materials, products and by-products will most likely be known at this time, since it is typically included in the evaluation of the basic concept, when the overall process idea is formulated.

The utility prices need to be found, however, they are usually heavily dependent on geographical location, local taxes and even worldwide market conditions, since the fuel prices tend to follow the oil prices very closely. It might be necessary to establish a set of different scenarios, especially for the fuel price, since this can be fairly difficult to predict on a medium to long term time scale. E.g. (Hoffman 03) reports that

> *"Natural gas markets have undergone extreme volatility in the past three years, to prices no one ever thought possible prior to 2000."*

This is supported by the data from (Vasnetsov 03), since natural gas prices have doubled since 1999. This both effect the fuel price, but in many cases also the feed costs, as natural gas is used for feed in several large scale chemical processes, including e.g. ammonia, methanol, polyethylene.

There is no doubt that the price forecast has a significant impact on the optimal solution, however, it is beyond the scope of this thesis to go into this field of study. It will thus be considered adequate to compare solutions from the hierarchical approach with the solutions from the integrated design using the *same objective function and price correlations* for both cases. The economic model used for this work is described in section 3.3.

Step 2: Formulation of process superstructure

Having identified a set of alternatives both for reaction, recycle and separation it is necessary to formulate a set of simplified unit operation models that can be used in the optimisation. Common simplifications include

- Use of ideal gas models rather than rigorous thermodynamic models
- Exclusive use of 1-D models, no 2 or 3-D effects are accounted for
- Only steady state models
- Using fixed unit operation parameters wherever doing so can be considered reasonable.

- Use of simple mean values instead of integral values wherever possible, since integrated values often requires solution of integrals of differential equations.

The advantage of fixing certain variables in the models is that the models are then simpler and the equations become easier to solve. Examples of parameters that might be considered fixed include pump and compressor efficiencies.

In general we will use simplifications such as outlined above, but there must always be a reasonable balance between simplifications, and correct prediction of the unit operation.

Step 3: Enhancement of process superstructure

Before proceeding to optimisation of the process and utility system, it might be beneficial to examine the process from an energy point of view, rather than the chemical point of view, which has probably been used for setting up the initial superstructure. There might exist several options for increasing energy efficiency even inside the process. Exergy analysis is a valuable tool here, since it will reveal where there are significant potentials for increasing efficiency. For instance reduction valves over big pressure differences might be substituted with gas expanders. Heuristics and rules of thumbs might also be used in this phase. Most importantly the issue is that the utility supply are not only to be interfaced with the process, but optionally also integrated partly inside the process. All the relevant options that are found during this phase are included in the superstructure.

Step 4: Integrated optimisation of superstructure

In the integrated optimisation one can either use the "standard" superstructure for the utility system, which will be proposed in chapter 4, or a set of additional technologies might be added. For instance the superstructure presented in chapter 4 does not include heat pumps, and thus this must be added if it is of interest to the designer. The "standard" superstructure does include all the relevant interfaces as outlined in fig. 3-1, and these are hereby modelled and an integrated superstructure optimisation problem is formulated. The solution of the problem then provides the optimal design given these constraints. As mentioned in step 1, a number of scenarios might be set up for evaluation.

It must be noted that the models are likely to include several non-convex terms, and a global optimum cannot be assured. Therefore a detailed review of the optimisation results, carried out by experienced designers is needed. It is also a good idea to try several starting points for the optimisation, in order to verify if the result is a local or a near-global optimum.

One of the large uncertainties in the formulation is that it is often impossible to predict how close the found solution is to the global optimum. To overcome this either deterministic global optimisation or stochastic optimisation can be used, however, these are much more computational expensive. Hence, there is no obvious choice if a global optimum is wanted, it will not be addressed further in this thesis.

Step 5: Verification of results

Finally the results from the optimisation need to be verified. As the method is used during conceptual design it is unlikely that any real data are available from the process. The verification is therefore most likely to be based on well-established simulation software, that

includes more rigorous models, e.g. Pro/II by (Invensys 03) for verification of the process it self and GateCycle by (GE Enter 03) for verification of the utility system.

The verification might also be used to perform exergy analysis or some other ways to uncover significant potentials for increasing the efficiency. It might be that potentials still exists, and that a new superstructure can be formulated based upon the result of the first. If any potential are uncovered a new superstructure is formulated and step 5 (and optionally step 4) is repeated again.

3.2.3 Discussion of methodology

One of the most important aspects to acknowledge is that the proposed methods still requires a competent user. The superstructures are only as good as the engineer that proposes them allows. Exergy analysis can be applied to help enhancing the superstructure, but there is still a risk that good solutions are overlooked.

The success of the method also depends on the ratio of utility prices to raw material prices. If the process is very energy intensive and utility cost comprise a significant part of the overall running costs, the expected benefits of using the integrated method are much larger than for processes where utility cost only are a small part of the overall operating costs.

The important details of economic modelling will be discussed in the next section.

3.3 Economic modelling

Here the economic model used in this work will be presented. The model is based on various sources, but since it is not the key topic of this thesis it will be presented "as-is" and no comparison with different methods will be carried out.

First the method for calculation of profitability are described, this is based on the net present worth method. Afterwards the prediction of economic development along with prices for fuel, wages etc. will be presented in the scenarios.

3.3.1 Method for calculation of profitability

The method used for economic evaluation (or calculation of profitability) is the one suggested by (Peters *et al.* 03). The profitability of the plant is evaluated using the net present worth method. This method calculates the present worth of all cash flows minus the present worth of all capital investments. The method discounts all future earnings and investments back to the present. The net present worth is calculated as follows

$$NPW = \sum_{i=1}^{n} \frac{(s_i - c_i - d_i)(1-\Phi) + d_i}{(1+r)^i} - \sum_{i=-2}^{n} \frac{C_i}{(1+r)^i} \tag{3.1}$$

where s_i *is the sales revenue in year i*
c_i *is the total product cost in year i*
d_i *is the depreciation in year i*
r *is the internal rate*

Φ is the tax rate
C_i is the capital investment in year i

Note that year 1 is the first year of operation, and year -2 is the year where the first estimate is being made, i.e. plant construction phase is from year -2 to end of year 0.

Capital investment

Fixed capital investments (FCI) are spent over a period of time. It is assumed that it takes 3 years to spend the investments from the beginning of the estimate to the start of operation. 15% of the FCI is assumed to be spent at the end of the first year, 35% is assumed to be spent at the end of the second year and the remaining 50% at the end of the third year, i.e. just before operation will begin.

The working capital that must be available at beginning of operation is assumed to be 15% of the FCI.

Operating costs

The operating costs can be divided into variable operating costs and fixed operating costs, where the first depends depend purely on the operation of the plant, whereas the latter is charged even if the plant is offline.

The variable costs can be summarised as follows

- The raw material cost is normally the dominating cost, and depends on the chemicals in question.
- Operating labour cost are estimated using the estimate for operating labour pr. unit operation (Peters *et al.* 03) and the wages and work hours listed in section 3.3.2.
- Supervision is assumed to be 15% of the operating labour cost
- Maintenance and repairs is assumed to be 6% of FCI
- Operating supplies is assumed to be 15% of maintenance and repairs
- Laboratory charges is assumed to be 15% of operating labour cost

The fixed costs can be summarised as

- Insurance: 1% of FCI
- Plant overhead: 60% of labour cost, supervision cost plus maintenance and repair cost.
- Administration: 20% of the operating labour cost
- Finally it is assumed that sales and R&D amounts to 8% of the total product cost

Depreciation

According to (Skatteministeriet 00) the declining balance depreciation is the most frequently used method in Europe. This method allows a fixed fraction of the current book value to be depreciated every year. The maximum fraction is typically around 30% per year.

3.3.2 Scenarios

The net present worth method requires knowledge of the expenses and incomes for all the years of operation (e.g. 10 years). The estimation of these prices is of course difficult, thus it is interesting to investigate the result of the optimisation for significantly different scenarios. Since the objective function is chosen to be the net present worth of the plant, it is primarily of interest to look further into the assumed prices in the model. Especially the prices for utility systems contain considerable uncertainty, and one way to examine this uncertainty is to analyse the solution for a set of different alternative price developments.

The different developments will be based on three scenarios for the development of the European economies and especially the European energy market. The scenarios are developed by (Elsam 03), and fully accessible at the website indicated in the reference list. A brief outline of the major political and economical development for each scenario is provided here.

- Scenario 1: The Free Market. A steady economical development is expected, along with the continuous globalisation. The power balance of today remains.
- Scenario 2: Crisis. A sudden economic collapse occurs and lasts for the next 10 years, followed by a catch-up. The political development is characterised by increased nationalism, weakening of the present superpowers and spreading of the power.
- Scenario 3: Grassroots. A high economic growth in the EU prevails all the years from now to 2025. The political development is characterised by a new world order, where USA's power is reduced because of economical collapse, and in the wake EU and China/Asia increase their regional influence.

Note that the colours used in the text will be used to describe the scenarios will be used in the following to make identification easier. The predicted overall economic trend of the northern European region and the inflation is shown in fig. 3-2.

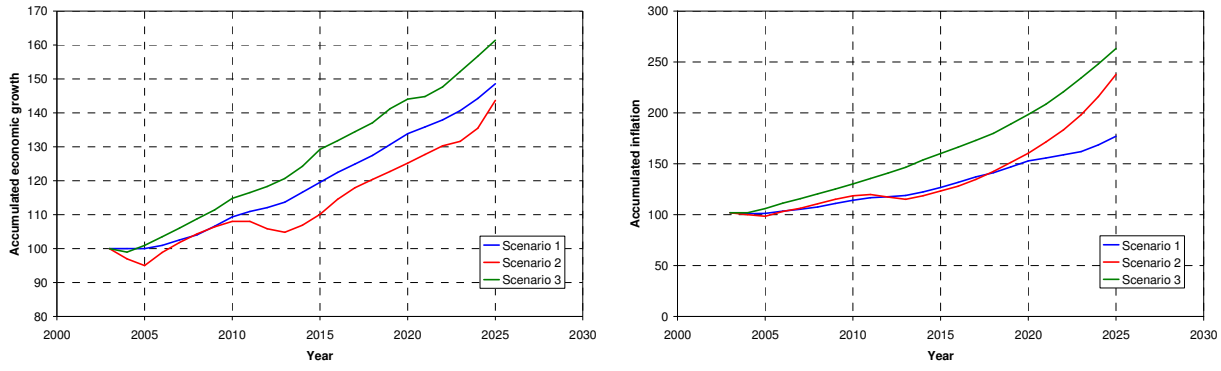

fig. 3-2 To the left the overall economic growth for the Northern European economy, and to the right the inflation. Year 2003 is used as index 100.

In addition to the overall trend in the economy the scenarios also try to predict the development in the fuel prices. Based on these inputs the scenario model calculates the

broad development of the European power plant fleet over the next 20 years, and based hereupon a set of electricity prices are derived.

Electricity prices

The market model in the scenarios does predict the electricity prices, but only in the form of sale prices, which for an electricity generator are the interesting price. For industry, there are typically a number of taxes and transmission charges to pay, in addition to the sale price from the generator. In this work, the electricity can both be bought from the electricity grid or if there is an excess of heat and the price is right, it is possible to export electricity to the grid.

In accord with this, it is assumed that electricity generated at the plant can be sold at spot market prices. The electricity prices are predicted by the scenarios as shown in fig. 3-3.

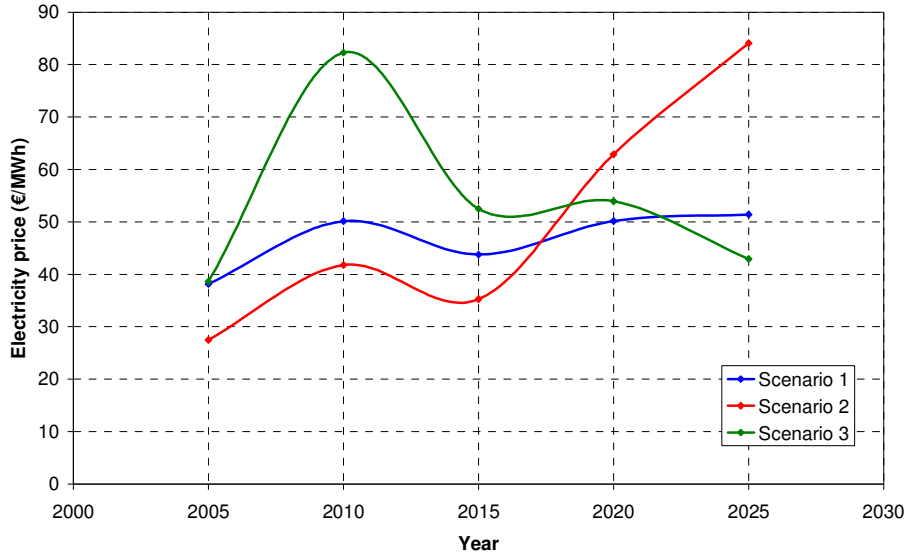

fig. 3-3 Electricity prices predicted by the scenarios. Note that prices are calculated in fixed prices for 2003.

Oil and gas prices

Crude oil prices as well as average fuel oil prices are based on (IEA 03), which reports the prices on a monthly basis. In fig. 3-4 the spot price for brent crude oil is compared with the end-user price for heavy fuel oil.

Not surprisingly, the two prices correlate relatively closely, and therefore it seems to be reasonable to base the forecast of the fuel oil price on the prediction on the crude oil price. The scenarios predict the crude oil price, as shown in fig. 3-5.

Note that the prices were predicted in 2003, and now near the end of 2005 it is very easy to see that none of the scenarios have foreseen the large increases in oil prices experiences the last couple of years (shown in black). In spite of this observation we will still use the predicted scenarios for the sake of consistency. It should, however, still be pointed out that

the higher fuel prices will in fact increase the economic advantages of integrated utility design.

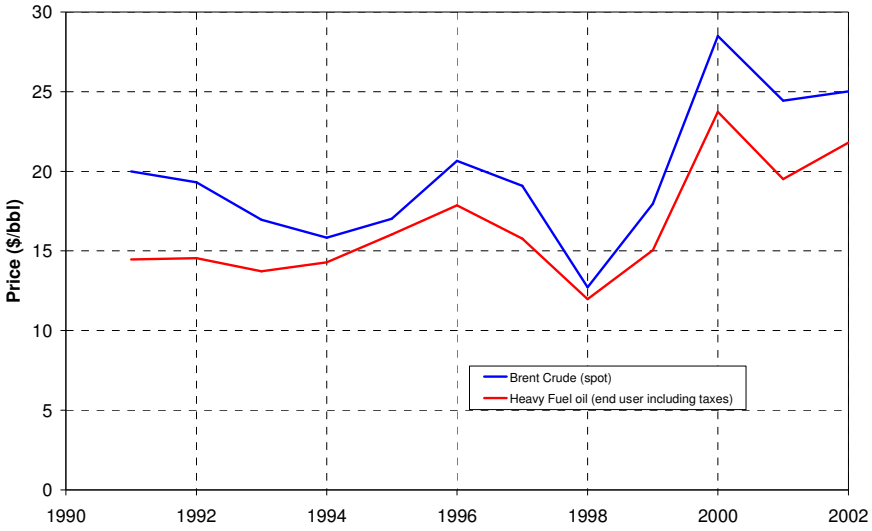

fig. 3-4 Comparison of Brent crude oil spot price and the end user price of heavy fuel oil in Europe, the data are based on. (IEA 03)

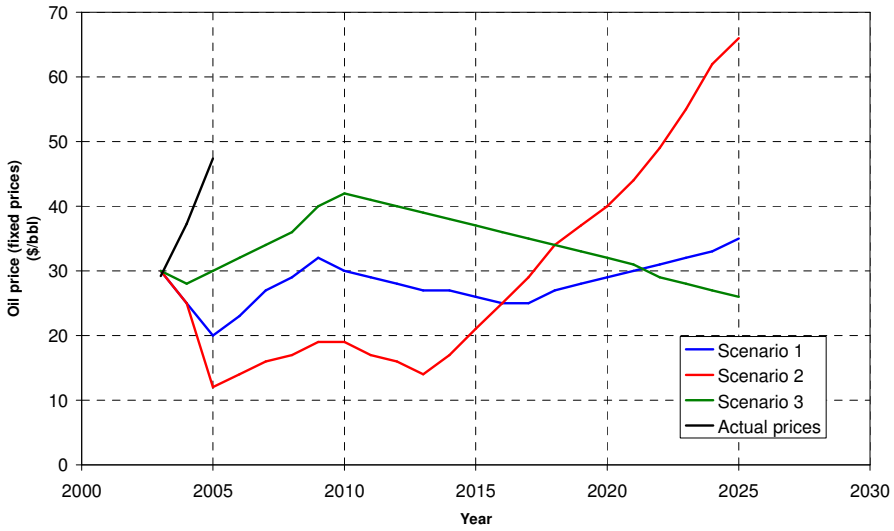

fig. 3-5 Crude oil prices predicted by the scenarios and the actual prices by (IEA 05).[14]

The crude oil price is converted to a price for heavy fuel oil, according to the relation between the two shown in fig. 3-4. When the prices for both fuel oil and gas are converted to €/GJ the prices follow the curves in fig. 3-6.

[14] The prices are average prices, and therefore the peak prices of more than 60 US$ pr barrel that occurred several times during 2005 are not shown.

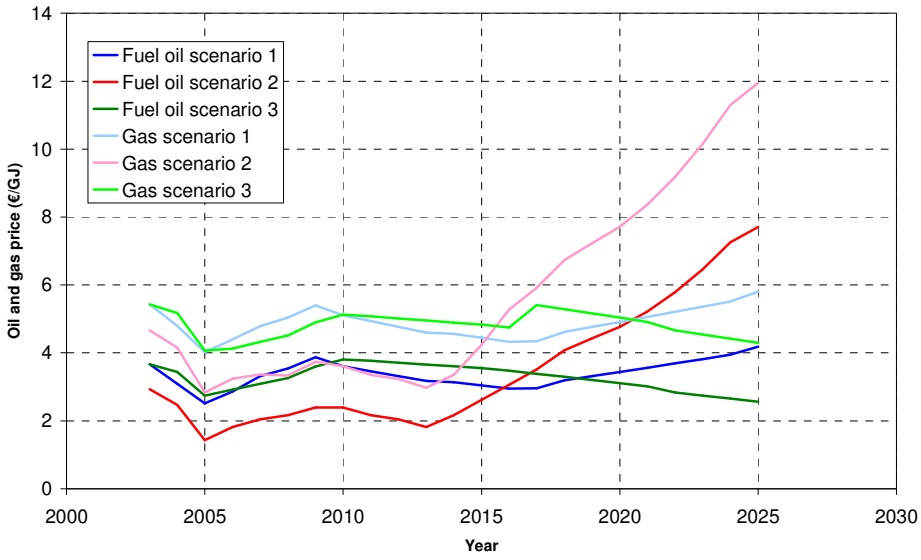

fig. 3-6 Oil and gas prices from the scenarios converted to €/GJ.
Note that the gas price includes transmission fees.

These prices are used as fuel prices in the optimisation; note that the prices shown here do not include taxes.

Taxation

The general company tax is set to 35% based on EU-average according to (Skatteministeriet 00), and is considered to be fixed for the entire time period. The taxation of energy products and electricity is based on the minimum requirements set down by (European Union 03); the following minimum taxes are to be enforced in all member states in 2007, though some exemptions do exist, see table 3-1.

table 3-1 Taxation of energy products and electricity in the EU from 2007

Energy product	EU minimum taxation
Natural gas (€/GJ HHV)	0.15
Heavy Fuel Oil (€/tons)	15.00
Electricity (€/MWh)	0.50

In addition it might be necessary to apply a either a CO2-tax or fee, which reflects the price of the CO2 due to the Kyoto-protocol. For the sake of simplicity, tt has been chosen not to include this into the economic model.

Wages for operators

Wages for operators at chemical plants are based on the statistical data from (Eurostat 00), and shown in fig. 3-7.

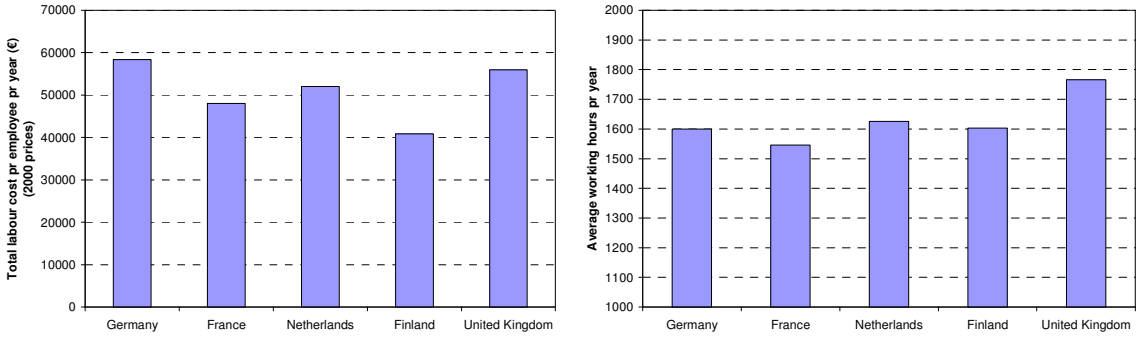

fig. 3-7 Labour cost and working hours in the chemical industry, for a number of northern European countries (Eurostat 00). Note that the cost is in 2000 prices.

Even though there are significant regional differences in the cost, it is chosen to use a simple average cost of 51000 €/year and a standard working year of 1600 hours.

It is assumed that the labour cost will be inflated by the general inflation.

Investment costs

The investment costs in chemical plants have been tracked by the Chemical Engineering magazine (Chemical Engineering 05), as shown in fig. 3-8.

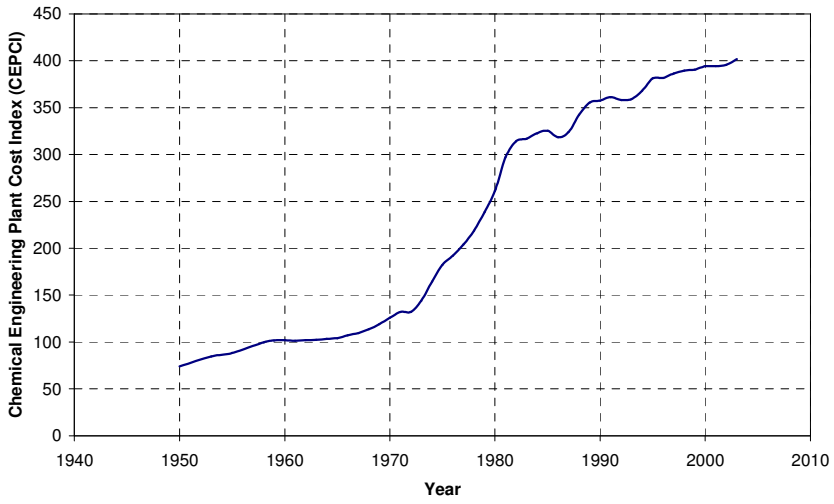

fig. 3-8 The chemical engineering cost plant index for the last 50 years (Chemical Engineering 05)

The cost for the plant will be calculated based on the 2003 index, and inflated by the inflation until 2005 (see fig. 3-2).

3.4 Summary

In this chapter the methodology for integrated design has been proposed. Based on the experience in each of the fields of hierarchical design method it was considered impossible

to include every single aspect of process design in one large problem. Instead it was proposed to include a limited reactor and separation superstructure with the optimisation of the utility system. To make the method general the utility system and the process is still considered different parts of the overall system, but the interaction between the two are described in detail in section 3.2.1. The individual steps of the method are described in detail, and the assumptions required for the model are discussed. Economics as well as modelling plays a central role in formulating the optimisation problem and both are of course bound with uncertainty. In addition the solution process itself might be difficult as the problems are usually non-convex.

Finally the economic modelling used in this work is described, it is based on the net present worth method, and thereby need estimation of investment cost and operating expenses / income for all the years of operation.

To estimate the prices the scenario analysis by (Elsam 03) is used. It is evident that none of the scenarios have foreseen the rise of crude oil prices in the last couple of years. In spite of this significant disagreement the scenarios are anyway used in this work, as price forecasting is not a topic of this work.

4

SYNTHESIS OF UTILITY SYSTEMS

The synthesis of utility system is a major part of the overall methodology; here the detailed models for the utility system are described. The models are based on existing work, but improved in a number of ways. A new set of steam property correlation are developed to ensure that pressure can be selected freely during optimisation. Models for steam- and gas turbines are also developed. The entire superstructure for the utility system is completely connected to the heat integration method. Furthermore the heat integration model is presented, followed by the model for the driver selection.

Synthesis of the utility systems for a chemical process is in itself a major task and has been addressed by several authors, e.g. (Bruno *et al.* 98; Manninen and Zhu 99a; Manninen and Zhu 99b). However, to accommodate the methodology presented in chapter 3, the utility system must now be integrated with the rest of the process, which cannot be completely handled by the existing models. Besides each of the models include a number of shortcomings that it is desirable to address.

For this study, the utility system is limited to considering steam- and gas-turbines, along with steam boilers and heat-recovery-steam-generators (HRSG). The synthesis model lends inspiration from various sources, most of which are improved in this model:

- The superstructure method are derived from (Bruno *et al.* 98)
- The simplified gas turbines models are an improved version of the work by (Manninen and Zhu 99b)
- The steam properties are improved compared to the ones proposed by both (Bruno *et al.* 98), (Mavromatis and Kokossis 98b) and (Manninen 99).
- The heat integration model is an improved version of the one proposed by (Duran and Grossmann 86b)

In this chapter the method and models for synthesis of the utility system is described first (section 4.1). Subsequently an overview of the heat integration model is described (section

4.2); the heat integration model functions as the "glue" between the utility system and the process. Finally, based on the steam turbine and gas turbine models the superstructure for the driver interface is presented (section 4.3).

4.1 Utility system

In this section the model for the utility system is formulated. First the overall utility system is introduced, along with a discussion on the use in combination with integrated design.

Afterwards models for the individual part of the utility system are described, starting out with the steam property prediction (section 4.1.2), followed by models for boiler, condensate/feed water systems, steam turbines, gas turbines and HRSGs (section 4.1.3, 0, 4.1.5, and 4.1.6 respectively).

4.1.1 General consideration and superstructure

In the design of the utility system for this work it is necessary to formulate the utility system within the context of integrated design. Even though the utility system is still considered different from the process (see fig. 3-1), it is important that it can be designed simultaneously with the rest of the process, and all the interfaces between the process and the utility system must be taken into consideration.

The heat integration serves as the interface for heat transfer between the process and the utility system. From a general viewpoint it is desirable that the utility system can both supply and receive heat from the heat integration. Hereby excess heat from the process can be put to use in the utility system, and heat deficits in the process can be properly supplied from the utility system. Thus almost the entire heat transfer area in the utility system is considered part of the heat integration.

The selection of steam turbines needs to match the driver interface. Thus, the utility system must include various combinations of steam turbines to supply mechanical and electric energy to both the process and the electricity grid, or if needed buy electricity.

Based on these considerations the superstructure for the utility system that has been used in this work is shown in fig. 4-1.

The superstructure includes three different pressure headers[15] (HP, MP and LP) and a condensing pressure level, which is only used by the steam turbines. Steam can be generated at each pressure level using a boiler and/or a heat recovery steam generator.

[15] More pressure levels can be added without difficulty.

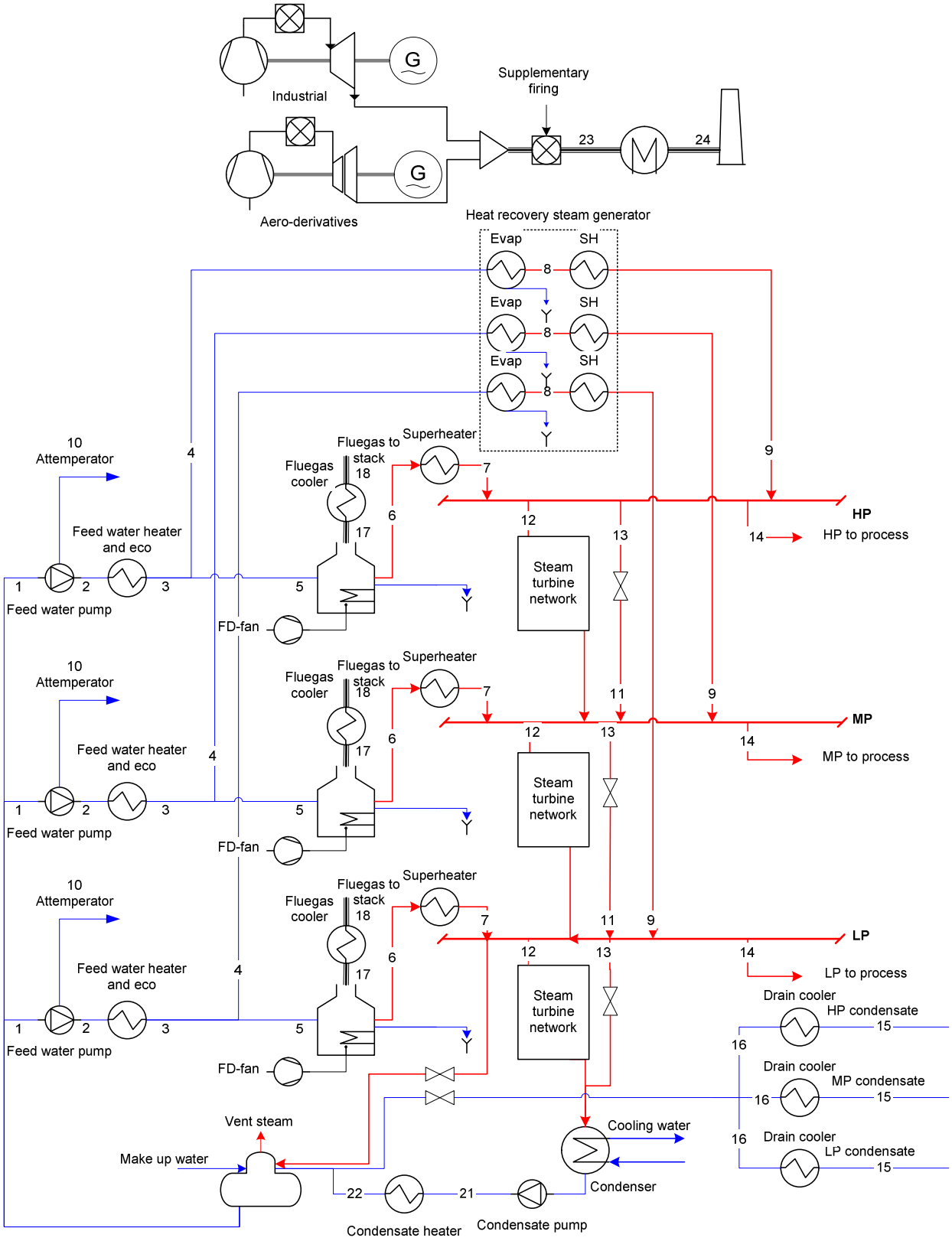

fig. 4-1 Superstructure for the utility system

Heat integration is a very important part of this superstructure formulation, since almost all streams are considered either hot or cold streams, instead of belonging to a specific device.

For example the heat recovery steam generator is made up of six cold streams, three isothermal streams for evaporators to each level and three superheaters, one for each level. None of these streams are bound to obtain heat from the gas turbine exhaust gas, but might just as well be heated by any other hot stream in the associated process. It is also seen that the high pressure feed water heating and the economising sections are considered as just one cold stream for each pressure level. Thus, there is no constraint on the way that feed water heating and economising takes place; it is up to the heat integration with the process to establish the optimal heat recovery system.

The work requirements by both the process and the utility system itself can be met by either steam turbine drives or electric drives. The steam turbines and the steam turbine network for selection of turbines are discussed in detail in 4.3.

Before describing the models in detail, the thermodynamic foundation of steam properties are addressed.

4.1.2 Steam properties

In utility systems correct prediction of steam properties is very important, and in general the ideal gas law provides an inadequate formulation of the property data. For instance pressure effects on the enthalpy term are not included in the ideal gas law. Instead the international certified steam properties (IF-97) (Wagner 00) are normally used. However, for this work these correlations are considered to be too non-linear and complicated for practical use in the optimisation. Furthermore, the IF-97 steam properties model the sub- and supercritical regions in great detail, but since the aim is conceptual design for process utility systems, it is not expected that any of the steam boilers will be supercritical. For this reason, a set of simplified properties will be proposed and compared to the IF-97 steam data.

Vapour pressure and saturation conditions

The vapour pressure is estimated from the Antoine equation, but a new set of parameters are generated to fit into the region of interest from 0°C and up to the critical point. The resulting equation

$$\log_{10}\left(p_{sat}\,[bar]\right) = 5.166 - \frac{1721.77}{T_{sat}\,[C] + 233.425} \tag{4.1}$$

This correlation actually fits quite well with the accurate data, as seen in fig. 4-2. The Antoine equation is non-linear, but it is impossible to avoid this. Instead, the non-linearity will be exploited to obtain improved, yet simple data for the enthalpy.

Instead of letting the enthalpy of saturated water depend on temperature alone, we will also include the pressure, which leads to the following curve fit.

$$h_f\left[\frac{kJ}{kg}\right] = 4.145 \cdot T_{sat}\,[C] + 1.142 \cdot p_{sat}\,[bar] + 4.491 \tag{4.2}$$

In fig. 4-3 the function is compared to the IF-97 data and good agreement is observed.

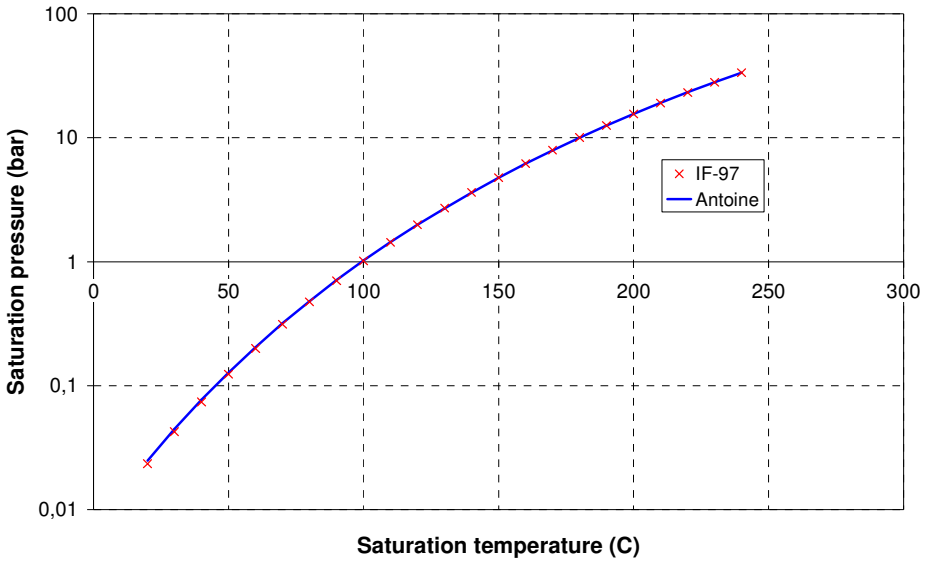

fig. 4-2 Saturation pressure for water/steam

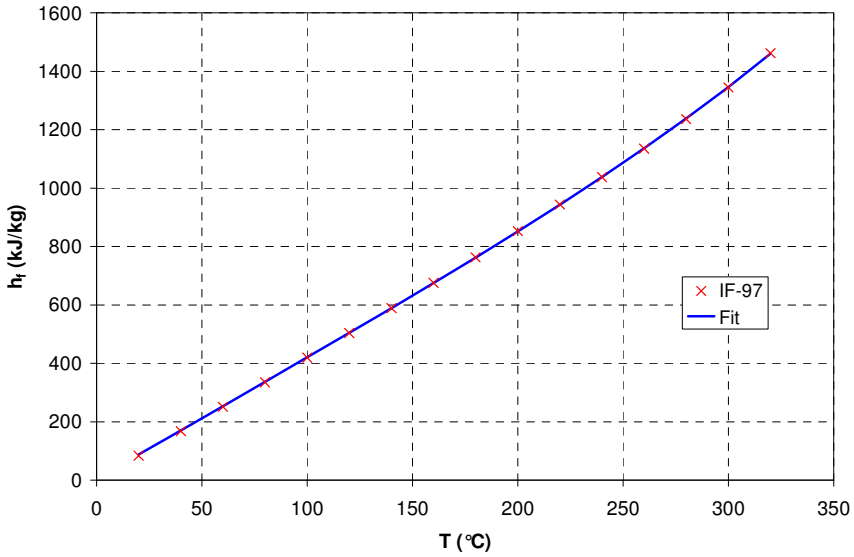

fig. 4-3 Enthalpy of water, comparison between IF-97 data and the correlation in (4.2).

For moderate saturation temperatures, the saturation enthalpy fits reasonably well with the saturation temperature alone.

Often, it will be very useful to know the enthalpy of vaporisation. Once again, the non-linearity from the Antoine equation is exploited to build a linear function.

$$h_{fg}\left[\frac{kJ}{kg}\right] = \text{-}2.566 \cdot T_{sat}\,[C] \text{-}\, 4.024 \cdot p_{sat}\,[bar] + 2517.2\left[\frac{kJ}{kg}\right] \tag{4.3}$$

In fig. 4-4, the correlation is compared to both the IF-97 data and a linear curve fit, based on temperature alone. The correlation fits quite well, even though some deviations occur near the critical point. Still, it is much better than a function of temperature alone.

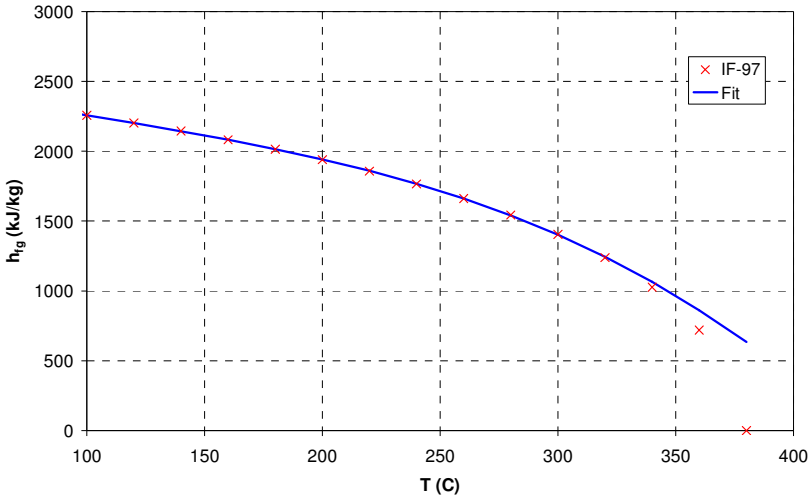

fig. 4-4 Enthalpy of vaporisation plotted against saturation temperature.

A combination of the saturated liquid enthalpy and the enthalpy of vaporisation gives the saturated vapour enthalpy.

Superheated steam

(Manninen 99) proposed a simplified formulation of the enthalpy in the superheated region.

$$T = 2.833p^2 + 6.562 \cdot 10^{-5}h^2 - 6.891 \cdot 10^{-4}h \cdot p - 307 \tag{4.4}$$

From fig. 4-5 it is obvious that there are significant deviations in the entire region; moreover, it is also inconsistent at the interface to the two-phase region.

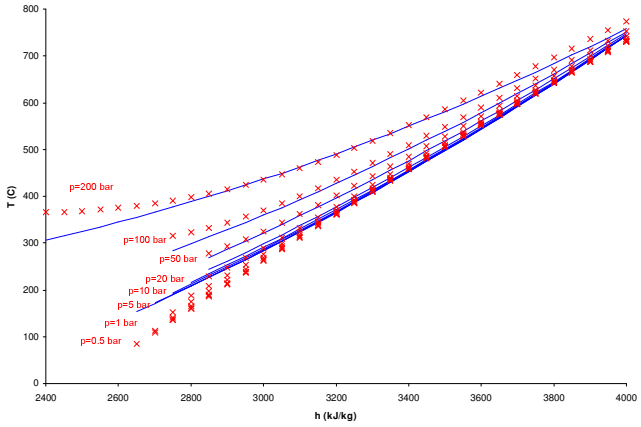

fig. 4-5 Temperature as function of enthalpy and pressure in the superheated region.

(Bruno *et al.* 98) proposed to formulate a specific correlation for the enthalpy at every fixed pressure header. In the present model the pressure is free, and therefore this approach is also inadequate.

Instead a new formulation is proposed based on the formulation by (Hellmann and Grossman 96). The formulation is given as

$$\Delta h_{sh} = \Delta T_{sh}\left[(a_0 + a_1 p_{sat}) + b_1 (T_{sat} + T)\right] + \left(1 - \exp\left(\frac{-\Delta T_{sh}}{d}\right)\right)\sum_{i=0}^{4} c_i T_{sat}^{i} \qquad (4.5)$$

As for the formulas above units are in (°C), (bar) and (kJ/kg), respectively. Compared to the original formulation by (Hellmann and Grossman 96) some higher order terms are removed. The parameters for the equation are given in table 4-1.

table 4-1 Coefficients for the correlation in equation (4.5)

$\mathbf{a_0}$	$\mathbf{a_1}$	$\mathbf{b_1}$	**d**	
1.611	0.05472	3.383×10^{-4}	45.00	
$\mathbf{c_0}$	$\mathbf{c_1}$	$\mathbf{c_2}$	$\mathbf{c_3}$	$\mathbf{c_4}$
1708.0	−16.99	0.06275	-1.025×10^{-4}	6.351×10^{-8}

The formulation is compared with the IF-97 data as shown in fig. 4-6, and it is clear that for pressures up to 150 bar it gives very good results, with less than 5% error.

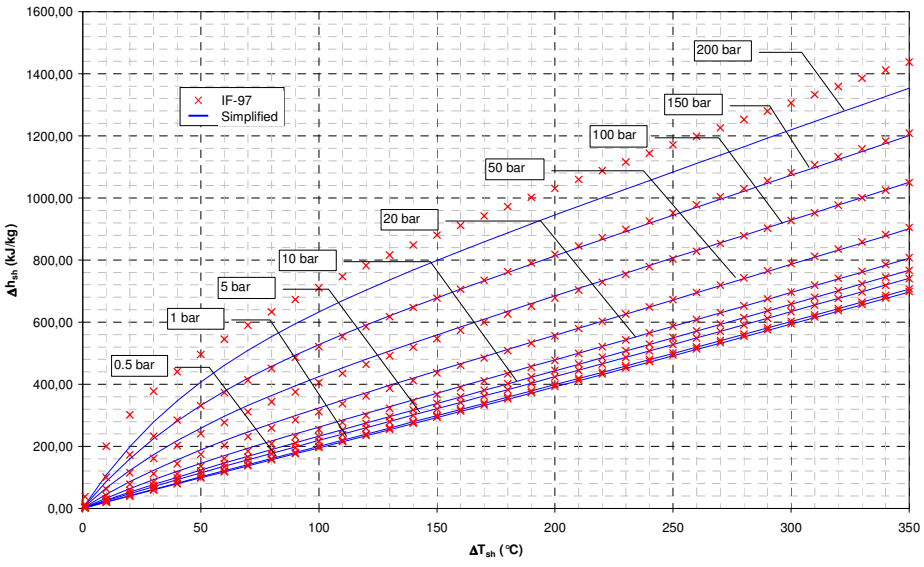

fig. 4-6 Comparison of the simplified Hellmann formulation and the IF-97 data.

The above formulation constitutes a sound formulation for the steam property data, well below the critical point.

Discussion of steam properties

The above formulation allows for calculation of enthalpy-temperature-pressure relations for steam data. Especially for the superheated region the formulation is much more precise than the correlations that have previously been used in optimisation. Please note that only the enthalpy has been addressed here, whereas the entropy is in this case only used for steam turbine, and is discussed in 4.1.4.

4.1.3 Condensate, feed water systems and steam boilers

The feed water- and boiler systems are outlined below. The condensate and feed water preheating systems are usually quite complicated, facilitating both indirect heat exchangers and direct heat exchangers, e.g. deaerators. It is reasonable to assume that the only direct heat exchange will take place in a deaerator, and hence both condensate heaters and feed water preheaters can be considered of the indirect type. Normally it would then be necessary to make a detailed design of the feed water preheating train, but in this case, both condensate heaters and feed water preheaters are considered a set of cold streams that are assigned to the heat integration. The real benefit of including it into the heat integration is that the feed water can both be preheated by steam as well as surplus heat from the process, depending on the process in question. Hereby an optimal integration between process and utilities is ensured. Of course it must be noted that due to practical constraints it might not be desirable to use a certain process stream in the feed water preheating, but for now these issues are not taken into account.

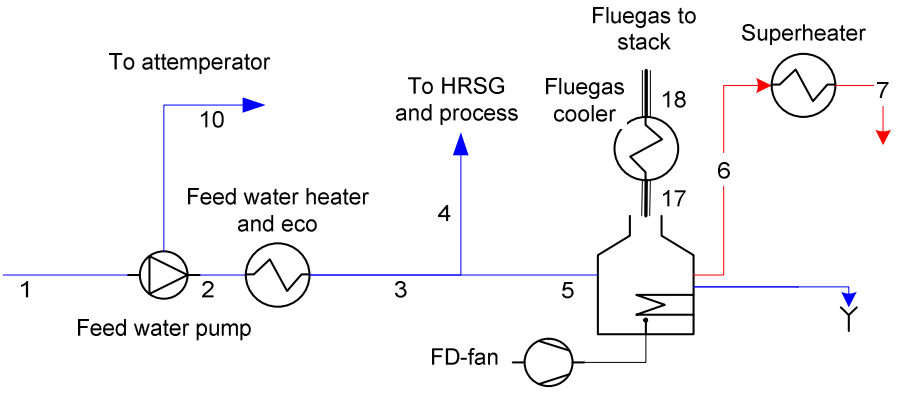

fig. 4-7 Feed water system for a single steam pressure

The boiler is also somewhat different from normal boilers in that it is assumed that the evaporator is placed in the panel walls around the radiation section. On the other hand, the convective part of the boiler is considered to be a set of cold and hot streams. The economiser is a cold stream, and actually included in the feed water preheating, and the steam superheating is also considered a cold stream. The flue gas is considered to be a hot stream. It might very well be that the resulting design of the boiler is somewhat impractical, but it is interesting to examine this freedom of integration with the process.

In the following, the disjunctive formulation for the feed water system is presented. Please note that all redundant variables have been removed from the system of equations, e.g. since $\dot{m}_1 = \dot{m}_2$ only $\dot{m}_1$ is included in the system of equation, which also removes the mass balance equation for the feed water pump. The feed water can be used for two purposes:

- Steam generation in the HRSG or by process waste heat, designated by the boolean variable Y_{HRSG}
- Steam generation in the boiler, designated by the boolean variable Y_{boiler}

If we let the existence of the feed water pump be described by the boolean variable Y_{FWP} the following logical propositions for the feed water system can be formulated

$$\begin{aligned} &Y_{HRSG} \vee Y_{boiler} \Rightarrow Y_{FWP} \\ &\neg Y_{HRSG} \wedge \neg Y_{boiler} \Leftrightarrow \neg Y_{FWP} \end{aligned} \tag{4.6}$$

This can be formulated in terms of binary variables as

$$\begin{aligned} &Y_{HRSG} \vee Y_{boiler} \Rightarrow Y_{FWP} \quad \Leftrightarrow \\ &\left(\neg Y_{HRSG} \wedge \neg Y_{boiler}\right) \vee Y_{FWP} \quad \Leftrightarrow \\ &\left(\neg Y_{HRSG} \vee Y_{FWP}\right) \wedge \left(\neg Y_{boiler} \vee Y_{FWP}\right) \quad \Leftrightarrow \\ &\begin{cases} 1 - y_{HRSG} + y_{FWP} \geq 1 & \Leftrightarrow \quad y_{FWP} - y_{HRSG} \geq 0 \\ 1 - y_{boiler} + y_{FWP} \geq 1 & \Leftrightarrow \quad y_{FWP} - y_{boiler} \geq 0 \end{cases} \end{aligned} \tag{4.7}$$

In the second logical proposition, it actually turns out that only one side of the implication is necessary, since the other is covered by the first logical proposition.

$$\begin{aligned} &\neg Y_{HRSG} \wedge \neg Y_{boiler} \Leftrightarrow \neg Y_{FWP} \quad \Leftrightarrow \\ &\neg\left(\neg Y_{HRSG} \wedge \neg Y_{boiler}\right) \vee \neg Y_{FWP} \wedge Y_{FWP} \vee \left(\neg Y_{HRSG} \wedge \neg Y_{boiler}\right) \quad \Leftrightarrow \\ &\left(Y_{HRSG} \vee Y_{boiler}\right) \vee \neg Y_{FWP} \wedge Y_{FWP} \vee \left(\neg Y_{HRSG} \wedge \neg Y_{boiler}\right) \\ &\Rightarrow y_{HRSG} + y_{boiler} + 1 - y_{FWP} \geq 1 \quad \Leftrightarrow \quad y_{HRSG} + y_{boiler} - y_{FWP} \geq 0 \end{aligned} \tag{4.8}$$

Feed water pump

If we let the boolean variable Y_{FWP} designate the existence of the feed water pump the following disjunctive model can be formulated

$$\begin{bmatrix} Y_{FWP} \\ \dot{W}_{FWP} = \dfrac{\dot{m}_1 \left(p_2 - p_1\right)}{\eta_s \rho} \\ \dot{W}_{FWP} + \dot{m}_1 \left(h_1 - h_2\right) = 0 \\ C_{GR}^{pump} = \dfrac{C_{cepci}}{382}\left[1.18\left(1.8 + 1.51 f_M f_p\right) + 0.35\left(1.8 + 1.51\right)\right] 3878.8 \dot{W}^{0.3656} \\ \dot{m}_1 \geq \dot{m}_{min} \end{bmatrix} \vee \begin{bmatrix} \neg Y_{FWP} \\ \dot{W}_{FWP} = 0 \\ \dot{m}_1 = 0 \\ C_{GR}^{pump} = 0 \end{bmatrix} \tag{4.9}$$

The isentropic efficiency, η_s , is assumed constant.

Splitter to HRSG and process

If we let the boolean variable Y_{HRSG} designate the existence of the steam level in the HRSG the following disjunctive model can be formulated for the splitter

$$\begin{bmatrix} Y_{HRSG} \\ \dot{m}_1 - \dot{m}_4 - \dot{m}_5 = 0 \end{bmatrix} \quad \vee \quad \begin{bmatrix} \neg Y_{HRSG} \\ \dot{m}_4 = 0, \dot{m}_1 = \dot{m}_5 \end{bmatrix} \tag{4.10}$$

Feed water heater and economizer

For the combined feed water heater and economizer we have the following disjunction

$$\begin{bmatrix} Y_{boiler} \vee Y_{HRSG} \\ \dot{Q}_{eco} + \dot{m}_1 \left(h_2 - h_f \right) = 0 \end{bmatrix} \quad \vee \quad \begin{bmatrix} \neg Y_{boiler} \wedge \neg Y_{HRSG} \\ \dot{Q}_{eco} = 0 \end{bmatrix} \tag{4.11}$$

Note that we have assumed that the feed water is at saturation condition at the outlet of the economiser. This will most likely not be the case in real life, and as a consequence, a certain margin is included.

Boiler evaporative system

For the evaporator in the boiler the following disjunctions are formulated

$$\begin{bmatrix} Y_{boiler} \\ \left(1 + AF_{boiler}\right) \dot{m}_{fuel} c_{p,FG} \left(T^{FG}_{flame} - T_{17} \right) - \dot{m}_6 h_{fg} = 0 \\ \dot{m}_6 = 0{,}97 \dot{m}_5 \\ \dot{m}_5 \leq \dot{m}^{boiler}_{max} \\ T_{sat} + 50 \leq T_{17} \leq 1500 \end{bmatrix} \quad \vee \quad \begin{bmatrix} \neg Y_{boiler} \\ \dot{m}_{fuel} = 0 \\ \dot{m}_6 = \dot{m}_5 = 0 \end{bmatrix} \tag{4.12}$$

Note that the flue gas is assumed to be at least 50°C higher than the steam temperature at the exit of the evaporative part of the boiler; normally the flue gas temperature is much higher. Nevertheless is it chosen to use this constraint in order to give as much freedom to the optimisation as possible.

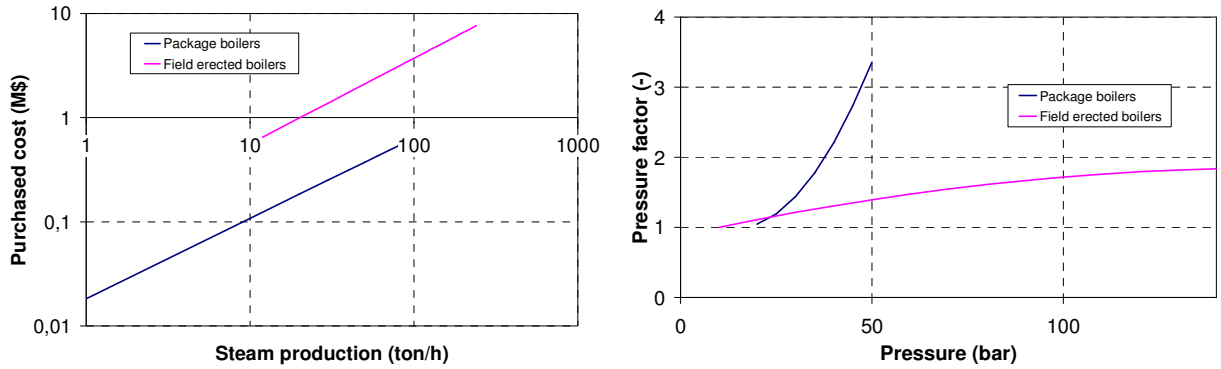

fig. 4-8 Purchased cost and pressure correction for boilers, according to (Turton et al. 98).

Small boilers can be purchased as package boilers, which are assembled at the manufacturer and delivered as a complete package at the site. Larger boilers must be erected on the site, which is more expensive. In fig. 4-8 the price estimates for the two different boilers are plotted next to the pressure correction for the cost.

The boiler cost functions includes the cost of the boiler and the forced draught fan, it is assumed that the boilers are small enough that no induced draught fans are necessary.

$$\begin{bmatrix} Y_{boiler} \\ C_{GR}^{fan} = \frac{C_{cepci}}{382}\left(1.18 f_p^{fan} f_M^{fan} + 0.35 \cdot 1 \cdot 2.2\right) C_p^{fan} \\ C_{GR}^{boiler} = \frac{C_{cepci}}{382}(1.18 f_p^{boiler} + 0.35) f_{BM}^{boiler} \frac{A}{1.8 \cdot 0.15} \dot{m}_6{}^{B} \end{bmatrix} \quad \vee \quad \begin{bmatrix} \neg\, Y_{boiler} \\ C_{GR}^{fan} = 0 \\ C_{GR}^{boiler} = 0 \end{bmatrix} \tag{4.13}$$

$$C_p^{fan} = \left[0.8184 \left(\frac{AF_{boiler} \dot{m}_{fuel}}{\rho_{air}} \right)^2 + 383.53 \left(\frac{AF_{boiler} \dot{m}_{fuel}}{\rho_{air}} \right) + 2027.4 \right]$$

The air-to-fuel ratio, AF , is calculated by the combustion of a fuel consisting of only carbon, C, and hydrogen, H:

$$\begin{aligned} xC + yH + \lambda\left(x + \frac{y}{4}\right)\left(O_2 + \frac{0.79}{0.21} N_2\right) \quad \rightarrow \\ xCO_2 + \frac{y}{2} H_2O + (\lambda - 1)\left(x + \frac{y}{4}\right) O_2 + \lambda\left(x + \frac{y}{4}\right)\frac{0.79}{0.21} N_2 \end{aligned} \tag{4.14}$$

Hereby the air-to-fuel-ratio (AF) can be found as

$$AF = \frac{\lambda\left(x + \frac{y}{4}\right)\left(1 + \frac{0.79}{0.21}\right) 29 \frac{kg}{kmole}}{x \cdot 12 \frac{kg}{kmole} + y \cdot 1 \frac{kg}{kmole}} \tag{4.15}$$

The constants in the boiler cost functions are all given in table 4-1.

table 4-1 Constants for calculation of boiler capital cost

Boiler	A	B	$F_{p,A}^{boiler,i}$	$F_{p,B}^{boiler,i}$	$F_{p,C}^{boiler,i}$	F_{BM}
Package boiler	18348	0.77	1.3794	-0.05438	0.001879	1.8
Field erected boiler	85074	0.82	0.8824	0.01214	-0.00003798	1.8

The energy balance and work requirement for the forced draught fan are as follows

$$\dot{W}_{fan} + \dot{m}_{air} c_p^{air} \left(T_{in}^{air} - T_{out}^{air}\right) = 0 \tag{4.16}$$

And the temperature rise over the fan, can be calculated assuming ideal gas properties

$$\frac{T_{out}^{fan}}{T_{in}^{fan}} = \left(\frac{p_{out}^{fan}}{p_{in}^{fan}} \right)^{\frac{\gamma-1}{\gamma \eta_s^{fan}}} \tag{4.17}$$

It is assumed that the forced draught fan will be driven by an electric motor.

Steam superheating

For superheating of the steam at the boiler outlet the following disjunction is formulated

$$\begin{bmatrix} Y_{boiler} \\ \dot{Q}_{SH} + \dot{m}_6 \left(h_g - h_7 \right) = 0 \\ T_7 = f\left(h_7 \right) \end{bmatrix} \quad \vee \quad \begin{bmatrix} \neg\, Y_{boiler} \\ \dot{Q}_{SH} = 0 \\ h_7 = h_g \end{bmatrix} \tag{4.18}$$

4.1.4 Steam turbine models

The next issue is the modelling of steam turbines. First the overall model for the turbines is described. Afterwards the prediction of isentropic expansion work and isentropic efficiencies are discussed.

Extraction steam turbines can be decomposed into a number of simple turbines, as shown by (Chou and Shih 87), see fig. 4-9. Therefore it is only necessary to consider the simple turbine.

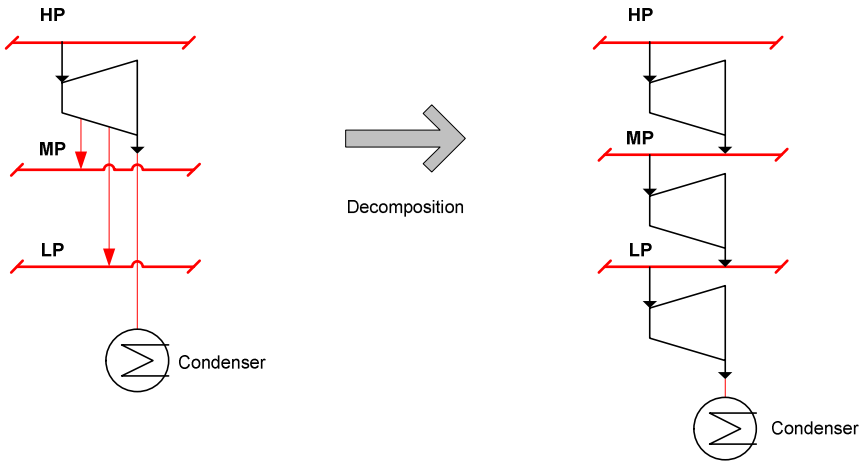

fig. 4-9 Decomposition of an extraction turbine into a set of simple turbines, according to (Chou and Shih 87).

The energy balance for each expansion stage is

$$\dot{W}_t = \dot{m}\left(h_{in} - h_{out} \right) \tag{4.19}$$

The outlet enthalpy can be found from the isentropic efficiency

$$\eta_s = \frac{\Delta h}{\Delta h_s} = \frac{(h_{in} - h_{out})}{(h_{in} - h_{out,s})} \quad ; \quad h_{out,s} = h(s_{in}, p_{out}) \tag{4.20}$$

However, this requires the calculation of the entropy at the inlet, and a correlation of the entropy in the superheated region is thus needed. To avoid this, (Mavromatis and Kokossis 98b) has proposed the following method for prediction of Δh_s in the superheated region

$$\frac{\Delta T_{sat}}{\Delta h_s} = a_1 + a_2 (\Delta h_{sh} + h_{fg}) \tag{4.21}$$

In the figure below the IF-97 data (Wagner 00) for a large range of different expansion conditions are plotted, even though the overall trend is clear, there are still significant deviations.

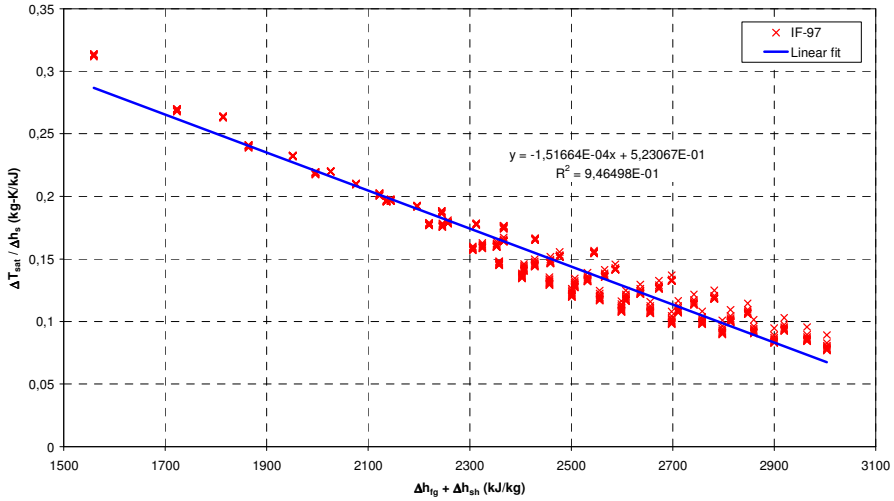

fig. 4-10 Prediction of the isentropic expansion enthalpy compared to the IF-97 data. The data covers a large range. Inlet pressure from 0.5 – 100 bar and outlet pressure from 2-90% of inlet pressure. Superheat at the inlet is varied from 50K to 300K.

Because of the deviations in the model above it is desirable to formulate a new and more precise model. First, it is important to observe that there are significant differences between expansion in the superheat region and in the condensing region. This is both in terms of thermodynamic properties for steam and isentropic efficiencies for the turbines. Therefore, the expansion path is divided into two sub sections, namely superheated and condensing sections.

In the superheated region, a more precise estimate of the isentropic expansion enthalpy is needed, still without having to predict the entropy. Various correlations have been tried, and it is found that Δh_s can be expressed quite precisely as a linear function of the isentropic expansion temperature difference, see fig. 4-11.

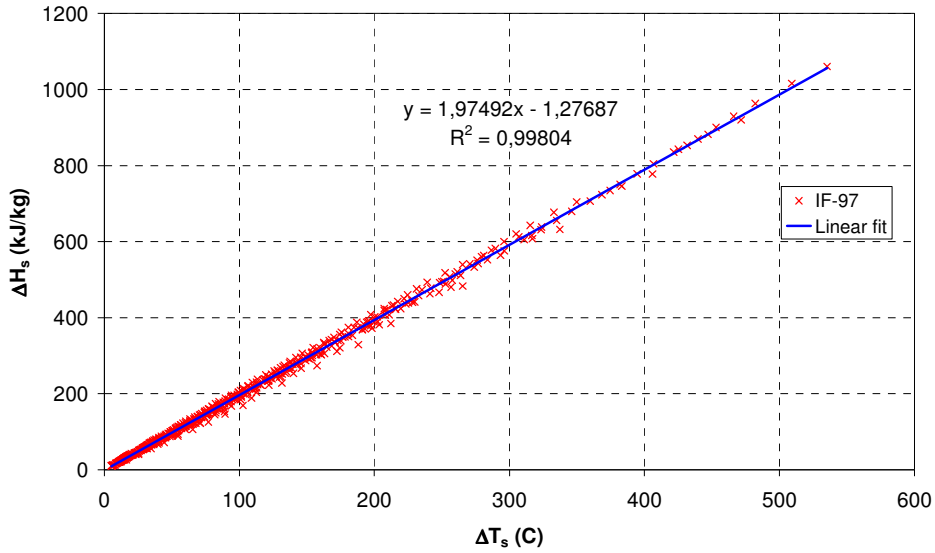

fig. 4-11 the isentropic expansion enthalpy as a function of the isentropic expansion temperature difference.

The isentropic temperature difference can be estimated from the ideal gas law; even though it might seem like a rough estimate, it actually shows very good agreement in superheated region.

$$\left(\frac{p_{out}}{p_{in}}\right)^{\frac{\gamma-1}{\gamma}} = \frac{T_{out,s}}{T_{in}} \tag{4.22}$$

In fig. 4-12 the model is compared to the IF-97 data and good agreement is observed.

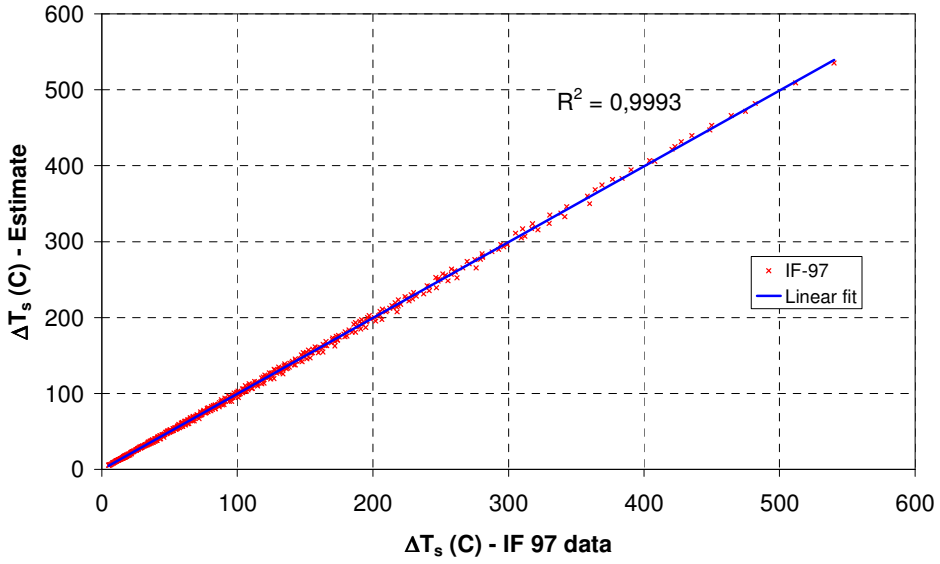

fig. 4-12 Plotting the isentropic expansion temperature difference for different conditions versus the one obtained by equation (4.22).

For the condensing sections, the expansion enthalpy is somewhat more complicated to model, since the data deviates more from the linear approximation. Nonetheless, it has been found that within the region of interest the following simple fit is satisfactory:

$$\begin{aligned}
\Delta h_s &= A + B \cdot T_{sat,in} + C \cdot T_{in} = A + B \cdot T_{sat,in} + C \cdot \left(T_{sat,in} + T_{sh,in}\right) \\
A &= -8.0145 \cdot T_{sat,out} + 222.88 \\
B &= 0.0137 \cdot T_{sat,out} + 3.3437 \\
C &= -0.004 \cdot T_{sat,out} + 0.9682
\end{aligned} \tag{4.23}$$

In fig. 4-13 the correlation are plotted for a number of inlet pressures at an outlet pressure equivalent to 25°C.

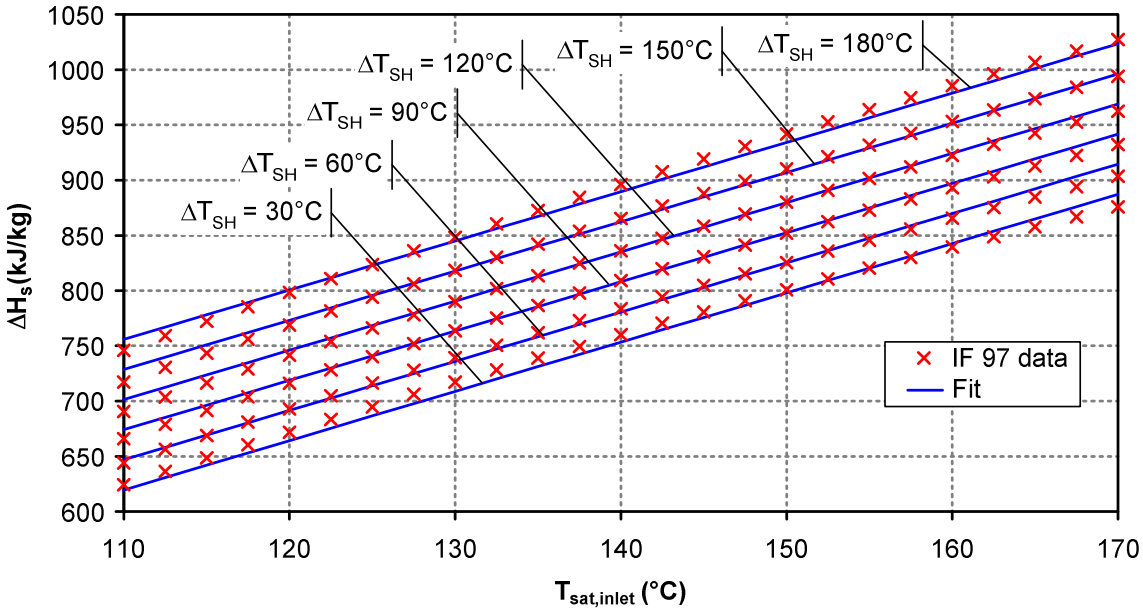

fig. 4-13 The correlation in equation (4.23) compared to the IF-97 data. Plotted for a large range of inlet temperatures and inlet pressures (i.e. saturation temperatures). The outlet pressure is at equivalent to 25°C saturation temperature.

As the outlet pressure is usually fixed by the temperature of the cooling water, the parameters A, B and C are also fixed; thus (4.23) is linear. In appendix 9 a number of plots various outlet pressures can be found.

Hereby the isentropic expansion enthalpy can be estimated both for the superheated and the condensing region. Even though deviations still exist compared to the IF-97 data, it is far superior to the models proposed earlier.

Estimation of isentropic efficiency for back pressure turbines

The design point isentropic efficiency of a steam turbine depends on the design of the turbine, and according to (Spencer *et al.* 63) the performance can be accurately predicted based on the following parameters.

- Volume flow
- Pressure ratio
- Initial pressure and temperature
- Governing stage design (if applicable)
- Exhaust loss
- Leakage flow
- Mechanical and generator losses

It is obvious that the inlet conditions have significant importance as small turbines tend to have a larger relative leakage flow, which lowers the isentropic efficiency. The efficiency is also affected by the outlet conditions, in particular if the steam is wet in the outlet. The exhaust loss is primary of concern for condensing turbines caused by the high annulus velocities at the exit from the last stage.

An estimation procedure can be found in (Spencer *et al.* 63)[16], and even though 40 years old the correlations are still widely used in commercial software like SteamPro (Thermoflow 00) and GateCycle (GE Enter 03). The method is based on a set of highly non-linear functions, why it is desirable to use a simplified method. Furthermore it must be observed the aforementioned method is only applicable for steam turbine larger than 16.5 MW and is only presented for 3600 and 1800 rpm applications. Nevertheless it is often used for prediction of performance at other speeds, e.g. in SteamPro and Gatecycle.

For back pressure turbines a simplified method is proposed by (Mavromatis and Kokossis 98b), where the efficiency is based on:

- Turbine size in terms of power output
- Saturation temperature (i.e. pressure) at the inlet:

The formulation is defined as

$$\frac{\dot{W}_{max}}{\eta_{is}} = A + B\dot{W}_{max} \quad ; \quad A = a_1 + a_2 T_{sat} \quad ; \quad B = b_1 + b_2 T_{sat} \tag{4.24}$$

The coefficients are given in

Turbine size	a_1	a_2	b_1	b_2
< 1.2 MW	-0.131	0.00117	0.9	0.00152
> 1.2 MW	-0.928	0.00623	1.12	0.00047
Averaged	-0.538	0.00364	1.112	0.00052

In fig. 4-14 the functions for isentropic efficiency are plotted for various pressure levels. It is not stated explicitly in the work by (Mavromatis and Kokossis 98b) why there is a

[16] This method is referred to as the SCC-method (Spencer-Cotton-Cannon) in the rest of the text.

significant discontinuity at 1.2 MW, but it might be caused by a change from radial to axial turbines.

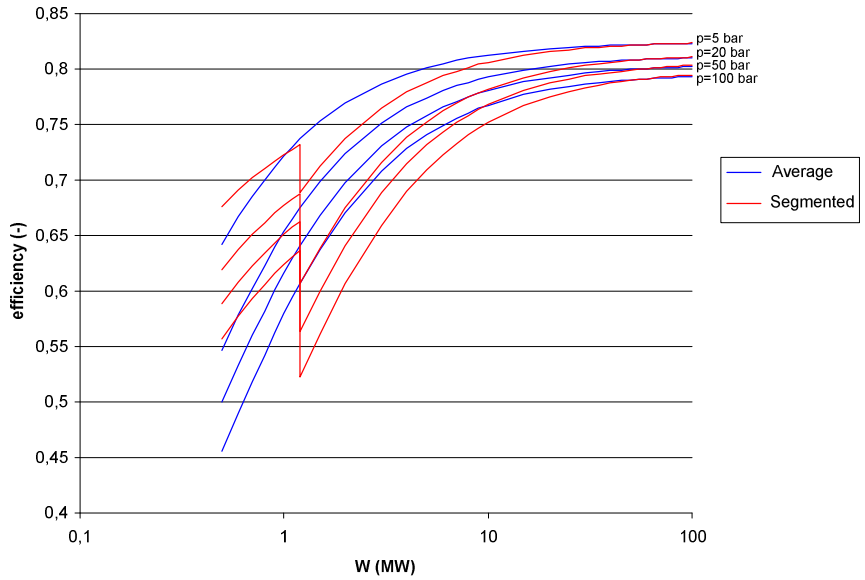

fig. 4-14 Isentropic efficiency as a function of turbine size, at four different pressure levels. Both the averaged model and the segmented model are plotted.

The simplified method does not take the turbine pressure ratio into account, even though it has a significant impact on the efficiency estimate if the SCC-method is applied.

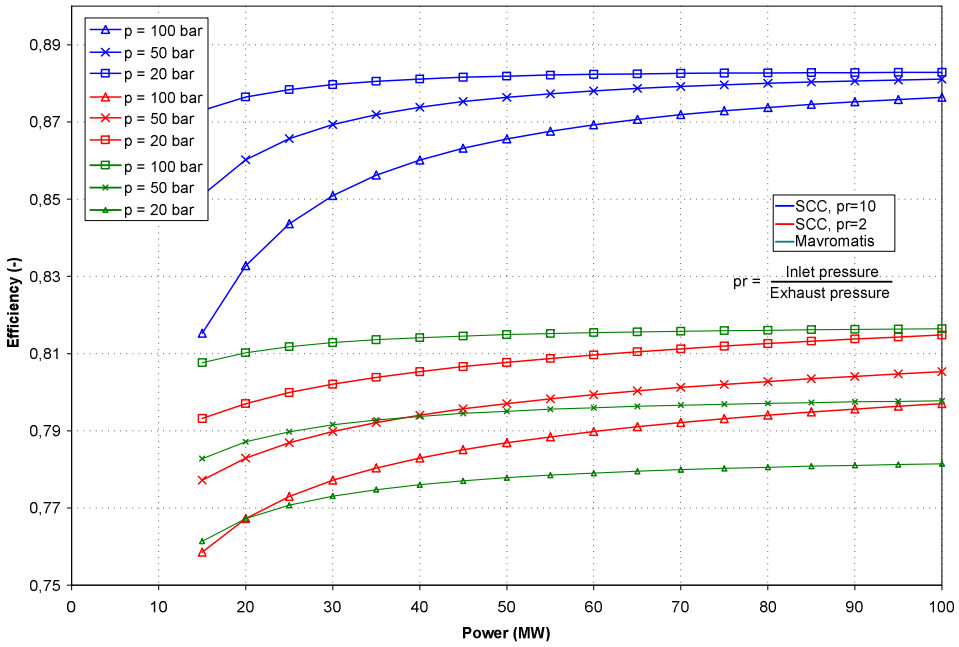

fig. 4-15 Comparison of the isentropic efficiency prediction by the SCC method and the simplified method for various inlet pressures.

Comparison with the simplified method in fig. 4-15 shows that the simplified method provides a conservative estimate, especially when it is noted that the performance prediction by the SCC-method is likely to be 2-4% below the performance of turbines of today (Thermoflow 01). Comparing the simplified formula with data from an actual backpressure turbine at a small CHP-plant (Grue and Bach 00) also shows that the formula is conservative. The turbine has an efficiency of 77% based on plant measurement data, whereas (4.24) predicts an efficiency of 73%.

Estimation of isentropic efficiency for condensing turbines

The efficiency for the condensing section is fundamentally based on the same correlation, but is corrected for the steam wetness and outlet losses. For condensing turbines the velocity at the exhaust is typically quite high, and since kinetic energy is not recovered for work purposes the apparent efficiency of the turbine decreases as a function of the exhaust velocity. In addition, the efficiency also decreases as a function of the moisture content at the turbine exhaust; this is due to the formation of water droplets, which do not follow the streamlines of the steam flow. The expansion line construction for a condensing turbine must include the exhaust loss as outlined in the mollier-chart in fig. 4-16.

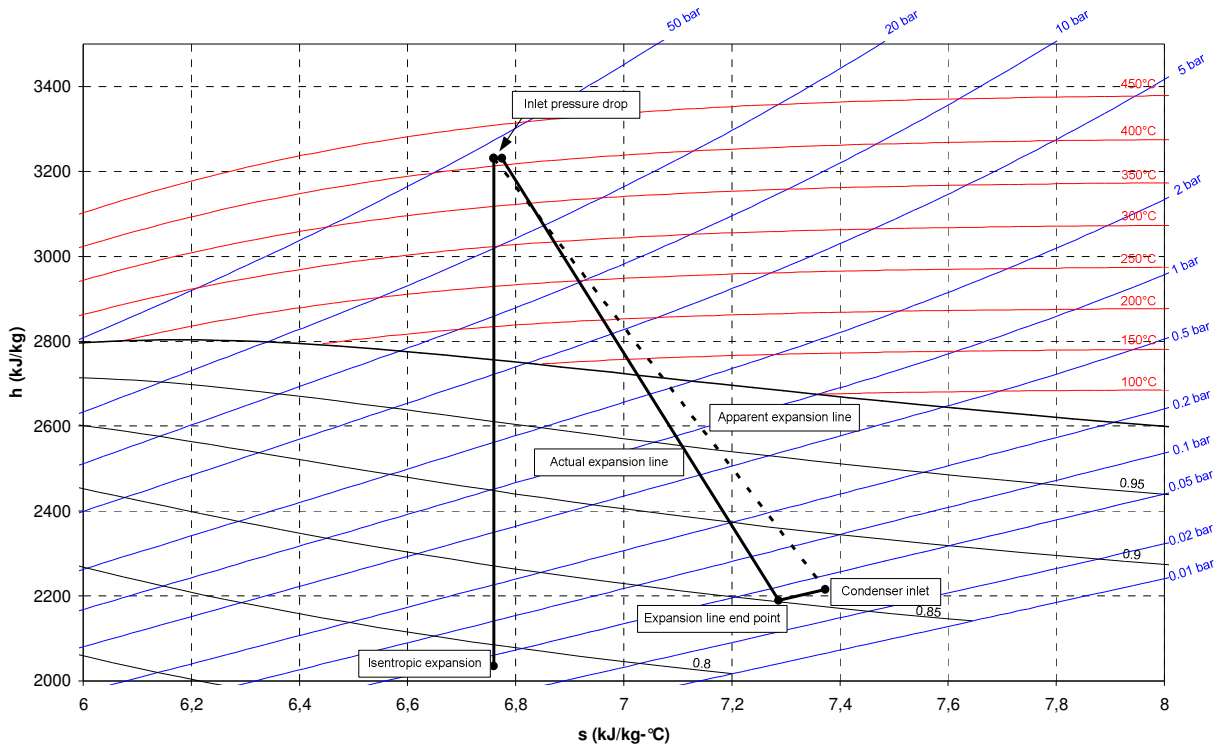

fig. 4-16 Expansion path for condensing turbine. Note the difference between the state at the outlet of the last stage (expansion line end point) and the inlet to the condenser.

The exhaust loss for a number of different turbine configurations is shown in fig. 4-17, along with an outline of the typical region for the design point. The turbine is normally not designed at the minimum exhaust loss is a trade-off between design-point efficiency and

part-load efficiency. If a turbine were designed at the minimum exhaust loss at the design flow, a very significant exhaust loss would occur even at moderate part-load.

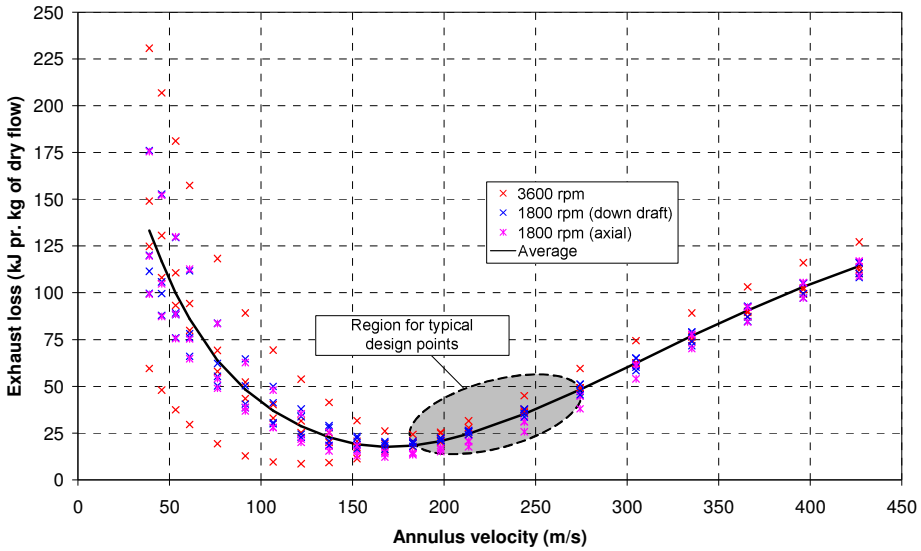

fig. 4-17 Exhaust loss prediction by the SCC-method, all the data are found in (Spencer et al. 63). Furthermore the region for typical design points is shown.

The overall efficiency is shown in fig. 4-18. This includes both the efficiency of the expansion and the exhaust loss.

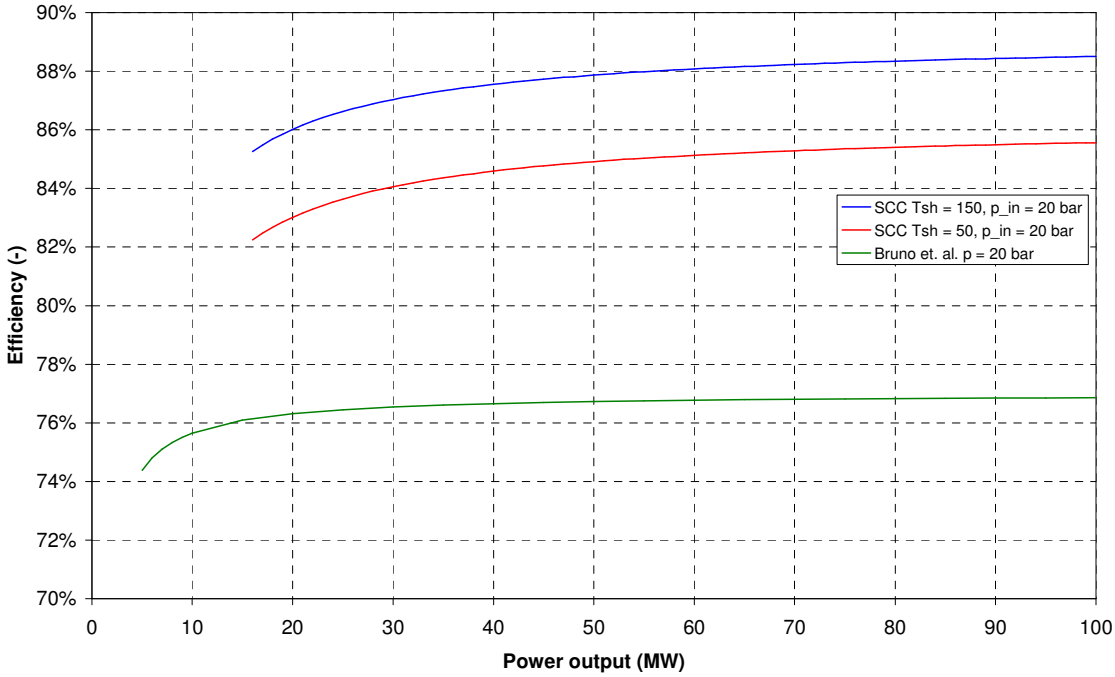

fig. 4-18 Comparison of efficiencies for condensing steam turbines by the SCC method and the method by (Bruno et al. 98). Note that the efficiencies by the SCC method includes exhaust loss

The SCC method depends on the inlet temperature, since this affect the wetness at the exhaust. Therefore the efficiency is shown for different degrees of superheat at the inlet. The model by (Bruno *et al.* 98) seems to make a significant underestimation of the efficiency. It has nonetheless still been chosen to use this method, as the SCC method is considered too complicated for use in the optimisation for the condensing sections. It is thus likely that condensing turbines will be deselected more often than necessary.

4.1.5 Gas turbine models

Unlike most other process equipment, gas turbines are only available in discrete sizes, although more than 100 different machines are available on the market.

For modelling purposes, it seems reasonable to differentiate between industrial gas turbines and aero derivatives. The former are heavy duty single shaft machines whereas the latter are modified twin shaft aircraft engines. Typically, the aero derivatives have higher efficiency and are more expensive than the industrial gas turbines. Consequently, the exhaust gas from aero derivatives often has lower temperature and oxygen content, which limits the potential level of supplementary firing.

In the design of utility systems along with optimisation of the process plant, only a rough estimate of the power requirements might be known. Furthermore, it might be feasible to use gas turbines for covering the entire requirement, only part of it or nothing at all. In principle, this requires an enormous superstructure including all the gas turbines that might be used in this utility system; it is obvious that the approach will be both cumbersome and computationally expensive (if solvable at all). To overcome this problem the pre-screening methods by (Manninen and Zhu 99b) can be used in the preliminary phase of flowsheet generation. In this method, a gas turbine is considered as a continuously scaled unit. In order to create a correlation for gas turbines manufacturer data for 83 industrial gas turbines and 87 aero-derivatives were collected. All data is provided at ISO-conditions, that is, inlet conditions of 15°C at sea level and a relative humidity of 60%. The data were obtained directly from the manufacturers (Alstom 03; GE 03; Mashproekt 03; Mitsubishi 03; Pratt and Whitney 03; Rolls Royce 03; Vericor 03). The price estimations were obtained from (Thermoflow 00).

Industrial gas turbine models

In fig. 4-19 fuel consumption (in kW based on LHV), exhaust gas flow and exhaust gas temperature are all correlated to the power output. Both fuel consumption and exhaust gas flow correlates quite good, even with linear models. On the other hand, the exhaust gas temperature does not really show any correlation with any parameter. This is also observed in the work by (Manninen and Zhu 99b). Instead it is obviously far better to calculate the exhaust gas heat content as a function of the power output, which exhibits much better agreement.

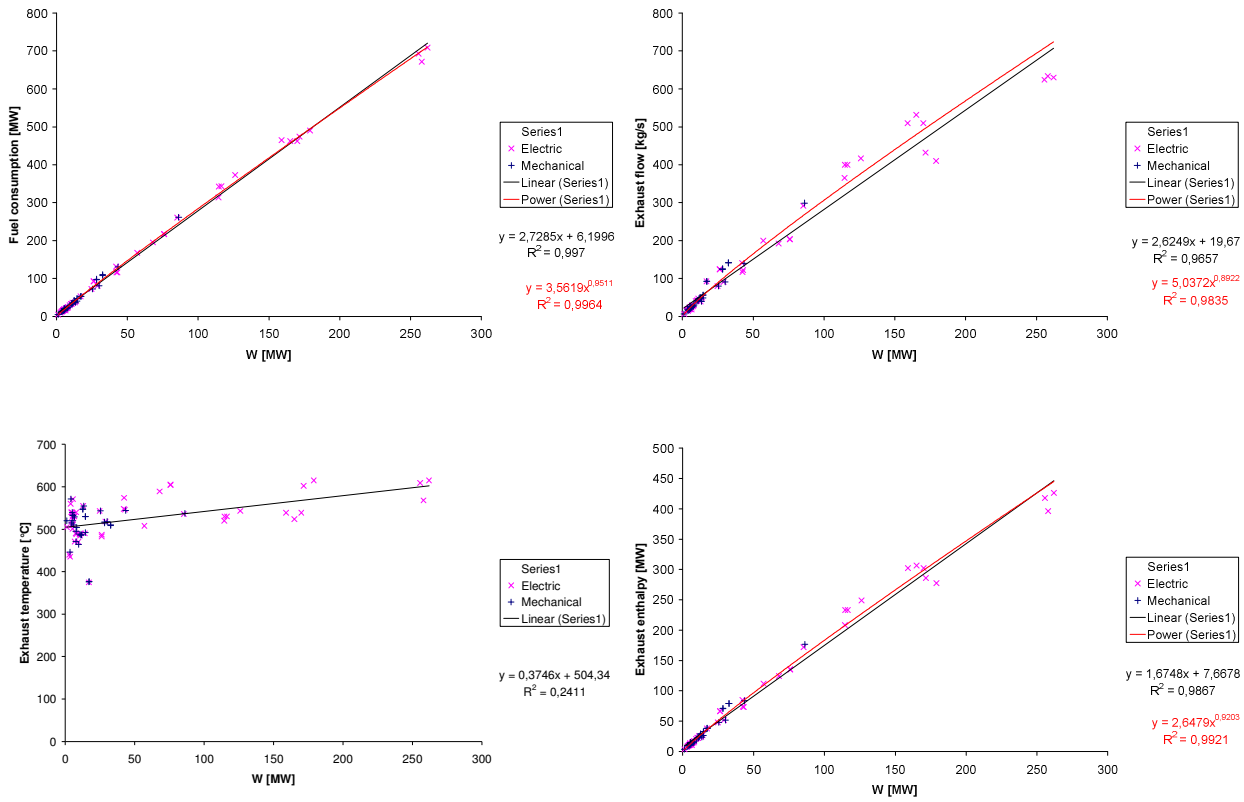

fig. 4-19 Modelling of industrial gas turbines based on manufacturer data at ISO-conditions.

A closer examination of the industrial gas turbines reveals that several manufacturers provide very large gas turbines with high efficiencies, primarily for power generation in combined cycles. These gas turbines, even though still single shafted, have high efficiencies and generally do not fit into the overall definition of industrial gas turbines. In many cases, however, it would be obvious that 150 MW or more power will not be needed, and therefore a reduced space with more accurate correlations can be used, see fig. 4-20. Here the correlation for the investment price is also shown.

Aero derivative models

The models for the aero-derivative gas turbines are also based on manufacturer data at ISO-conditions. As for industrial gas turbines, it is far better to base the exhaust flow condition on the heat content instead of the temperature. The correlations for the aero-derivative turbines are shown in fig. 4-21.

With these correlations, it is possible to make an overall model for both aero-derivative gas turbines and industrial gas turbines. Details and larger charts are found in appendix 12.

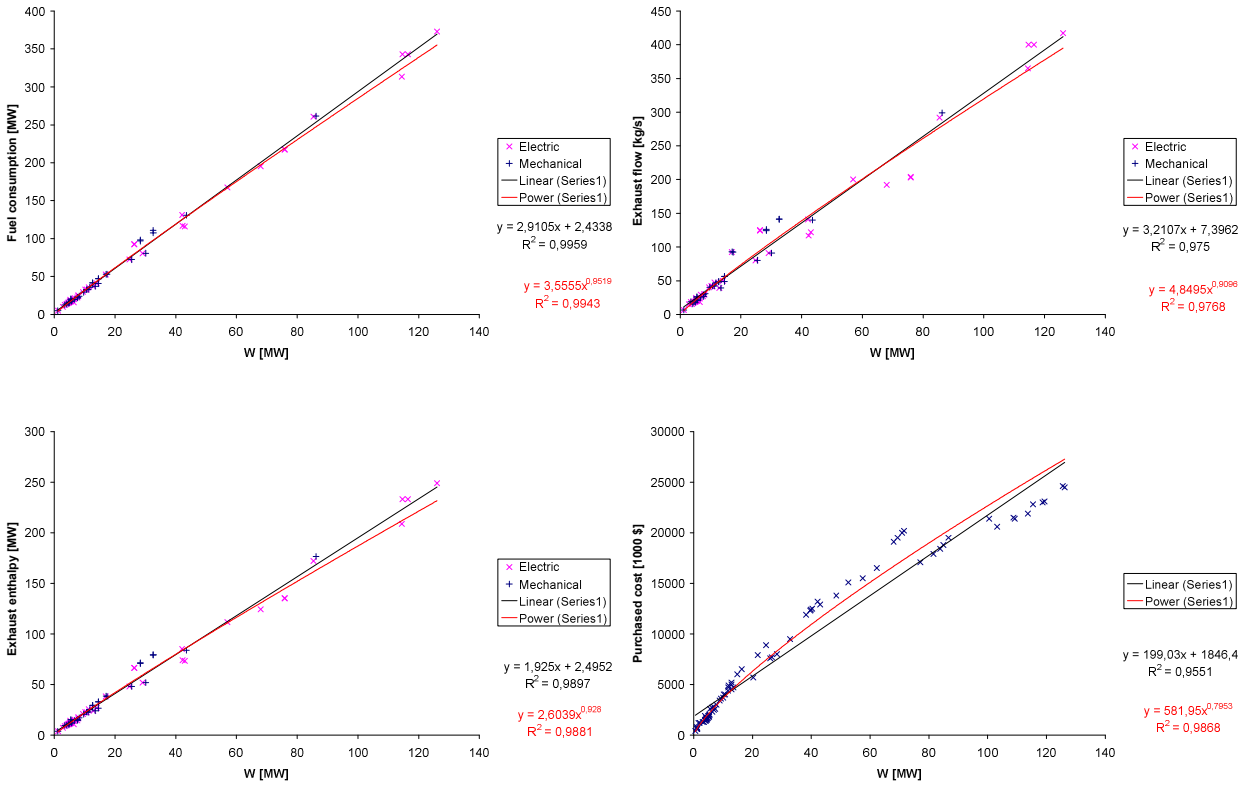

fig. 4-20 Industrial gas turbine correlation, for power output below 150 MW.

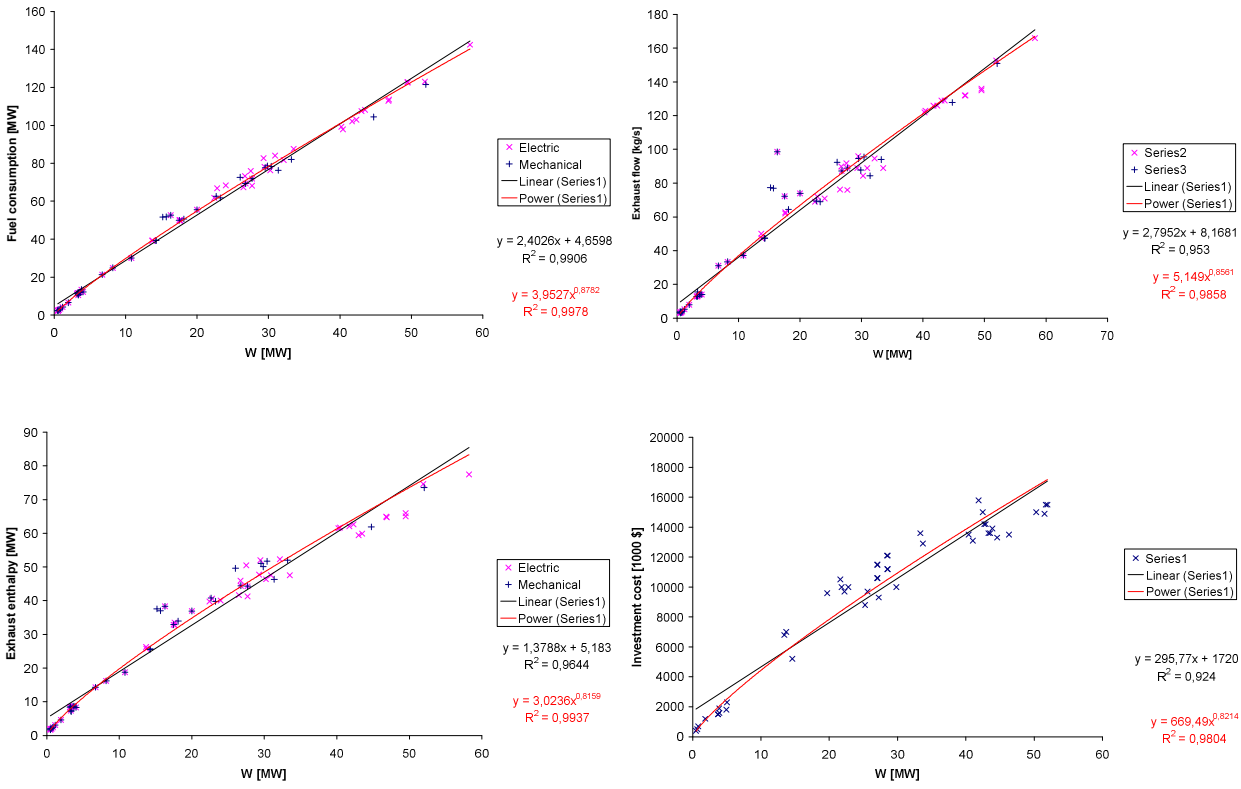

fig. 4-21 Models for aero-derivative gas turbines.

4.1.6 Heat recovery steam generator

The heat-recovery-steam-generator (HRSG) is used to raise steam from the heat of the exhaust gas from the gas turbine or any other available hot stream in the process flow sheet. For a complete integration between the systems the HRSG is consequently modelled as just another set of streams in the heat integration model.

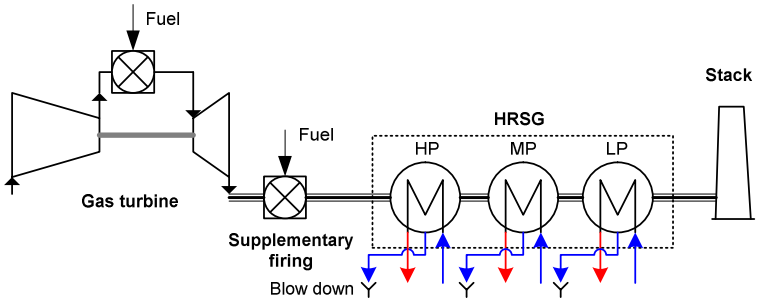

fig. 4-22 Gas turbine with supplementary firing and heat recovery steam generator.

On the other hand it might in some situations be desirable to design a utility system, which is not completely integrated with the process plant. For this purpose a more traditional HRSG must be modelled, where the exhaust gas from the gas turbine is used to raise steam; this is outlined in fig. 4-22.

For a HRSG with only one pressure level the design of the heat transfer area is fairly simple, but when multiple pressure levels are present the design depends on the relative flow in the different pressure levels and the degree of superheat for each pressure level. In the flowsheet optimisation phase, blowdown is required and it is assumed that the blowdown water is at saturation conditions, i.e. blowdown from the steam drum.

In the modelling of the HRSG it is assumed that the heat exchanger surfaces are coupled to provide the optimal cooling curve, i.e. the one that is obtained if pinch analysis is used on the HRSG, see fig. 4-23. In this figure it is also shown that the pinch point can only be located at 5 different locations (number of steam levels + one for inlet and one for final outlet). It cannot be ruled out that in some rare cases the pinch point will actually be located at a position along the "superheating" parts of the curves; but for all practical purposes it seems reasonable to neglect this option, and still if it happens it will appear as a pinch violation, which can easily be identified by inspection of the curves.

Each steam level can be divided into three sections, i.e. economising, evaporating and superheating. The energy balance for each of these sections is:

$$\begin{aligned} \dot{Q}^i_{eco} &= \dot{m}^i_{in}\left(h^i_f - h^i_{in}\right) && \forall i \in \{HP, MP, LP\} \\ \dot{Q}^i_{evap} &= \dot{m}^i_{out} h^i_{fg} && \forall i \in \{HP, MP, LP\} \\ \dot{Q}^i_{SH} &= \dot{m}^i_{out}\left(h^i_{out} - h^i_g\right) && \forall i \in \{HP, MP, LP\} \end{aligned} \tag{4.25}$$

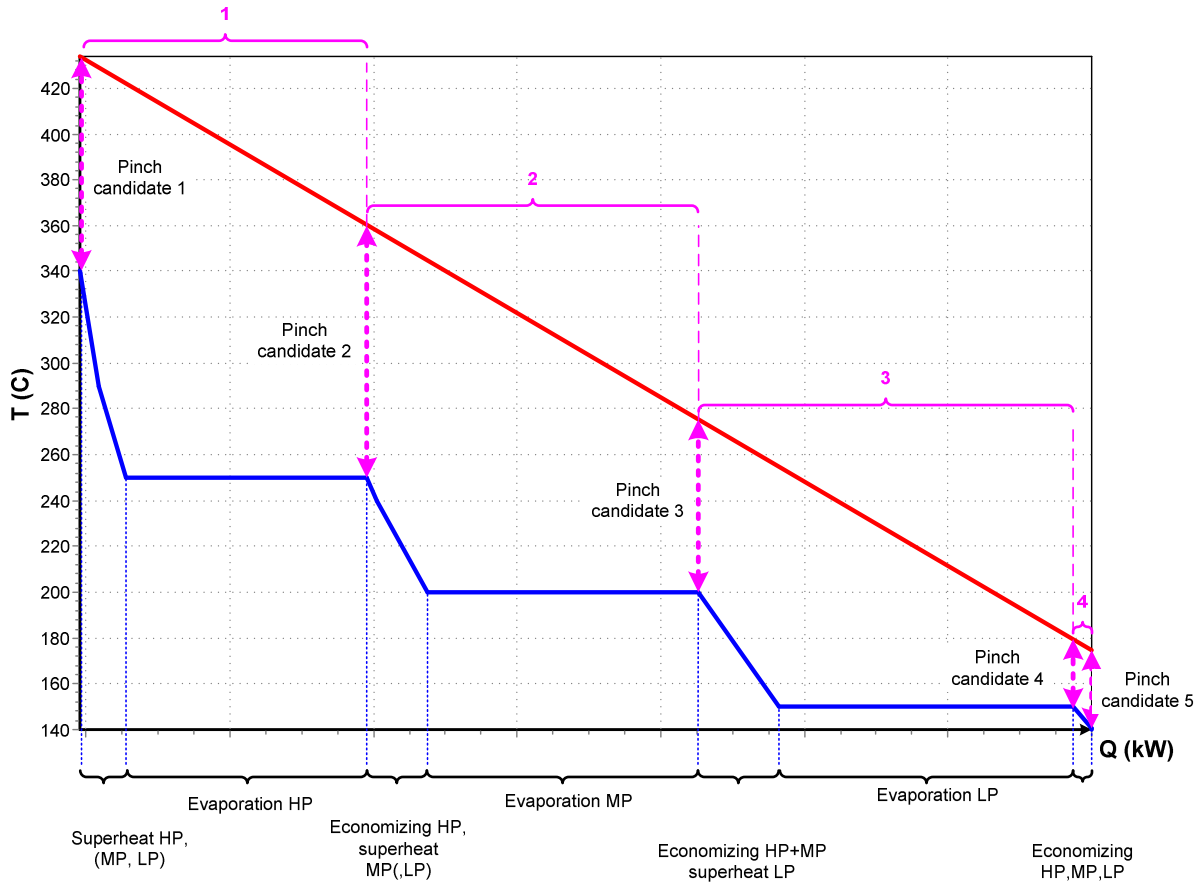

fig. 4-23 Optimal cooling curve for the fluegas in an HRSG. Three pressure levels are present (LP, MP, HP). The heating curve (blue) can be divided into a number of sections. The pinch point can only be located at 5 locations, i.e. number of steam levels + 2, and this in turn divides the heating/cooling curves into 4 intervals

Based on the definition of the five pinch candidate points, the flue gas cooling curve (red) can in turn be divided into four intervals, also shown in fig. 4-23. To ensure that none of the potential pinch points violate the desired $\Delta T_{\min}$ it is necessary to derive a model that calculates the amount of heat in each of the sections. The heat needed in each section depends on the degree of superheat for each steam level, e.g. LP-steam might require heating in both interval 1, 2, 3 and 4 if there is a significant degree of superheat, but only from interval 3 and 4 for no or moderate degrees of superheat. A boolean variable Y_i^j is introduced to determine in which interval i the outlet temperature of steam at level j is placed. Depending on the boolean variable a set of constraints apply to the outlet temperature as well as a set of energy balances for each interval. The outlet of the LP stream can be in any of the three intervals (1-3).

$$\begin{bmatrix} Y_1^{LP} \\ T_{out}^{LP} \leq T_{\max} \\ T_{out}^{LP} \geq T_{sat}^{HP} \\ \dot{Q}_1^{LP} = \dot{m}_{out}^{LP} c_{p,SH}^{LP} \left(T_{out}^{LP} - T_{sat}^{HP} \right) \\ \dot{Q}_2^{LP} = \dot{m}_{out}^{LP} c_{p,SH}^{LP} \left(T_{sat}^{HP} - T_{sat}^{MP} \right) \\ \dot{Q}_3^{LP} = \dot{m}_{out}^{LP} \left(h_{fg}^{LP} + c_{p,SH}^{LP} \left(T_{sat}^{MP} - T_{sat}^{LP} \right) \right) \end{bmatrix} \veebar \begin{bmatrix} Y_2^{LP} \\ T_{out}^{LP} \leq T_{sat}^{HP} \\ T_{out}^{LP} \geq T_{sat}^{MP} \\ \dot{Q}_1^{LP} = 0 \\ \dot{Q}_2^{LP} = \dot{m}_{out}^{LP} c_{p,SH}^{LP} \left(T_{out}^{LP} - T_{sat}^{MP} \right) \\ \dot{Q}_3^{LP} = \dot{m}_{out}^{LP} \left(h_{fg}^{LP} + c_{p,SH}^{LP} \left(T_{sat}^{MP} - T_{sat}^{LP} \right) \right) \end{bmatrix} \veebar \begin{bmatrix} Y_3^{LP} \\ T_{out}^{LP} \leq T_{sat}^{MP} \\ T_{out}^{LP} \geq T_{sat}^{LP} \\ \dot{Q}_1^{LP} = 0 \\ \dot{Q}_2^{LP} = 0 \\ \dot{Q}_3^{LP} = \dot{m}_{out}^{LP} \left(h_{fg}^{LP} + c_{p,SH}^{LP} \left(T_{out}^{LP} - T_{sat}^{LP} \right) \right) \end{bmatrix} \tag{4.26}$$

The outlet of the MP stream can only be in interval 1 or 2, hence:

$$\begin{bmatrix} Y_1^{MP} \\ T_{out}^{MP} \leq T_{\max} \\ T_{out}^{MP} \geq T_{sat}^{HP} \\ \dot{Q}_1^{MP} = \dot{m}_{out}^{MP} c_{p,SH}^{MP} \left(T_{out}^{MP} - T_{sat}^{HP} \right) \\ \dot{Q}_2^{MP} = \dot{m}_{out}^{MP} \left(h_{fg}^{MP} + c_{p,SH}^{MP} \left(T_{sat}^{HP} - T_{sat}^{MP} \right) \right) \\ \dot{Q}_3^{MP} = \dot{m}_{out}^{MP} c_{p,eco}^{MP} \left(T_{sat}^{MP} - T_{sat}^{LP} \right) \end{bmatrix} \veebar \begin{bmatrix} Y_2^{MP} \\ T_{out}^{MP} \leq T_{sat}^{HP} \\ T_{out}^{MP} \geq T_{sat}^{MP} \\ \dot{Q}_1^{MP} = 0 \\ \dot{Q}_2^{MP} = \dot{m}_{out}^{MP} \left(h_{fg}^{MP} + c_{p,SH}^{MP} \left(T_{out}^{MP} - T_{sat}^{MP} \right) \right) \\ \dot{Q}_3^{MP} = \dot{m}_{out}^{MP} c_{p,eco}^{MP} \left(T_{sat}^{MP} - T_{sat}^{LP} \right) \end{bmatrix} \tag{4.27}$$

For the HP stream only a single option exists, and therefore the energy balance becomes

$$\begin{aligned} \dot{Q}_1^{HP} &= \dot{m}_{out}^{HP} c_{p,SH}^{HP} \left(h_{fg}^{MP} + c_{p,SH}^{MP} \left(T_{out}^{HP} - T_{sat}^{HP} \right) \right) \\ \dot{Q}_2^{HP} + \dot{Q}_3^{HP} &= \dot{m}_{out}^{HP} c_{p,eco}^{HP} \left(T_{sat}^{HP} - T_{sat}^{LP} \right) \end{aligned} \tag{4.28}$$

For interval 4 the heat transfer is quite simple, since all streams are below saturation conditions.

$$\dot{Q}_4^i = \dot{m}_{in}^i c_{p,eco}^i \left(T_{sat}^{LP} - T_{in}^i \right) \quad \forall i \in \{HP, MP, LP\} \tag{4.29}$$

In addition a set of logical constraints must ensure that each level only has one outlet

$$\begin{aligned} & Y_1^{HP} \\ & Y_1^{MP} \veebar Y_2^{MP} \\ & Y_1^{LP} \veebar Y_2^{LP} \veebar Y_3^{LP} \end{aligned} \tag{4.30}$$

The overall energy balance for each steam level is

$$\dot{Q}_{eco}^{i} + \dot{Q}_{evap}^{i} + \dot{Q}_{SH}^{i} = \sum_{j=1}^{4} \dot{Q}_{j}^{i} \qquad \forall i \in \{HP, MP, LP\} \tag{4.31}$$

The overall energy balance for the HRSG is

$$\dot{Q}_{FG}^{in} - \dot{Q}_{FG}^{out} = \sum_{i} \dot{Q}_{eco}^{i} + \dot{Q}_{evap}^{i} + \dot{Q}_{SH}^{i} \qquad i \in \{HP, MP, LP\} \tag{4.32}$$

The energy balance for the flue gas in each interval is

$$\dot{m}_{FG} c_p^{FG} \left(T_j^{FG} - T_{j+1}^{FG} \right) = \sum_{i} \dot{Q}_{j}^{i} \qquad i \in \{HP, MP, LP\} \quad \forall j \in \{1,2,3,4\} \tag{4.33}$$

Based on the energy balances the temperature of the flue gas at each pinch candidate point can be evaluated through (4.33). A constraint on each temperature will ensure that there are no pinch violations:

$$\begin{aligned} & T_1^{FG} + \Delta T_{\min} \geq T_{out}^{i} \qquad \forall i \in \{HP, MP, LP\} \\ & T_2^{FG} + \Delta T_{\min} \geq T_{sat}^{HP} \\ & T_3^{FG} + \Delta T_{\min} \geq T_{sat}^{MP} \\ & T_4^{FG} + \Delta T_{\min} \geq T_{sat}^{LP} \\ & T_5^{FG} + \Delta T_{\min} \geq T_{in}^{i} \qquad \forall i \in \{HP, MP, LP\} \end{aligned} \tag{4.34}$$

With equation (4.25) to (4.34) the HRSG is modelled, and it is ensured that no pinch violation occurs.

4.2 Heat integration

Simultaneous process optimisation and heat integration was first reported by (Duran and Grossmann 86b), who calculated the minimum hot and cold utility requirements simultaneously with the process optimisation. The method does not include an area estimate, which implies that ΔT_{min} must be defined a priori and the investment cost of the network cannot be incorporated into the objective function. Nevertheless the method has been used in several papers, as a simple way to include the heat integration potential. (Yee *et al.* 90a) proposed a superstructure model for the synthesis of heat exchanger networks, without fixed ΔT_{min}, see also chapter 1.1.4. In (Yee *et al.* 90b) the method was used in a small scale example for simultaneous process optimisation and heat integration. The method is

thorough and provides near optimal trade-off between heat exchanger area and operational costs, but is combinatorially prohibitive and therefore found unsuitable for use in this work.

A brief summary on the method by (Duran and Grossmann 86b) is provided here for a set of hot stream N_H and at set of cold stream N_c .

$$\begin{aligned}
&\min z = \dot{Q}_{steam} + \dot{Q}_{water} \\
&\quad s.t. \\
&\dot{Q}_{steam} \geq \underbrace{\sum_{j=1}^{N_C} F_j^c \left[\max\left(0; T_j^{c,out} - \left(T_k^p - \Delta T_{min}\right)\right) - \max\left(0; T_j^{c,in} - \left(T_k^p - \Delta T_{min}\right)\right)\right]}_{\text{Heat requirement by cold streams above pinch point } T_k^p} \\
&\quad \underbrace{- \sum_{i=1}^{N_H} F_i^h \left[\max\left(0; T_i^{h,in} - T_k^p\right) - \max\left(0; T_i^{h,out} - T_k^p\right)\right]}_{\text{Heat available from hot streams above pinch temperature } T_k^p} \qquad \forall k \in N_c \cup N_h \\
&\dot{Q}_{water} = \dot{Q}_{steam} + \underbrace{\sum_{i=1}^{N_H} F_i^h \left[T_i^{h,in} - T_i^{h,out}\right]}_{\text{Total heat content of hot streams}} - \underbrace{\sum_{j=1}^{N_C} F_j^c \left[T_j^{c,in} - T_j^{c,out}\right]}_{\text{Total heat requirement by cold streams}} \\
&T_k^p = \begin{bmatrix} T_k^{h,in} & \forall k \in N_H \\ T_k^{c,in} + \Delta T_{min} & \forall k \in N_C \end{bmatrix}
\end{aligned} \tag{4.35}$$

In this example the hot (steam) and cold (water) utility input is minimised. The first constraint ensures that the hot utility supply at least covers the difference between the heat needed and the heat available above the given pinch point temperature. This constraint is applied for all pinch candidates T_k^p . The second constraint is the overall energy balance and the final constraint simply defines the pinch candidates; here it is seen that the inlet temperature of every hot and cold stream is considered a pinch candidate. The cold pinch candidates are shifted by the value of ΔT_{min} .

The problem is formulated from a traditional pinch analysis point of view, where the process and utility is two separate systems. However, in integrated design the process system is not considered different from the utility system, and therefore the hot utility and cold utility supplies are simply additionally hot and cold streams. As mentioned before the cold pinch temperatures are shifted towards the hot temperatures, but it has turned out to be more beneficial to shift both the hot and cold temperatures by the amount $\frac{1}{2}\Delta T_{min}$, thus moving the entire formulation to a mean temperature between hot and cold. The reason for shifting each stream by $\frac{1}{2}\Delta T_{min}$ is that it is easier to substitute the global ΔT_{min} with an individual addition from each stream. In this way streams with poor heat transfer properties can be associated with a larger $\frac{1}{2}\Delta T_{min}$ than streams with high heat transfer properties. Therefore the formulation used in this work is:

$$\min z = f(\mathbf{x},\mathbf{y})$$

s.t.

$$0 \geq \underbrace{\sum_{j=1}^{N_C} F_j^c \left[\max\left(0; T_j^{c,out} + \tfrac{1}{2}\Delta T_{min} - T_k^p\right) - \max\left(0; T_j^{c,in} + \tfrac{1}{2}\Delta T_{min} - T_k^p\right)\right]}_{\text{Heat requirement by cold streams above pinch point } T_k^p}$$

$$- \underbrace{\sum_{i=1}^{N_H} F_i^h \left[\max\left(0; T_i^{h,in} - \tfrac{1}{2}\Delta T_{min} - T_k^p\right) - \max\left(0; T_i^{h,out} - \tfrac{1}{2}\Delta T_{min} - T_k^p\right)\right]}_{\text{Heat available from hot streams above pinch temperature } T_k^p} \qquad (4.36)$$

$$\forall k \in N_c \cup N_h$$

$$0 = \underbrace{\sum_{i=1}^{N_H} F_i^h \left[T_i^{h,in} - T_i^{h,out}\right]}_{\text{Total heat content of hot streams}} - \underbrace{\sum_{j=1}^{N_C} F_j^c \left[T_j^{c,in} - T_j^{c,out}\right]}_{\text{Total heat requirement by cold streams}}$$

$$T_k^p = \begin{bmatrix} T_k^{h,in} - \tfrac{1}{2}\Delta T_{min} & \forall k \in N_H \\ T_k^{c,in} + \tfrac{1}{2}\Delta T_{min} & \forall k \in N_C \end{bmatrix}$$

The objective function is here related to the entire process, and the hot and cold utilities are now just hot and cold streams. Furthermore the temperatures are now all at the mean condition.

The max-functions in the formulation have discontinuous derivatives and are therefore unsuitable for continuous optimisation methods. Therefore a smooth-approximation of the max-functions was proposed by (Duran and Grossmann 86b):

$$\max(0;a) \approx \frac{a + \sqrt{a^2 + \varepsilon}}{2} \qquad (4.37)$$

Here ε is a small number, the approximation for various values of ε is shown in fig. 4-24.

Now the problem is formulated as an NLP-problem. The smooth-approximations are somewhat sensitive however, since the derivatives around zero change dramatically, and for negative values of *a* the derivatives of the smooth approximation is very small. This can lead to numerical difficulties as reported by (Grossmann *et al.* 98), who instead proposed a rigorous MINLP-formulation. This MINLP-formulation is rewritten for this work, and can be found in appendix 11. While making the model much more robust it also introduce $3N^2$ integer variables (N being the number of hot + cold streams), which potentially makes the problem combinatorially prohibitive for cases of practical scale.

The MINLP-formulation has been tested in the present work with the methanol-case described in chapter 5. Even though significant efforts were made to tighten the formulation the problem turned out to be combinatorially prohibitive, and unusable in practice. Therefore the smooth-approximations are used, despite their numerical problems. To make

the smooth approximation stable a value of $\varepsilon = 0.01$ has been used; this has worked out satisfactory even though small discrepancies exist. The result is that the pinch temperature requirements are not completely fulfilled, although practical experience has shown that this problem can usually be overcome by selecting slightly higher values of $\Delta T_{\min}$ than would normally be applied.

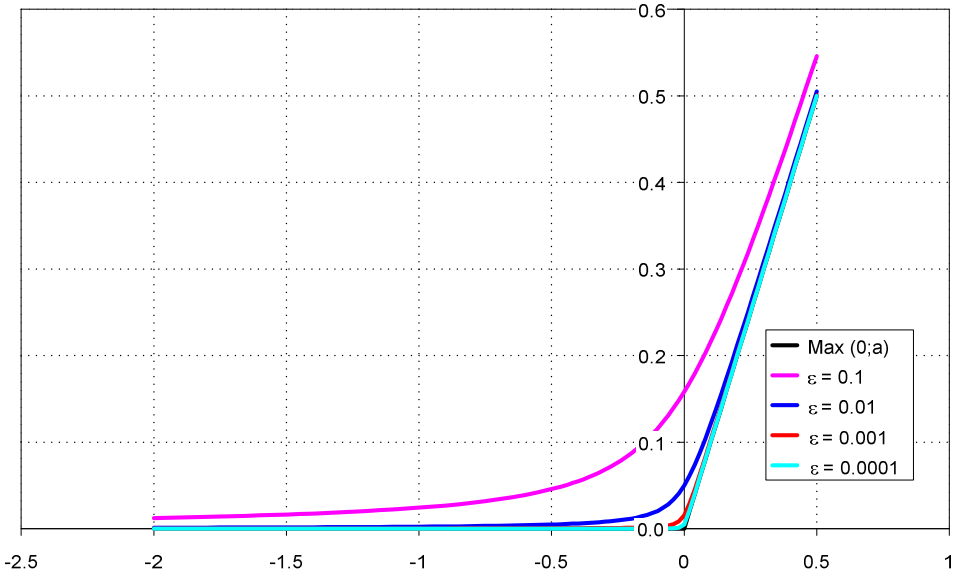

fig. 4-24 Plot of the max-function approximation for different values of ε

Apart from the numerical difficulties that can be introduced by this method, two serious limitations are found:

- The ΔT_{min} must be defined a priori
- The area of the heat exchangers are not calculated and thus cannot be included in the investment cost in the objective function.

These limitations are significant, but to the best of our knowledge no present method is able to deal with them in a completely satisfactory manner, without at the same time introducing a large MINLP-problem.

Regarding the minimum approach temperature ΔT_{min}, it is obvious that the strength of the method by (Yee *et al.* 90a) is that it is handled implicitly by optimising the area cost instead of minimising utility consumption at an arbitrary ΔT_{min}.

The problem formulated by equation (4.36) is used for this work, with the addition that individual values of $\frac{1}{2}\Delta T_{min}$ are used for each stream. The idea is to use large values for streams with low heat transfer coefficients and vice-versa. Hereby the actual ΔT_{min} will not be completely arbitrary, but will reflect the properties of all streams around the pinch point. The approach of selecting different temperature contributions from each stream has also been proposed by (Zhu *et al.* 95) and (Briones and Kokossis 99).

4.3 Driver selection

In a process plant, each work requirement must be met be some kind of driver. In this work, the drivers are limited to electrical drives and steam turbines. The gas turbine are only utilised for on-site generation of electricity.

When three different steam levels are available, there exist 6 different turbine configurations for each work requirement, see fig. 4-25. The network includes both backpressure turbines and condensing turbines, and extraction turbines. Each work requirement in the process can be fulfilled by either one of the turbine combinations or an electric drive.

Electricity can be produced on-site with either a gas turbine or steam turbine. Alternatively electricity can both be bought and sold from/to the electric grid.

To formulate the disjunctive model for the steam turbine network we first define a number of sets. Let the set of utility levels be defined as $i \in \{HP, MP, LP, cond\}$. If there are N work-requirements in the process and one electricity requirement to cover all on-site electricity production the combined work requirement set is defined as $j \in \{E, M_1 \ldots M_N\}$. Furthermore let the turbine configuration and electric driver be defined in the set $k \in \{T1, T2, \ldots, T6, Elec\}$. Based on the superstructure then it is possible to define a set of ordered pairs, that describes the inlet pressure level to each turbine $l \in \{(T1, HP), (T2, HP), (T2, MP), (T3, HP), (T3, MP), (T3, LP), \ldots\}$

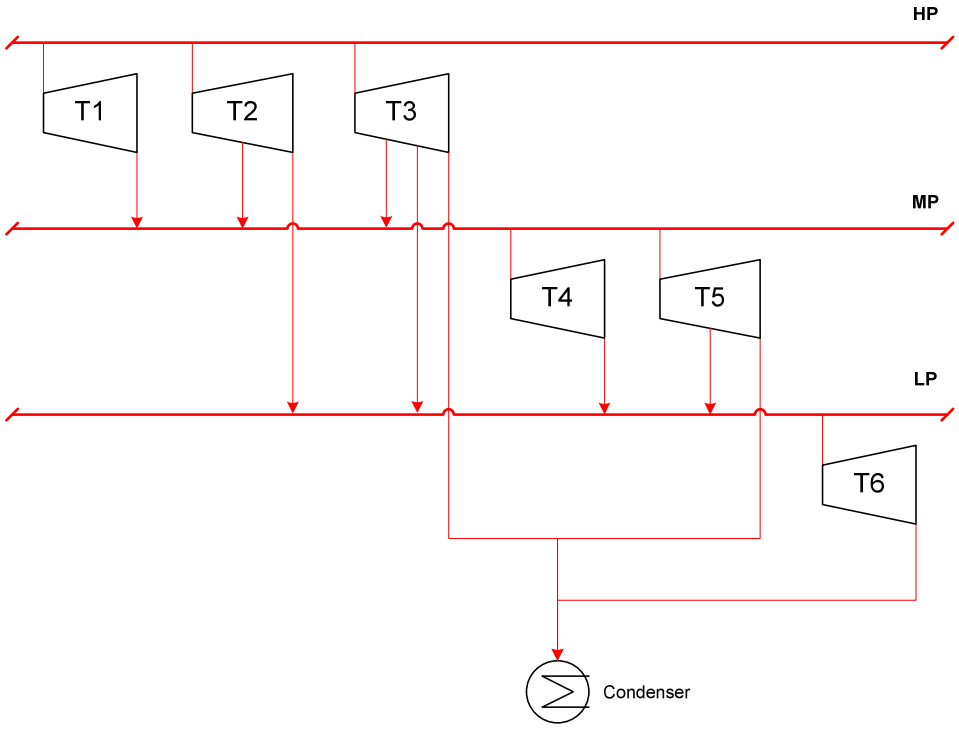

fig. 4-25 Outline of the steam turbine network.

Each mechanical work requirement in the process must be combined with exactly one driver. The on-site electricity production can on the other hand be satisfied by one or more drives. This is formulated using a set of boolean variables

$$\begin{aligned} Y_{j,Elec} \veebar Y_{j,T1} \veebar Y_{j,T2} \veebar Y_{j,T3} \veebar Y_{j,T4} \veebar Y_{j,T5} \veebar Y_{j,T6} \quad & \forall j \in \{M_1 \dots M_N\} \\ Y_{j,T1} \vee Y_{j,T2} \vee Y_{j,T3} \vee Y_{j,T4} \vee Y_{j,T5} \vee Y_{j,T6} \quad & \forall j \in \{E\} \end{aligned} \tag{4.38}$$

The disjunctive turbine model is formulated as follows

$$\begin{bmatrix} Y_{jk} \\ \dot{W}_{j,l(i,k)} = \dot{m}_{j,l(i,k)} \left(h^{in}_{j,l(i,k)} - h^{out}_{j,l(i,k)} \right) \\ h^{in}_{j,l(i,k)} = h\left(T^{in}_{j,l(i,k)}, p_i \right) \\ h^{out}_{j,l(i,k)} = h\left(T^{in}_{j,l(i,k)}, p_{i+1} \right) \\ h^{out}_{j,l(i,k)} = f\left(\dot{W}_{j,l(i,k)} \right) \\ C_{GR,jk} = 12106 \frac{C_{cepci}}{382} \left[\sum_l \dot{W}_{j,l(i,k)} \right]^{0.4401} \end{bmatrix} \vee \begin{bmatrix} \neg Y_{jk} & \\ \dot{W}_{j,l(i,k)} = 0 & \forall i \\ \dot{m}_{j,l(i,k)} = 0 & \forall i \\ C_{GR,jk} = 0 & \end{bmatrix} \quad \forall k \in \{T1,\dots,T6\}, \forall j \tag{4.39}$$

The model consists of the energy balance for each turbine cylinder, the thermodynamic relation between enthalpy, pressure and temperature as described in section 4.1.2. The outlet enthalpy from each cylinder is found by the isentropic efficiency (here denoted using the function f for brevity) as described in 0. Finally the grassroot cost of the turbine is formulated as a power law, according to (Turton *et al.* 98).

4.4 Summary

In this chapter the utility and heat integrations models have been formulated.

A new set of steam properties for optimisation purposes was proposed; this includes a new model for calculation of isentropic expansion enthalpy in turbines. The new steam properties allow for free selection of the pressure levels, since pressure is properly taken into account by the steam properties. The superstructure for the optimisation has heavy emphasis on the heat integration with the process, thus almost all streams in the superstructure are considered part of the heat integration. The formulation of the gas turbine model is very similar to the work of (Manninen 99), but some minor enhancements are included.

If a separate utility system model, which is less integrated with the process, is desired, this can easily be accomplished by replacing the HRSG model.

The heat integration model is updated compared to (Duran and Grossmann 86b) in the sense that different temperature differences are associated with each stream. This makes the overall minimum temperature difference more realistic. Two different methods have been tested for formulation of the heat integration problem, and it is concluded that the MINLP-

formulation is unsuitable for the integrated design, since the formulation becomes combinatorially prohibitive.

The driver interface is modelled by disjunctions to select the proper driver among a number of steam turbine and electrical driver combinations.

To highlight some of the elements in the methods a number of small test cases for both utility design and heat integration will be presented in the next chapter.

5

CASE STUDIES ON UTILITY SYSTEMS

In this chapter a number of small cases for optimisation of utility systems and heat integration are presented. They serve to test the models developed in the previous chapter, and in addition a test of different optimisation algorithms are carried out for the first test case. Generally the proposed superstructure and disjunctive model is able to find solutions superior to those found earlier. The disjunctive branch-and-bound solver is a particular strong solver for the superstructure, and is able to find significantly better solutions than the commercial solvers.

The purpose of this chapter is to provide a number of case studies that focus on utility system design. This is both to highlight some of the issues of the models in the last chapter, and to discuss the disjunctive solver and the economic models.

5.1 Example 1

This example is formulated by (Bruno *et al.* 98). A set of demands for heat and power are given in table 5-1.

table 5-1 Heat and power demands for the example

Electricity	4500 kW
Mechanical demand 1	1200 kW
Mechanical demand 2	1500 kW
Mechanical demand 3	700 kW
HP heating	0 kW
MP heating	20000 kW
LP heating	55000 kW

The steam headers are fixed and listed in table 5-2.

table 5-2 pressure levels at each header

Pressure level	Pressure (bar)	Temperature (°C)	Enthalpy of vaporization (kJ/kg)
HP	45.0	257.4	1676
MP	17.0	204.3	1923
LP	4.5	147.9	2120

The net present worth method (NPW) is used as objective function, in which a lifetime of 10 years is expected along with an internal rate of return of 8%. Since there is no income associated with the utility plants the NPW will inevitably be a cost. The plant with the *lowest* NPW-cost is thus the optimal plant.

As the heat demands for the plant are fixed at certain pressure levels, the utility system cannot be integrated with the rest of the plant. To make the problem more in line with the work of (Bruno *et al.* 98), it is chosen to model the HRSG with the model formulated in 4.1.6. Furthermore the boilers are assumed to have a fixed efficiency of 95%, and there is no possibility of heat integrating the boilers with the rest of the plant. Therefore the utility superstructure is slightly different from the one for integrated design.

The resulting flowsheet using the disjunctive model formulated in the previous chapter is shown in fig. 5-1.

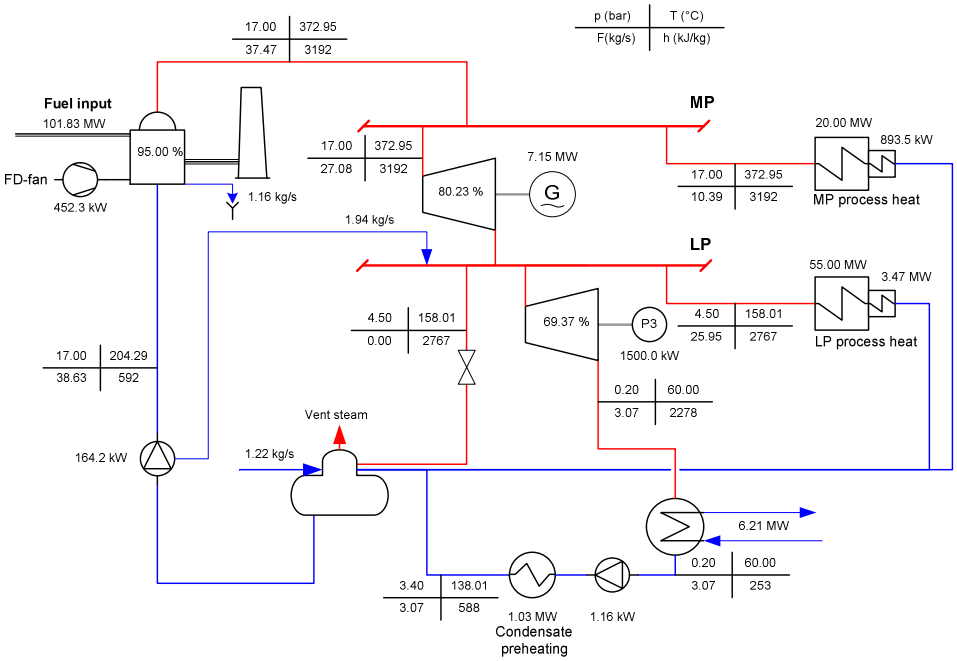

fig. 5-1 The optimal flowsheet for example 1.

For comparison the optimal flowsheet predicted by (Bruno *et al.* 98) is shown in fig. 5-2.

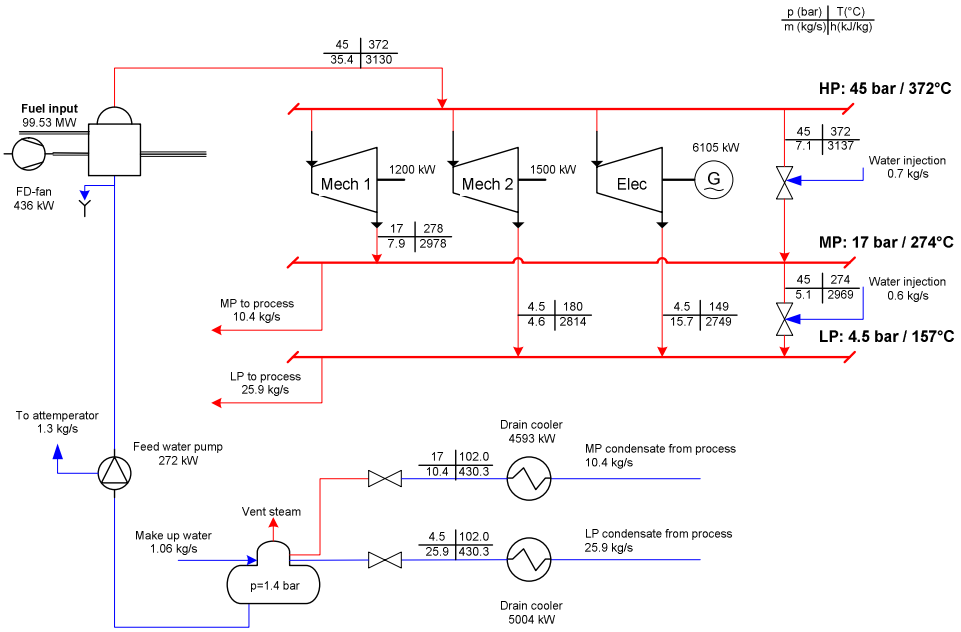

fig. 5-2 The optimal flowsheet predicted by (Bruno et al. 98). Please observe that there are some disagreements compared to the original work, this is primarily due to some errors in the reported heat balance and the use of a different set of steam property equations.

The NPW cost for the two solutions along with statistics on the solution is found in table 5-3, the objective has also been calculated using the cost function used in the original paper. A reduction of 7.5% in the NPW cost is obtained using the new flowsheet, instead of the one proposed by (Bruno *et al.* 98), but if the original objective function is used the improvement is smaller. The CPU time is of course much higher for the new flowsheet since the topology needs to be found, whereas it is specified in the other case.

table 5-3 Solution summary for example 1

	MINLP-optimum (NPW cost)	**Relaxed optimum (NPW cost)**	**Objective function used by (Bruno *et al.* 98)**	**CPU time (s)**	**Number of B&B iterations**
New solution	83.0 M€	76.6 M€	14.2 M€	105	63
(Bruno *et al.* 98)	89.5 M€	83.7 M€	14.6 M€	5	7

The most significant difference is the fact that the solution of (Bruno *et al.* 98) uses a boiler to produce HP-steam and a set of HP-turbines to cover the mechanical demands of 1200 kW and 1500 kW. The new solution on the other hand only raises MP-steam and uses electricity for the mechanical demand at 1200 kW, thus only providing a turbine drive for the 1500 kW demand. It is clear that the boiler is cheaper since the steam is raised at a much lower pressure, and in addition the relatively small turbines have a significantly higher efficiency at the low inlet pressure. On the other hand the steam temperature is 372°C compared to 274°C, which increases the electric efficiency. All together, the new method is able to find an improved plant compared to the originally reported results.

5.1.1 Scenario analysis

The results have so far been presented for scenario 1 (Elsam 03), but in order to evaluate the sensitivity of the solution towards the prices of utility, solutions has also been found for scenario 2 and 3. However, it turns out the solution is the same for all three scenarios. The reason is that the ratio between heating and work demands for this case is high and therefore a boiler is needed to cover the demands, they simply cannot be covered by raising steam in a HRSG from a gas turbine. Furthermore, since steam must be provided at MP-pressure the only choice left is whether to include a HP-steam level and HP-turbines, but the cost of the boiler and the reduction in the turbine efficiency rules out this option.

5.1.2 Numerical analysis

The case has also been used for a numerical study, comparing different solvers. The following solvers where tested

- The disjunctive Branch-and-Bound solver from this work
- DICOPT 2.0, included in GAMS and first presented by (Duran and Grossmann 86a)
- SBB (Simple Branch-and-Bound) included in GAMS.

The DICOPT and SBB solvers are the only solvers in GAMS that can handle large scale MINLP-problems. Typically DICOPT is better for problems with a complex combinatorial part and a simple non-linear part, whereas SBB is stronger for difficult non-linear problems, though with simpler combinatorial parts. Both solvers rely just as the disjunctive solver on an NLP-solver to solve the relaxed problems, and CONOPT 3 where used for all three cases. In addition DICOPT uses a MILP-solver to solve the master-problems, and CPLEX was used in this case.

The optimal object function by the three solvers is compared in fig. 5-3. It is clear that the disjunctive B&B solver is superior to the other solvers.

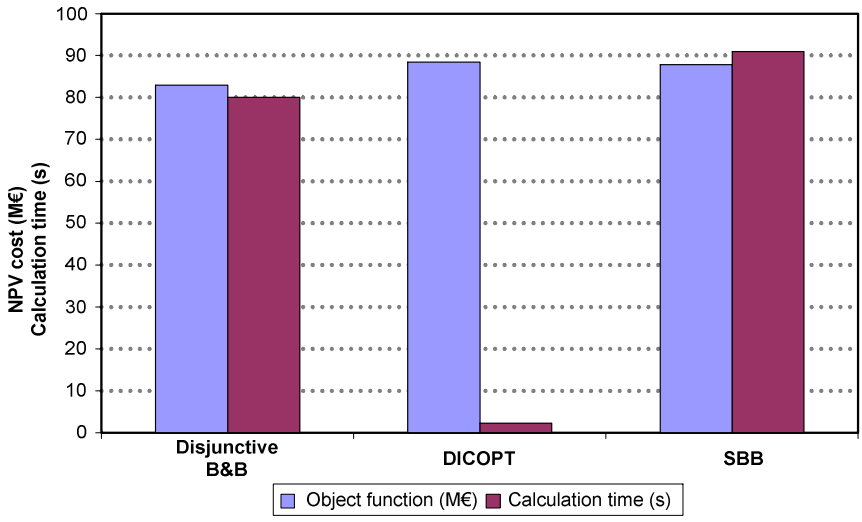

fig. 5-3 Comparison of different solvers for the problem.

The reason is to be found in several places. Part of the model is very non-linear and therefore it can more or less be expected that DICOPT have problems finding an optimal solution. Several solver options has been tried out in order to improve the solution, but none were found to improve the results. The SBB works in much the same way as the disjunctive solver, but the ability of the disjunctive solver to exclude constraints for disabled parts of the superstructure makes it much more robust and furthermore it has the option of restarting from several initial points. None of these features are found in SBB, which is most likely the explanation that the disjunctive solver is better; during the SBB iterations a far larger number of nodes are judged infeasible and thus excluded from further search than in the disjunctive solver. The calculation times for the two B&B solvers are almost identical, whereas DICOPT is much faster.

5.2 Example 2

This example is originally formulated by (Papoulias and Grossmann 83a). A set of demands for heat and power are given in table 5-5. .

table 5-4 Heat and power demands for the example

Electricity	33000 kW	Mechanical demand 6	1265 kW
Mechanical demand 1	3120 kW	Mechanical demand 7	1940 kW
Mechanical demand 2	1800 kW	Mechanical demand 8	640 kW
Mechanical demand 3	550 kW	HP heating	0 kW
Mechanical demand 4	818 kW	MP heating	31500 kW
Mechanical demand 5	2600 kW	LP heating	85500 kW

The optimal utility system is shown in fig. 5-4.

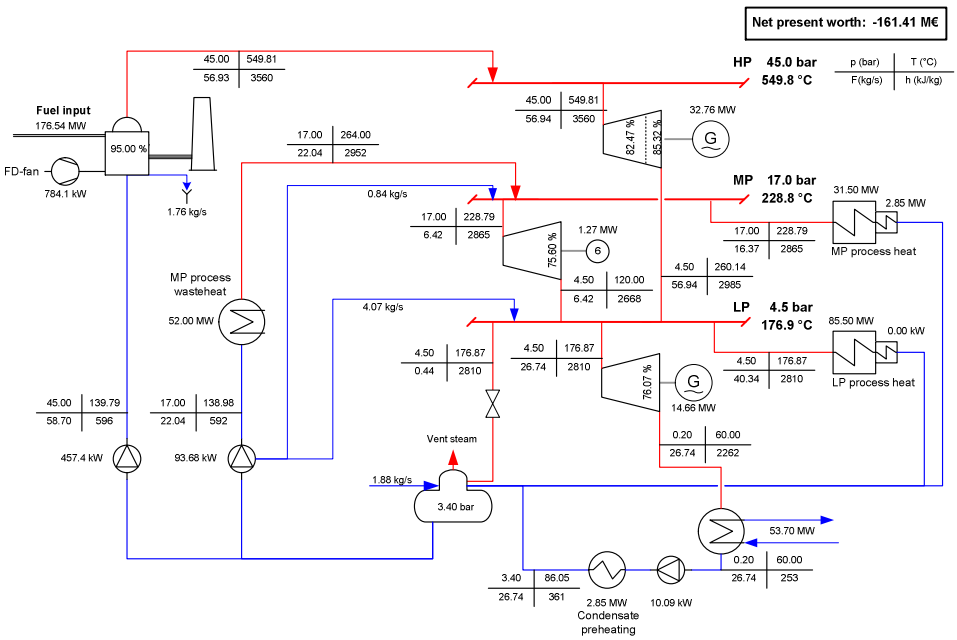

fig. 5-4 Optimal utility system for example 2.

The system uses a HP-boiler and the waste heat at MP level to generate steam. The HP-steam is expanded through a turbine to the LP-level, generating most of the electricity requirements. There is more MP-wasteheat available than MP heat demand, and thus a small turbine expands excess MP-steam from the MP to the LP level, covering mechanical demand no. 6 by a direct drive. At the LP level most of the steam is used for process heating, and the excess steam is expanded through a condensing turbine, that also generates electricity. All mechanical demands except no. 6 are consequently covered by electricity. The drain cooler of the MP-steam is used for condensate preheating, and therefore a deaerator pressure of 3.4 bar is selected. It should be noted that the HP-steam temperature is very high (550°C), which clearly increases the efficiency.

The system has been optimised using the fixed pressure headers, but actually only the MP and LP level needs to be fixed since there is a process heat demand at these level. However, the HP-level can as such be freely selected. The resulting flowsheet is shown in fig. 5-5.

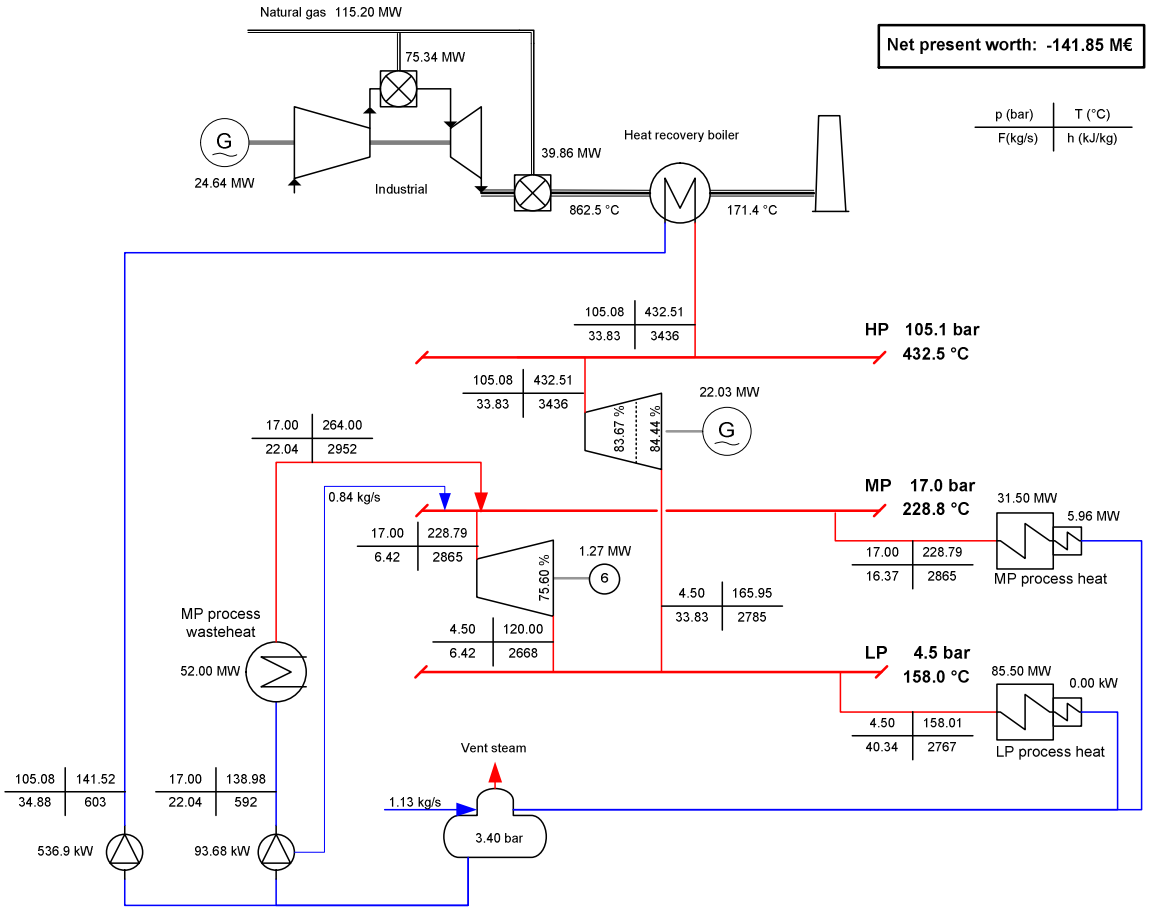

fig. 5-5 Optimal utility system for example 2, with optimised HP-pressure.

In this case the HP-pressure level is increased to 105 bar, and a gas turbine with a supplementary fired HRSG is used to generate electricity and raise steam. The net present worth cost for the plant is reduced by 12.5% and the fuel consumption is reduced by 35%. This shows the very important aspect of selection of the pressure level. The plant with the

gas turbine is only competitive because the pressure level of the HP-header is increased, otherwise the matching of the gas turbine, the HRSG and the steam turbines would have been impossible and the electric efficiency would have been too small. Another interesting feature of the plant is that the condensing turbine is eliminated; this can on one hand be considered a result of the quite low efficiencies that are estimated for the condensing turbines and on the other hand it increases the overall efficiency since no heat is rejected in the condenser. Finally a brief note on the drain cooler at the MP level, where 5.95 MW of heat is rejected, since there is no feed water preheating in the selected design, this heat is rejected to cooling water.

5.3 Heat integration example

The new heat pinch method stated in chapter 4.2, will be illustrated in this example. The stream data is a modified version of the example found in (Zamora and Grossmann 98). It is a small problem with 2 hot streams and 2 cold streams, as listed in table 5-5.

table 5-5 Stream specification for the small test example

	T_{in} (°C)	T_{out} (°C)	F (kW/K)	Base case h_c (W/m²K)	Case 1 h_c (W/m²K)	Case 2 h_c (W/m²K)
H1	180	75	30	150	150	10
H2	240	60	40	100	500	100
C1	40	230	35	200	200	200
C2	120	300	20	100	100	100
Hot utility	325	325		2000	2000	2000
Cold utility	25	40		500	500	500

Three different cases for the convection coefficients are listed, where the base case refers to the one in the work by (Zamora and Grossmann 98), and the other two cases are simply modified versions of the original problem.

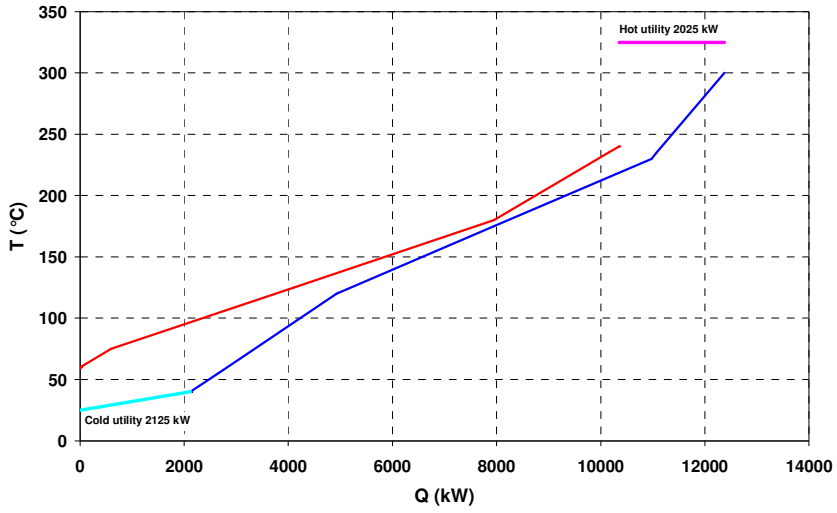

fig. 5-6 Composite curves for the streams specified in table 5-5.

For the base case the convection coefficients are generally high and $\Delta T_{min} = 5°C$ is selected for the pinch analysis. This leads to the composite curves shown in fig. 5-6.

The fixed temperature difference corresponds to a stream temperature difference of 2.5°C for each of the streams. However, the convection coefficients for the streams differ by a factor of 2, and therefore it is realistic to associate different temperature differences with each stream. The temperature contribution for each stream is shown in table 5-6.

table 5-6 Minimum temperature differences for each stream

ΔT_{min}^{stream}	H1	H2	C1	C2
Base case	2.5	3.75	1.875	3.75
Case 1	2.5	0.10	1.875	3.75
Case 2	37.5	3.75	1.875	3.75

The selected temperature contributions are in this case thought to be a linear function of the convection coefficient. Other dependencies can be used, e.g. (Franck *et al.* 98) suggests

$$\Delta T \sim \frac{1}{\sqrt{h_c}}$$

Using the temperatures of the base case leads to a heat integration curve as shown in fig. 5-7.

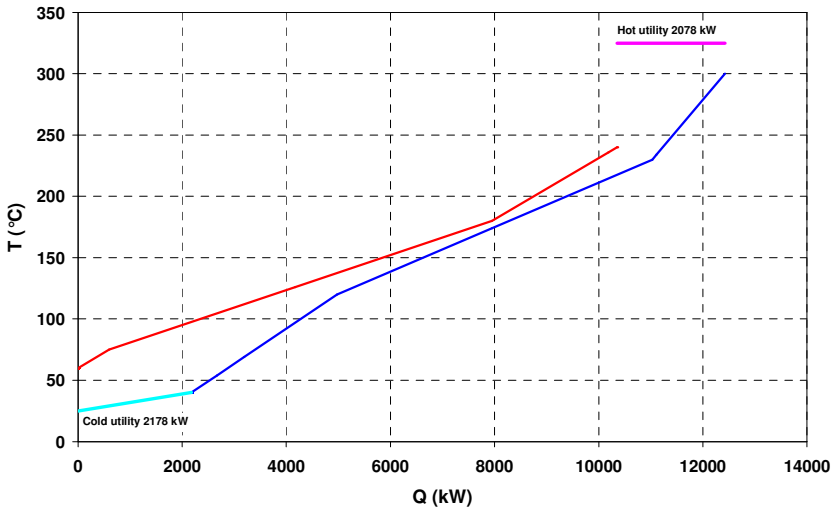

fig. 5-7 Composite curves for the basecase

The heat consumption is slightly increased compared to the overall temperature difference of 5°C. Using a superstructure approach[17] a possible heat exchanger network can be found, as shown in fig. 5-8.

[17] The superstructure from (Yee *et al.* 90a) is used to derive the network

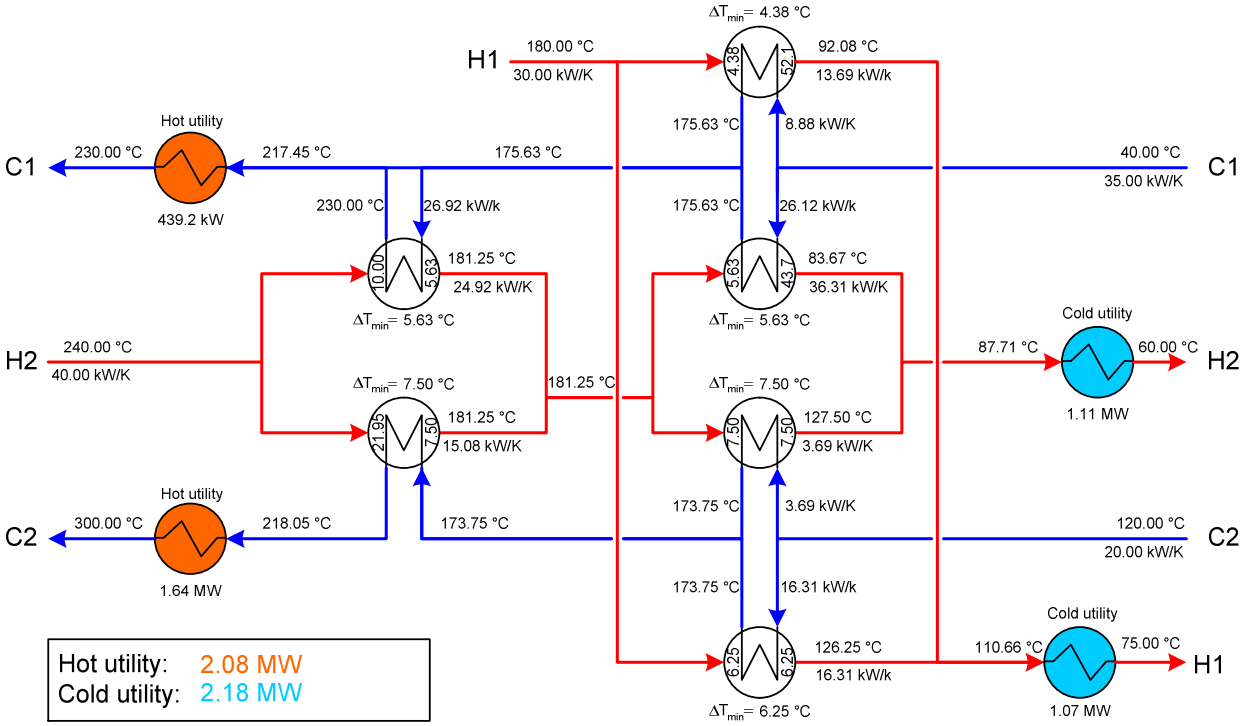

fig. 5-8 Heat exchanger network for the basecase. The exchanger matches at each end of the exchanger are the small numbers inside each exchange symbol. Note that the network only fulfils minimum hot and cold utility given the approach temperatures of table 5-6.

In case 1, hot stream 2 has a much higher convection coefficient, and therefore a much lower minimum temperature. This reduces the need for hot and cold utility as shown by the composite curves

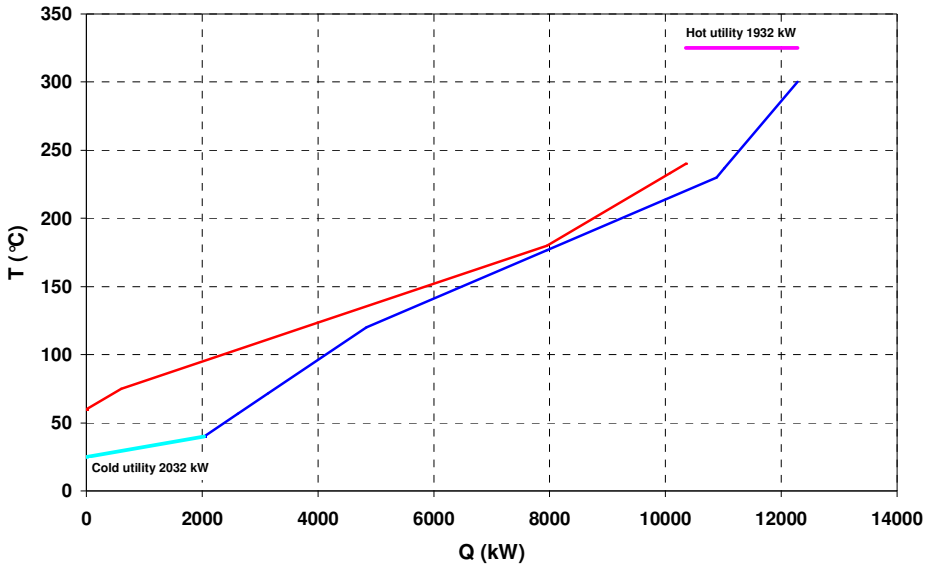

fig. 5-9 Composite curves for case 1. The heat integration is found using the model in chapter 4.2.

The heat exchanger network that fulfils the minimum requirements and the minimum temperature differences are shown in fig. 5-10

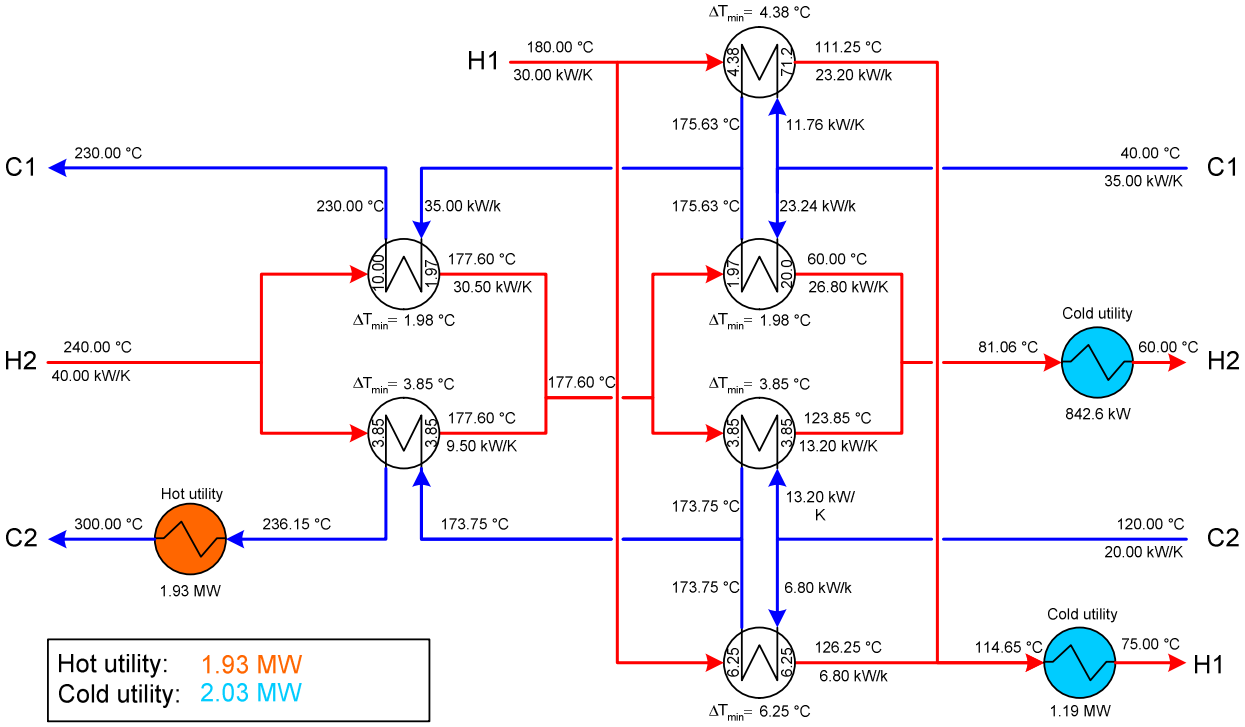

fig. 5-10 heat exchanger network for case 1.

In the final case (case 2), the convection coefficient for hot stream 1 is assumed to be very low, in the typical range for gases. Therefore the minimum temperature for this case is increased very much compared to the other streams.

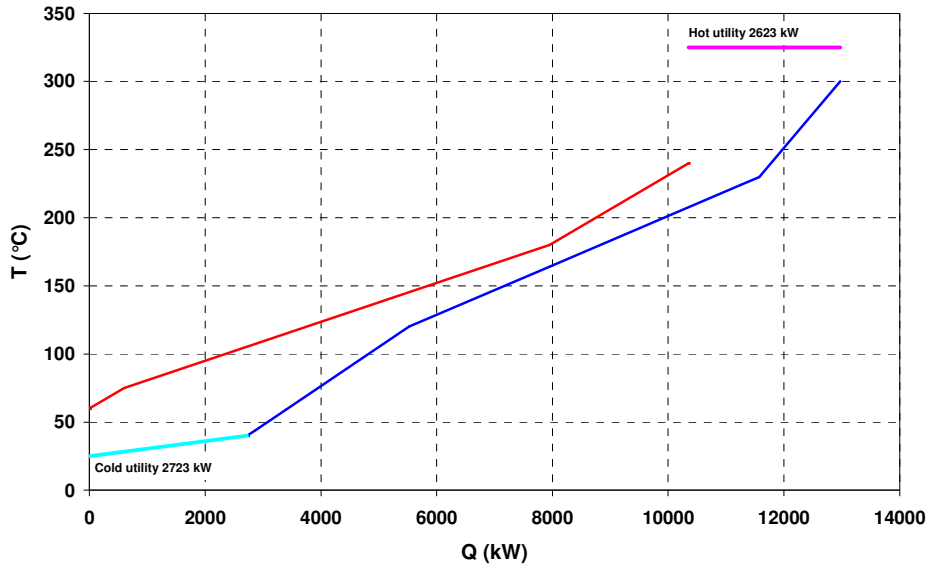

fig. 5-11 Composite curves for case 2

The most interesting aspect of this case is that even though one of the streams has a very high minimum temperature difference (37.5°C) the HRAT for the composite curves is still as low as 15.5°C. This is because of the low temperature differences accepted by the other hot stream in the problem. The network in fig. 5-12 shows clearly that the heat integration is feasible.

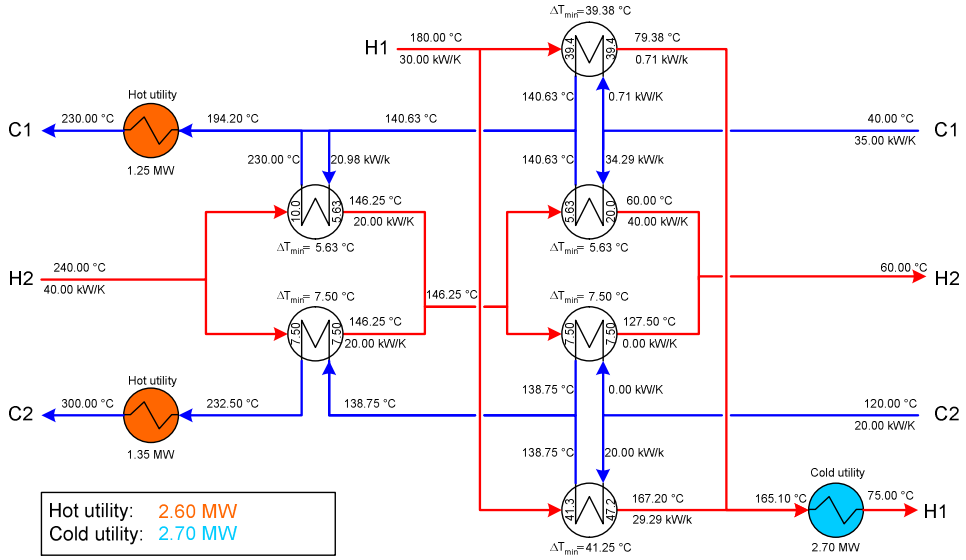

fig. 5-12 Network structure for case 2

The three cases shown here prove that fixing the individual stream temperature differences instead of the global minimum temperature difference certainly is possible with the formulation in chapter 4.2. It is interesting to see that for most of the cases many of the heat exchangers in the network actually operate either exactly at the limiting temperature difference or very close to it. The usefulness of the method is highlighted by the fact that setting the individual stream temperature differences are based on the convection coefficients.

5.4 Summary

The small cases here proved both the strength of the proposed superstructure formulation, as well as the strength of the disjunctive branch-and-bound solver.

In the first example an improved flowsheet compared to the original is found. Even more importantly, the improvement can most likely be contributed to the robustness of the disjunctive solver, which finds a significantly better optimum than the two commercial solvers (DICOPT and SBB).

In the second example an improved flowsheet were also identified. The more important lesson from this example was that fixing the pressure a priori can lead to significantly suboptimal design. Thus the importance of the steam properties that allow free selection of pressure is highlighted.

The heat integration example illustrates the effect of associating different temperature differences with each stream. For the examples used here the different temperatures turns out to produce a network where several exchanger operate at the minimum temperature difference. However, this is not generally the case, but highly dependent on the actual case.

6

METHANOL SYNTHESIS

The conversion of natural gas to methanol is used as a test case for integrated design. Only some of the steps in integrated design are addressed by this example, e.g. no effort is put into improving the process superstructure, however there is a discussion of relevant additions to the superstructure that might be interesting. The methanol process described along with the relevant unit operation models, and the process is optimised. It turns out that the integrated design finds a better solution than the traditional sequential design.

In this chapter an example of integrated design will be treated, where the conversion of natural gas into methanol will be used as the test case. The case will be optimised both using sequential design and integrated design, so the two methods can be compared.

6.1 Process description

Methanol is one of the most important bulk chemicals, and is synthesized in large-scale plants. Most of the processes revolve around the production of methanol from syngas, consisting of H_2, CO and CO_2. The process was first invented by BASF in the early 20th century where they found a catalyst that would make the process run at 300 bar. The very high reaction pressure means both high capital costs and operating expenses for the plant. New catalysts have emerged, always seeking a trade-off between effectiveness in terms of converted syngas and operating pressure and today the process can run at pressures as low as 40-50 bar (Moulijn *et al.* 01).

The synthesis of methanol are typically divided into three steps

- Production of syngas from natural gas (or other fossil fuels)
- Conversion of syngas into crude methanol
- Purification of methanol

The conversion of natural gas into syngas are usually described by the reactions

$$
\begin{aligned}
CH_4 + H_2O &\rightleftarrows 3H_2 + CO & \Delta H_{rx} &= 206169 \tfrac{kJ}{kmole} & (I) \\
CH_4 + 2H_2O &\rightleftarrows 4H_2 + CO_2 & \Delta H_{rx} &= 165012 \tfrac{kJ}{kmole} & (II) \\
CO + H_2O &\rightleftarrows CO_2 + H_2 & \Delta H_{rx} &= -41157 \tfrac{kJ}{kmole} & (III)
\end{aligned}
\tag{6.1}
$$

From the reactions it is obvious that it is a highly endothermic reaction to convert methane to syngas. The conversion of syngas to methanol can be described by

$$
\begin{aligned}
CO_2 + 3H_2 &\rightleftarrows CH_3OH + H_2O & \Delta H_{rx} &= -49316 \tfrac{kJ}{kmole} & (I) \\
CO_2 + H_2 &\rightleftarrows CO + H_2O & \Delta H_{rx} &= 41157 \tfrac{kJ}{kmole} & (II)
\end{aligned}
\tag{6.2}
$$

A simplified flowsheet for the process is outlined in fig. 6-1.

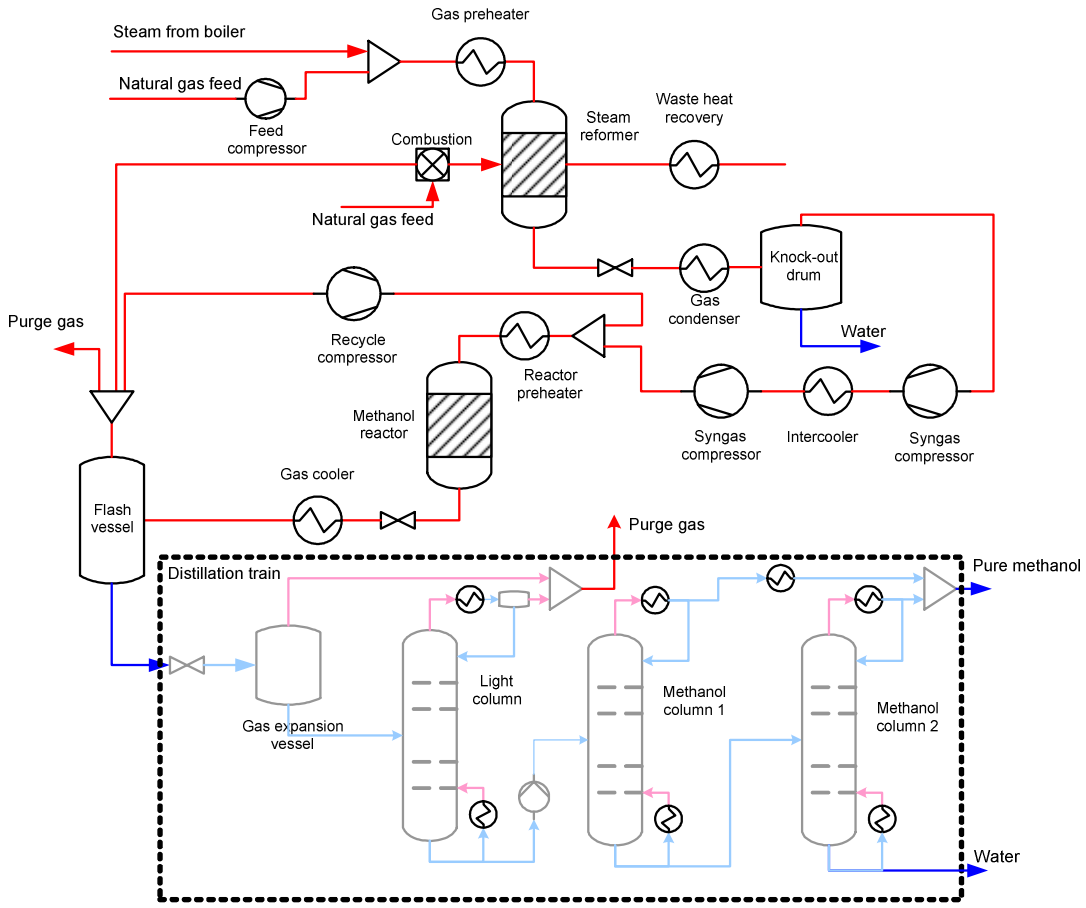

fig. 6-1 Outline of the methanol process.

The natural gas is mixed with steam and fed into the steam reformer, where catalytic conversion to syngas takes place. The reactions are highly endothermic, therefore the reformer is heated by a direct natural gas burner. Both the syngas and the flue gas leaves the reactor at very high temperature, providing a large potential for waste heat recovery. Before compression and conversion into methanol the syngas is cooled and steam is condensed. The conversion into methanol usually takes place at a higher pressure and thus a syngas

compressor is needed, here shown as a two-stage compressor with intercooler. The syngas is then mixed with the recycle gas and fed into the methanol reactor. Here the catalytic conversion to methanol takes place, but as the conversion is not complete, the outlet gas is cooled and split in a flash vessel. The unreacted syngas is recycle or purged, whereas the methanol/water mixture in the liquid phase of the flash is sent to the distillation train. Here the remaining gases in the liquid phase is removed by first a gas expansion vessel and afterwards in a column[18]. Afterwards the methanol is separated from water, in this case two columns are used, though a single column is also possible.

The syngas-to-methanol loop have already been used for simultaneous process optimisation and heat integration by (Duran and Grossmann 86b; Yee *et al.* 90b).

6.1.1 Use of method

The method proposed in chapter 3 includes a number of steps. However, only some of the steps are considered relevant for this study.

1. Process economics. This step is included to define the assumptions regarding the economy.
2. Formulation of process superstructure. In this step unit operation models for the flowsheet in fig. 6-1 are described.
3. Enhancement of process superstructure. For the sake of simplicity this step is omitted, though several suggestions for enhancements are mentioned in section 6.1.2.
4. Integrated optimisation of utility system and process superstructure. Here the findings of the optimisation are reported.
5. Verification of results, e.g. comparison with rigorous simulation tools. This step is omitted; the results are thus alone discussed based on the modelling for the optimisation. For real life applications this step is of course very important.

6.1.2 Limitations of the case

The process shown in fig. 6-1 is a traditional methanol process. Several other options do exists. Some will be briefly outlined here, but for the sake of simplicity the present example will not be extended any further.

Syngas production

Reforming of natural gas can also be done in an autothermal reformer. This works by initially combustion of some of the natural gas with pure oxygen, and thus the temperature of the feed gas rises significantly (around 2000 K). Afterwards the very hot gas is passed over an catalyst in a refractory lined vessel, which makes the operation more or less

[18] This also includes some undesired side products from the reaction

adiabatic. A reviews of recent developments in autothermal reforming is given by (Aasberg-Petersen *et al.* 03).

The oxygen for the autothermal reformer is supplied from an air-separation unit, which is quite expensive. Therefore autothermal reformers are usually only attractive for very large methanol plants (5000 metric tons pr day or more) (Rostrup-Nielsen 00). The technology will not be considered any further in this example.

Conversion of syngas to methanol

Two major methanol reactor designs are dominant on the world market, the ICI-process and the Lurgi-process. The former is an adiabatic reactor with a single catalyst bed. The reaction is quenched by adding cold gas at several points. The latter is essentially a shell and tube heat exchanger, where the catalyst material is placed inside the tubes and steam is raised on the outside. This makes the reactor more or less isothermal, depending on the heat transfer. An excellent overview of reactor technology is provided by (Tijm *et al.* 01). It is beyond the scope to go into detail with all the different types.

A single interesting option draws attention however; this is a variant of the "isothermal reactor". Instead of using a single reactor, two reactors are operated at different temperature levels, the first at high temperature to obtain a fast partial conversion combined with generation of high pressure steam, and a second reactor at lower temperature to obtain full conversion.

Besides the reactor type, the catalysts are also very important. Often these are either proprietary or at the development state at various universities. Even though a new catalyst might have a significant impact on the performance of the conversion it is considered beyond the scope of this example. It should be noted that it is often difficult or impossible to obtain rate-equations for proprietary catalysts.

In the recycle loop around the reactor a novel proposal by (Greeff *et al.* 02) suggests to include an expander in the reactor loop, thus recovering work and cooling the gas, see fig. 6-2.

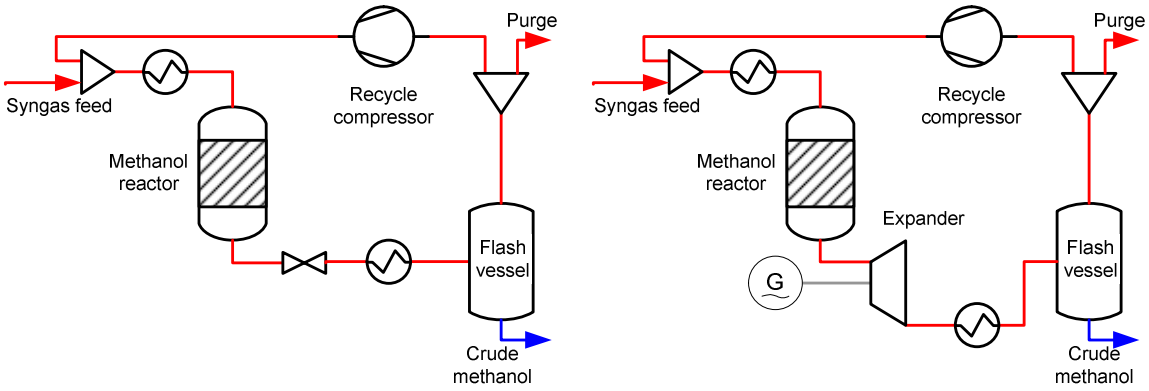

fig. 6-2 To the left the traditional methanol reactor loop, to the right an expander is placed after the methanol reactor. Here it is indicated that the expander drives a generator, but it might just as well drive the compressor.

The recycle compressor is larger in the case where the expander is included. In the traditional loop the pressure in the flash vessel is normally identical to the pressure at the outlet from the methanol reactor. For the case with the expander the pressure in the flash vessel will necessarily be lower, and therefore require a larger compressor. It depends on the utility cost and investment cost whether the expander is economically feasible.

Purification of methanol

In this example the distillation train is modelled as a black box. It is reasonable to believe that there is potential for even further optimisations in the matching of the temperature levels in the distillation columns with the utility system. In the current example the black-box model includes three distillation columns, but often two columns are used. The use of three columns saves energy, but costs more (Lurgi Chemie 05). This will not be discussed any further here, but the example in chapter 7 highlight the selection of temperature levels in the distillation columns.

6.2 Step 1: General process specifications

The prices for natural gas are based on the scenarios mentioned in chapter 3.3. In addition to the prices found in the scenarios, prices for methanol, cooling water and demineralised water are needed. These are based on various sources and assumed fixed.

- Methanol: 280 $/ton (Methanex 05)
- Cooling water: 0.04 $/ton (Peters *et al.* 03)
- Demineralised water: 0.85 $/ton (Peters *et al.* 03)

Together with the scenarios these prices make up all that is needed to estimate the running cost for the methanol process.

The process is specified to

- Production of 1000 tons methanol/day
- Natural gas feed available at 10 bar
- Ambient conditions are 1.013 bar and 25°C

The investment prices are taken from (Turton *et al.* 98), and updated to 2003 levels[19]. The costs of the pressure vessels are given for discrete diameters, which is unsuitable for the continuous optimisation, and hence a new continuous fit is proposed.

$$\begin{aligned} C_{GR} &= \frac{C_{cepci}}{382}\left(4.27 + 2.03 \cdot F_p F_M\right) 132.03 \cdot H^{0.87} \cdot 26.60 \cdot D^{0.63} \\ F_p &= 0.0369 \cdot p[bar] + 1.3644 \end{aligned} \tag{6.3}$$

Comparison of the new fit and the model by (Turton *et al.* 98) is shown below.

[19] Price updates are according to CEPCI see chapter 3.3.

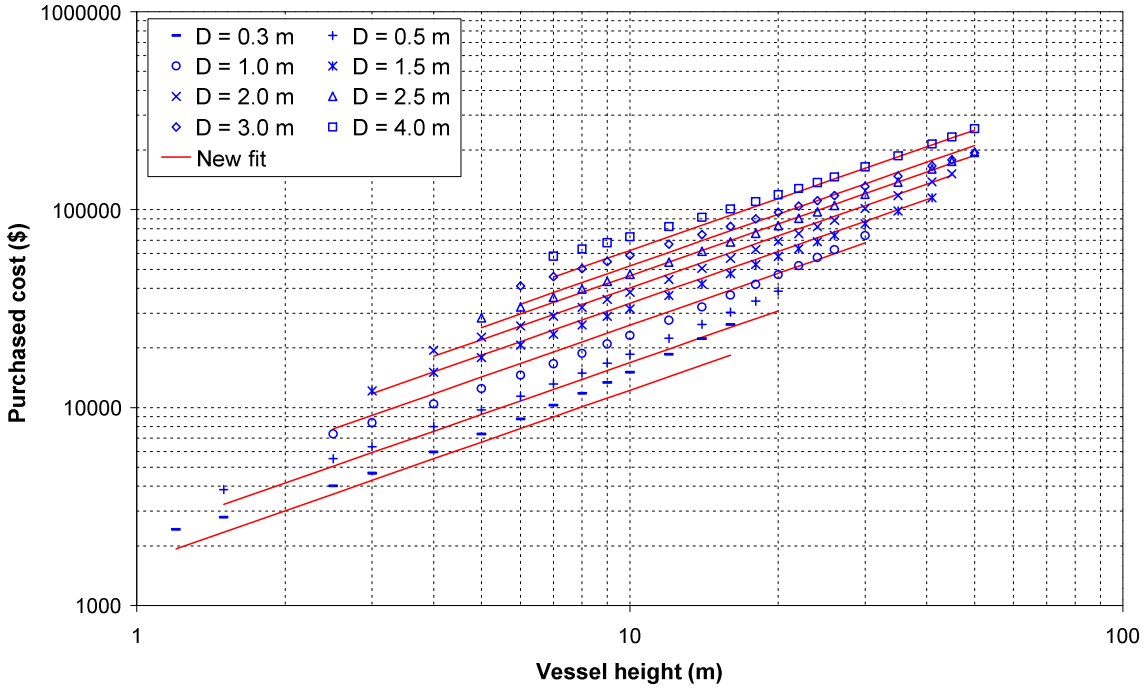

fig. 6-3 Comparison of the cost data by (Turton et al. 98) and the proposed fit in (6.3).[20]

Even though there are some discrepancies, the overall fit is quite good, with less than 5% deviations for most of the area. Only in the extremes the deviations grows larger.

6.3 Step 2: Formulation of process superstructure

In order to keep the present example simple, the process flowsheet in fig. 6-1 is used together with the utility structure in fig. 4-1. Thus no additional unit operations or alternative process paths are included. In the following the thermodynamics and unit operation models for the process is formulated.

6.3.1 Reactor modelling

Both the steam reformer and the methanol reactor are modelled as plug-flow reactors. The working principle of the steam reformer is outlined in fig. 6-4.

The natural gas and steam mixture is fed into pipes filled with catalyst material, while the outside the pipes are heated by gas burners. As the conversion to syngas takes place at high temperatures, the heat in the flue gas can be utilised for preheating the reactants and generation of steam.

[20] Note that only the purchased cost is shown, i.e. $132.03 \cdot H^{0.87} \cdot 26.60 \cdot D^{0.63}$.

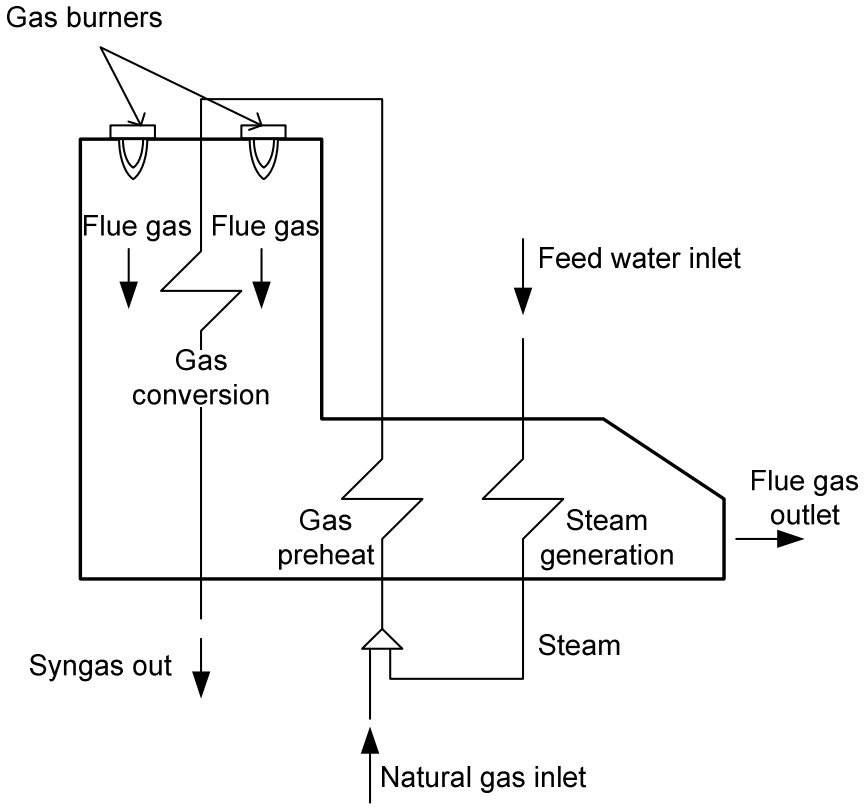

fig. 6-4 Steam reformer working principle.

The methanol reactor is assumed to be of the isothermal type, i.e. the Lurgi reactor. The syngas is fed into the reactor, that is essentially a shell'n'tube heat exchanger, see fig. 6-5. Inside the tubes are filled with the catalyst pellets, and as the reaction is exothermic heat is rejected to the boiling water on the shell side of the reactor.

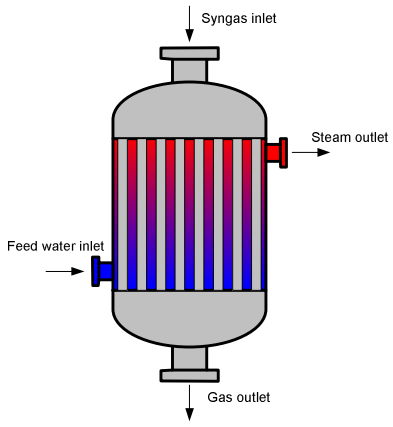

fig. 6-5 "Isothermal" methanol reactor.

General plug flow reactor model

The reactor is modelled as a plug-flow reactor with a packed catalyst bed. The mole balance for the reactor is based on catalyst weight; this is convenient, as differences in porosity etc. will not affect the solution. The mole balance for m species in q reactions are formulated as:

$$\frac{dF_i}{dW} = \sum_{j=1}^{q} \tilde{r}_{ij} \qquad \forall i \in \{1,2,\ldots,m\} \tag{6.4}$$

Note that the actual rates are used, i.e. rates compensated for the efficiency of the catalyst pellets.

The energy equation for a plug-flow reactor with q reactions and m species can according to (Fogler 99) be formulated as:

$$\frac{dT}{dW} = \frac{\frac{Ua}{\rho_b}(T_a - T) + \sum_{i=1}^{q} \tilde{r}_{ij} H_{RXij}(T)}{\sum_{j=1}^{m} F_j c_{p,j}} \tag{6.5}$$

It should be noted that an adiabatic reactor also can be modelled by this equation by setting the U-value to zero, reflecting that there is no heat exchange.

Conservation of momentum in a packed bed can be described by Ergun equation (Fogler 99).

$$\begin{aligned} \frac{dp}{dW} &= -\frac{\alpha}{2}\frac{T}{T_0}\frac{p_0}{p/p_0}\frac{F_t}{F_{t0}} \\ \alpha &= \frac{2\beta_0}{A_c\rho_c(1-\phi)p_0} = \frac{2\beta_0}{A_c\rho_b p_0} \\ \beta_0 &= \frac{G(1-\phi)}{\rho_0 D_p \phi^3}\left(\frac{150(1-\phi)\mu}{D_p} + 1.75G\right) \end{aligned} \tag{6.6}$$

Together, these three balance equations describe the reactor. To model the two reactors the rate equations for the reactions are needed. In the following the rate equations for both steam reforming and methanol conversion are presented.

Steam reforming reactions

(Xu and Froment 89) reports that the steam reforming reaction can be described by the following three reactions

$$\begin{aligned} &CH_4 + H_2O \rightleftarrows 3H_2 + CO && \Delta H_{rx} = 206169\,\tfrac{kJ}{kmole} && (I) \\ &CH_4 + 2H_2O \rightleftarrows 4H_2 + CO_2 && \Delta H_{rx} = 165012\,\tfrac{kJ}{kmole} && (II) \\ &CO + H_2O \rightleftarrows CO_2 + H_2 && \Delta H_{rx} = -41157\,\tfrac{kJ}{kmole} && (III) \end{aligned} \tag{6.7}$$

Where (I) and (II) are steam reforming reactions and (III) is the water-gas-shift-reaction. The steam reforming reactions are highly endothermic, and hence a large energy input to the reactor is needed.

In addition to the three reactions mentioned here, there are a number of undesired side reactions, especially carbon formation. This must be avoided as carbon inhibits the catalysts. The equilibrium composition for reforming of a typical natural gas is shown below (fig. 6-6), and the composition of the natural gas is found in table 6-1.

table 6-1 Typical composition of Danish natural gas.

Component	Molar fraction
CH_4	87.2%
C_2H_6	6.8%
C_3H_8	3.1%
C_4^+	1.5%
CO_2	1.4%

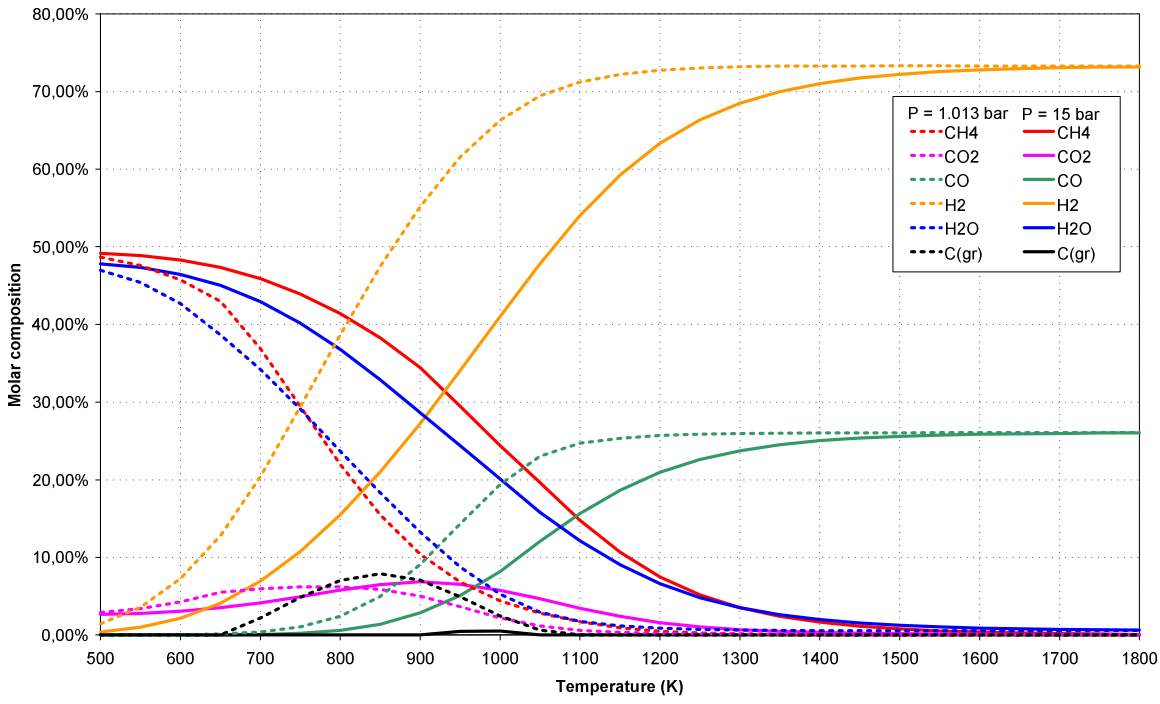

fig. 6-6 Equilibrium composition for steam reforming of natural gas with S/C-ratio of 1

It is obvious that carbon formation is potentially very high at low pressure; hence the higher operating pressure is usually favoured. The carbon formation can also be reduced by

increasing the S/C-ratio[21], and industrial reformers are thus typically operated with a S/C-ratio of 2.5 for natural gas, and even higher for reforming of heavier hydrocarbons (Moulijn *et al.* 01).

The following reaction rates for the steam reforming of methane have been proposed by (Xu and Froment 89)

$$r_I = \frac{\frac{k_1}{p_{H_2}^{2.5}}\left(p_{CH_4}p_{H_2O} - \frac{p_{H_2}^3 p_{CO}}{K_{eq,1}}\right)}{\left(1 + K_{CO}p_{CO} + K_{H_2}p_{H_2} + K_{CH_4}p_{CH_4} + K_{H_2O}\frac{p_{H_2O}}{p_{H_2}}\right)^2} \quad \left[\frac{kmole}{kg_{catalyst}\,s}\right]$$

$$r_{II} = \frac{\frac{k_2}{p_{H_2}^{3.5}}\left(p_{CH_4}p_{H_2O}^2 - \frac{p_{H_2}^4 p_{CO_2}}{K_{eq,2}}\right)}{\left(1 + K_{CO}p_{CO} + K_{H_2}p_{H_2} + K_{CH_4}p_{CH_4} + K_{H_2O}\frac{p_{H_2O}}{p_{H_2}}\right)^2} \quad \left[\frac{kmole}{kg_{catalyst}\,s}\right] \qquad (6.8)$$

$$r_{III} = \frac{\frac{k_3}{p_{H_2}}\left(p_{CO}p_{H_2O} - \frac{p_{H_2}p_{CO_2}}{K_{eq,3}}\right)}{\left(1 + K_{CO}p_{CO} + K_{H_2}p_{H_2} + K_{CH_4}p_{CH_4} + K_{H_2O}\frac{p_{H_2O}}{p_{H_2}}\right)^2} \quad \left[\frac{kmole}{kg_{catalyst}\,s}\right]$$

The indices of the rate-terms refer to the reactions above. The Arrhenius and Van 't Hoff parameters is found in table 6-2 and table 6-3 respectively.

table 6-2 Arrhenius parameters for the steam reforming reactions (Smet et al. 01)

$k = A\exp(-E_A/RT)$	A	E_A [kJ/kmole]
k_1 [kmole bar$^{0.5}$ kg^{-1} s^{-1}]	1.1736e12	240.1e3
k_2 [kmole bar$^{0.5}$ kg^{-1} s^{-1}]	2.8333e11	243.9e3
k_3 [kmole bar^{-1} kg^{-1} s^{-1}]	543.055	67.13e3

table 6-3 Van 't Hoff adsorption parameters by (Smet et al. 01)

$k = A\exp(-\Delta H/RT)$	A	ΔH [kJ/kmole]
K_{CO} [bar^{-1}]	8.23e-5	-70650
K_{H_2} [bar^{-1}]	6.12e-9	-82900
K_{CH_4} [bar^{-1}]	6.65e-4	-38280
K_{H_2O} [-]	1.77e5	88680

[21] Steam-to-Carbon-ratio

The equilibrium parameters are calculated using the NASA CEA-program (McBride 84), and the result are shown in table 6-4.

table 6-4 Equilibrium parameters for the steam reforming reaction.

$k = A\exp(-B/RT)$	A	B
$K_{eq,1}$ [bar²]	1.22473E+13	223064.62
$K_{eq,2}$ [bar²]	2.10621E+11	186483.02
$K_{eq,3}$ [-]	0.01719735	-36581.6

The reactions in a steam reformer are diffusion limited. The diffusion can either be modelled by using a heterogeneous-model, e.g. (Froment and Bischoff 90), or a pseudo homogeneous model. In the first the diffusion inside the catalyst pellets is modelled, which gives a very detailed description of the reaction and diffusion phenomena at the expense of computational complexity. The pseudo homogeneous model is simpler and uses an efficiency factor to account for the diffusion limits. This model will be used in this work, since it seems to provide a reasonable trade-off for utilisation in the flow sheet design. The efficiency factors can be considered approximately constant (DeGroote and Froment 96)

- $\eta_I = 0.07$ (CO-formation by steam reforming)
- $\eta_{II} = 0.06$ (CO2-formation by steam reforming)
- $\eta_{III} = 0.7$ (Water-gas-shift)

Based on the efficiency factors the actual rate of reactions is defined as

$$\tilde{r} = \eta r \tag{6.9}$$

Together with the general model for the plug flow reactor, this is the model of the steam reformer.

Methanol reaction

The conversion of syngas to methanol can according to (Vanden Bussche and Froment 96) be described by the hydrogenation of CO_2 (6.10) and the reverse-water-gas-shift reaction (6.11):

$$CO_2 + 3H_2 \rightleftarrows CH_3OH + H_2O \quad \Delta H_{rx} = -49316 \tfrac{kJ}{kmole} \tag{6.10}$$

$$CO_2 + H_2 \rightleftarrows CO + H_2O \quad \Delta H_{rx} = 41157 \tfrac{kJ}{kmole} \tag{6.11}$$

According to (Graaf *et al.* 86) the equilibrium constant for the methanol formation reaction can be expressed as:

$$\left(K_1^{eq}\right) = \left(\frac{p_{CH_3OH}\, p_{H_2O}}{p_{CO_2}\, p_{H_2}^3}\right) = 10^{\left(-10.592+\frac{3066}{T}\right)} \approx \exp\left(-24.389 + \frac{7059.726}{T}\right) \tag{6.12}$$

The equilibrium for the reverse-water-gas-shift is equivalent to the water-gas-shift reaction in the steam reformer.

Several expressions for the rate equation have been proposed, e.g. (Askgaard *et al.* 95; Graaf *et al.* 88; Vanden Bussche and Froment 96). Earlier studies by (Hostrup 02; Løvik 01) both suggest that the rate equation developed by (Vanden Bussche and Froment 96) provides an acceptable trade-off between precision and simplicity. The rate equations can be recast into the following form.

$$\begin{aligned} r_{1,CH3OH} &= \frac{k_d p_{CO_2} p_{H_2} \left(1 - \frac{1}{K_1^{eq}} \left(\frac{p_{H_2O} p_{CH_3OH}}{p_{CO_2} p_{H_2}^3}\right)\right)}{\left(1 + k_c \frac{p_{H_2O}}{p_{H_2}} + k_a \sqrt{p_{H_2}} + k_b p_{H_2O}\right)^3} \frac{p_{H_2}^3}{p_{H_2}^3} \\ &= \frac{\left(k_d p_{CO_2} p_{H_2}^4 - \frac{k_d}{K_1^{eq}} p_{H_2} p_{H_2O} p_{CH_3OH}\right)}{\left(p_{H_2} + k_c p_{H_2O} + k_a p_{H_2}^{3/2} + k_b p_{H_2} p_{H_2O}\right)^3} \quad \left[\frac{kmole}{kg_{catalyst} s}\right] \end{aligned} \tag{6.13}$$

$$r_{2,H2O} = \frac{k_e p_{CO_2} \left(1 - K_2^{eq} \left(\frac{p_{H_2O} p_{CO}}{p_{CO_2} p_{H_2}}\right)\right)}{1 + k_c \frac{p_{H_2O}}{p_{H_2}} + k_a \sqrt{p_{H_2}} + k_b p_{H_2O}} \frac{p_{H_2}}{p_{H_2}} = \frac{k_e p_{CO_2} p_{H_2} - k_e K_2^{eq} p_{H_2O} p_{CO}}{p_{H_2} + k_c p_{H_2O} + k_a p_{H_2}^{3/2} + k_b p_{H_2} p_{H_2O}} \quad \left[\frac{kmole}{kg_{catalyst} s}\right] \tag{6.14}$$

This leads to an introduction of two new rate constants k_d / K_1^{eq} and $k_e K_3^{eq}$. The rate constants for the recast equations are given in table 6-5.

table 6-5 Parameter values in the kinetic model[22]

k = A exp(B / (R_gT))	**A**	**B**
k_a [bar $^{-0,5}$]	0.499	17197
k_b [bar $^{-1}$]	6.62e-11	124119
k_c [-]	3453.38	0
k_d [mole / (kg s bar^2)]	1.07	36696
k_e [mole / (kg s bar)]	1.22e10	-94765
k_d / K_1^{eq} [mole / (kg-s)]	4.182e10	-22005
$k_e K_2^{eq}$ [mole / (kg-s-bar)]	1.142e8	-55078

[22] T is given in (K) and R_g is 8.315 kJ/kmole-K

The catalyst in the methanol reactor becomes deactivated over time, and several methods have been proposed to model the deactivation. (Løvik 01) provides an excellent summary of the different methods, and formulates a new model

$$\frac{da}{dt} = -K_d \exp\left(\frac{-E_d}{R_g}\left(\frac{1}{T} - \frac{1}{T_0}\right)\right) a^5$$
$$K_d = 4.39 \cdot 10^{-3} h^{-1} \quad E_d = 91270 \frac{kJ}{kmole} \tag{6.15}$$

In the model it is assumed that the initial activity is $a(t=0) = a_0 = 0.4$, and that a rescaled activity coefficient can be formulated as

$$\tilde{a} = 1 - \frac{a_0 - a}{a_0} \tag{6.16}$$

The actual rate can be found from the rescaled activity coefficient, the efficiency of the catalyst bed and the theoretical rate proposed for the reactions.

$$\tilde{r}_i = \tilde{a} \eta r_i \tag{6.17}$$

The actual rate is used in the models for the reactor. The efficiency is assumed to be 70% (Løvik 01).

6.3.2 Two-phase flash

The flash unit is simply a pressure vessel, where the inlet flow is split into a vapour and a liquid fraction, see fig. 6-7. The flash is assumed to be adiabatic.

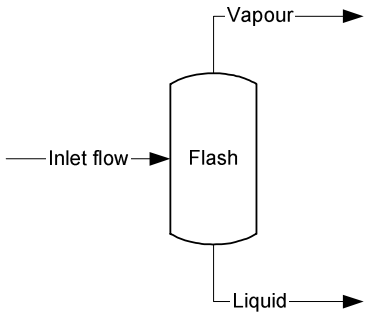

fig. 6-7 Outline of a flash vessel

This unit model requires the calculation of the equilibrium between the liquid and the vapour phase. Depending on the species of interest a number of different methods are available. The most simplified method assumes that the mixture is ideal, i.e. the mixture observe the rule

$$x_i p_{sat,i} = y_i p \tag{6.18}$$

For polar mixtures the ideal rule is not really adequate, and more advanced mixing rules, e.g. the UNIFAC method would normally be used. However, in this preliminary design phase the ideal model is used, and the simplified flash model proposed by (Biegler *et al.* 97) is used here. A key-component is selected from which the recovery of the non-key components can be calculated as:

$$\xi_k = \frac{\frac{p_0^k}{p_0^n}\xi_n}{1+\left(\frac{p_0^k}{p_0^n}-1\right)\xi_n} \quad \Leftrightarrow \quad p_0^n\xi_k = \xi_n\left(p_0^n\xi_k + \left(1-\xi_k\right)p_0^k\right) \tag{6.19}$$

Normally a component of intermediate volatility is selected as the key-component, otherwise the uncertainties might become larger, and besides the equations will be poorly scaled. The vapour pressure is found according to the Antoine equation. Finally, the bubble-point equation must be fulfilled for the liquid phase:

$$p = \sum_i y_{liquid,i} p_0^i \tag{6.20}$$

Based on the recovery coefficients, the mole balance can be formulated.

$$\begin{aligned} F_{vapour,i} &= \xi_i F_{inlet,i} \\ F_{liquid,i} &= \left(1-\xi_i\right)F_{inlet,i} \end{aligned} \tag{6.21}$$

Since the flash is considered adiabatic, the conservation of energy simplifies to:

$$T_{vapour} = T_{liquid} = T_{inlet} \tag{6.22}$$

Finally it is assumed that no pressure drop occurs in the flash vessel, and hence

$$p_{vapour} = p_{liquid} = p_{inlet} \tag{6.23}$$

Normally the volume of the vessel is designed to have a liquid hold-up time of approx. 5 min and an equal size for the vapour phase (Biegler *et al.* 97)

$$V_{flash} = 2\frac{F_{liquid}\tau}{\rho_{liquid}} \tag{6.24}$$

The flash vessel is assumed to have a height-diameter ratio of 4 and correlation (6.3) is used to calculate the investment cost.

6.3.3 Compressor

Compressors are used to raise the pressure of the gas. In large-scale plants compressors are normally either radial or axial type, depending on the desired flow and pressure ratio. In the case of methanol synthesis, a radial compressor would probably be the choice.

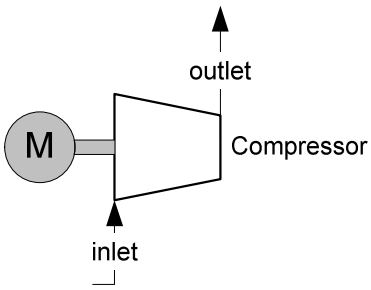

fig. 6-8 Compressor

The compressor is modelled assuming constant specific heat values during compression, and ideal gas behaviour. This assumption is quite reasonable, especially when average values for c_P and γ are used. The model is based on (Bathie 96).

The compression is assumed adiabatic, so the energy balance becomes

$$\dot{W}_{mech}\eta_{mech} + T_{in}\sum_i F_{in,i}c_{p,i} - T_{out}\sum_i F_{out,i}c_{p,i} = 0 \tag{6.25}$$

In this case, the outlet temperature can be related to the pressure ratio of the compression:

$$\frac{p_{out}}{p_{in}} = \left(\frac{T_{out}}{T_{in}}\right)^{\frac{\eta_P\gamma}{(\gamma-1)}} \quad ; \quad \gamma = \frac{c_p}{c_v} = \frac{c_p}{c_p - R_u} \tag{6.26}$$

The investment cost for the compressor is based on (Turton *et al.* 98)

$$C_{GR} = \frac{C_{cepci}}{382}\left(1.18 \cdot F_{BM} + 0.875\right) \cdot 987.42 \cdot \dot{W}^{0.9542} \tag{6.27}$$

It can be observed that the compressor is very close to being a linear function of the work-input.

6.3.4 Distillation train

In this example the distillation train is modelled as a black-box. The energy requirements for the condensers and reboilers are taken from (Kovac and Glavic 95), along with the stream temperatures for the involved streams. It is obvious that this is a very crude model, and that the full integration potential between process and utility system is probably not achived when the distillation columns are fixed.

6.4 Optimisation of integrated process and results

A number of different optimisations have been carried out in order to compare two different approaches:

- Sequential design, i.e. the process is optimised first and the utility system is optimised afterwards.

- Simultaneous design, i.e. the process and the utility system are optimised simultaneously.

First the sequential design approach is discussed.

6.4.1 Sequential design

The sequential design is of course much easier, since the optimisation problem is much smaller, but it also poses a difficulty in the formulation of the objective function. Since the utility system is unknown at the time of the process design it is uncertain how the process can be heat integrated and how much external utility that is required. There exists two ways to deal with this

- Assume that the process can be completely heat integrated, i.e. no cost is associated with heating, cooling and work requirements anywhere in the process
- Assume that no heat integration can take place at all, i.e. all heating, cooling, and work requirements must be met by external utility supply.

The first approach is somewhat optimistic, since it assumes that the process is completely self-contained, and no external utility supply is needed. The latter approach is very pessimistic, since heat integration is assumed impossible. Still this approach can be interesting as a reference point.

For the present process it is obvious that the steam reformer operates at a very high temperature. This means that there is plenty of excess heat, both in the syngas at the reactor outlet and in the flue gas used to heat the reactor. It is therefore reasonable to believe that heat for the rest of the process can be obtained purely from the excess heat. This corresponds to the first of the two alternatives mentioned above.

Solutions for both approaches have been obtained, and are compared with the simultaneous process in the following.

For the first case, where utility cost is ignored, the optimal process design is shown in fig. 6-9.

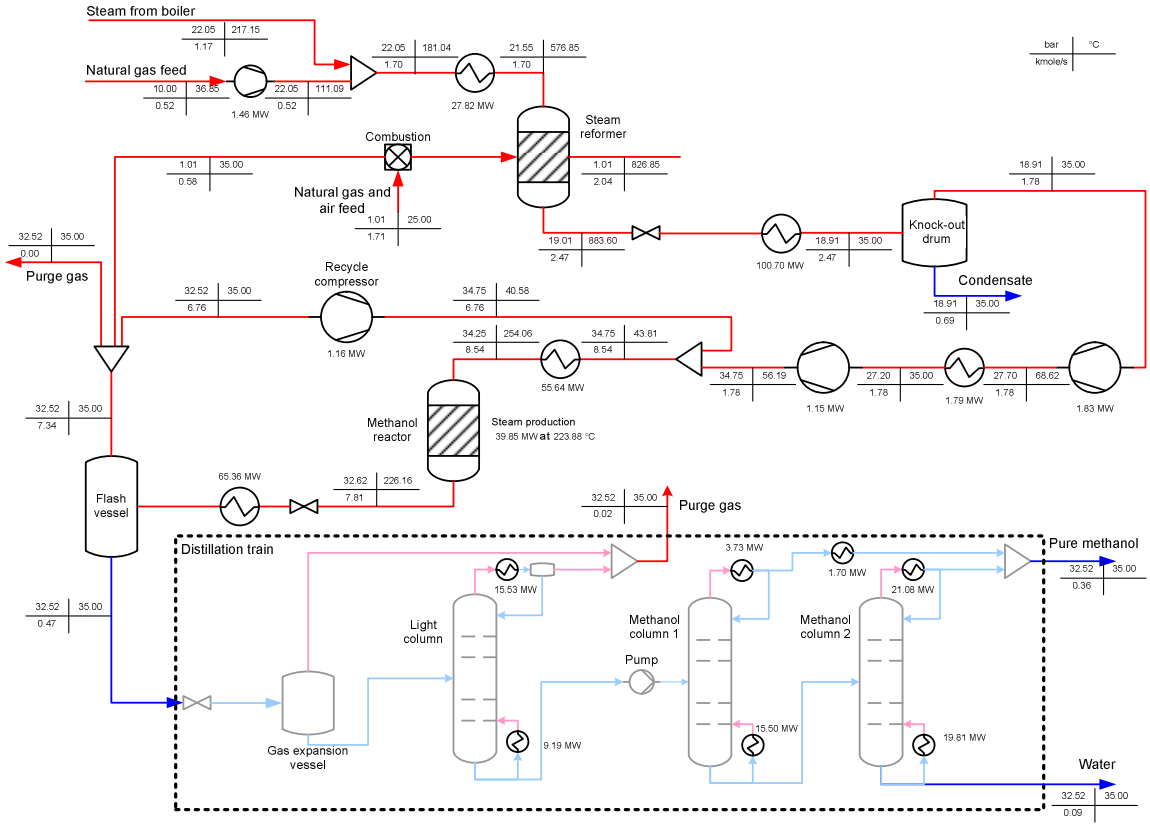

fig. 6-9 Optimal design for the process, when the utility cost is ignored.

The stream composition for a selected number of streams is shown in table 6-6.

table 6-6 Stream composition for the process flowsheet in fig. 6-9.

Component	Reformer feed	Reformer outlet	Dry syngas	MeOH rector in	MeOH reactor out	Flash vapour	Flash liquid
CO_2	1.47%	4.66%	6.46%	5.17%	4.56%	4.82%	0.45%
CO	0.02%	12.03%	16.70%	5.62%	2.56%	2.71%	0.23%
H_2	3.19%	52.82%	73.33%	80.69%	77.80%	82.63%	2.28%
H_2O	69.15%	28.19%	0.30%	0.09%	1.18%	0.03%	19.17%
CH_4	26.17%	2.32%	3.22%	7.95%	8.69%	9.19%	0.84%
CH_3OH	0.00%	0.00%	0.00%	0.49%	5.21%	0.62%	77.03%

For the case where all the utility duties are associated with full cost, the optimal flow sheet is shown in fig. 6-10.

For both processes the purge gas is used in the steam reformer. For the case “Full utility cost”, the purge rate is somewhat higher. This saves a bit on the recycle compressor, but the real save is on the heating duty before the methanol reactor and in the condenser at the reactor outlet. The lower recycle rate of course potentially makes the conversion into methanol lower, and to compensate for this the pressure in the reactor is a higher. The steam temperature in the methanol reactor is practically identical in the two cases, and a higher

steam production rate is observed in the case of "ignored utility cost", caused by the larger recycle rate. The reaction rate in the reactor is, as mentioned earlier influenced by the deactivation of the catalyst, and therefore the catalyst needs replacement from time to time.

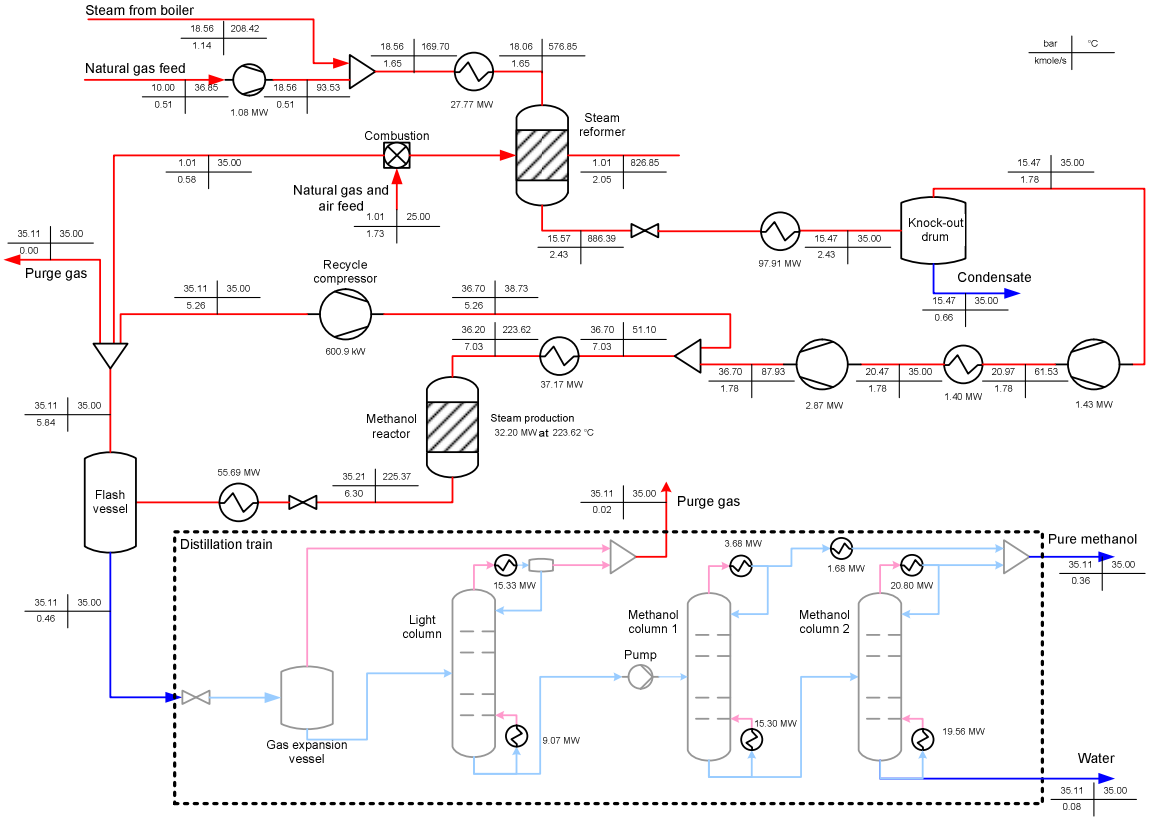

fig. 6-10 The optimal design for the case where all heating and cooling duties are associated with the fuel cost, i.e. no heat integration is assumed.

The stream composition for this case is provided in the table below.

table 6-7 Stream composition for the flowsheet shown in fig. 6-10

Component	Reformer feed	Reformer outlet	Dry syngas	MeOH rector in	MeOH reactor out	Flash vapour	Flash liquid
CO_2	1.47%	4.58%	6.27%	5.65%	5.08%	5.44%	0.55%
CO	0.02%	12.50%	17.13%	6.26%	2.42%	2.59%	0.24%
H_2	3.19%	53.93%	73.91%	82.02%	78.72%	84.76%	2.52%
H_2O	69.15%	27.30%	0.36%	0.11%	1.35%	0.03%	18.00%
CH_4	26.17%	1.70%	2.34%	5.53%	6.17%	6.60%	0.65%
CH_3OH	0.00%	0.00%	0.00%	0.43%	6.27%	0.58%	78.04%

The case for full utility cost has already a higher conversion rate due to the increased pressure, but also the time for replacement of the catalyst are reduced to 8644 hours

opposed to 11229 hours for the case without utility cost, this leads to a higher mean activity level for the catalyst.

The higher reaction pressure means that the syngas-compressors needs more power, but even this increased power consumption is easily covered by the save in heating duty before the reactor.

The pressure in the steam reformer is 3-4 bars lower for the case of full utility cost; it does not have any significant influence on the syngas composition, eventhough the different pressure levels at the steam reformer inlet influences the steam pressure at which steam must be raised.

Pinch analysis

The pinch analysis for the heat integration is presented here for both cases. In the design of the process the flue gas at the outlet of the steam reformer is very hot (825°C), and unused. It is of course obvious to utilise this heat potential. The grand composite curve for the case "ignored utility cost" is shown below.

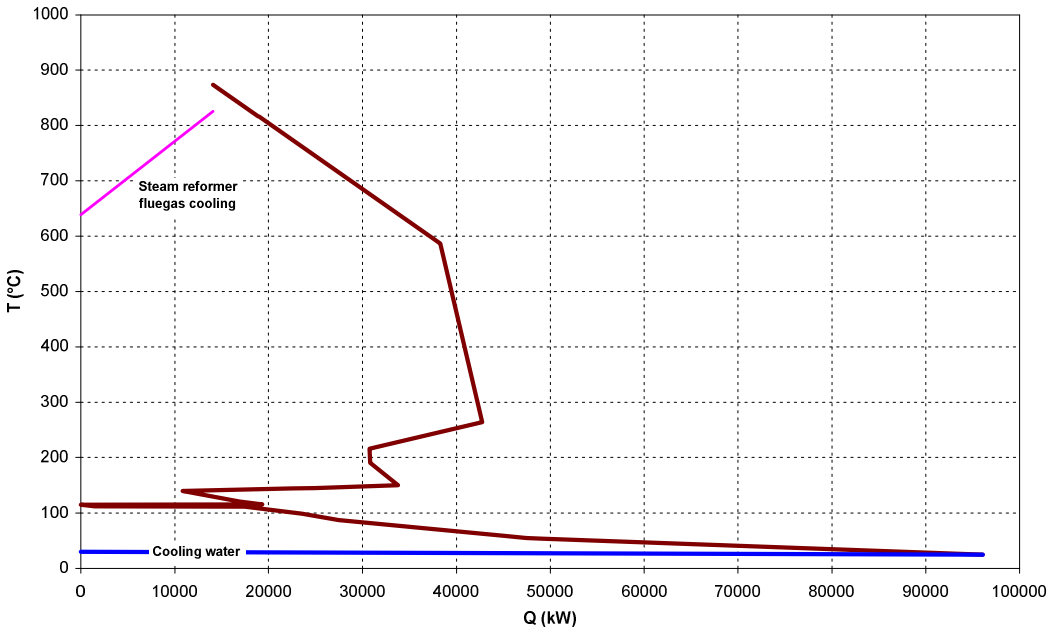

fig. 6-11 Grand composite curve for the case without utility cost.

The flue gas from the steam reformer easily covers the heating demand of the process, and still has significant heat content (625°C). This indicates that there is probably even a possibility for raising steam.

On the other hand there is a large requirement for cooling, almost 100 MW. In addition the surplus heat cannot really be used, since it is around 100°C or lower.

The grand composite curve for the case with full utility cost is almost identical, though the heating requirement is a little lower.

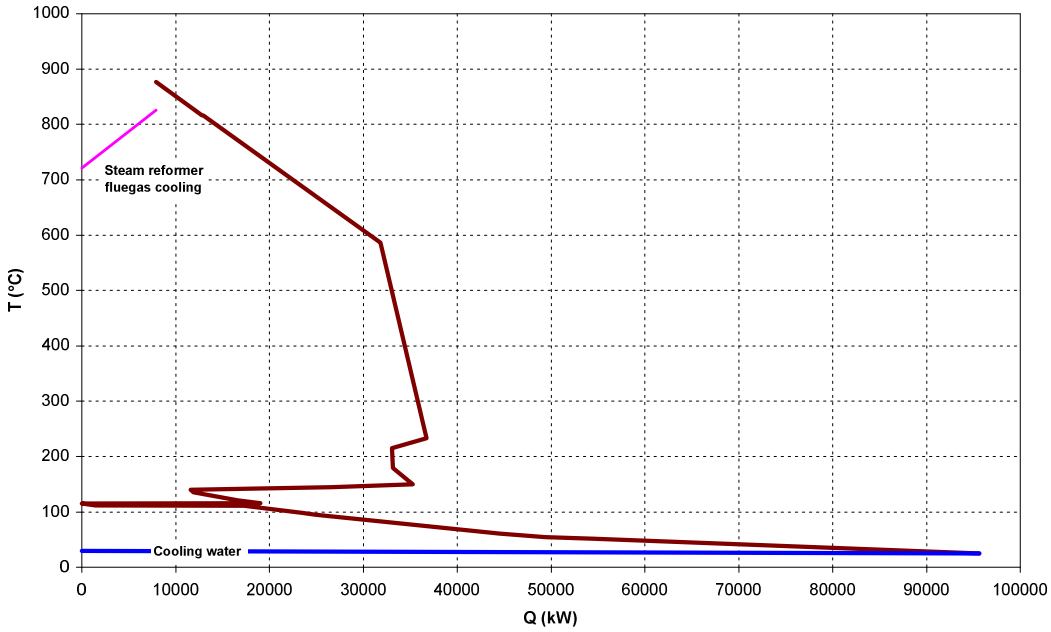

fig. 6-12 Grand composite curve for the case with full utility cost.

In this case the steam reformer flue gas is also able to cover the full heating demand.

Utility system

For each of the two cases the utility system is designed based on the set of stream data, which are found in the process flow sheets. The pinch analysis indicated that the process can supply itself with heat, but nevertheless all streams are included in the design of the utility system. In this way all options for generation of steam, and preheating of feed water will be investigated.

The utility system for the case "ignored utility cost" is shown in fig. 6-13. It is worth noting that the HP and MP pressure levels are close, 22 bar and 25 bar respectively. The steam feed to the reformer defines the MP-level, whereas the HP-level is defined by the methanol reactor. Since the pressure levels are so close the optimisation has determined that the best way to utilise the steam from the methanol reactor, is simply to let it down to the MP-level. From the MP-level a single large steam turbine is utilised for generation of electricity, both for covering the demands in the process and for selling electricity to the grid.

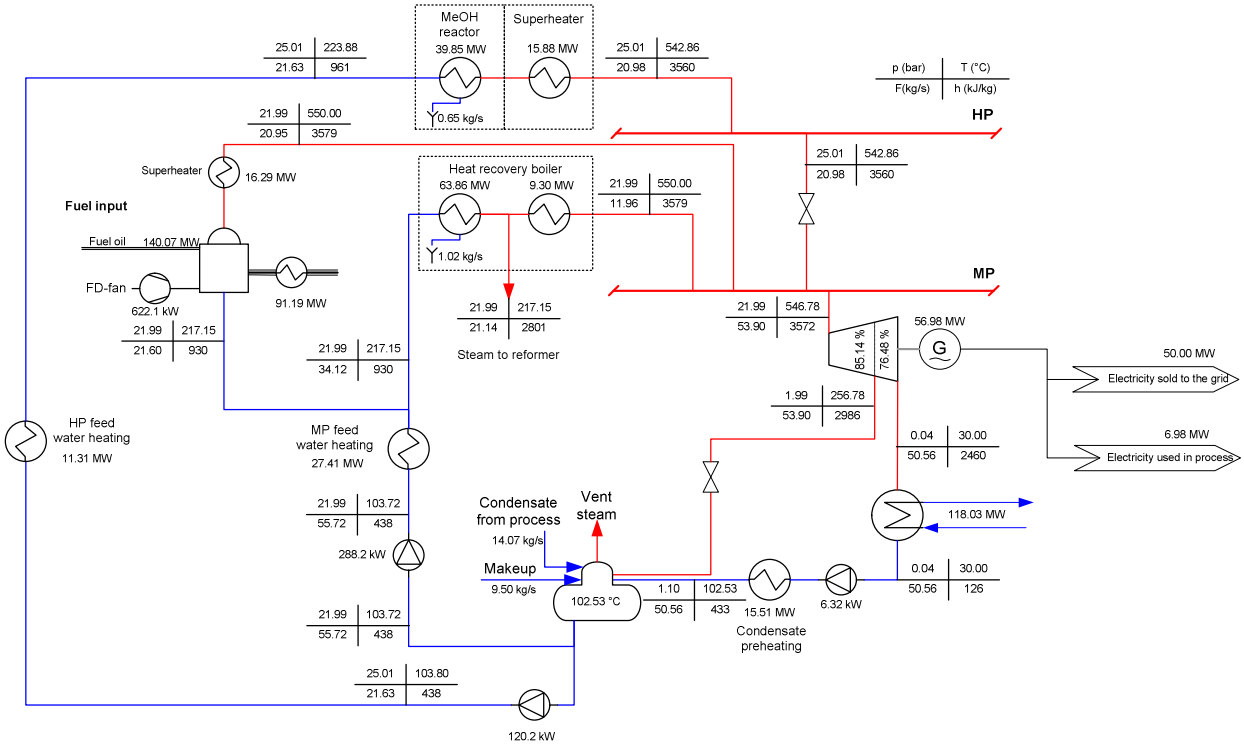

fig. 6-13 Utility system for the case "ignored utility cost"

The design of the utility system for the case of full utility cost is shown in fig. 6-14.

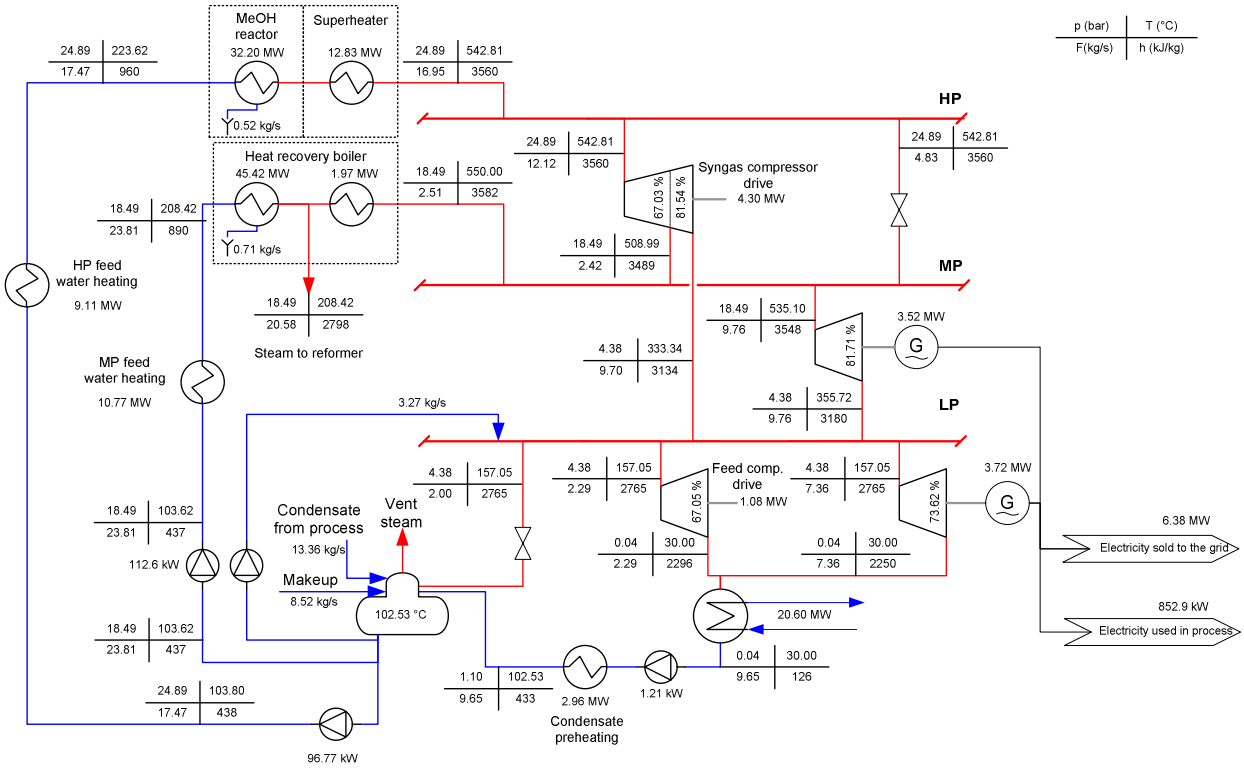

fig. 6-14 Utility system for the process design, where utility cost is included.

In this case the MP and HP headers are also very close because of the demands from the steam reformer and the temperature in the methanol reactor. A turbine drive is selected both for the feed compressor and the syngas compressor. It is worth noting that only 6.4 MW electricity is sold to the grid, and as a consequence there is no need for fuel input to the process.

6.4.2 Simultaneous design

For the simultaneous optimisation the process flow sheet is shown in fig. 6-15.

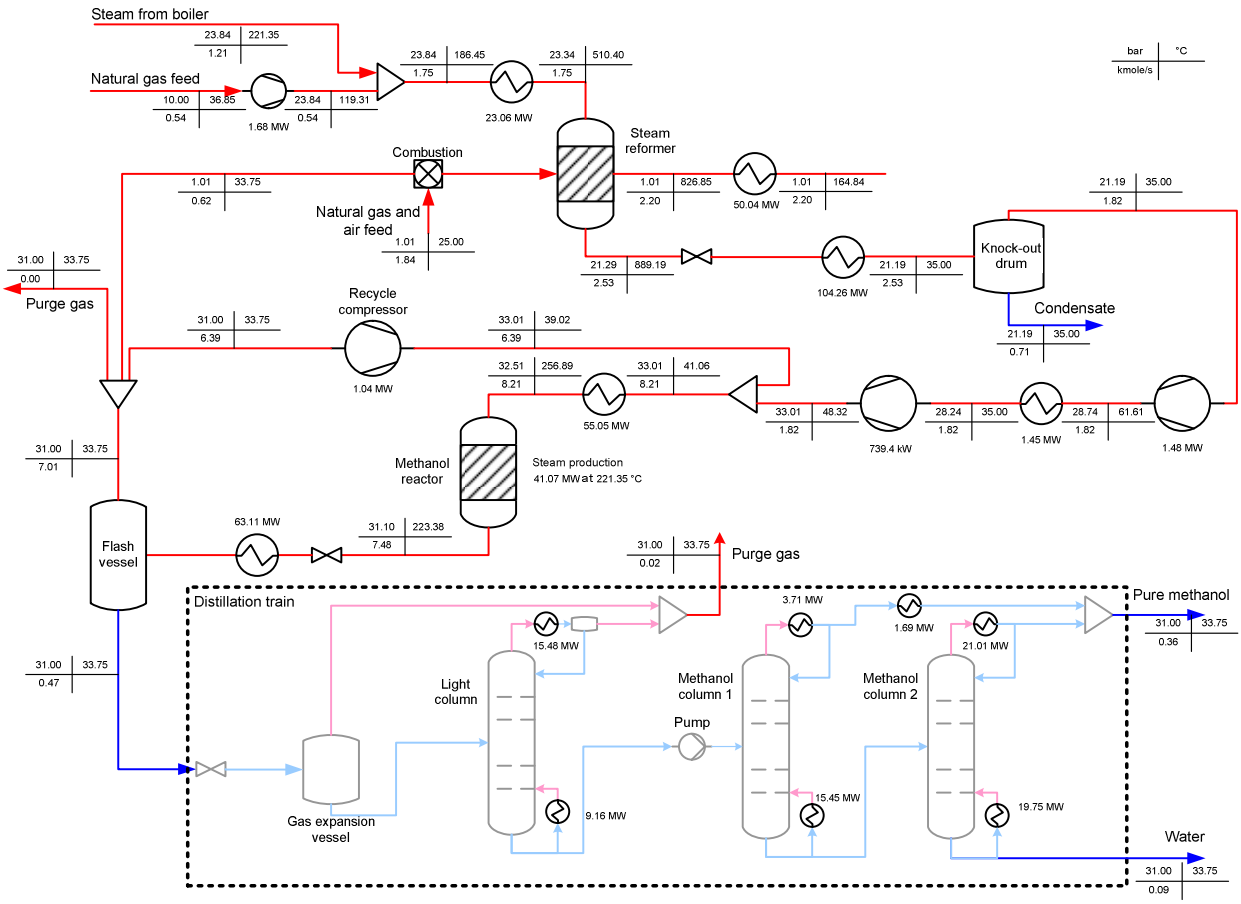

fig. 6-15 Optimal process flowsheet for simulateneous optimisation

The stream composition is shown in the table below

Component	Reformer feed	Reformer outlet	Dry syngas	MeOH rector in	MeOH reactor out	Flash vapour	Flash liquid
CO_2	1.47%	4.76%	6.63%	5.73%	5.16%	5.47%	0.51%
CO	0.02%	11.81%	16.44%	5.78%	2.59%	2.74%	0.22%
H_2	3.19%	52.58%	73.20%	79.75%	76.64%	81.61%	2.15%
H_2O	69.15%	28.36%	0.26%	0.08%	1.22%	0.03%	18.99%
CH_4	26.17%	2.49%	3.47%	8.19%	8.99%	9.53%	0.84%
CH_3OH	0.00%	0.00%	0.00%	0.48%	5.41%	0.61%	77.28%

Inspection of the solution shows that the methanol reactor has a lower operating pressure in this case than in the two previous cases, and also a slightly lower temperature. To compensate for the lower temperature the reactor is larger than in any of the two previous cases. The steam fed to the reformer matches the steam level in the reactor, thus the reactor raises the steam for use in the reformer. This is a clear sign of the interactions accounted for by the utility system, since there is now a connection between the two pressure levels.

Another interesting point is the syngas composition, which in this case is more CO- and CO_2 rich, i.e. better matched to the methanol process. It is not quite clear why the other two solutions failed to recognise this important fact.

The steam reformer is operated at a higher pressure than in the previous cases and combined with the lower pressure in the methanol reactor, which leads to a significantly lower work requirement of the syngas compressors. On the other hand there is a slight rise in the feed compressor requirement. In the previous flowsheets the steam generation for the reformer was not really accounted for until the design of the utility system. In the simultaneous case the heat and power consumption for raising steam is completely transparent for the optimisation. The utility system for the simultaneous optimisation is shown in fig. 6-16.

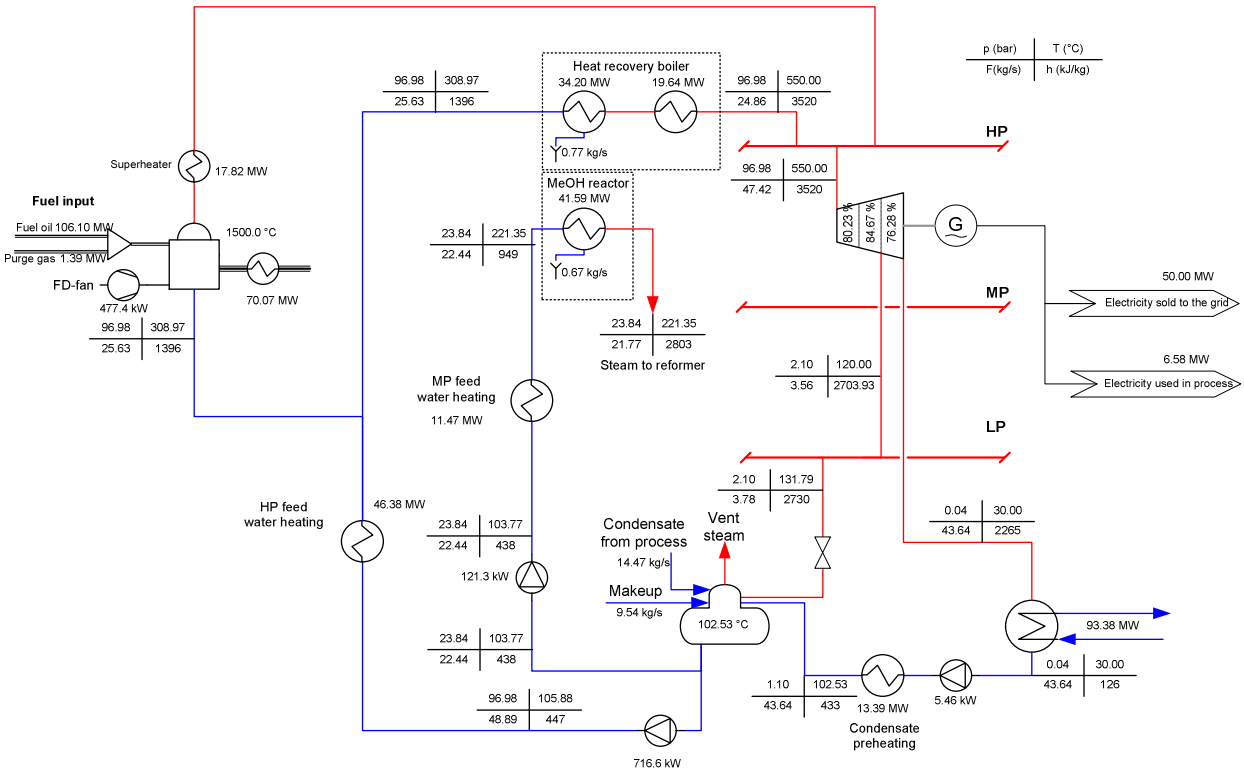

fig. 6-16 Utility system for simultaneous optimisation

In this case 50 MW electricity is sold to the grid, an therefore a single steam turbine with a high efficiency is selected to produce both electricity for sale and for the compressor drives.

The methanol reactor is used to raise steam for the steam reformer, and the heat recovery boiler along with the fuel oil fired boiler produces high pressure steam at 96 bar. The steam parameters are much higher than in the two previous cases, and it is clear that this increases the electric efficiency of the utility system. Consequently the fuel oil consumption has dropped by 35 MW compared to the system in fig. 6-13.

The net present worth for the complete plant (process and utility) for all the cases are compared in fig. 6-17.

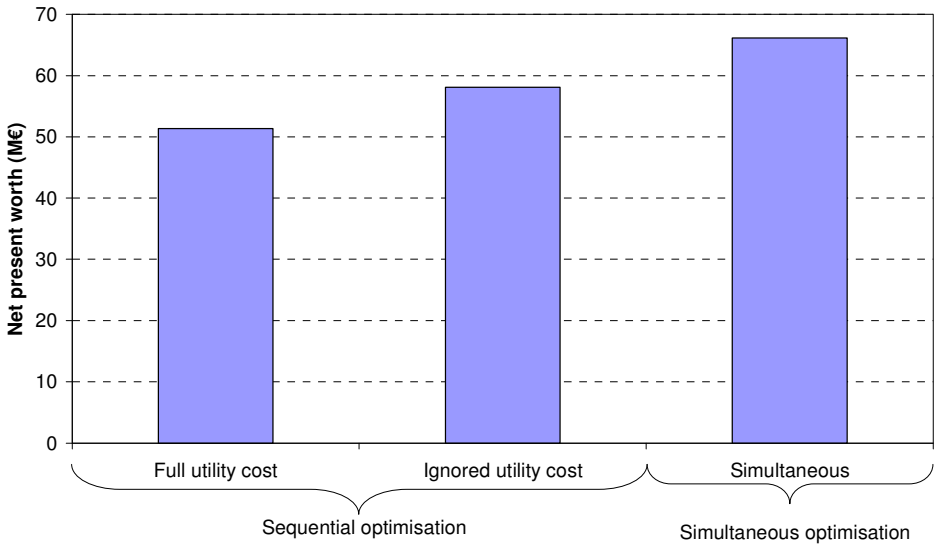

fig. 6-17 Comparison of the net present worth for the three different cases. Economics are all from scenario 1.

It is clear that the simultaneous method is better than the two sequential cases.

6.5 Summary

In this chapter the synthesis of methanol from natural gas was used as an example for integrated design. It has been shown that for this example the simultaneous method is able to find a better optimum than the sequential method. The net present worth of the integrated approach is 12% higher than for the best of the sequential approaches. The model of the methanol synthesis plant was limited to include a steam reformer and a single methanol reactor. Both these reactors were modelled with differential equations, providing a detailed estimate of the operating conditions. The models are highly non-linear; primarily because of the complicated reactions that takes place in the two reactors. On the other hand the distillation train was assumed fixed, and thus not included in the optimisation. In total there was around 10000 constraints and more variables. This proved that the disjunctive solver could handle problems of a realistic scale, although most of the workload was of course on the NLP-solver.

It is interesting to notice that not only does the utility system change for the simultaneous case, but also a number of process parameters changes. This suggests that there is an interaction between the utility system and the process that the sequential method does not include.

All the results have been calculated using price scenario 1, but calculations using scenario 2 and 3 shows a similar tendency.

A number of interesting process alternatives can be investigated in future work, and was briefly outlined in the beginning of the chapter.

7

HYDRO-DEALKYLATION OF TOLUENE TO BENZENE AND METHANE

The well-known HDA-test case is used here for examination of the integrated design method. Initially the process is described, the process superstructure proposed and the unit operation models are formulated. The base case by (Douglas 88) is used for an exergy analysis and discussion of the process and the superstructure. The optimisation of the superstructure both with traditional hierarchical design and integrated design are carried out. Comparison of the results shows an increased net present worth for the plant designed with integrated design.

The hydro-dealkylation of toluene into benzene and methane is one of the most well established test cases in process engineering. It was first presented by (Douglas 88) and afterwards it has been used by many others as a test case for process integration.

7.1 Process description

The process will be shortly described; the flowsheet is outlined in fig. 7-1. The primary reaction for production of benzene from toluene:

$$Toluene + H_2 \rightarrow Benzene + CH_4 \quad \Delta H_{rx} = -41910 \frac{kJ}{kmole} \tag{7.1}$$

In addition, diphenyl is produced in an undesired side reaction

$$2\ Benzene \rightleftarrows Diphenyl + H_2 \quad \Delta H_{rx} = 16140 \frac{kJ}{kmole} \tag{7.2}$$

The superstructure for the process was first presented by (Kocis and Grossmann 89). First, a short description of the system is provided, and afterwards a number of issues related to their formulation are pointed out.

The process is fed with toluene and hydrogen (actually 95% hydrogen and 5% methane). The hydrogen feed can optionally be purified in a membrane separator, though this results

in pressure loss and the gas must be recompressed. Afterwards the hydrogen is mixed with the toluene feed and the recycle streams for both hydrogen and toluene, this forms the reactant gas. The reaction takes place at high temperatures (around 900 K), which means that the reactant gas must be heated. Optionally, waste heat can be used in a preheater, and afterwards a furnace is needed to raise the temperature even further. The reaction can take place in either an adiabatic or an isothermal reactor. Immediately after the reaction, the products must be quenched to prevent coking. The products are cooled even further and flashed, to separate the products in a vapour stream (methane and unreacted hydrogen) and a liquid stream (benzene, toluene, and diphenyl). Since the purity of the benzene must be around 99.9% a liquid separation system is needed to separate the benzene from the toluene and diphenyl.

The liquid flow also contains a small amount of hydrogen and methane, which must be removed from the liquid flow. This can either be done in a stabilising column or in another flash unit. It is assumed that the stabilising column has a partial condenser, since hydrogen is very volatile. A small amount of benzene will inevitably remain in the vapour flow from the stabilising column, so the vapour can be run through a gas absorber to recover the benzene. In the benzene column the benzene is separated from the toluene and diphenyl, leaving toluene and diphenyl at the bottom. Finally, the diphenyl can be separated from the toluene, either in another distillation column or in a flash unit.

In the vapour recovery system the hydrogen/methane flow can be recycled, either with a purge to avoid building up methane in the system, or with a membrane separator to purify the hydrogen. The small amounts of benzene in the vapour flow can optionally be recovered in the gas absorber.

The optimisation problem is provided as one of the standard test cases with GAMS (Brooke *et al.* 98) and is actually provided through the work of (Kocis and Grossmann 89). The original formulation has a number of shortcomings however, which are improved in this work.

- The toluene feed is at liquid conditions, so a two phase mixer must be used
- The condensers and reboilers of the distillation columns are included.
- The investment price for the membrane separator are improved, and now take the area cost into account
- The heat of reaction is no longer assumed independent of temperature, and the side-reaction is no longer assumed to have the same heat of reaction as the main reaction.

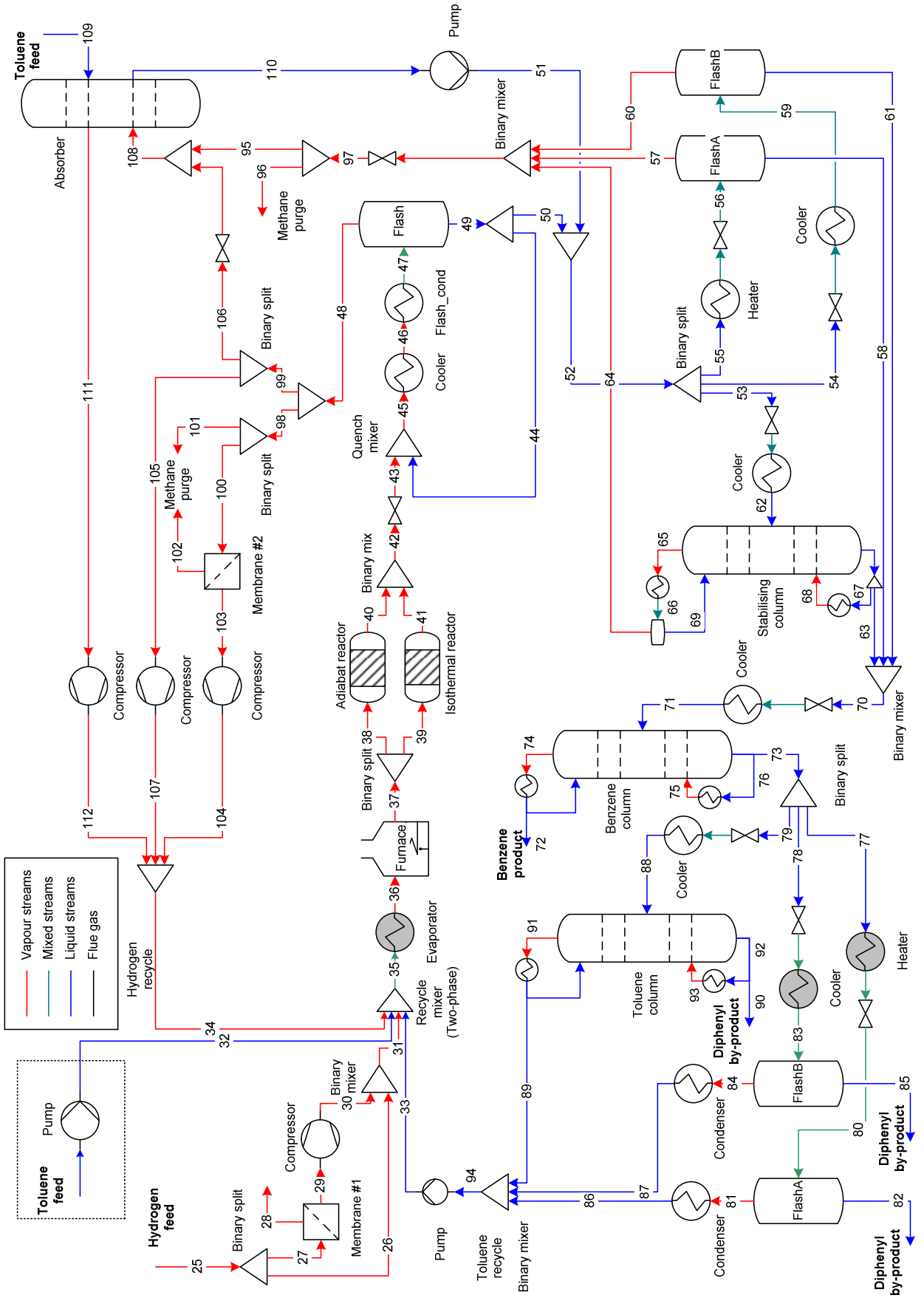

fig. 7-1 Flowsheet for the HDA-process.

7.1.1 Use of method

The method proposed in chapter 3 includes a number of steps. However, only some of the steps are considered relevant for this study.

1. Process economics. This step is included to define the assumptions regarding the economy.
2. Formulation of process superstructure. In this step unit operation models for the flowsheet in fig. 7-1 are described.
3. Enhancement of process superstructure. Here the base case provided by (Douglas 88) is used for an exergy analysis to identify potentials for increasing efficiency.
4. Integrated optimisation of utility system and process superstructure. Here the findings of the optimisation is reported.
5. Verification of results, e.g. comparison with rigorous simulation tools. This step is omitted, the results are thus alone discussed based on the modelling for the optimisation. For real life this step is of course very important.

7.2 Step 1: Process specifications

A number of specifications are needed in order to optimise the process.

- 265 kmole/hr of benzene shall be produced at 99.7% purity
- Hydrogen feed is 95% hydrogen and 5% methane, available at 40 bar and 300 K
- Toluene feed is 100% toluene and available at ambient conditions.
- Ambient conditions are 1.013 bar and 15°C

All the investment prices are updated to 2002 levels. The prices for the feeds and product are chosen to be

- Hydrogen feed 4.2 $/kmole (Kirschner 03a)
- Toluene feed 27.5 $/kmole (Bianchi and Uctas 03; Kirschner 03b)
- Benzene product 35.0 $/kmole (Bianchi and Uctas 03; Brown 03)
- Diphenyl product 20 $/kmole (Kocis and Grossmann 89)

Note that no updated price for the cost of diphenyl has been found; instead, it has been updated with same ratio as for benzene and toluene.

The utility prices are all based on (Peters *et al.* 03)

- Cooling water cost 0.04$/ton

It is chosen to use an objective function that is based on the net present worth method, with the following parameters

- Internal rate of return 8%
- Time horizon 10 years

Generally, the economic parameters are associated with significant uncertainties which means that the result must be checked for the sensitivity of these parameters.

7.3 Step 2: Formulation of process superstructure

In this section the thermodynamics and reaction are presented first, and afterwards the unit operation modelling is described.

7.3.1 Thermodynamics and reaction

The thermodynamics for this example is based on the ideal gas equation of state. This is not entirely correct, but has been chosen to keep the example simple. Vapour-liquid equilibria are also modelled using ideal separation models, and the vapour pressure is calculated by the Antoine equation. Data for the thermodynamic properties can be found in appendix 10.

Reaction

According to (Douglas 88) the rate equation for the toluene formation (7.1) is

$$r_{tol} = -k\sqrt{C_{H2}} \tag{7.3}$$

In addition, the kinetic constant can be evaluated through Arrhenius' law.

$$k = 6.3 \cdot 10^{10} \exp\left(-\frac{52000\left[\frac{cal}{mole}\right]}{R_u T}\right)\left[\sqrt{\frac{mole}{L}}\,\frac{1}{s}\right] \tag{7.4}$$

The undesired formation of diphenyl is relatively small compared to the main reaction, and therefore it can be modelled through a simplified method, suggested by (Douglas 88). Instead of a separate rate equation for this reaction, the selectivity S towards conversion of toluene into benzene can be described in terms of the overall conversion x from toluene to benzene.

$$S = \frac{\text{Moles of benzene produced}}{\text{Moles of toluene converted}} = 1 - \frac{0.0036}{(1-x)^{1.544}} \tag{7.5}$$

7.3.2 Unit operation models

Reactor modelling

If isothermal operation is assumed, the volume of a plug flow reactor can be evaluated using the design equation. For isothermal operation the integration along the reactor length can be found analytically.

$$V = F_{H_2}\int_0^X \frac{dX}{-r} = \frac{2\sqrt{F_{tot,0} R_U T_0 F_{H,0}}}{k\sqrt{p_0}}\left(1-\sqrt{1-X}\right) \tag{7.6}$$

It is obvious that the assumption of isothermal operation does not hold for the adiabatic reactor, but in this case, the mean temperature between inlet and outlet is used as the "isothermal temperature".

Distillation models

The modelling of a distillation column can be very complicated, but fortunately a number of short-cut methods are available that will fit into this framework. For these models to work a number of assumptions are made

- The distillation is sharp, e.g. components lighter than the light key[23] are 100% recovered, and vice-versa for components heavier than the heavy key.
- There are no intermediate components between the light and the heavy key

The modelling of the distillations column follows simplified methods, usually referred to as the Fenske-Underwood-Gilliland method, e.g. (Douglas 88; Peters *et al.* 03). Given a desired purity specification for both the heavy and the light key-components ξ_{lk} and ξ_{hk} the minimum number of theoretical equilibrium trays $N_{\min}$ can be determined from the Fenske-equation

$$N_{\min} = \frac{\ln\left(\frac{\xi_{lk}\left(1-\xi_{hk}\right)}{\xi_{hk}\left(1-\xi_{lk}\right)}\right)}{\ln \alpha_{lk/hk}} \tag{7.7}$$

Afterwards the minimum reflux ratio $R_{\min}$ can be determined from the Underwood equation

$$\sum_{i=1}^{n} \frac{\alpha_i y_{F,i}}{\alpha_i - \Theta} = 1 - \overline{q} \quad ; \quad R_{\min} + 1 = \sum_{i=1}^{n} \frac{\alpha_i y_{D,i}}{\alpha_i - \Theta} \tag{7.8}$$

According to (Douglas 88), this can be simplified for the case of high purity separations and for saturated liquid feed, that is $\overline{q} = 1$.

$$R_{\min} \approx \frac{1}{\left(\alpha_{lk/hk} - 1\right) x_{feed}^{lk}} \tag{7.9}$$

The actual reflux ratio is assumed to be $1.2R_{\min}$ and hereby the number of theoretical trays N can be found from Gillilands equation

$$\frac{N - N_{\min}}{N+1} = 0.75\left[1 - \left(\frac{R - R_{\min}}{R+1}\right)^{0.566}\right] \tag{7.10}$$

Gilliland have also proposed a simplified equation, specially for the case where $R = 1.2R_{\min}$ (Douglas 88)

$$N \approx 2N_{\min} \tag{7.11}$$

[23] In distillation the objective is to separate a light component (light key) from a heavy component (heavy key). The light key surfaces at the top of the column, whereas the heavy key leaves the column at the bottom.

In fig. 7-2 equation (7.10) is plotted for different values of N_{min} and R_{min} to illustrate the simplification in (7.11). It is clear that (7.11) represents the lower bound and more trays are needed when either the minimum reflux is small or the number of theoretical trays is small.

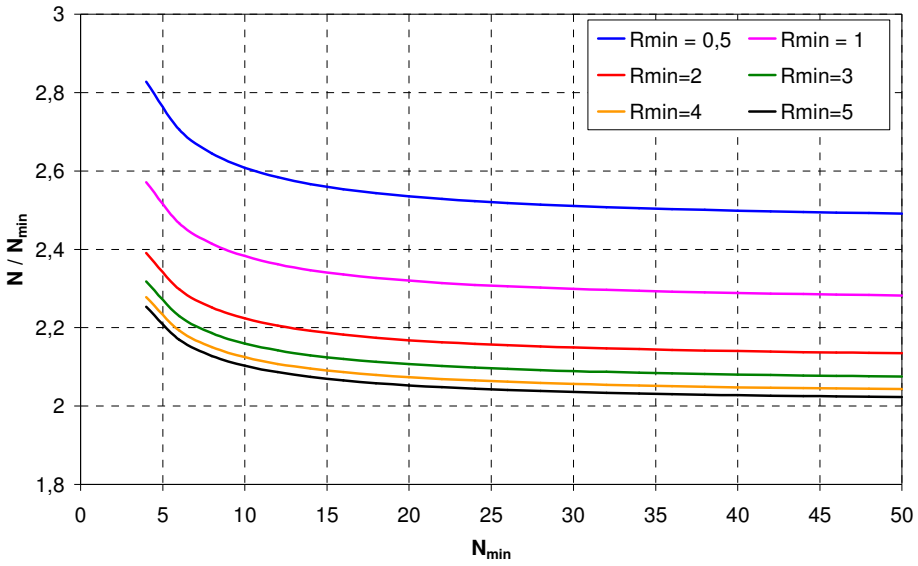

fig. 7-2 Plot of equation (7.10) for different values of N_{min} and R_{min}, with $R = 1.2R_{\min}$

Finally, the actual number of trays can be found from the tray efficiency:

$$N_{act} = \frac{N}{\eta_{tray}} \tag{7.12}$$

For distillation column tray efficiencies around 80% can be expected (Biegler *et al.* 97).

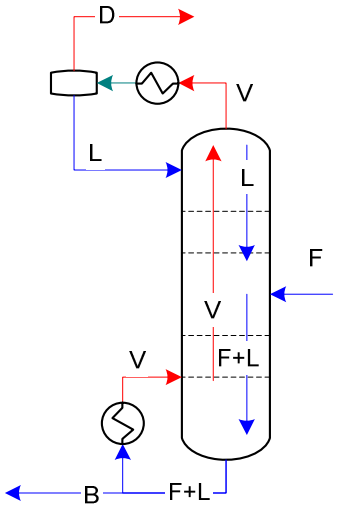

fig. 7-3 Column with partial condenser

The columns considered so far have a reboiler at the bottom and a condenser at the top. For columns operating with very volatile components, it might be difficult or very expensive to condense at the components at the top; thus, a partial condenser can be used instead, as outlined in fig. 7-3.

The partial condenser is followed by a flash vessel, and therefore the column model must be combined with a flash model, as the one described in chapter 6.3.2.

For estimation of the column diameter, the flooding velocity is obtained through the following simplified expression based on (Biegler *et al.* 97).

$$U = 0.101\sqrt{\frac{\rho_{liquid}}{\rho_{vapor}}} \quad ; \quad \rho_{vapor} = \frac{p}{R_u T} \tag{7.13}$$

From this the column diameter can be estimated

$$V = \rho_{vapor} U \varepsilon \pi \frac{D^2}{4} = 0.101 \rho_{vapor} \sqrt{\frac{\rho_{liquid}}{\rho_{vapor}}} \varepsilon \pi \frac{D^2}{4} = 0.101 \sqrt{\rho_{liquid} \rho_{vapor}} \varepsilon \pi \frac{D^2}{4} \tag{7.14}$$

The investment cost is calculated from equation (6.3).

Membrane separator

The membrane separator is used to separate methane from hydrogen, based on differences in permeability through the membrane material. As all the aromatics are much larger molecules than the hydrogen and methane it is assumed that none of them can diffuse through the membrane.

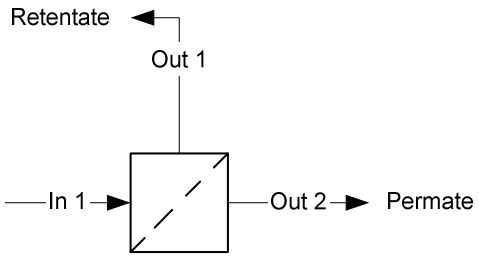

fig. 7-4 Definitions for the membrane separator

The driving force for a membrane separator is the pressure drop across the membrane. The mole balance across the membrane are modelled using a shortcut model, assuming an average concentration as driving force

$$F_p^i = P_i A\left(p_r^i - p_p^i\right) \tag{7.15}$$

The partial pressure of the retentate p_r^i is assumed to be a simple average of inlet and outlet.

$$p_r^i = p_r^{tot}\left(\frac{y_{in}^i + y_{out}^i}{2}\right) \tag{7.16}$$

The permeability constants are found in (Brandrup and Immergut 75). The investment cost for the vessel is estimated using the correlations in (6.3). The size of the vessel is estimated based on the area of the membrane and the packing (m^2 membrane pr. m^3 volume). The cost of the membrane itself is assumed to be a function of the area. (Peters *et al.* 03).

Absorber model

The absorber is used to recover benzene in the vapour flow, thereby ensuring that only a minimum amount of the benzene is purged. Liquid toluene is used as solvent in the absorber.

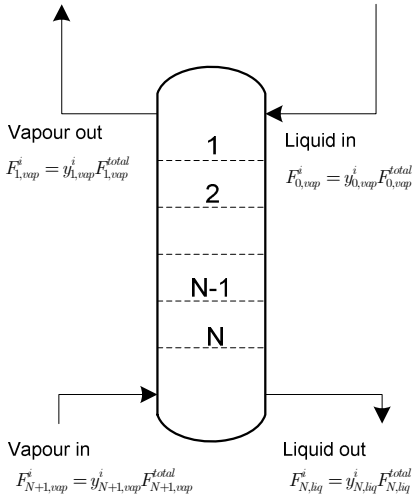

fig. 7-5 Outline of an absorber with N trays

The short-cut method described by (Biegler *et al.* 97) is used. This method uses an averaged effective absorption coefficient for the entire tower, instead of each individual tray. According to (Douglas 88) the effective absorption coefficient for the selected key component n are usually around $A^n_E = 1.4$. Based on this this, effective absorption coefficients for the non-key components can be found through

$$A^i_E = \frac{A^n_E}{\alpha_{i/n}} \quad ; \quad \alpha_{i/n} = \frac{p^0_i(T)}{p^0_n(T)} \quad ; \quad i \neq n \tag{7.17}$$

The variable β is defined for each key-component (benzene and toluene) as

$$\beta^i_N = \frac{\left[1 - \left(A^i_E\right)^{N\eta_{tray}+1}\right]}{1 - A^i_E} \quad ; \quad \beta^i_{N-1} = \frac{\left[1 - \left(A^i_E\right)^{N\eta_{tray}}\right]}{1 - A^i_E} \tag{7.18}$$

For the non-key components (methane and hydrogen) it is assumed that they are non-condensible and thus not absorbed in the liquid stream. This can be modelled by setting $\beta_N = \beta_{N-1} = 1$. Based on the β variables the mole balance for each component can be formulated as

$$F^i_{1,vap} = \frac{F^i_{N+1,vap} + \beta^i_{N-1} F^i_{0,liq}}{\beta^i_N} \tag{7.19}$$

For the complete derivation of the model see (Biegler *et al.* 97).

In order to simplify the equations, the number of trays is treated as a continuous variable, instead of a discrete variable. The tray efficiency in absorbers is usually quite low, around 20%.

The volume and the cost of the absorber is found in the same way as for the distillation column, see (7.14).

7.4 Step 3: Enhancement of the superstructure

The superstructure formulated by (Kocis and Grossmann 89), already includes a number of enhancements compared to the original flowsheet by (Douglas 88).

- An absorber is included to facilitate recovery of benzene from the flash separation
- A membrane separator is included to recover hydrogen from the purge.
- The overhead from the stabiliser column can be recycled
- Both the stabiliser column and the toluene column can be replaced with flash separation units.

The superstructure thus includes a number of options not included in the original work. To investigate the process, an exergy analysis is performed on the base-case as formulated by (Douglas 88), which is shown in fig. 7-6. Furthermore an economic analysis is performed.

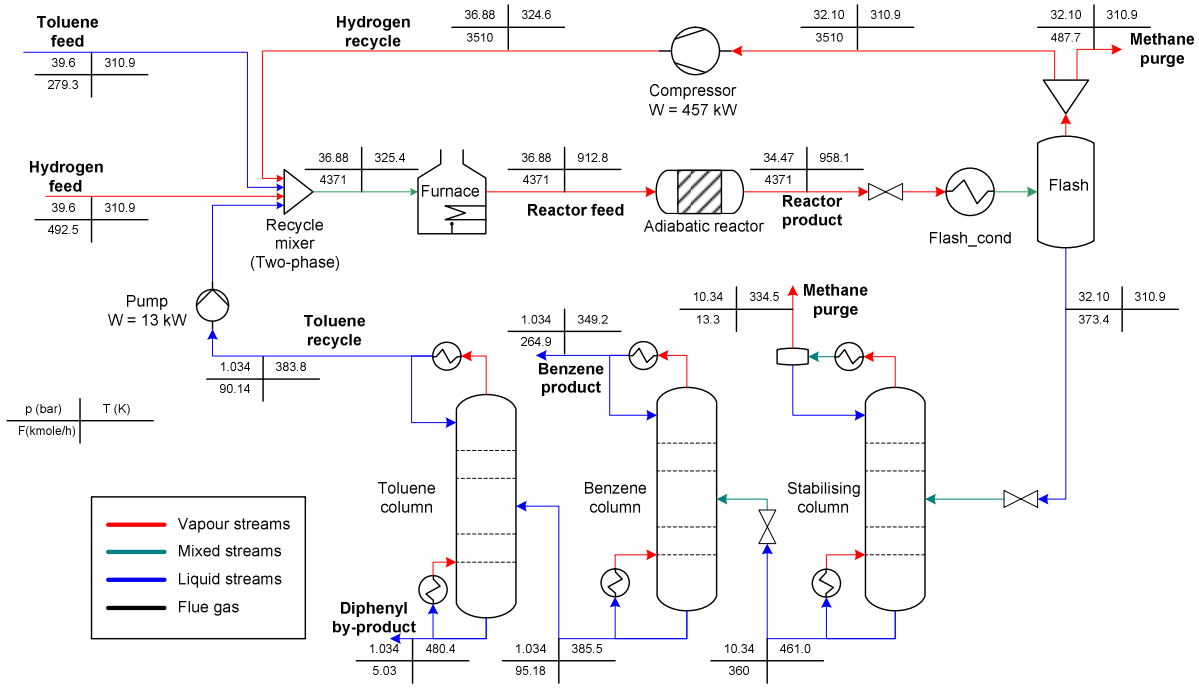

fig. 7-6 Base case, the original process proposed by (Douglas 88)

The flow composition is given in table 7-1.

table 7-1 Stream composition for the original flowsheet by (Douglas 88)

Component (mole %)	Hydrogen feed	Toluene feed	Hydrogen recycle	Toluene recycle	Reactor feed
H2	95.0%	0.0%	39.42%	0.00%	42.35%
CH4	5.0%	0.0%	59.75%	0.00%	48.53%
C6H6	0.0%	0.0%	0.74%	1.48%	0.63%
C7H8	0.0%	100.0%	0.09%	98.50%	8.49%
C12H10	0.0%	0.0%	0.00%	0.03%	0.00%
Component	**Reactor product**	**Flash liquid**	**Methane purge**	**Benzene product**	**By-product**
H2	36.09%	0.40%	11.10%	0.00%	0.00%
CH4	54.90%	2.98%	82.90%	0.02%	0.00%
C6H6	6.79%	71.47%	6.00%	99.95%	0.00%
C7H8	2.12%	23.92%	0.00%	0.03%	8.87%
C12H10	0.11%	1.23%	0.00%	0.00%	91.13%

The results of the exergy analysis on the above system are summarised in fig. 7-7.

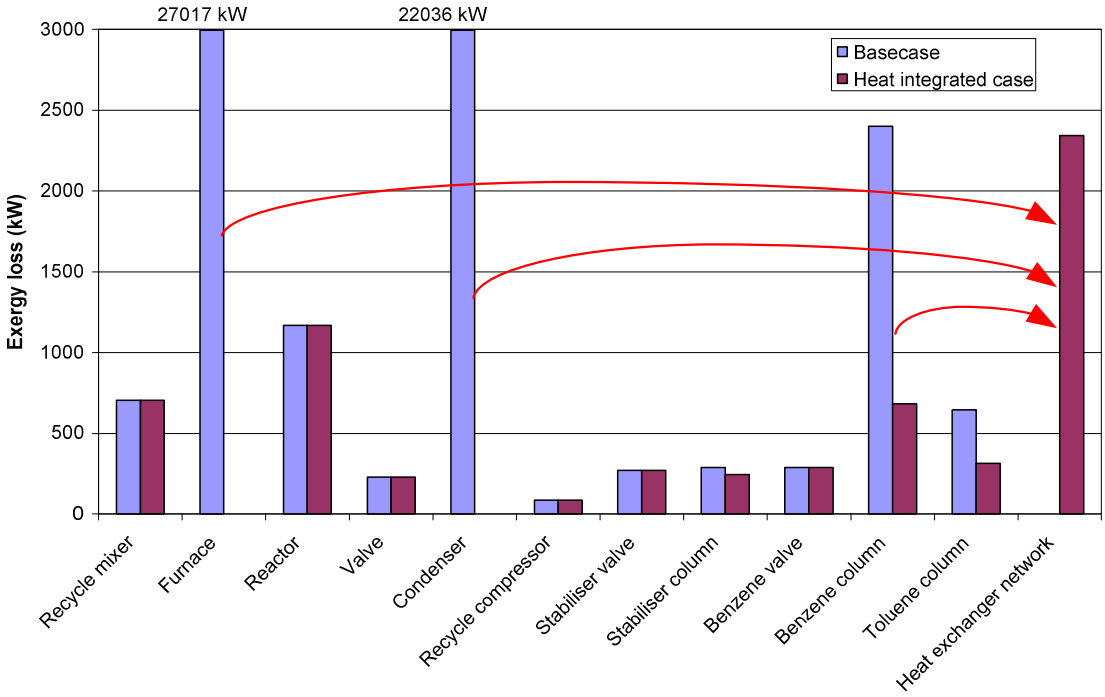

fig. 7-7 Exergy analysis on the basecase by Douglas and the heat integrated case. Note that the significant decrease in exergy loss in the furnace, condenser and benzene column is somewhat transferred to a large exergy loss in the heat exchanger network.

The largest exergy loss occurs in the furnace and in the condenser before the flash unit. This result can be somewhat misleading since these two operations can benefit very much from heat integration. Therefore, an exergy analysis on an idealised heat integrated case is also shown. The heat-integrated case is ideal in the sense that it is assumed that the minimum utility requirements predicted by the pinch analysis can be achieved. In this case the total exergy loss in the process is reduced dramatically, and at the same time it becomes evident that a number of minor exergy losses need to be addressed.

The total exergy loss is reduced from around 55 MW to 6 MW only because of heat integration. The grand composite curve for the heat integration is shown in fig. 7-8.

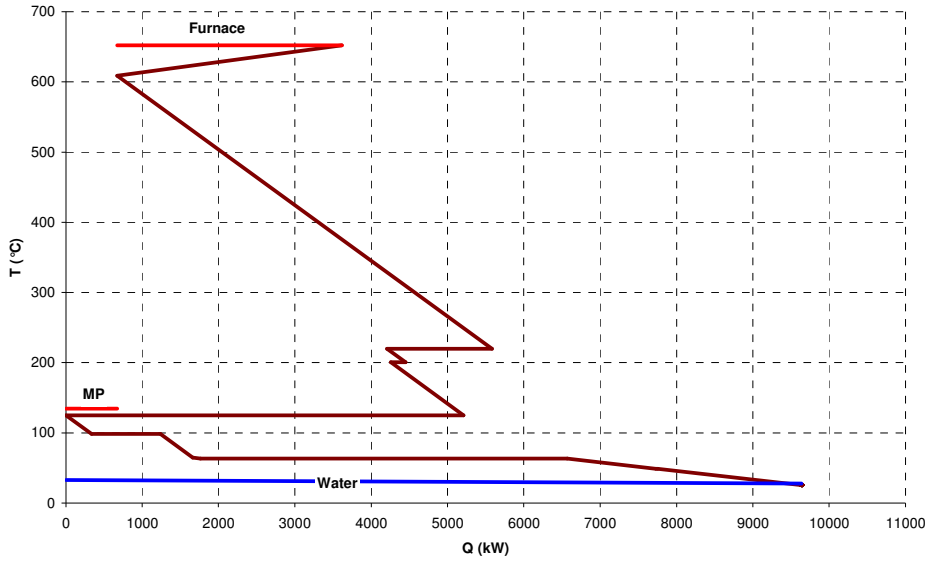

fig. 7-8 Grand composite curve for the basecase design, utility supply is MP-steam and furnace..

The MP-steam level is specified by (Douglas 88), but in reality a lower level around 130°C, i.e. 2.5 bar, would be usable. On the other hand the potential for generation of LP-steam is almost non-existing, and a large supply of cooling water is needed.

If the economy of the plant is analysed, the yearly operating costs for the plant are summarised in table 7-2. The variable production costs are primarily due to raw material costs, which constitute more than 80% of the total variable cost, while primary energy (e.g. natural gas) for steam generation and cooling water are the second and third. Even though the raw material cost is the dominating part of the costs, it is obvious from the stoichiometry in (7.1) that production of one mole of benzene requires one mole of hydrogen and one mole of toluene, which means that it is impossible to eliminate the use of raw materials. Instead it seems more appropriate to set up minimum targets for both raw material and utility. The minimum target for the raw material use is given by stoichiometry, and neglecting the side-reaction, since the most ideal process would convert a mole hydrogen and a mole toluene into a mole benzene. The target for steam and cooling water can be set by the pinch analysis. Using these targets leads to the minimum variable costs, also listed in table 7-2.

table 7-2 Variable operating costs for the first year of operation.[24]

Variable costs	Variable cost (M€)	Minimum target (M€)
Raw materials (hydrogen and toluene)	60.990	52.972
Electricity	0.154	0.154
Steam	7.161	0.356
Cooling water	2.551	0.474
Operators	1.191	1.191
Maintenance and repair	0.866	0.866
Total variable cost	*72.912*	*56.012*

In fig. 7-9 the potential savings are shown, and it is seen that the saving of utility and raw material show almost identical potentials.

One might argue that the saving in utility is easily realised through heat integration, which can be carried out without interfering with the process flowsheet. Savings in raw materials are in this sense somewhat more difficult, requiring a new process. Therefore the economic targets might not be completely comparable, and indeed a new flowsheet that saves raw material might or might not have the same heat integration potential as the original process.

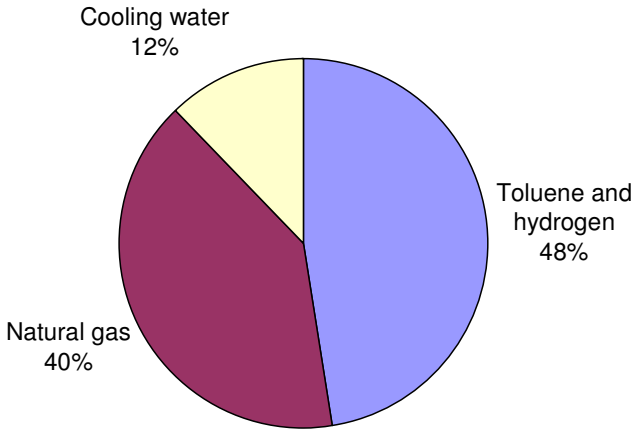

fig. 7-9 potential economic saving in variable cost. Note that savings in electricity and wages are not included here.

Additionally, the electricity requirements and the need for operators and maintenance have not been included in these targets. The electricity is overall a limited expense, and it might be disregarded as uninteresting; however this could prove a wrong decision since a significant amount of high temperature waste heat is available in the process, see fig. 7-8.

[24] Note that the prices are based on the first year of scenario 1, see section 3.3.2

This waste heat could in turn be used for producing electricity, and furthermore since there is a significant production of methane in the reaction this can be utilised as fuel in a utility system. Altogether it might be that the expense for electricity is in itself insignificant but the potential for generating electricity and selling electricity to the grid does seem to be available.

The expenses for wages, maintenance and repair need to be addressed, since it is very dependent on the process design. When the method of (Turton *et al.* 98) is used a certain unit operation requires a certain number of operators, and according to (Peters *et al.* 03) the maintenance and repair cost can be estimated as a fraction of the investment price. Since nearly all savings are associated with a further complication of the process (e.g. heat integration requires a number of heat exchangers), the savings will be accompanied by not only larger investments but also larger expenses for wages and maintenance.

Since all these considerations are reflected in the economic model the optimal solution can be found. This assumes that the superstructure actually includes the optimal process and that the optimisation algorithm does not stop at a local optimum.

The saving potential is equal for raw-materials and utility, as this was based on a certain set of prices. Since the raw-material cost is the dominating part of the variable cost it is clear that the solution will be much more sensitive to changes in raw material costs than changes in utility cost. The scenarios described in 3.3.2 primarily deals with general economic development and particularly energy prices. Since no future scenario for the development in demand for toluene and benzene is available it is somewhat more difficult to predict the prices of these commodities.

7.4.1 Discussion

The above analysis showed several important issues. First of all the major exergy loss in a heat integrated process will be in the heat exchanger network. To remedy this, the integrated design is excellent since waste heat can be used to raise steam and generate power in the utility system. This also addresses the potential savings in both natural gas and cooling water consumption.

The raw material cost can only be cut by avoiding purge loss and undesirable side product formation. In the super structure in fig. 7-1, several options for reducing the purge exists. The hydrogen can be recovered in a membrane and benzene can be recovered in the absorber. Furthermore purge streams can be directed to the utility system for fuel use, and hereby the purge is also becoming useful.

Based on this it is considered that the integrated design and the proposed process superstructure will be able to address most of the problems identified by analysing the base case.

7.5 Optimisation of integrated process and results

The results of the optimisation of the HDA system are primarily interesting when they are compared with more traditional solutions of the problem. First of all it must be noted that it is not straightforward to compare the original flowsheet by (Douglas 88) with the ones presented here. This is due to the fact that different unit operation models and thermodynamic data are used in the present work compared with the work of (Douglas 88). Most of the current work is more detailed, and the flowsheet includes options that are either not described or only mentioned briefly. To make a thorough comparison therefore requires that the different approaches be based on the same fundamental thermodynamics and unit operation models. It is of course debatable whether the assumptions of the models are acceptable for a given purpose, but for comparison of optimisation results, the foundation must be the same for all cases.

Two cases are of interest

- Sequential (or hierarchical) optimisation, i.e. the HDA-process is optimised first, the energy requirements are fixed, and afterwards the utility system is optimised to cover the fixed demands.
- Simultaneous optimisation of the combined HDA and utility system, as described by the method in this work

The objective function for the prior case is somewhat difficult to define, since it is ambiguous how to associate cost with the utility supply. This is discussed further in the following section.

7.5.1 Sequential optimisation

There exist two extremes for the objective function of this case.

- All mechanical energy is provided by electricity from the grid, all heat is supplied by natural gas fired furnaces, and all cooling is provided by cooling water.
- No utility cost is associated with the process at all

The first option is very pessimistic since it assumes that no heat integration or co-generation can take place. The latter is on the other hand very optimistic since it assumes that the process does not have any need for utility supply at all, i.e. all heating, cooling and mechanical demands can be covered by heat integration. A number of options can be made up in between the two extremes, but no method really seems to be able to include a realistic utility price.

table 7-3 Summary of objective function and problem size for the two formulations

Case	Net present worth (M€)	No. of constraints	No. of variables	CPU time (s)	Nodes evaluated
No utility cost	31.1	900-1200	800-1100	116	74
Full utility cost	-1.43	900-1200	800-1100	158	126

As a demonstration of the differences, the flowsheet for the HDA-process with the two extreme objective functions are shown in fig. 7-10 and fig. 7-11.The problem characteristics are summarised in table 7-3. Note that the variable number of constraints and variables is due to the disjunctive formulation.

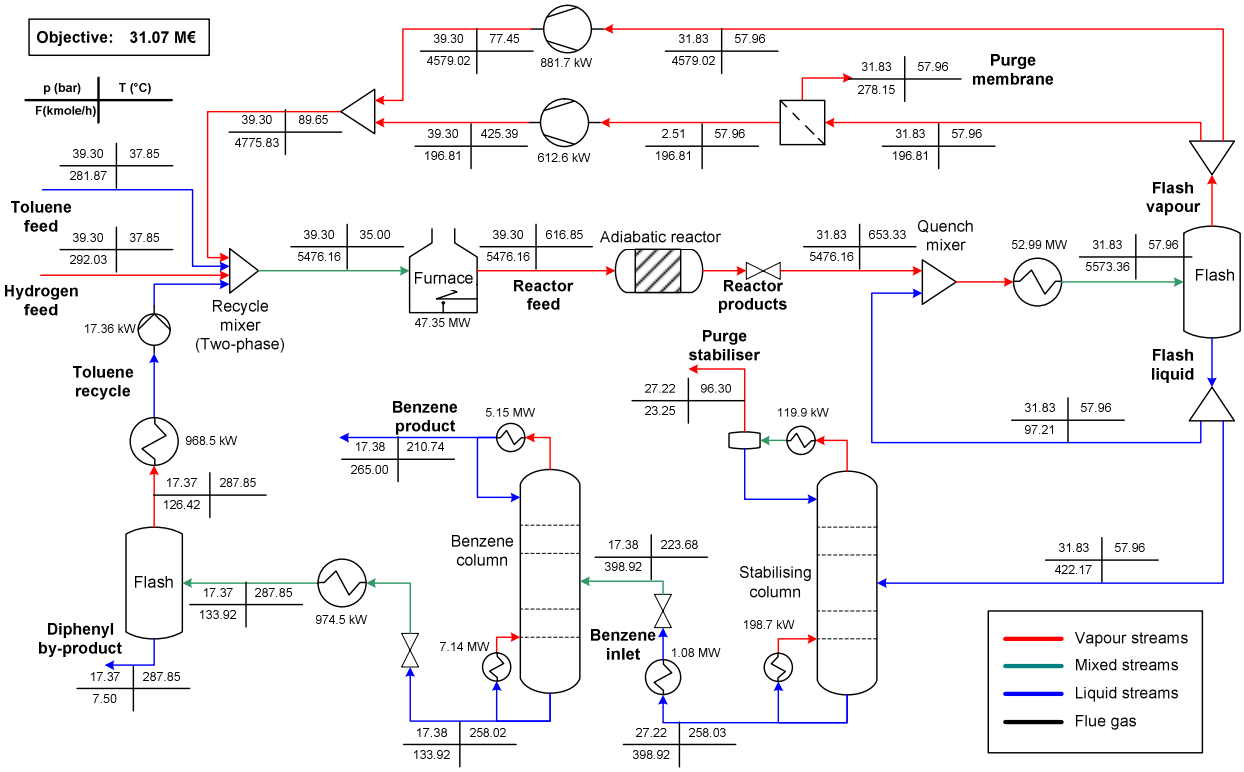

fig. 7-10 Results for the case with no utility costs

The stream summary for the "no-utility-cost" flowsheet is found in table 7-4.

table 7-4 Stream composition for a selected set of streams in fig. 7-10.

Component	Hydrogen feed	Toluene feed	Reactor feed	Reactor product	Flash vapour	Flash liquid
H_2	95.00%	0.00%	42.00%	37.01%	40.02%	1.03%
CH_4	5.00%	0.00%	49.60%	54.64%	58.85%	4.20%
C_6H_6	0.00%	0.00%	0.86%	5.79%	0.97%	63.53%
C_7H_8	0.00%	100.00%	7.44%	2.40%	0.16%	29.27%
$C_{12}H_{10}$	0.00%	0.00%	0.10%	0.15%	0.00%	1.97%
Component	**Purge membrane**	**Hydrogen recycle**	**Purge stabiliser**	**Benzene inlet**	**Benzene product**	**By-product**
H_2	0.00%	42.35%	18.76%	0.00%	0.00%	0.00%
CH_4	98.07%	56.57%	75.47%	0.04%	0.07%	0.00%
C_6H_6	1.66%	0.93%	5.77%	66.90%	99.70%	0.82%
C_7H_8	0.27%	0.15%	0.00%	30.97%	0.23%	61.22%
$C_{12}H_{10}$	0.00%	0.00%	0.00%	2.08%	0.00%	37.97%

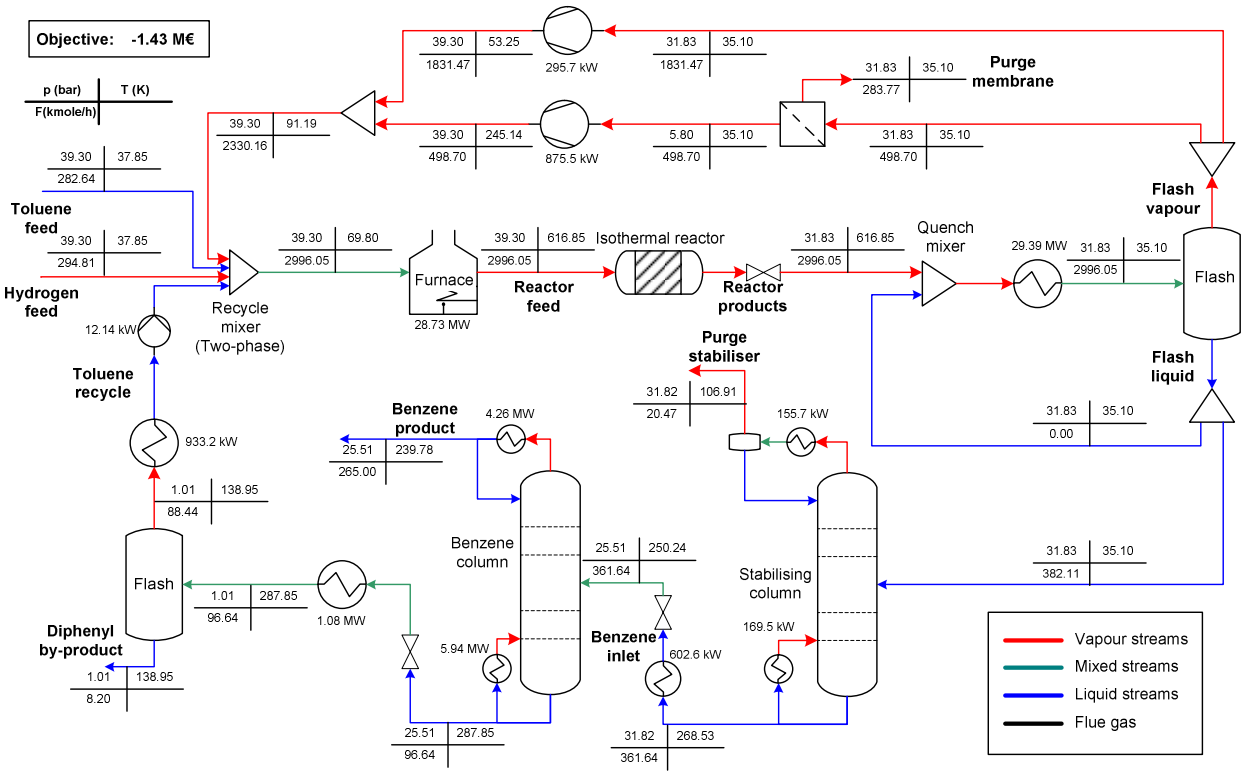

fig. 7-11 Resuls for the case with full utility cost

The stream summary for the "full-utility-cost" flowsheet is found in table 7-5.

table 7-5 Stream composition for a selected set of streams in fig. 7-11.

Component	Hydrogen feed	Toluene feed	Reactor feed	Reactor product	Flash vapour	Flash liquid
H_2	95.00%	0.00%	51.94%	45.20%	50.35%	1.36%
CH_4	5.00%	0.00%	37.67%	44.49%	49.20%	4.41%
C_6H_6	0.00%	0.00%	0.37%	7.04%	0.40%	63.54%
C_7H_8	0.00%	100.00%	9.90%	3.08%	0.06%	28.84%
$C_{12}H_{10}$	0.00%	0.00%	0.12%	0.19%	0.00%	1.85%
Component	**Purge membrane**	**Hydrogen recycle**	**Purge stabiliser**	**Benzene inlet**	**Benzene product**	**By-product**
H_2	0.00%	54.48%	22.46%	0.00%	0.00%	0.00%
CH_4	99.05%	45.11%	72.29%	0.05%	0.07%	0.00%
C_6H_6	0.83%	0.36%	5.26%	67.29%	99.70%	0.34%
C_7H_8	0.12%	0.05%	0.00%	30.69%	0.23%	32.29%
$C_{12}H_{10}$	0.00%	0.00%	0.00%	1.97%	0.00%	67.37%

In the case with full utility cost the net present worth becomes negative, i.e. the investment will not pay off compared to other investments.

The topologies of the two cases are almost identical, though with one important exception, the reactor. In the case of full utility cost an isothermal reactor is selected and it operates at the lowest permissible temperature, thus saving heat input to the furnace and cooling water for the condenser. The isothermal reactor is larger and more expensive than the adiabatic counterpart in fig. 7-10, and also has a larger conversion, which reduces the need for recycling. The problem with the recycle is primarily the operating cost for the furnace and the condenser, whereas the electricity requirements of the recycle compressors are negligible in this case.

Furthermore the case with full utility cost has a slightly higher consumption of raw materials and thus a higher purge rate. This is not particularly surprising since the focus in this case is shifted from almost pure raw-material cost toward energy cost.

Finally the benzene column operates at significantly different pressures in the two cases; it is most likely the saving of cooling water before the column that has motivated this choice. It turns out the investment price levels are not widely different for the two columns, since the high pressure column is somewhat smaller, and thereby compensates for the cost involved in the increased pressure.

Both cases includes the membrane separator for purifying the methane purge, this choice is quite obvious, and results in a significant saving on the hydrogen feed. Comparing to the base case by (Douglas 88) in fig. 7-6 the hydrogen feed is reduced by 40%.

The case with no utility cost has a much larger recycle rate than the case with full utility cost. This choice is linked to the fact that there is no additional operating cost for the heating and cooling of the larger flow.

Pinch analysis

The heat integration potential for the two solutions is seen in the grand composite curves, in fig. 7-12 and fig. 7-13. There is a significant difference between these curves, primarily because of the different reactors. In the case of full utility cost the isothermal reactor provides a significant amount of high temperature excess heat. Both cases need a furnace and HP steam for covering the heat requirements and both cases also have surplus heat below pinch for generation of MP-steam.

On close inspection especially the latter case have an excess of heat at 600°C (the isothermal reactor), but the heat must be exchanged to a level around 300-350°C. This is clearly not thermodynamically optimal; on the other hand it can be difficult to capitalise on the high quality heat, since the most obvious choice would be to generate VHP-steam, and expand it before it was to be used for heating. However, since the HP pressure level is already around 130 bar, it would probably be quite difficult to built a turbine that could handle the VHP-steam and the limited flow rate.

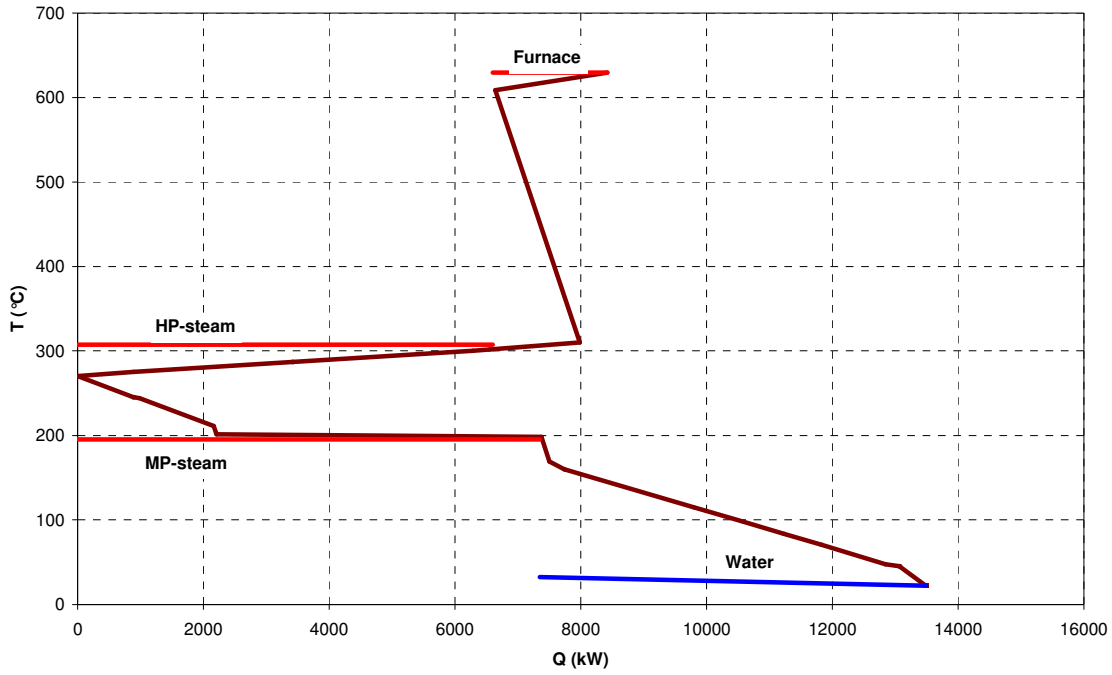

fig. 7-12 The grand composite curve for scenario 1 without utility costs

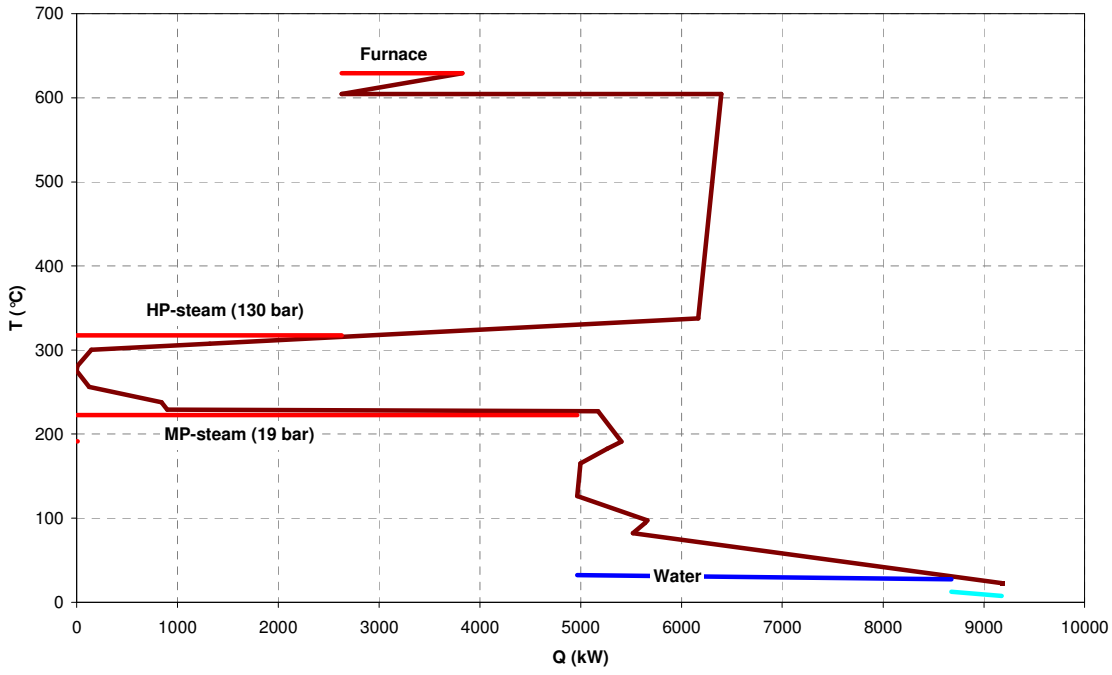

fig. 7-13 Grand composite curve for scenario 1 with full utility cost.

Utility systems

Based on the process flowsheet for the two cases the utility system for each system is designed. For the case without utility cost the utility system the optimal utility system is shown in fig. 7-14.

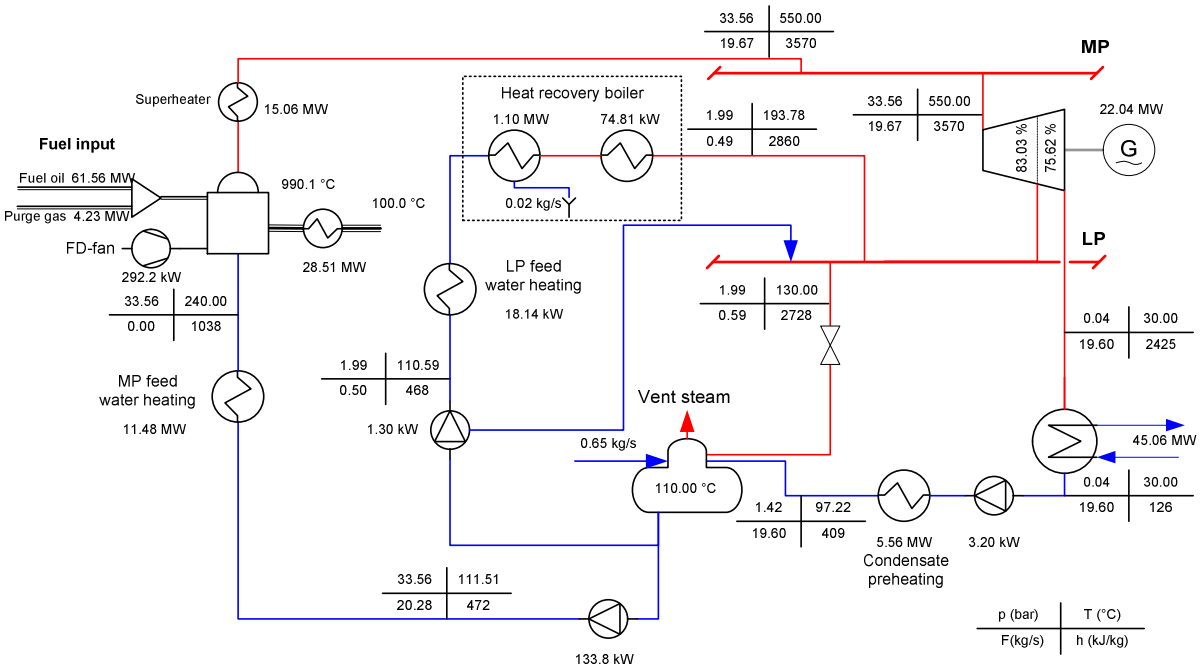

fig. 7-14 Utility system for the process in fig. 7-10. Note that the percentages shown inside the turbine symbol are the estimated isentropic efficiencies for each section.

All the drivers are electrical and electricity is generated in a single steam turbine using 33.5 bar steam. The majority of the steam is generated in a fuel oil fired boiler, which also uses the purge gas from the process. A minor steam flow (LP) is generated by recovering heat from the process; this is only used for driving the deaerator. The steam turbine generates around 22 MW electricity, of which 2 MW is used by the process and 20 MW is sold to the electricity grid.

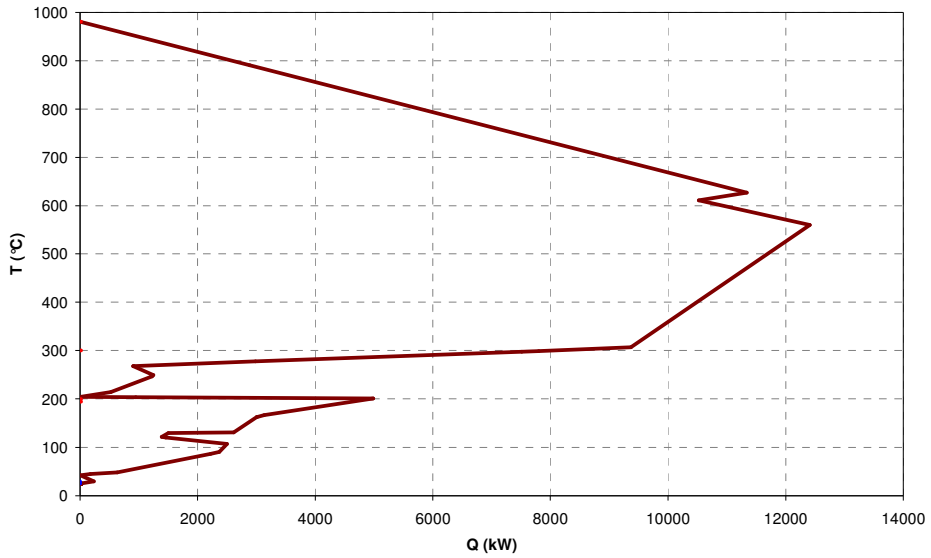

fig. 7-15 Grand composite curve for the combined process and utility system. The process case for no utility cost.

The utility system for the case with full utility cost included in the HDA-optimisation is shown in fig. 7-16.

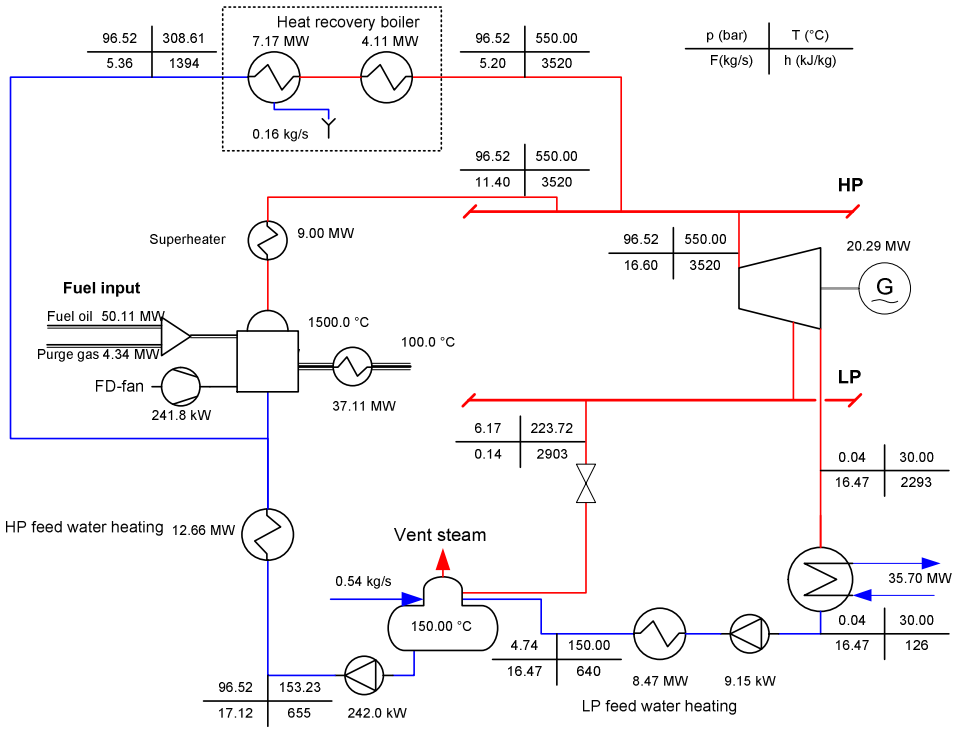

fig. 7-16 Utility system for the case with full utility cost

The major difference is the steam pressure level used in the two systems, where the system in fig. 7-16 has a pressure of 96 bar, significantly higher than the other system. Apart from this, the two utility systems are fairly identical.

If we combine the process models and the utility system models the total net present worth for process and utility system can be calculated.

table 7-6 Total net present worth for process and utility system

Case	Net present worth for both process and utility system (M€)
No utility cost	26.1
Full utility cost	29.1

In this case it is apparently the model with the full utility cost that turns out to provide the best total system.

7.5.2 Simultaneous optimisation

The object function for this case is as such simpler than for the previous, since the utility is automatically included in the combined case. The drawback is that the problem is much

larger and therefore requires much more computational power. The optimal flowsheet is shown in fig. 7-17.

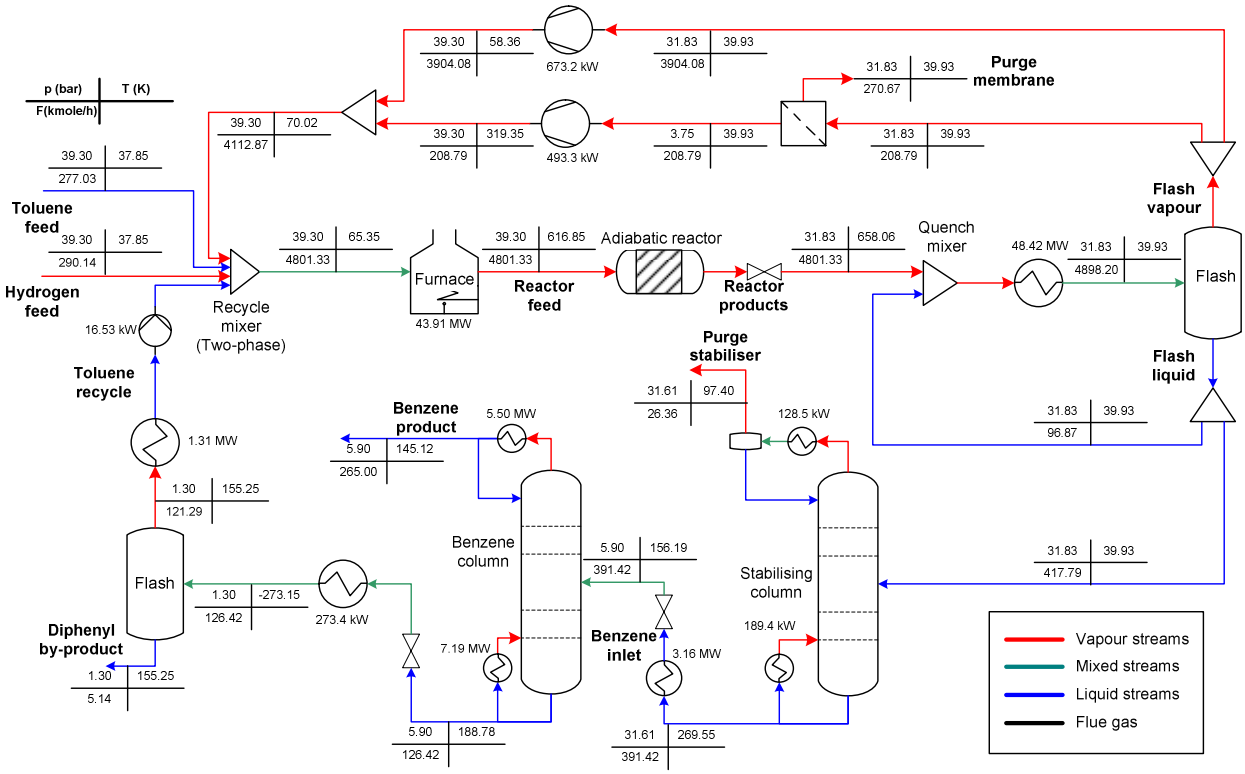

fig. 7-17 Results for the simultaneous optimisation, scenario 1 and fixed raw material costs

The composition of the individual streams is summarised in table 7-7.

table 7-7Stream composition for the flowsheet in fig. 7-17.

Component	Hydrogen feed	Toluene feed	Reactor feed	Reactor product	Flash vapour	Flash liquid
H_2	95.00%	0.00%	43.76%	38.12%	41.64%	1.11%
CH_4	5.00%	0.00%	47.49%	53.20%	57.80%	4.93%
C_6H_6	0.00%	0.00%	0.45%	6.03%	0.49%	64.20%
C_7H_8	0.00%	100.00%	8.23%	2.52%	0.07%	28.20%
$C_{12}H_{10}$	0.00%	0.00%	0.07%	0.14%	0.00%	1.56%
Component	**Purge membrane**	**Hydrogen recycle**	**Purge stabiliser**	**Benzene inlet**	**Benzene product**	**By-product**
H_2	41.64%	44.38%	17.62%	0.00%	0.00%	0.00%
CH_4	57.80%	55.08%	77.29%	0.05%	0.08%	0.00%
C_6H_6	0.49%	0.47%	5.09%	68.18%	99.70%	0.44%
C_7H_8	0.07%	0.07%	0.00%	30.10%	0.22%	39.81%
$C_{12}H_{10}$	0.00%	0.00%	0.00%	1.66%	0.00%	59.75%

The noticeable differences compared with the systems in the sequential optimisation, i.e. fig. 7-10 and fig. 7-11, are as follows

- The reactor is adiabatic
- The operating pressure for the benzene column is shifted to around 5 bar
- The vapour recycle rate is significantly higher than for any of the two other cases
- The raw material usage is slightly lower than for the other cases.

Even though the differences might seem small and almost insignificant it is these differences that makes the system superior to those found by the sequential approach. A comparison of the objective functions for the three different systems are shown in fig. 7-18.

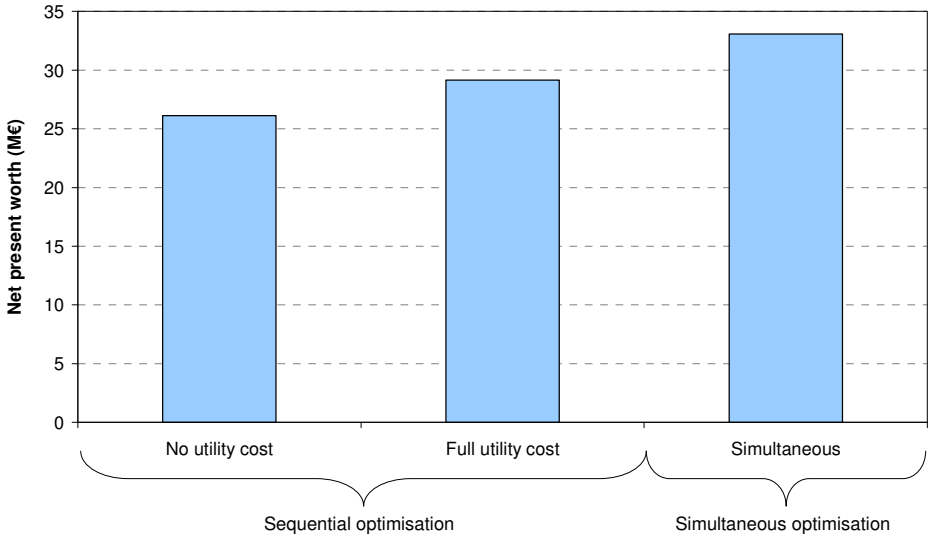

fig. 7-18 Comparison of the net present worth for the three different processes.

It is evident that the simultaneous optimisation offers the best objective function, approximately 13% better than the best from the sequential optimisation.

The utility system is shown in fig. 7-19. The utility system is designed so that all the recycle compressors are driven by electric motors. Totally the utility plant produces 2.88 MW of electricity, of which 1.25 MW is used in the process and 1.63 MW is sold to the electricity grid. The electricity is generated both in the small industrial gas turbine and in a small steam turbine. The gas turbine is supplementary fired in order to cover the high temperature heat demands in the process, i.e. the preheating of the reactants. The steam system has a single pressure header at approx. 2 bar, i.e. LP steam. This pressure is obviously selected to recover the heat from the benzene condenser at the benzene column.

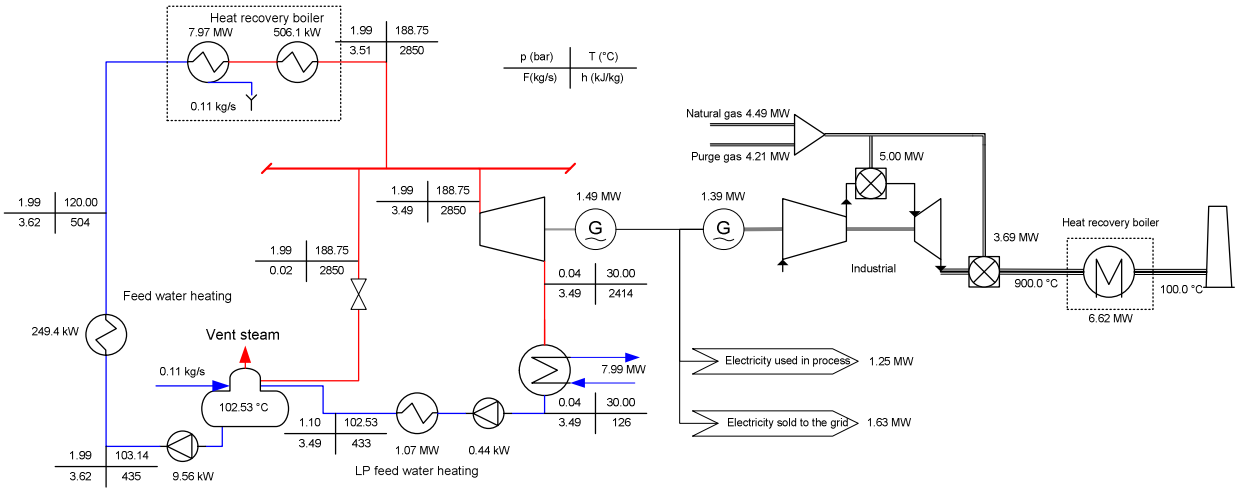

fig. 7-19 Utility system for the process in fig. 7-17.

There are some practical problems with a utility of this size, since only a limited number of industrial gas turbines are available at this size, but e.g. the Solar Saturn 20 (Solar Turbines 05) which has a net power output of 1.25 MW might be an option.

Since the utility system and the process are optimised simultaneously the heat integration is "self-contained", i.e. no external heat or cooling is required. The grand composite curve for this case is shown in fig. 7-20. On inspection the grand composite curve shows that there is a better heat integration in this system, compared to the systems in fig. 7-12 and fig. 7-13. The reason is that the interaction between the utility system and the process are accounted for, for instance the pressure of the benzene column has in this case been shifted to a pressure (and temperature) more favourable to the utility system and heat integration potentials.

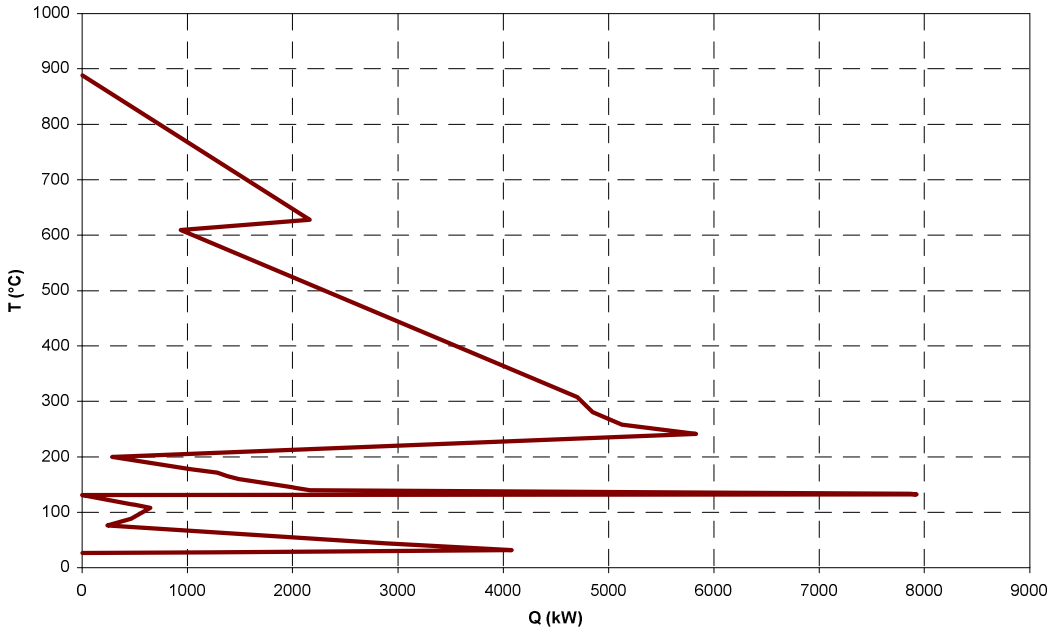

fig. 7-20 Grand composite curve for simultaneous optimisation with scenario 1 and fixed raw material costs.

The power generation of the utility system takes advantage of the option to operate as an electricity generator and sell power to the grid. The obvious question is whether this is due to overly favourable fuel and electricity prices or if it is a part of the integrated process. Therefore it is interesting to find the marginal efficiency, which is generally defined as the additional electricity that is generated ($\Delta\dot{W}_{el}$) relative to the additional fuel input ($\Delta\dot{Q}_{gas}$), as follows

$$\eta_{el}^{m} = \frac{\Delta \dot{W}_{el}}{\Delta \dot{Q}_{gas}} \tag{7.20}$$

In this case it is defined that the additional electricity production is the entire electricity production in the utility system, i.e. using as a reference the case where all electricity is bought from the electricity grid. The calculation of the additional fuel consumption is on the other hand less obvious, as the utility system will be simplified if no electricity is generated. Furthermore, since the process and the utility system are optimised simultaneously, the constraints imposed on the electricity generation will also affect the process. Basically this leaves two options:

- The process is fixed at the present worths and a simplified utility system, only providing heat to the process, is designed.
- The process and utility system are optimised simultaneously to generate an optimal flowsheet for the case where the utility system is constrained from generating electricity.

Neither of the options can be said to be entirely correct, since the first option would most likely base the marginal efficiency on a suboptimal process, as the process was optimised under the assumption that cogeneration was actually possible. The latter case is better in the sense that the process is optimised under the new constraints and thereby closer to the optimal process, but since the flowsheet is now changed, the marginal efficiency will be based on comparison between two different flowsheets. This can blur the result somewhat since plenty of factors are involved in the optimisation of this process, and the marginal efficiency is only a measure of a single aspect of the entire optimisation.

If the first method is used, the utility system is only used to supply heat to the process and the optimal flowsheet for this utility system is shown in fig. 7-21.

Comparing this system with the one for the integrated process, an impressive marginal efficiency of 98% is achieved. There are several reasons why such a high marginal efficiency can be found. Primarily, the process heating achieved by cooling of the flue gas from the boiler is associated with a large temperature difference, far larger than the pinch allows, which is evident from fig. 7-22. In addition the flue gas is cooled to 100°C in the integrated design, while it is only cooled to 208°C in this case, which obviously this leads to a higher loss.

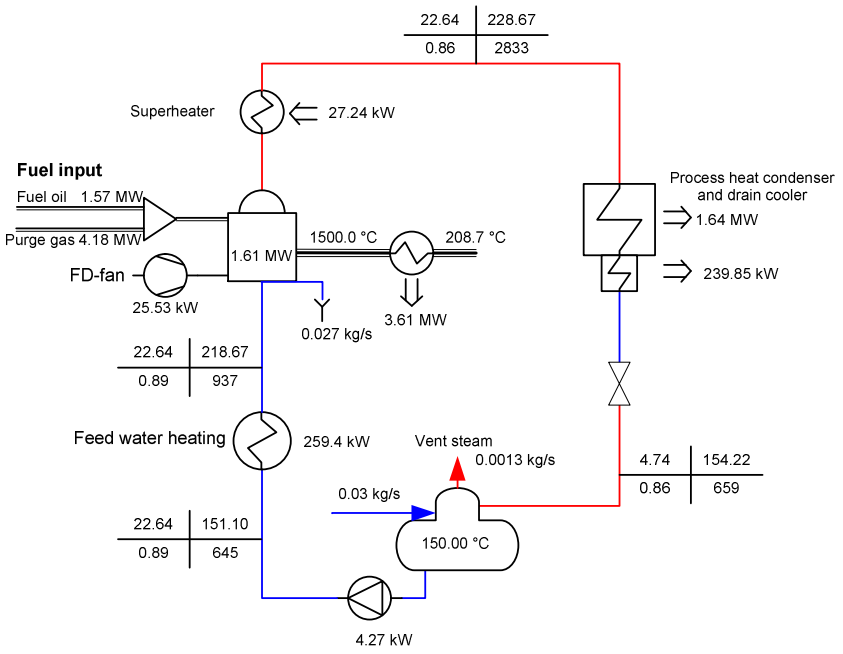

fig. 7-21 Utility system for the case where all power is generated off-site

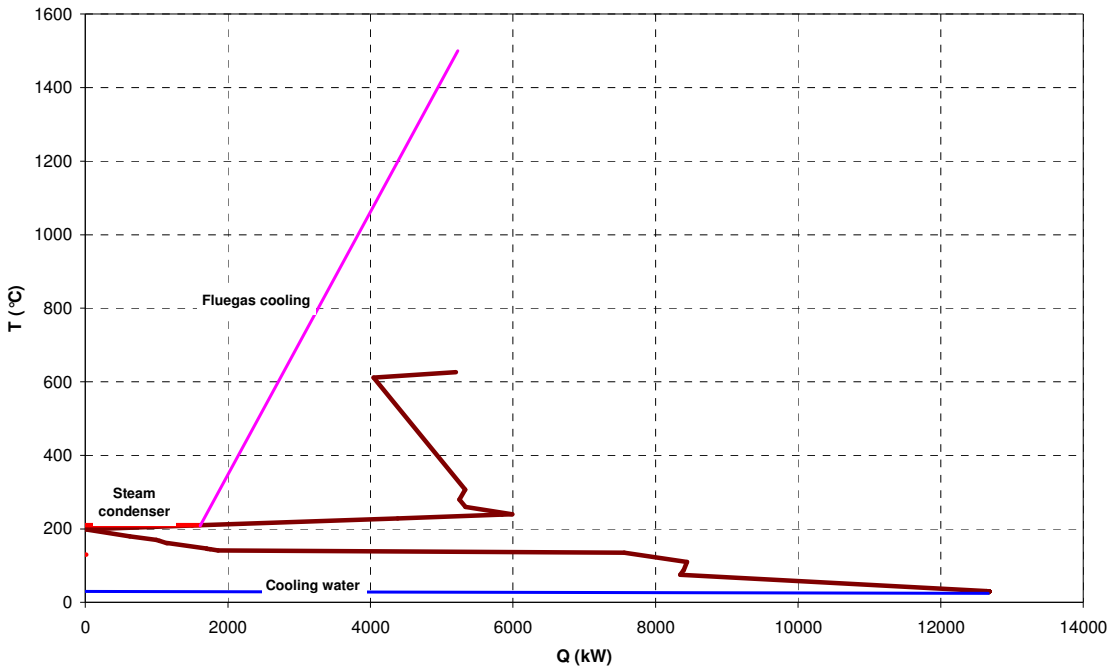

fig. 7-22 Grand composite curve for the simple utility system in fig. 7-21.

7.6 Summary

In this chapter the HDA process was used as an example for use of integrated design. The simultaneous optimisation results in a process with at least 13% higher net present worth.

The original base case was analysed with respect to exergy and economics. Based hereupon a number of inefficiencies could be identified, even if heat integration were used on the base case there would be a significant exergy loss in the heat integration. It was suggested that the integrated design can far better handle this, as waste heat can be put to use in steam turbines, thus recovering exergy. Similarly the purge gas can also be recovered for fuel.

The marginal electric efficiency was also higher for the integrated approach. The investment cost are almost identical for the three cases, with the simultaneous optimisation having a slightly lower investment cost than the others.

Once again the disjunctive solver was effective in solving the large scale problem. In this case it was particularly important, when e.g. one of the distillation columns were deselected. Here the disjunctive solver removed the equations for the column in the following nodes, this significantly reduced the problem size near the bottom of the search tree. Initially around 13000 constraint and a few more variables were present, but in the extreme cases this was reduced to just over 3000 constraints at the bottom of the search tree. This of course sped up the calculations near the bottom of the tree and also made the solution progress much more robust.

8

CONCLUSION AND CONTRIBUTIONS

This chapter includes a summary of the thesis, the main conclusions and suggestions for future work within this area.

In this chapter the conclusions for the work are given, starting out with a brief summary for each chapter. Afterwards the main conclusion and contributions are described, and finally outlines for interesting areas of future work are stated.

8.1 Summary of the thesis

Chapter 1

The main objective of this thesis has been the investigation of integrated design, or "process integration of core process and utility systems". This covers the subject of handling design of the chemical process flowsheet, the heat integration and the utility system simultaneously. In this way the interaction among the subsystems are taken into account and better systems can be designed. A brief background on process synthesis was provided. Much research has already been carried out in the individual fields of process synthesis but the integration of the fields is more limited. It is, however, widely recognised that the sequential design procedure by (Douglas 88) leads to suboptimal designs, since the interaction between the systems is not taken into account. The integration between process and utility system has only been very limited addressed. This motivates the subject of this thesis. Finally the outline of the thesis and the original contributions to science were summarised.

Chapter 2

In this chapter mathematical programming was introduced, formulations were divided into different classes, and algorithms for solving the problems were briefly described. The intuitive and easy formulation of problems using disjunctions was introduced, and the branch-and-bound solver that handles the disjunctions was described. The solver relies on a *depth-first-search* to establish the initial upper bound, and afterwards searches the tree with a

best-bound-search. The method of pseudo-costs by (Linderoth and Savelsbergh 99) was implemented, but was found only to be beneficial for cases where the solver is stopped when the lower and upper bound are within a given tolerance. As all problems in this work have been solved to completion, this option has not been used extensively. Afterwards exergy analysis was briefly described, and the evaluation of chemical exergy for hydro carbons was introduced. In addition, evaluation of exergetic efficiencies was described.

Chapter 3

In this chapter the main contribution of this thesis, a methodology for integrated design of process and utility system was proposed. Based on the experience in each of the fields of hierarchical design, it was considered impossible to include every single aspect of process design in one large problem. Instead it was proposed to include a limited reactor and separation superstructure with the optimisation of the utility system. To make the method general, the utility system and the process were still considered different parts, but the interaction of the two was described in detail in section 3.2.1. Finally the economic modelling used in this work was described; it is based on a scenario analysis by (Elsam 03). It is evident that none of the scenarios had foreseen the rise of crude oil prices in the last couple of years. In spite of this significant disagreement the scenarios were used in this work anyway, as price forecasting and updating was considered outside the scope of this work.

Chapter 4

In this chapter the utility and heat integrations models were formulated. A new set of steam properties for optimisation purposes were formulated as well; this included a new model for calculation of isentropic expansion enthalpy in turbines. The new steam properties allow for free selection of the pressure levels, since pressure is properly taken into account by the steam properties. The superstructure for the optimisation placed heavy emphasis on the heat integration with the process, thus almost all streams in the superstructure are considered part of the heat integration.

The formulation of the gas turbine model is very similar to the work of (Manninen 99), but some minor enhancements were included. If a separate utility system model that is less integrated with the process is desired, it can easily be accomplished by replacing the HRSG model.

The heat integration method combines the NLP-formulation by (Duran and Grossmann 86b) and the method of individual stream temperature differences by (Zhu *et al.* 95). This makes the overall minimum temperature difference more realistic. Two different methods have been tested for formulation of the heat integration problem, and it is concluded that the MINLP-formulation is unsuitable for the integrated design, since the formulation becomes combinatorially prohibitive. The method does not produce optimal heat exchanger networks, however.

The driver interface is modelled by disjunctions to select the proper drive among a number of steam turbine combinations and electrical drive.

Chapter 5

The small cases studied in this chapter demonstrated both the strength of the proposed superstructure formulation, as well as the strength of the disjunctive branch-and-bound solver.

In the first example, case 1 from (Bruno *et al.* 98), an improved flowsheet compared to the original was found. Even more importantly the improvement can most likely be contributed to the robustness of the disjunctive solver, which found a significantly better optimum than the two commercial solvers (DICOPT and SBB).

In the second example, case 2 from (Bruno *et al.* 98), an improved flowsheet was also identified. The more important lesson from this example was that fixing the pressure a priori can lead to significantly suboptimal design. Thus the importance of the steam properties that allow free selection of pressure was highlighted.

The heat integration example illustrated the effect of associating different temperature differences with each stream. For the examples used here the different temperatures turned out to produce a network where several exchangers operate at the minimum temperature difference. However, this is not the case in general, but highly dependent on the actual case.

Chapter 6

In this chapter the synthesis of methanol from natural gas was used as an example for integrated design. It has been shown that for this example the simultaneous method is able to find a better optimum than the sequential method. The net present worth of the integrated approach is 12% higher than for the best of the sequential approaches. The model of the methanol synthesis plant was limited to include a steam reformer and a single methanol reactor. Both these reactors were modelled with differential equations, providing a detailed estimate of the operating conditions. The models are highly non-linear; primarily because of the complicated reactions that takes place in the two reactors. On the other hand the distillation train was assumed fixed, and thus not included in the optimisation. In total there was around 10000 constraints and more variables. This proved that the disjunctive solver could handle problems of a realistic scale, although most of the workload was of course on the NLP-solver.

It is interesting to notice that not only does the utility system change for the simultaneous case, but also a number of process parameters changes. This suggests that there is an interaction between the utility system and the process that the sequential method does not include. All the results have been calculated using price scenario 1, but calculations using scenario 2 and 3 shows a similar tendency. A number of interesting process alternatives can be investigated in future work, and was briefly outlined in the beginning of the chapter.

Chapter 7

In this chapter the HDA process was used as an example for use of integrated design. The simultaneous optimisation results in a process with at least 13% higher net present worth.

The original base case was analysed with respect to exergy and economics. Based hereupon a number of inefficiencies could be identified, even if heat integration was used on the base

case there would be a significant exergy loss in the heat integration. It was suggested that the integrated design was far better handling this, as waste heat could be put to use in steam turbines, thus recovering exergy. Similarly the purge gas could be recovered for fuel as well.

The marginal electric efficiency was also higher for the integrated approach. The investment costs were almost identical for the three cases, with the simultaneous optimisation having a slightly lower investment cost than the others.

Once again the disjunctive solver was effective in solving the large scale problem. In this case it was particularly important, when e.g. one of the distillation columns were deselected. Here the disjunctive solver removed the equations for the column in the following nodes, which significantly reduced the problem size near the bottom of the search tree. Initially around 13000 constraint and a few more variables were present, but in the extreme cases this was reduced to just over 3000 constraints at the bottom of the search tree. This of course sped up the calculations near the bottom of the tree and also made the solution progress much more robust.

8.2 Main conclusions and contributions

The main achievement of the work is the formulation of a general method for handling the integrated design of processes and utility systems.

A methodology that simultaneously optimises the process, utility system and heat integrates both have been proposed. The method is formulated in general terms, but relies on the utility system optimisation method also developed for this work. The method provides a means of interfacing the utility model seamless with the process model for simultaneous optimisation. An important aspect of the method is that to ensure optimal heat integration between the process and the utility system, the traditional separation of process streams and utility streams in the pinch analysis have been removed, and allowing a complete integration across process to utility.

The method has been applied to two different test cases (Grue and Bendtsen 03a; Grue and Bendtsen 05). In both cases the conclusion is clear, that the integrated design method is able to find better designs than the traditional sequential method.

Another interesting feature of the integrated design is that the minimisation of total energy use is much more straightforward, since all heat integration is accounted for. If e.g. the specific energy consumption pr. unit of chemical products is to be minimised, it can be very difficult to tell if a design is optimal if the entire utility system is not included.

From a mathematical point of view, it is not surprising that better results are found by the simultaneous method. In the sequential method the individual models are constrained further than in the simultaneous case. In optimisation problems a better optimum can only be found by removing constraints, and this is exactly what the simultaneous method does.

In order for the integrated design method to work, a superstructure for synthesis of utility systems both for sequential design and integrated design is required. The superstructure is formulated with disjunctive programming. Unlike most other work within the field, the

superstructure allows for simultaneous selection of pressure levels in the utility system. In earlier work the pressure levels in the steam system have almost always been fixed. This is typical in the situation where the chemical process is already fixed, or where industrial steam levels are used. In this work, however, the pressure levels are allowed to be changed by the optimisation, thus removing a potentially important constraint on the utility system. It is clear that in many industrial situations there will be good arguments for selecting typical pressure levels for the process, but through the use of the novel method the cost of fixing the pressure headers can at least be highlighted.

To facilitate this a new formulation for steam properties is proposed, which is more detailed than the one usually used for optimisation, yet far simpler than the standard IF-97 formulation. The properties show good agreement for pressures below 150 bar. The unit operation models for steam turbines also have much better prediction capabilities of the isentropic expansion enthalpy, thus making the models much more reliable.

The utility system is formulated, so that heat integration between the utility system and the process is promoted. Excess heat from the process can be used at any level in the utility system, e.g. for preheating feed water or superheating steam. Thereby a complete heat integration of both the chemical process plant and the utility system can be computed, which will provide a far better heat integration than in normal systems where all interaction between the utility system and the process plant is carried out by steam. A number of different heat integration methods have been tried out, but all of the MINLP formulations become too combinatorially demanding for practical use. Therefore a NLP-formulation is used, although this has the drawback that the heat transfer area is not calculated. To partly alleviate this problem, the method allows for specification of different temperature differences for each stream, allowing the designer to specify temperature differences based on expected heat transfer coefficients for each stream.

The utility system also includes gas turbines, and the models for these have been improved. Based on manufacturer data for more than 150 different gas turbines, a general model has been developed for industrial and aero-derivative turbines.

It is important to notice, however, that this freedom of design in the utility system might lead to systems that are not desirable from a practical viewpoint. For instance material constraints or physical distances between equipment might make an integrated design impractical. However, the important issue is to make it clear to the designer what the cost is for putting constraints on the system.

In general, it has been necessary to create a robust solution framework for the optimisation. The entire method relies on disjunctive formulation of the problem, and therefore a disjunctive branch-and-bound algorithm has been implemented. Even on small systems this algorithm has proven superior to commercial solvers. For large systems the solver is robust, and has also proven the important feature of reducing the problem size as it moves down the search tree.

8.3 Future work

Several issues can be addressed by future work.

- More rigorous chemical models might be relevant, and in some cases one might even consider a direct coupling to a chemical process simulation program. The same can be said about the thermodynamic property evaluation and the important issue of vapour/liquid equilibrium. However, coupling the optimisation to a chemical simulation program will almost certainly increase the calculation time significantly.
- For the specific cases it is clear that a number of obvious options in methanol synthesis have not been investigated, e.g. using an autothermal reformer instead of a steam reformer, detailed simulation of the separation system etc. This is only a few examples of the general notion that it is always important to consider which options the superstructure should include.
- For heat integration it is clear that the major drawback of the present method is that the capital cost of the heat exchanger network is not accounted for simultaneously with the rest of the process design. This might have a significant impact on overall process design, and is thus desirable to include in the future.
- In general the method has only discussed plant design at the design point, but often the plant will operate off-design. Therefore it would be interesting in the future to include different operating scenarios in the integrated design. One simple example is in the utility system, where the condenser is subject to changes in the ambient temperature during the year. But other load cases might also be included, such as part load operation of the plant etc.
- The disjunctive solver used in this work has shown that disjunctive formulations are certainly beneficial, but better solver is still required. For the NLP-problems, the difficulty is that nearly all process models include a number of non-convexities, which makes the NLP-solver unable to guarantee finding the global optimum. The present state for global optimisation is promising from a mathematical point of view, but in practice the methods are still combinatorial expensive. The general problem of combinatorial expensive problems may of course be eased with the ever increasing computing power.
- For the utility system it is of importance to notice that the steam turbine efficiency correlations are simple, and as pointed out in the thesis this impacts the design. It would be desirable to formulate an improved efficiency estimate, although it would still have to be simpler than the method by (Spencer *et al.* 63).
- The economic model is difficult and more rigorous treatment of sensitivity toward different scenarios is desirable. Furthermore it could be interesting to include multi-objective optimisation, to investigate the trade-off between economic optimum and e.g. energy consumption.

9

APPENDIX: STEAM PROPERTIES

As mentioned in section 4.1.4, the isentropic expansion enthalpy for a number of different outlet pressures has been calculated. Here the fits are plotted for a range of outlet pressures. The plots are similar to fig. 4-15. In general all the plots show good agreement with the proposed fit (equation (4.23)).

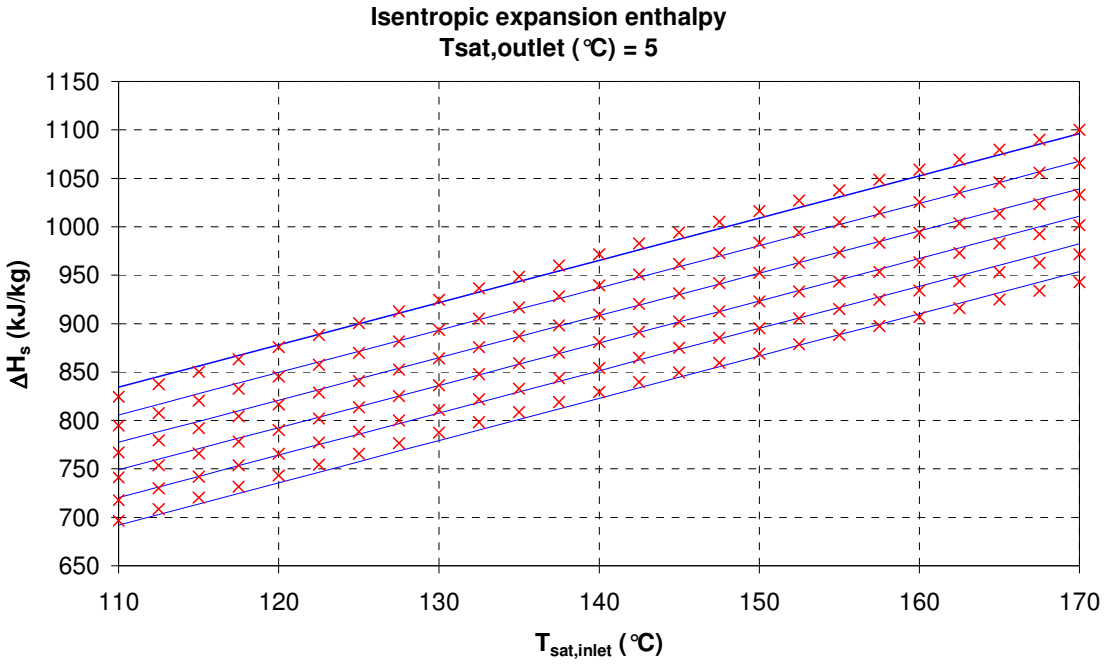

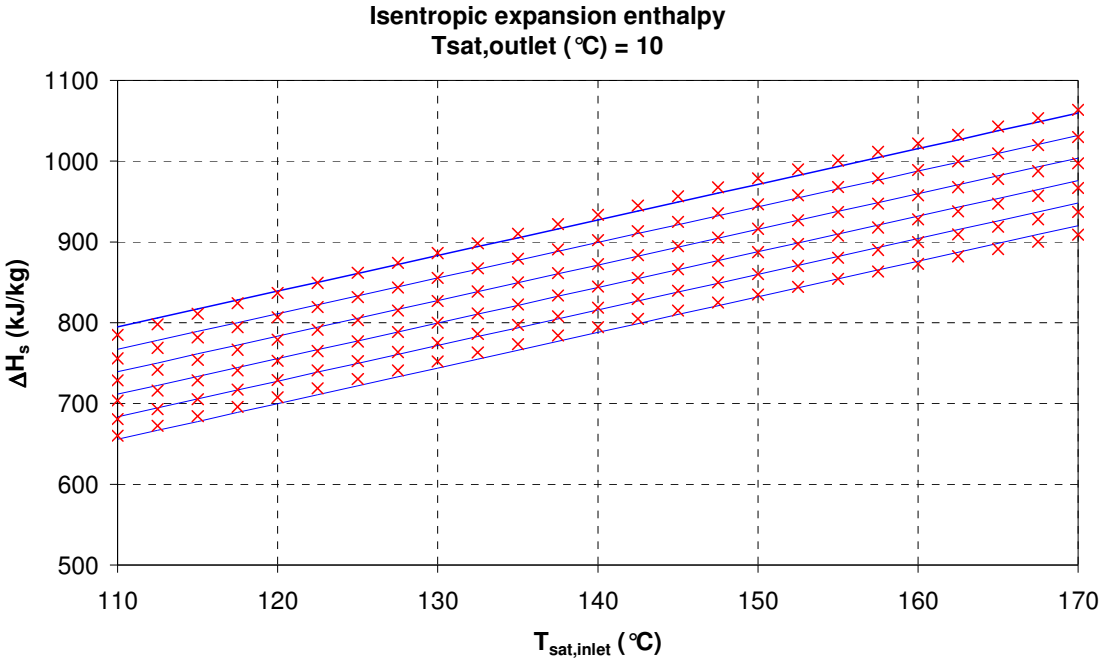
Isentropic expansion enthalpy
Tsat,outlet (°C) = 10
1100
1000
900
800
700
600
500
ΔHs (kJ/kg)
110
120
130
140
150
160
170
Tsat,inlet (°C)

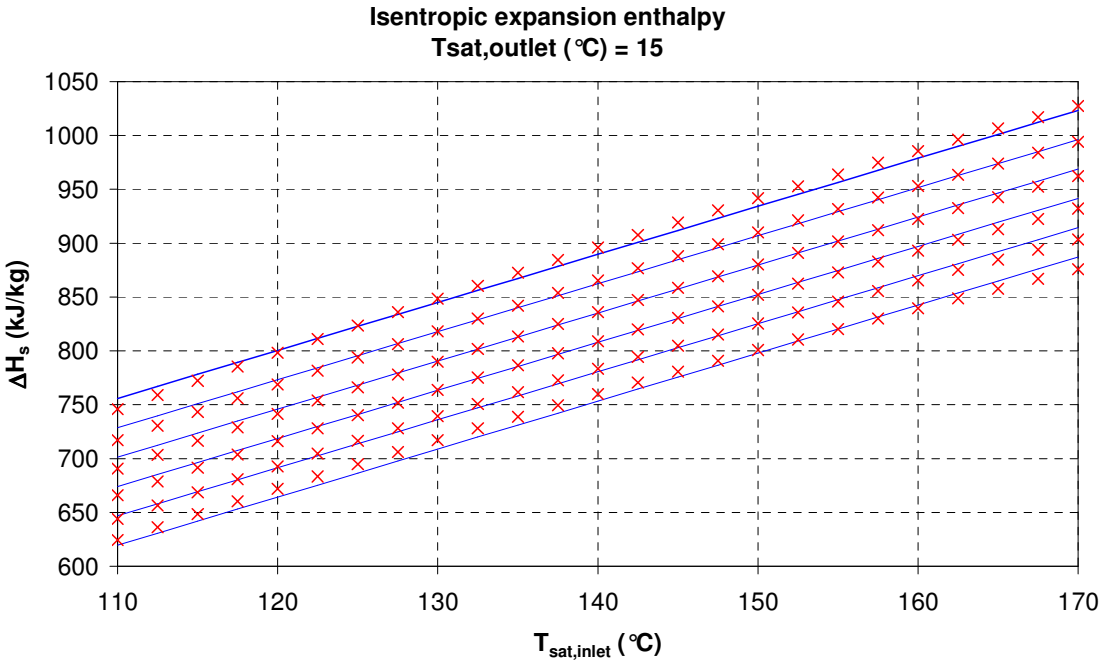
Isentropic expansion enthalpy
Tsat,outlet (°C) = 15
1050
1000
950
900
850
800
750
700
650
600
ΔHs (kJ/kg)
110
120
130
140
150
160
170
Tsat,inlet (°C)

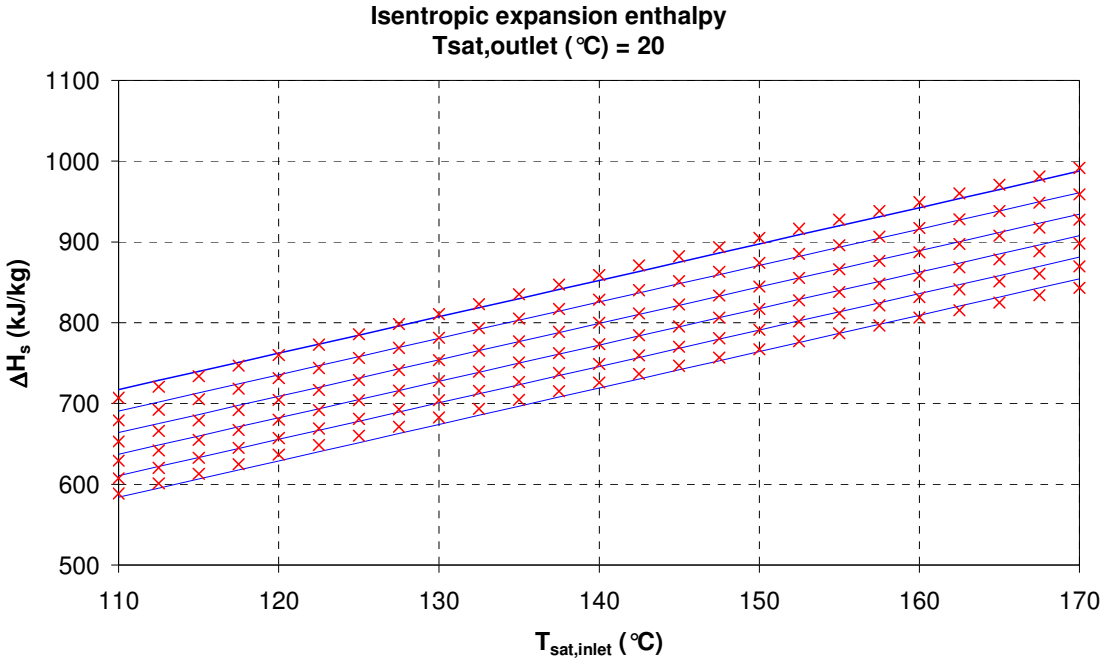
Isentropic expansion enthalpy
Tsat,outlet (°C) = 20
ΔHs (kJ/kg)
1100
1000
900
800
700
600
500
110
120
130
140
150
160
170
Tsat,inlet (°C)

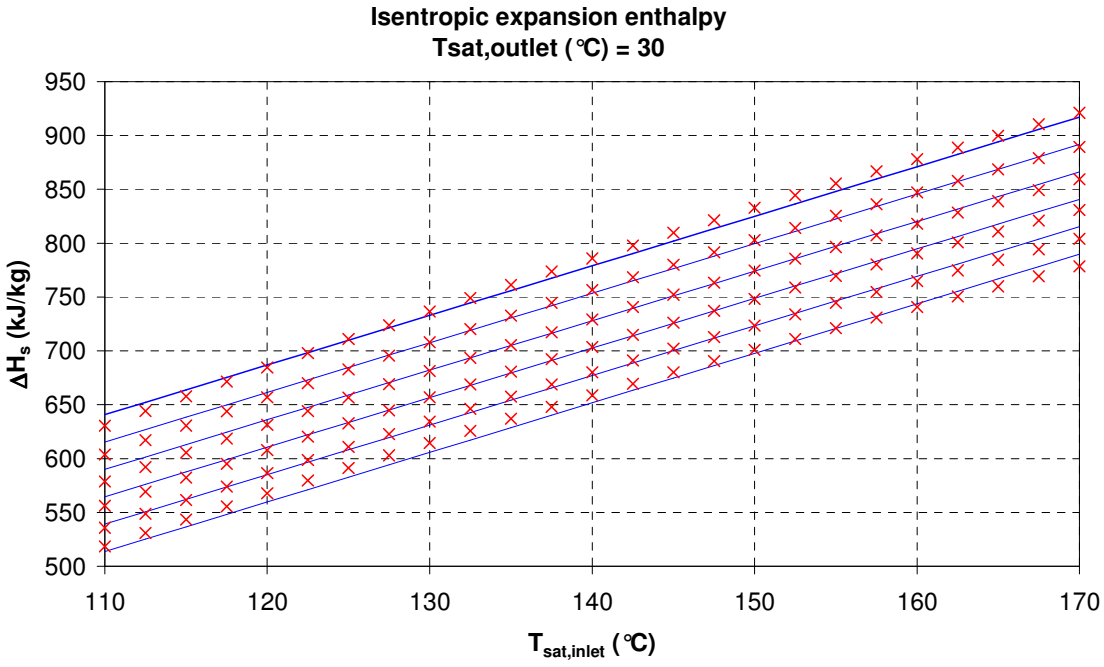
Isentropic expansion enthalpy
Tsat,outlet (°C) = 30
ΔHs (kJ/kg)
950
900
850
800
750
700
650
600
550
500
110
120
130
140
150
160
170
Tsat,inlet (°C)

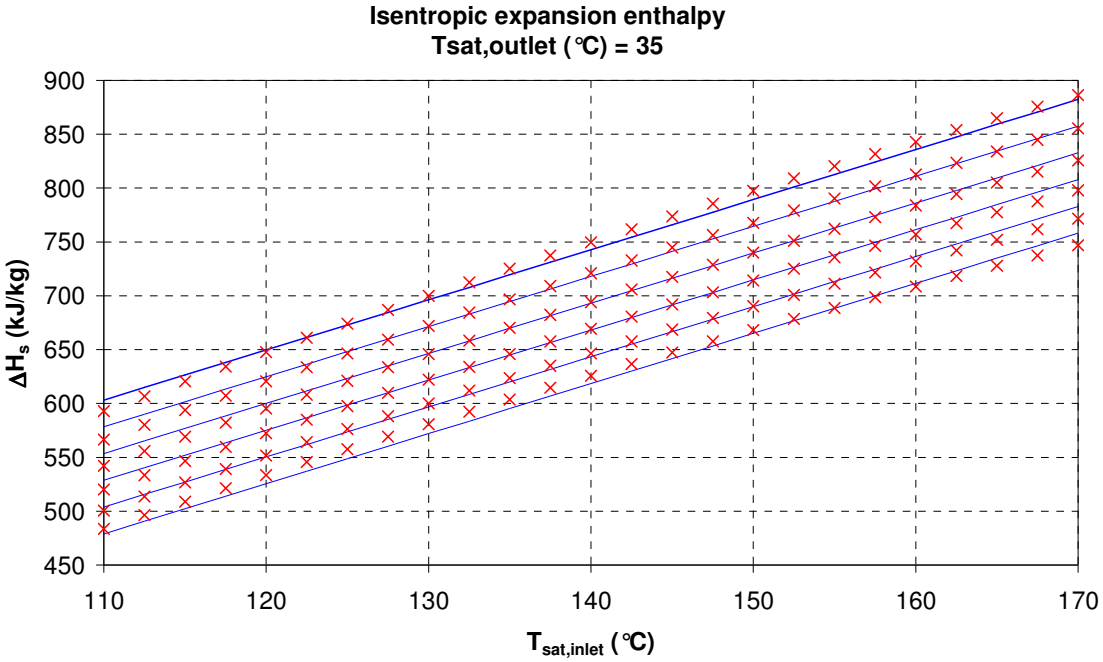
Isentropic expansion enthalpy
Tsat,outlet (°C) = 35
900
850
800
750
700
650
600
550
500
450
ΔHs (kJ/kg)
110
120
130
140
150
160
170
Tsat,inlet (°C)

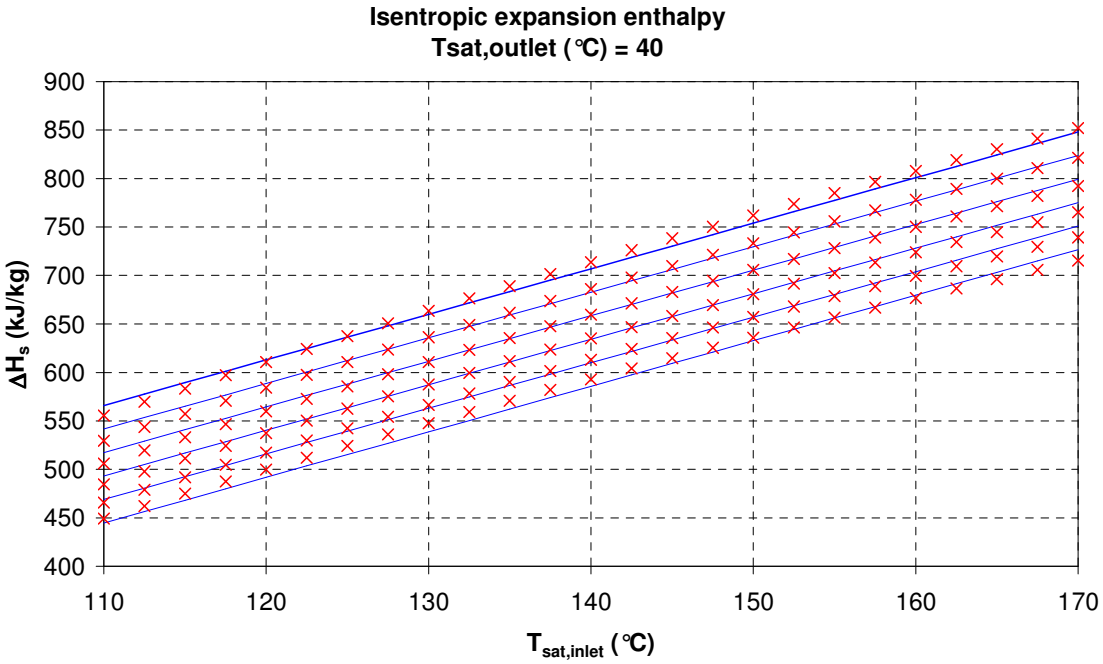
Isentropic expansion enthalpy
Tsat,outlet (°C) = 40
900
850
800
750
700
650
600
550
500
450
400
ΔHs (kJ/kg)
110
120
130
140
150
160
170
Tsat,inlet (°C)

10 APPENDIX: THERMODYNAMIC PROPERTIES

In this appendix the thermodynamic properties used in both the methanol test case and the HDA test case are presented.

10.1 Specific heat capacity

The ideal gas specific heat capacities are based on data from (Linstrom and Mallard 01). The specific heat capacity is linearised in the interval needed for the calculations, even though this is not entirely correct, it is considered sufficiently accurate for this work.

$$c_p = a + bT \tag{8.1}$$

where c_p *is the specific heat capacity [kJ/kmole-K]*
T *is the temperature [K]*
a and b are constants

In fig. 10-1 the heat capacities used in the methanol case are shown.

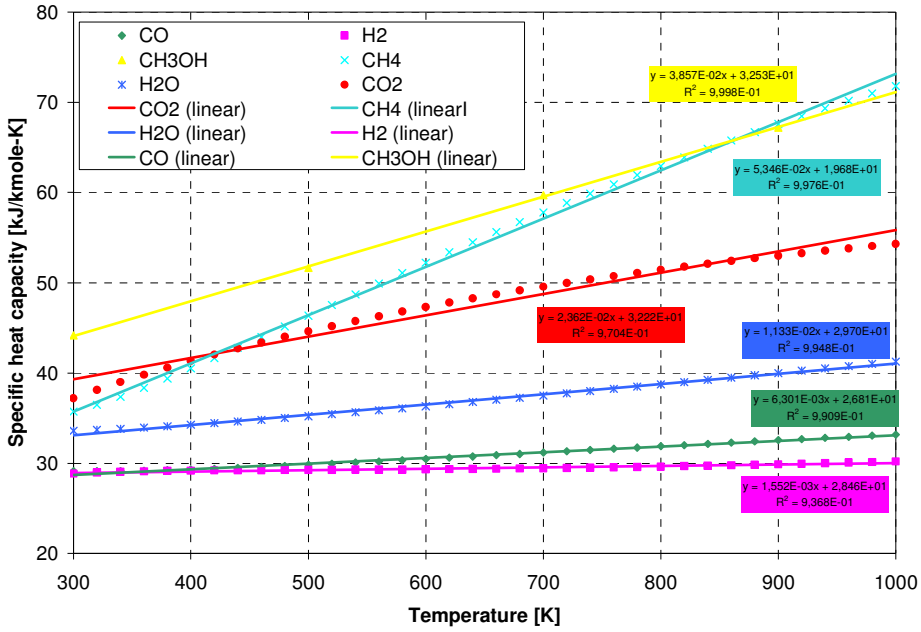

fig. 10-1 Specific heat capacities for the components in the methanol synthesis

The heat capacities for the aromatics in the HDA-process are shown in fig. 10-2.

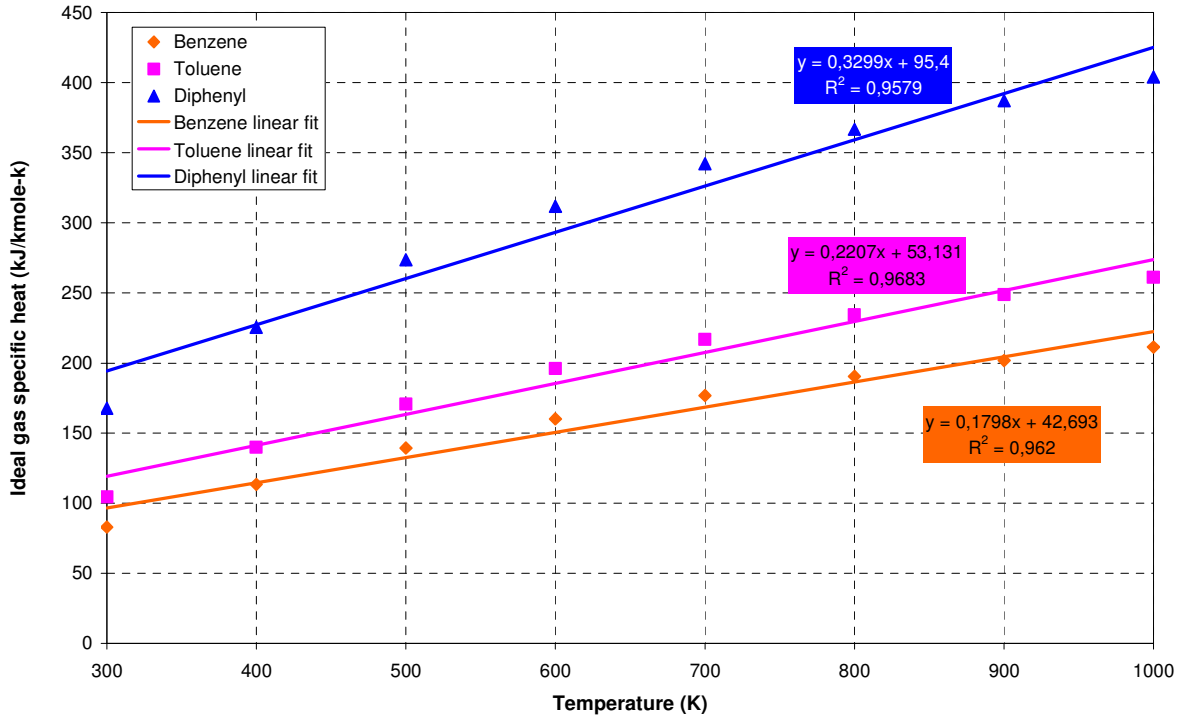

fig. 10-2 Ideal gas specific heat capacity for benzene, toluene and diphenyl (Perry 97).

The specific heat capacities in the liquid phase are assumed constant (Linstrom and Mallard 01)

	Benzene	Toluene	Diphenyl
C_p (kJ/kmole-K)	135	157	260

10.2 Heat of vaporisation

The enthalpy of vaporisation is found using the relation proposed by (Perry 97):

$$\Delta h_{fg}\left[\frac{kJ}{kmole}\right] = A\left(1-\frac{T[K]}{T_c[K]}\right)^B \tag{8.2}$$

Where the coefficients are found below

table 10-1 Coefficients for enthalpy of vaporisation.

	Water	Methanol	Benzene	Toluene	Diphenyl
A	54020	53926	46426	50144	75736
B	0.3317	0.3863	0.4039	0.3859	0.3975
T_c	647	512.6	562.0	591.7	780.0

10.3 Vapour pressure

The vapour pressure is found by the Antoine equation

$$\log_{10}\left(p_{sat}[bar]\right) = A + \frac{B}{T[K]+C} \tag{8.3}$$

The coefficients are all from (Linstrom and Mallard 01), and listed in table 10-2.

table 10-2 Antoine coefficients.

	CO	H2	CH3OH	CO2	H2O	CH4	Benzene	Toluene	Diphenyl
A	3.365	3.349	5.159	6.812	5.084	3.990	3.985	4.050	4.365
B	230.27	86.88	1569.61	1301.7	1663.1	443.01	1184.2	1327.041	1996.0
C	-13.14	5.584	-34.846	-3.504	-45.62	-0.49	-55.58	-55.53	-70.42

10.4 Liquid density

Liquid density are assumed to be a linear with respect to temperature, the curve fit are based on data from (Linstrom and Mallard 01).

$$\rho_{liquid}\left[\frac{kmole}{m^3}\right] = A\cdot T[K] + B \tag{8.4}$$

table 10-3 Coefficients for liquid density.

	Water	Methanol	Benzene	Toluene	Diphenyl

A	-0.0377	-0.0338	-0.0153	-0.0103	-0.0074
B	66.80	34.45	15.81	12.45	9.336

10.5 Entropy and exergy

The absolute entropy is defined as

$$s^0\left(T_g\right) = \int_{T=0}^{T=T_f} \frac{c_{p,s}}{T} dT + \frac{\Delta h_f}{T_f} + \int_{T=T_f}^{T=T_v} \frac{c_{p,l}}{T} dT + \frac{\Delta h_v}{T_v} + \int_{T=T_v}^{T=T_g} \frac{c_{p,g}}{T} dT \tag{8.5}$$

Normally the entropy at the reference conditions (298.15 K and 1.013 bar) can be found in literature, why the above equation reduces to

$$s^0\left(T_g\right) = s^0_{g,ref} + \int_{T=T_{ref}}^{T=T_g} \frac{c_{p,g}}{T} dT = s^0_{g,ref} + a\ln(T) + bT - a\ln\left(T_{ref}\right) + T_{ref}b \tag{8.6}$$

The meaning of the ideal gas standard entropy at 298.15 is somewhat arbitrary, since many chemical species can be in the liquid or even solid state at this temperature. Nevertheless, it is a useful basis for calculation of the entropy. In the HDA case it is necessary to calculate the liquid entropy for several streams. In order to find the liquid entropy it is therefore necessary to establish the liquid entropy at the standard state.

$$s^0_{g,ref} = s^0_{l,ref} + \int_{T=T_{ref}}^{T=T_v} \frac{c_{p,l}(T)}{T} dT + \frac{\Delta h_v}{T_v} + \int_{T=T_v}^{T=T_{ref}} \frac{c_{p,g}(T)}{T} dT \tag{8.7}$$

11

APPENDIX: RIGOROUS MINLP-FORMULATION OF HEAT-INTEGRATION

The rigorous formulation of the heat integration problem discussed in 4.2 is presented here. The resulting formulation is a MINLP-problem.

The following method is a revision of the work by (Grossmann *et al.* 98) and is a rigorous formulation of the heat integration problem in 4.2. Instead of using the relaxed formulation of the max-operators, that were used by (Duran and Grossmann 86b), integer variables are used instead.

For each pinch candidate it must be determined how much heat the hot streams can provide above the pinch, and how much heat is required by the cold streams below the pinch. Three options exist for every stream at every pinch candidate.

- The stream is completely above pinch
- The inlet temperature is above pinch, while the outlet temperature is below pinch (and vice-versa for cold streams)
- The stream is completely below pinch

A binary variable is associated with each of these possibilities, why it can hereby be determined how the stream is to be treated. Note that for isothermal streams the second mode, is not an option as inlet and outlet temperatures are both either above or below pinch.

Let us define a set of hot streams $H = H_N \cup H_I$, cold streams $C = C_N \cup C_I$, hot utility streams $H_U = H_{U,N} \cup H_{U,I}$ and cold utility streams $C_U = C_{U,N} \cup C_{U,I}$. Each of the sets is a union of non-isothermal streams (index N) and isothermal streams (index I).

The energy balance must be formulated for each of the sets, for each of the three possible modes (above, across or below) and for each pinch candidate. A set of temperature constraint must be associated with the binary variables in order to determine the position of

the stream. When a hot stream or hot utility is pinch candidate, the energy balance and temperature requirements for each of the hot streams and hot utilities can be expressed with big-M constraints and a set of binary variables $y_1^{i,k}, y_2^{i,k}, y_3^{i,k}$, index 1, 2, and 3 refers to above, across or below pinch.

$$\left.\begin{array}{l}
\dot{Q}_{i,k} - \dot{Q}_i \le U\left(1 - y_1^{i,k}\right) \\
T_i^{in} \ge T_k^{in} + \varepsilon - M\left(1 - y_1^{i,k}\right) \\
T_i^{out} \ge T_k^{in} + \varepsilon - M\left(1 - y_1^{i,k}\right) \\
\dot{Q}_{i,k} \le U\left(1 - y_3^{i,k}\right) \\
T_i^{in} \le T_k^{in} + M\left(1 - y_3^{i,k}\right) \\
T_i^{out} \le T_k^{in} + M\left(1 - y_3^{i,k}\right) \\
y_1^{i,k} + y_2^{i,k} + y_3^{i,k} = 1
\end{array}\right\} \begin{array}{l} i \in H \cup H_U \\ k \in H \cup H_U \end{array}$$

$$\left.\begin{array}{l}
\dot{Q}_{i,k} - F_i\left(T_i^{in} - T_k^{in}\right) \le U\left(1 - y_2^{i,k}\right) \\
T_i^{in} \ge T_k^{in} + \varepsilon - M\left(1 - y_2^{i,k}\right) \\
T_i^{out} \le T_k^{in} + M\left(1 - y_2^{i,k}\right)
\end{array}\right\} \begin{array}{l} i \in H_N \cup H_{U,N} \\ k \in H \cup H_U \end{array}$$

$$y_2^{i,k} = 0 \quad i \in H_I \cup H_{U,I}, k \in H \cup H_U \tag{8.8}$$

For the cold streams and cold utilities, the energy balance and temperature constraints are expressed as:

$$\left.\begin{array}{l}
\dot{Q}_{j,k} - \dot{Q}_j \ge -U\left(1 - y_1^{j,k}\right) \\
T_j^{in} \ge T_k^{in} - \Delta T_{min} - M\left(1 - y_1^{j,k}\right) \\
T_j^{out} \ge T_k^{in} - \Delta T_{min} - M\left(1 - y_1^{j,k}\right) \\
\dot{Q}_{j,k}^{HP} \le U\left(1 - y_3^{j,k}\right) \\
T_j^{in} \le T_k^{in} - \Delta T_{min} - \varepsilon + M\left(1 - y_3^{j,k}\right) \\
T_j^{out} \le T_k^{in} - \Delta T_{min} - \varepsilon + M\left(1 - y_3^{j,k}\right) \\
y_1^{j,k} + y_2^{j,k} + y_3^{j,k} = 1
\end{array}\right\} \begin{array}{l} j \in C \cup C_U \\ k \in H \cup H_U \end{array}$$

$$\left.\begin{array}{l}
\dot{Q}_{j,k} - F_j\left(T_j^{out} - \left(T_k^{in} - \Delta T_{min}\right)\right) \ge -U\left(1 - y_2^{j,k}\right) \\
T_i^{in} \le T_k^{in} - \Delta T_{min} + M\left(1 - y_2^{j,k}\right) \\
T_i^{out} \ge T_k^{in} - \Delta T_{min} - \varepsilon - M\left(1 - y_2^{j,k}\right)
\end{array}\right\} \begin{array}{l} j \in C_N \cup C_{U,N} \\ k \in H \cup H_U \end{array}$$

$$y_2^{j,k} = 0 \quad j \in C_I \cup C_{U,I}, k \in H \cup H_U \tag{8.9}$$

When the cold streams or cold utilities are pinch candidates, the hot stream energy balance and temperature constraints are

$$\left.\begin{aligned}
&\dot{Q}_{i,l} - \dot{Q}_i \le U\left(1 - y_1^{i,l}\right) \\
&T_i^{in} \ge T_l^{in} + \Delta T_{min} - M\left(1 - y_1^{i,l}\right) \\
&T_i^{out} \ge T_l^{in} + \Delta T_{min} - M\left(1 - y_1^{i,l}\right) \\
&\dot{Q}_{i,l} \le U\left(1 - y_3^{i,l}\right) \\
&T_i^{in} \le T_l^{in} + \Delta T_{min} - \varepsilon + M\left(1 - y_3^{i,l}\right) \\
&T_i^{out} \le T_l^{in} + \Delta T_{min} - \varepsilon + M\left(1 - y_3^{i,l}\right) \\
&y_1^{i,l} + y_2^{i,l} + y_3^{i,l} = 1
\end{aligned}\right\} \begin{array}{l} i \in H \cup H_U \\ j \in C \cup C_U \end{array} \tag{8.10}$$

$$\left.\begin{aligned}
&\dot{Q}_{i,l} - F_i\left(T_i^{in} - T_l^{in}\right) \le U\left(1 - y_2^{i,l}\right) \\
&T_i^{in} \ge T_l^{in} + \Delta T_{min} - M\left(1 - y_2^{i,l}\right) \\
&T_i^{out} \le T_l^{in} + \Delta T_{min} - \varepsilon + M\left(1 - y_2^{i,l}\right)
\end{aligned}\right\} \begin{array}{l} i \in H_N \cup H_{U,N} \\ l \in C \cup C_U \end{array}$$

$$y_2^{i,l} = 0 \quad i \in H_I \cup H_{U,I}, l \in C \cup C_U$$

The energy balance for cold streams with cold pinch candidates can be formulated as

$$\left.\begin{aligned}
&\dot{Q}_{j,l} - \dot{Q}_j \ge -U\left(1 - y_1^{j,l}\right) \\
&T_j^{in} \ge T_l^{in} - M\left(1 - y_1^{j,l}\right) \\
&T_j^{out} \ge T_l^{in} - M\left(1 - y_1^{j,l}\right) \\
&\dot{Q}_{j,l}^{HP} \le U\left(1 - y_3^{j,l}\right) \\
&T_j^{in} \le T_l^{in} - \varepsilon + M\left(1 - y_3^{j,l}\right) \\
&T_j^{out} \le T_l^{in} - \varepsilon + M\left(1 - y_3^{j,l}\right) \\
&y_1^{j,l} + y_2^{j,l} + y_3^{j,l} = 1
\end{aligned}\right\} \begin{array}{l} j \in C \cup C_U \\ l \in C \cup C_U \end{array} \tag{8.11}$$

$$\left.\begin{aligned}
&\dot{Q}_{j,l} - F_j\left(T_j^{out} - T_l^{in}\right) \ge -U\left(1 - y_2^{j,l}\right) \\
&T_i^{in} \le T_l^{in} - \varepsilon + M\left(1 - y_2^{j,l}\right) \\
&T_i^{out} \ge T_l^{in} - M\left(1 - y_2^{j,l}\right)
\end{aligned}\right\} \begin{array}{l} j \in C_N \cup C_{U,N} \\ l \in C \cup C_U \end{array}$$

$$y_2^{j,l} = 0 \quad j \in C_I \cup C_{U,I}, l \in C \cup C_U$$

Furthermore it must be noticed that, constraints in optimisation problems are always formulated using ≤ and≥, but never strictly greater than or less than. When the inlet temperature of a hot isothermal stream is pinch candidate, the isothermal stream can both be identified as being completely above pinch and completely below pinch. From fig. 11-1it is evident that the heat of the isothermal stream is only available below pinch, why it must

not be accounted for above pinch. The opposite holds for a cold isothermal stream with as pinch candidate, here the entire heat content of the isothermal stream must exchange heat above pinch. To overcome this problem a small slack variable ε is introduced, to ensure proper identification of these cases.

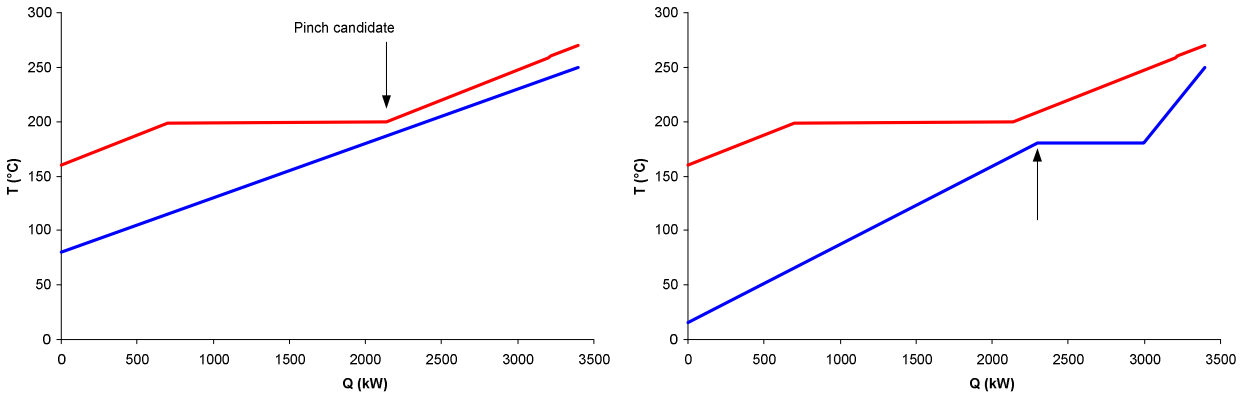

fig. 11-1 To the left is a simple example of composite curves with a hot isothermal stream. To the right is a simple example of composite curves with a cold isothermal stream.

12

APPENDIX: LIST OF GAS TURBINES

In this appendix the complete list of gas turbines used for the modelling in 4.1.5 are listed.

The gas turbines used for the modelling in 4.1.5 are listed in the following, along with large scale versions of the charts found in fig. 4-20 and fig. 4-21. The gas turbines are categorised as industrial and aero-derivatives.

12.1 Industrial gas turbines

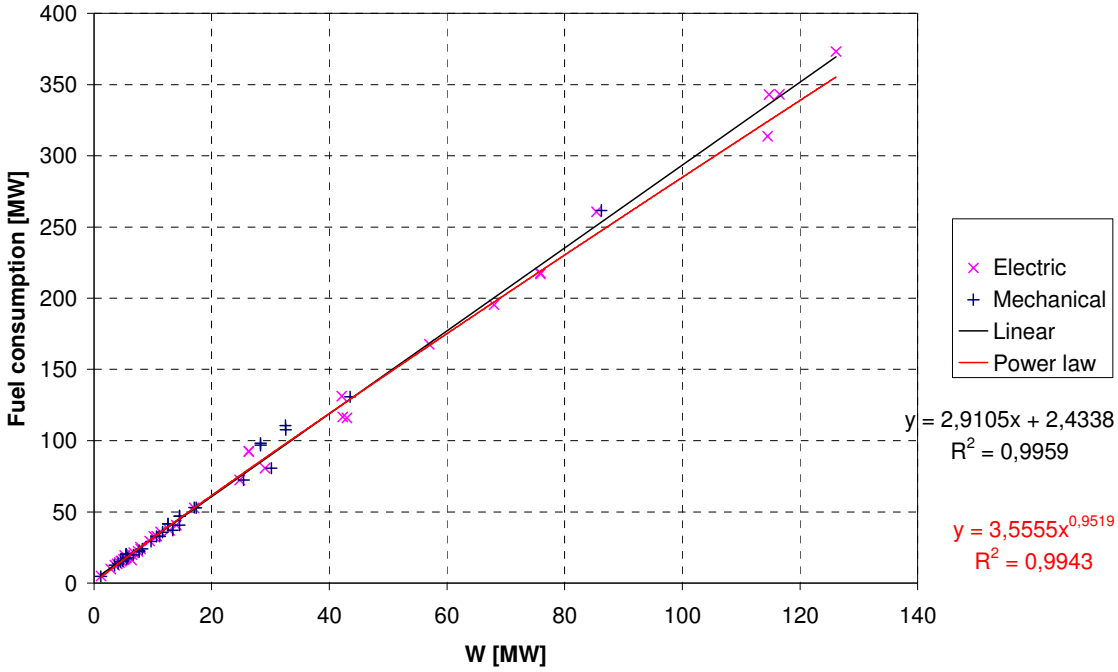

fig. 12-1 Correlation of fuel consumption to work output for industrial gas turbines.

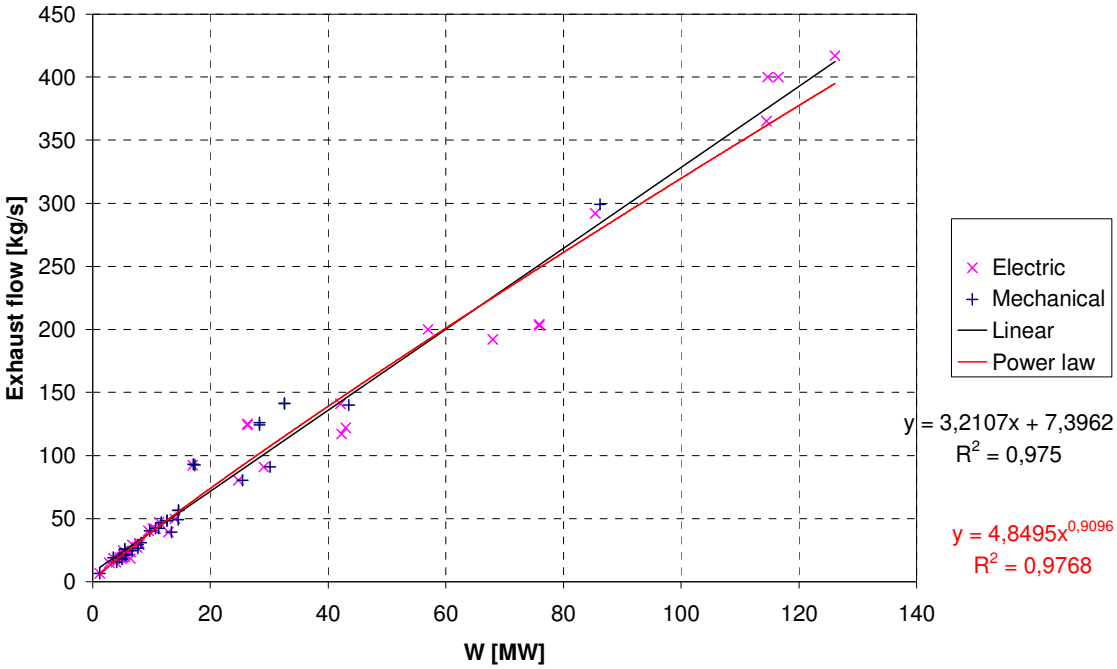

fig. 12-2 Correlation of exhaust gas flow to work output for industrial gas turbines

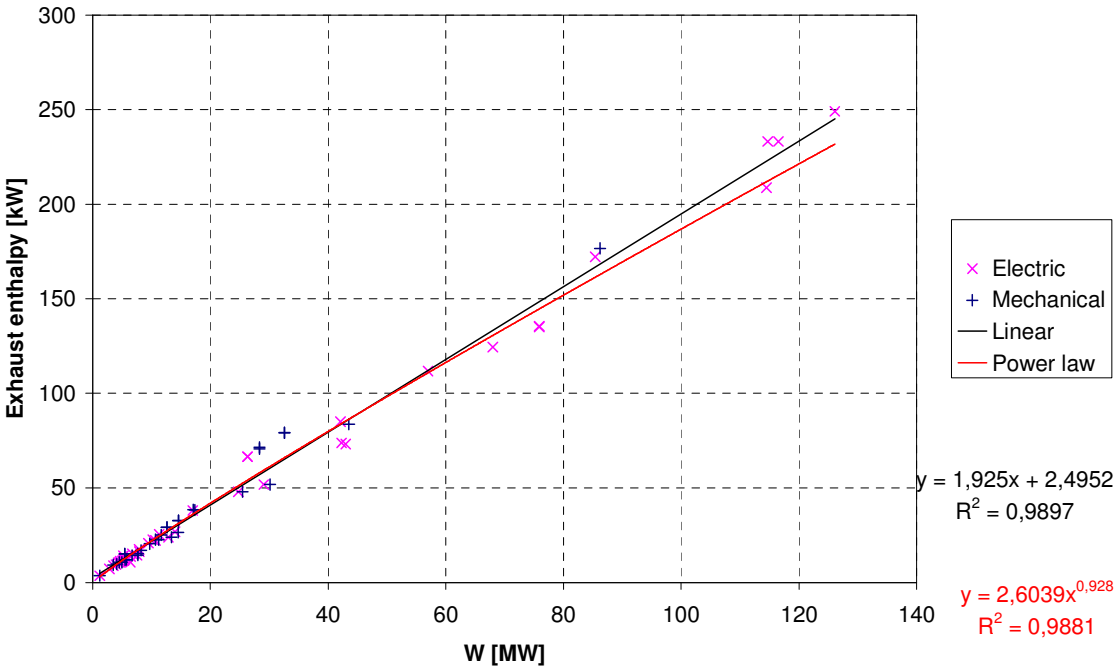

fig. 12-3 Correlation of exhaust enthalpy to work-output for industrial gas turbines

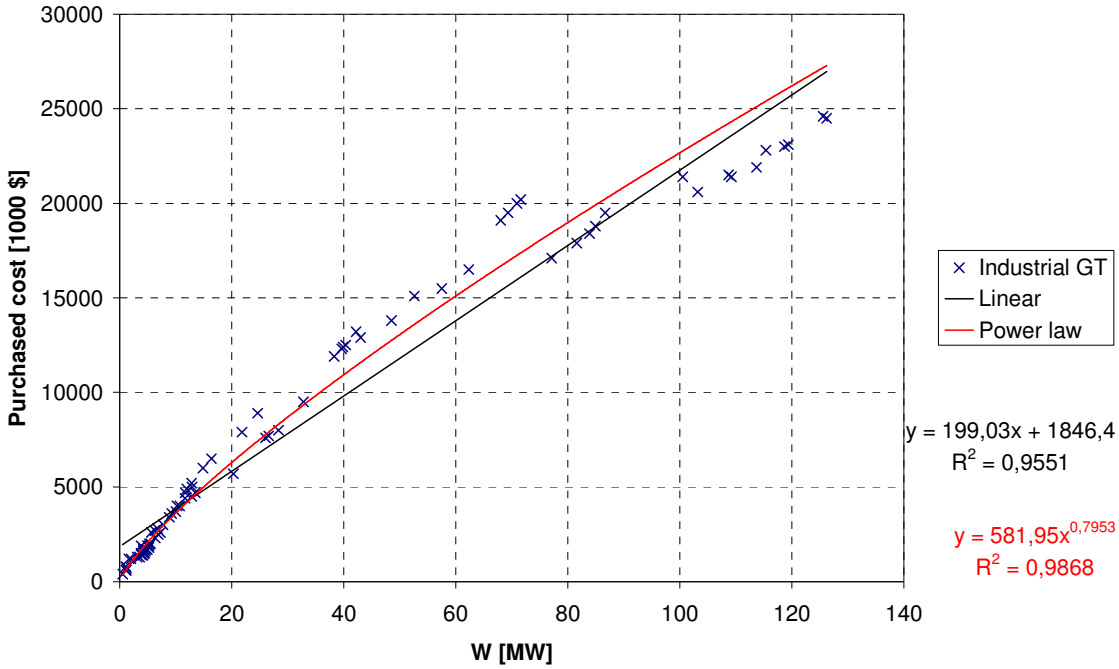

fig. 12-4 Correlation of purchased cost to work output for industrial gas turbines.

12.1.1 Table of industrial gas turbines

Manufacturer	Model	Output [kW]	Heat rate [kJ/kWh]	Pressure ratio	Mass flow [kg/s]	Turbine inlet temp [C]	Exhaust temp [C]
Solar Turbines Incorporated	Saturn 20	1185	14665	6.6	6.5		520
Solar Turbines Incorporated	Saturn 20	1210	14790	6.8	6.5		505
Zorya-Mashproekt	GT2500	2850	12631	12	14.9	951	440
Solar Turbines Incorporated	Centaur 40	3505	12909	10.2	19		446
Solar Turbines Incorporated	Centaur 40	3515	12910	9.8	18.6		435
Rolls-Royce	501-KB5	3938	12266	10.2	15.4		560
Rolls-Royce	501-KC5	4101	12019	9.4	15.5		571
Alstom Power	TYPHOON	4343	11995	13	17.67		540
Solar Turbines Incorporated	Centaur 50	4570	11958	10.6	18.9		515
Solar Turbines Incorporated	Centaur 50	4600	12260	10.6	19.1		510
Alstom Power	TYPHOON	4690	11933	14.1	19.05		540
Alstom Power	TYPHOON	4941	11248	13	17.96		540

Manufacturer	**Model**	**Output [kW]**	**Heat rate [kJ/kWh]**	**Pressure ratio**	**Mass flow [kg/s]**	**Turbine inlet temp [C]**	**Exhaust temp [C]**
Alstom Power	TYPHOON	5044	11918	14.3	19.56		529
GE Power - Nuovo Pignone	PGT5	5220	13420	9.1	24.6		523
Alstom Power	TYPHOON	5249	11819	14.9	20.8		538
Rolls-Royce	501-KB7	5300	11380	13.5	21.1		501
GE Power - Nuovo Pignone	PGT5	5440	13470	8.6	25.8		533
GE Aero Energy Products	GE5 (DLN)	5451	13411	14.8	25.8		533
GE Aero Energy Products	GE5 (DLN)	5500	11720	14.8	19.7		571
Solar Turbines Incorporated	Taurus 60	5500	11840	12.2	21.9		510
Rolls-Royce	501-KC7	5518	11180	13.5	20.9		520
Solar Turbines Incorporated	Taurus 60	5740	11265	12	21.6		510
Rolls-Royce	501-KH5	6420	9037	10.2	18.3		530
Rolls-Royce	601-K9	6449	11201	14.6	23.5		530
Rolls-Royce	601-K9	6711	10668	14.8	24.6		529
Alstom Power	TORNADO	6748	11419	12.3	29.3		471
Solar Turbines Incorporated	Taurus 70	7520	10650	16.1	27		490
Alstom Power	TORNADO	7672	10743	12.6	29.46		471
Solar Turbines Incorporated	Taurus 70	7690	10340	16.8	26.6		495
Alstom Power	TEMPEST	7908	11540	14.1	29.45	1122	540
Rolls-Royce	601-K11	7918	10921	19.4	30.4		488
Rolls-Royce	601-K11	8203	10611	19.4	30.7		504
Solar Turbines Incorporated	Mars 90	9450	11300	16	40.2		470
Solar Turbines Incorporated	Mars 90	9695	10881	16.5	40.2		464
GE Power - Nuovo Pignone	PGT10	10220	11536	13.8	42.3		488
GE Power - Nuovo Pignone	PGT10	10660	11060	13.8	42.3		488
Solar Turbines Incorporated	Mars 100	10690	11090	17.4	41.8		485
Solar Turbines Incorporated	Mars 100	11185	10598	17.6	42.3		486
GE Aero Energy Products	GE10 (DLN)	11300	11481	15.8	47.3		490
GE Aero Energy Products	GE10 (DLN)	11693	11050	15.8	46.9		487
Mitsubishi Heavy industries	MFT-111A	12610	11874		48.5		547
Mitsubishi Heavy industries	MFT-111A	12610	11874		48.5		547
Alstom Power	CYCLONE	12874	10357	16.8	39.38	1256	555
Alstom Power	CYCLONE	13412	9942	16.8	39.38		555
Solar Turbines Incorporated	Titan 130	14000	10460	16	49.8		490

Manufacturer	Model	Output [kW]	Heat rate [kJ/kWh]	Pressure ratio	Mass flow [kg/s]	Turbine inlet temp [C]	Exhaust temp [C]
Solar Turbines Incorporated	Titan 130	14540	10075	16.4	49		492
Mitsubishi Heavy industries	MFT-111B	14570	11631		56.36		530
Mitsubishi Heavy industries	MFT-111B	14570	11631		56.36		530
Alstom Power	GT35C	17000	11180	12	92.3	850	375
Alstom Power	GT35C	17065	11212	12.3	93		376
Alstom Power	GT35C	17365	10978	12	92.4		377
Alstom Power	GT10B	24770	10535	14	80.4		543
Alstom Power	GT10B	25430	10257	14	80.4		543
GE Aero Energy Products	MS5001	26300	12650	10.5	124.2		487
GE Power Systems	PG5371(PA) - MS5001	26300	12687	10.5	125.2		483
GE Aero Energy Products	MS5002C	28337	12309	8.9	126		515
GE Power Systems	M5002C	28340	12470	8.9	124.3		517
Alstom Power	GT10C	29060	10000	17.6	91		518
Alstom Power	GT10C	30120	9649	17.6	91		518
GE Power Systems	M5002D	32580	12239	10.8	141.4		509
GE Aero Energy Products	MS5002D	32595	11899	10.8	141.3		510
GE Power Systems	PG6581(B)	42100	11227	12.2	141		548
GE Power Systems	PG6591(C)	42300	9930	19	117		574
Alstom Power	GTX100	43000	9720	20	122		546
GE Power Systems	M6581(B)	43534	10823	12	140		544
Alstom Power	GT8C2	57000	10588	17.6	200	1100	508
Ansaldo Energia	V64,3A	68000	10345	16.2	192		589
GE Power Systems	PG6111(FA) 50 Hz	75900	10300	15.6	203		605
GE Power Systems	PG6111(FA) 60 Hz	75900	10330	15.7	204		604
GE Power Systems	PG7121(EA)	85400	10991	12.6	292		536
GE Power Systems	M7121(EA)	86230	10925	11.9	299		537
Zorya-Mashproekt	GT110000	114500	9862	14.7	365	1210	520
Alstom Power	GT11N2 (50Hz)	114700	10762	15.5	400	1085	530
Alstom Power	GT11N2 (60Hz)	116500	10603	15.5	400	1085	530
GE Power Systems	PG9171(E)	126100	10653	12.6	417		543

12.2 Aero derivatives

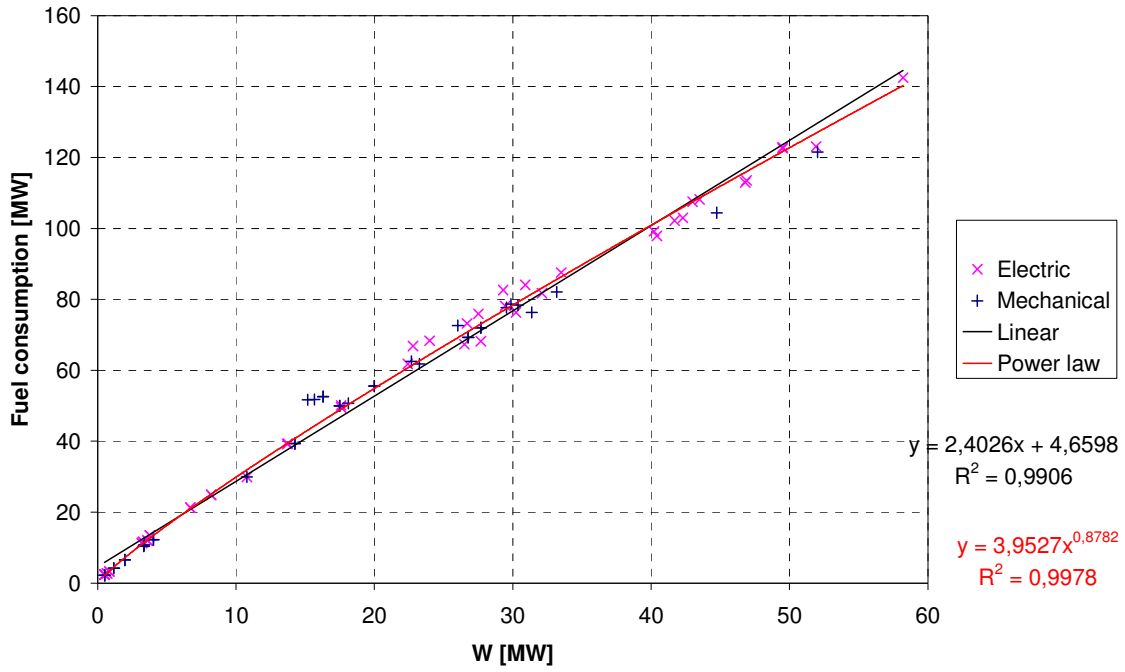

fig. 12-5 Correlation of fuel consumption to work output for aero-derivative gas turbines.

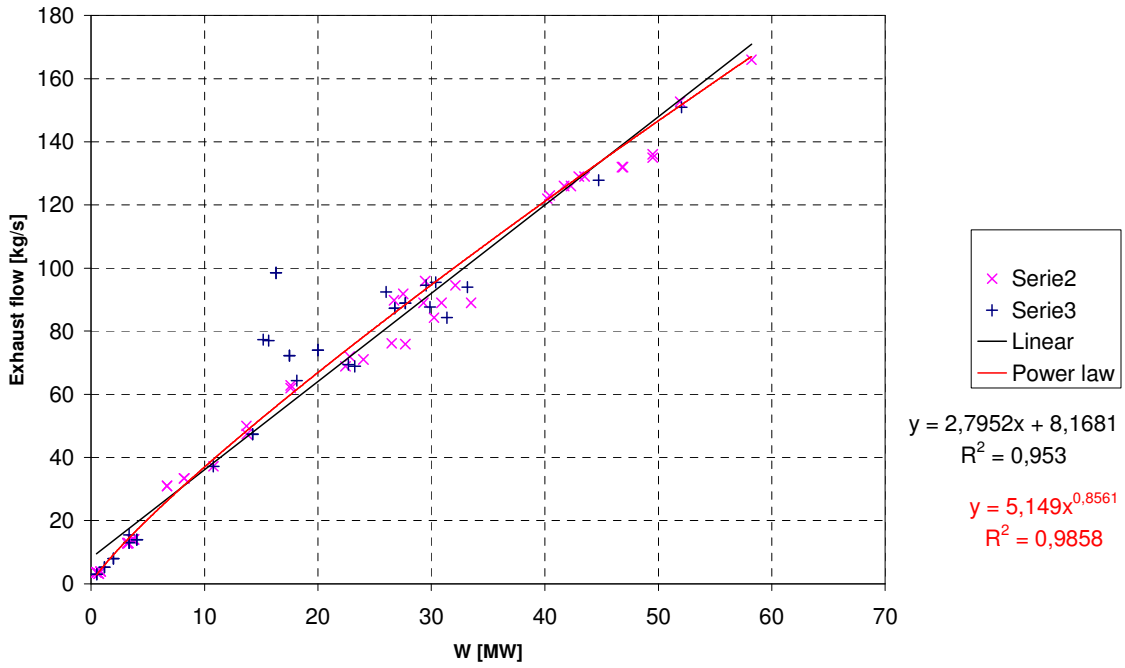

fig. 12-6 Correlation of exhaust gas flow to work output for aero-derivate gas turbines

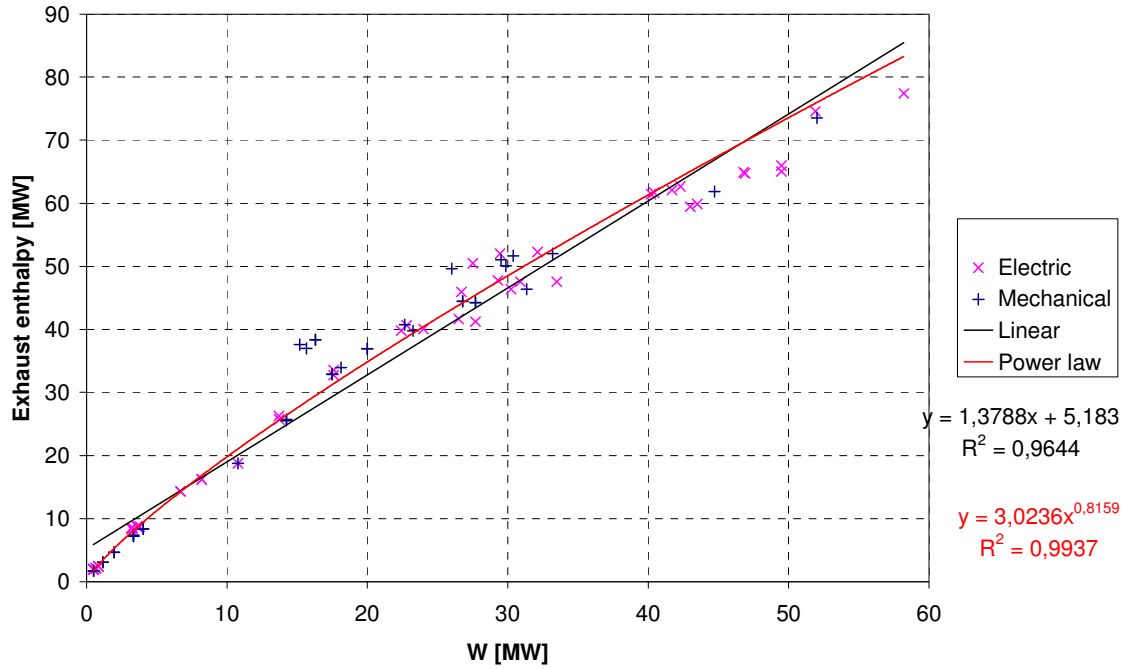

fig. 12-7 Correlation of exhaust enthalpy to work-output for aero-derivate gas turbines

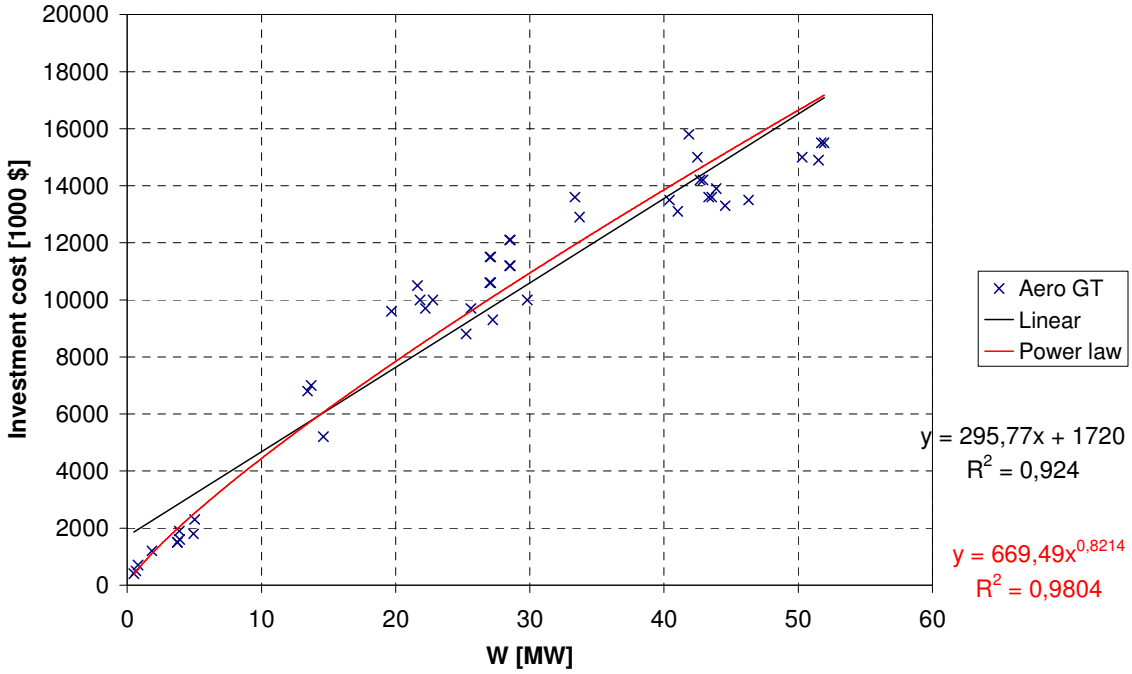

fig. 12-8 Correlation of purchased cost to work output for aero-derivate gas turbines.

Manufacturer	Model	Output [kW]	Heat rate [kJ/kWh]	Pressure ratio	Mass flow [kg/s]	Turbine inlet temp [C]	Exhaust temp [C]
Vericor Power Systems	ASE 8	490	17275	10.5	3.6		492
Vericor Power Systems	ASE 8	490	17275	10.5	3.6		492
Vericor Power Systems	ASE 8	506	17008	10.5	3.6		491
Vericor Power Systems	ASE 8	506	17008	10.5	3.6		491
Pratt & Whitney Power Systems	ST6L-721	508	15400	6.8	3		514
Pratt & Whitney Power Systems	ST6L-721	508	15400	6.8	3		514
Pratt & Whitney Power Systems	ST6L-795	678	14575	7.4	3.24		589
Pratt & Whitney Power Systems	ST6L-795	678	14575	7.4	3.24		589
Pratt & Whitney Power Systems	ST6L-813	848	13846	8.5	3.92		566
Pratt & Whitney Power Systems	ST6L-813	848	13846	8.5	3.92		566
Pratt & Whitney Power Systems	ST6L-90	1175	12857	10.4	5.26		536
Pratt & Whitney Power Systems	ST6L-90	1175	12857	10.4	5.26		536
Pratt & Whitney Power Systems	ST18A	1961	11921	14	7.97		532
Pratt & Whitney Power Systems	ST18A	1961	11921	14	7.97		532
Vericor Power Systems	ASE 40 (VPS3)	3188	12771	8.8	12.8		599
Vericor Power Systems	ASE 40 (VPS3)	3188	12771	8.8	12.8		599
Vericor Power Systems	ASE 40 (VPS3)	3286	12735	8.8	12.9		598
Vericor Power Systems	ASE 40 (VPS3)	3286	12735	8.8	12.9		598
Pratt & Whitney Power Systems	ST30	3340	11250	18	13.02		513
Pratt & Whitney Power Systems	ST30	3340	11250	18	13.02		513
Zorya-Mashproekt	GT3000	3360	11616	13.5	15.5		420
Vericor Power Systems	ASE 50 (VPS4)	3620	11862	10.2	14		565
Vericor Power Systems	ASE 50 (VPS4)	3620	11862	10.2	14		565
Vericor Power Systems	ASE 50 (VPS4)	3776	12762	10.2	14.1		562
Vericor Power Systems	ASE 50 (VPS4)	3776	12762	10.2	14.1		562
Pratt & Whitney Power Systems	ST40	4039	10878	19	13.97		544
Pratt & Whitney Power Systems	ST40	4039	10878	19	13.97		544
Zorya-Mashproekt	GT6000	6700	11432		31		420
Zorya-Mashproekt	GT6000	6700	11432		31		420
Zorya-Mashproekt	GT6000+	8200	10911	15.7	33.4	1102	442
Zorya-Mashproekt	GT6000+	8200	10911	15.7	33.4	1102	442
Zorya-Mashproekt	GT10000	10780	10003	19	37.2		458

Manufacturer	Model	Output [kW]	Heat rate [kJ/kWh]	Pressure ratio	Mass flow [kg/s]	Turbine inlet temp [C]	Exhaust temp [C]
Zorya-Mashproekt	GT10000	10780	10003	19	37.2		458
GE Aero Energy Products	LM1600 (PA)	13700	10295	20.2	50		478
GE Power - Nuovo Pignone	PGT16	13735	10314	20.1	47.4		493
GE Aero Energy Products	LM1600 (PA)	14243	9927	20.2	47.3		491
GE Power - Nuovo Pignone	PGT16	14252	9939	20.1	47.4		493
Rolls-Royce	COBERRA 2648	15182	12257	8.8	77.3		442
Rolls-Royce	COBERRA 2656	15660	11897	8.8	77		437
Zorya-Mashproekt	GT16000	16300	11616	12.8	98.5	865	354
Zorya-Mashproekt	GT16000	16300	11616	12.8	98.5	865	354
Zorya-Mashproekt	GT15000	17500	10284	19.6	72.2	1075	414
Zorya-Mashproekt	GT15000	17500	10284	19.6	72.2	1075	414
GE Aero Energy Products	LM2000 (PE) 50Hz	17600	10129	16.4	62.8		474
GE Aero Energy Products	LM2000 (PE) 60Hz	17600	10248	16.8	62		492
GE Aero Energy Products	LM2000 (PE)	18121	10069	16.4	64.4		479
Zorya-Mashproekt	GT15000+	20000	10000	19.4	74	1160	454
Zorya-Mashproekt	GT15000+	20000	10000	19.4	74	1160	454
GE Power - Nuovo Pignone	PGT25	22417	9919	17.9	68.9		525
GE Aero Energy Products	LM2500 (PE)	22669	9928	18.1	69.4		534
GE Aero Energy Products	LM2500 (PE) 50 Hz	22800	10556	18.1	72		513
GE Power - Nuovo Pignone	PGT25	23261	9560	17.9	68.9		525
GE Aero Energy Products	LM2500 (PE) 60 Hz	24000	10248	19.1	71		513
Rolls-Royce	COBERRA 6556	26025	10045	20.1	92.4		488
GE Aero Energy Products	LM2500 (PH) 50 Hz	26500	9148	18.2	76.2		497
Zorya-Mashproekt	GT25000	26700	9866	21	89.8	1245	465
Mitsubishi Heavy industries	MFT-8	26780	9316		87.28		463
Mitsubishi Heavy industries	MFT-8	26780	9316		87.28		463
Rolls-Royce	RB211- 6562DLE	27520	9933	20.8	91.8		500
Pratt & Whitney Power Systems	FT8	27700	9351	20.3	88.9		452.8
GE Aero Energy Products	LM2500 (PH) 60 Hz	27700	8862	17.8	75.9		494
Pratt & Whitney Power Systems	FT8	27700	9351	20.3	88.9		452.8
GE Aero Energy Products	LM2500 (PK) 50 Hz	29300	10152	22.8	89		488
Rolls-Royce	RB211- 6762DLE	29450	9554	21.5	95.9		493

Manufacturer	**Model**	**Output [kW]**	**Heat rate [kJ/kWh]**	**Pressure ratio**	**Mass flow [kg/s]**	**Turbine inlet temp [C]**	**Exhaust temp [C]**
Rolls-Royce	COBERRA 6562	29530	9472	20.8	94.5		491
GE Aero Energy Products	LM2500 (PK)	29861	9482	22.6	87.7		519
GE Power - Nuovo Pignone	PGT25+	30226	9084	21.5	84.3		500
Rolls-Royce	COBERRA 6762	30387	9288	21.5	95.5		492
GE Aero Energy Products	LM2500 (PK) 60 Hz	30900	9797	22.9	89		486
GE Power - Nuovo Pignone	PGT25+	31364	8754	21.5	84.3		500
Rolls-Royce	RB211- 6761DLE	32120	9158	21.5	94.5		503
Rolls-Royce	COBERRA 6761	33184	8899	21.5	94		503
GE Aero Energy Products	LM2500 (PV) 50 Hz	33500	9409	23	89		486
GE Aero Energy Products	LM6000 (PD) 60 Hz	40212	8878	28.1	122		458
GE Aero Energy Products	LM6000 (PD) 50 Hz	40417	8721	28.5	123		456
GE Aero Energy Products	LM6000 (PD) 50 Hz	41700	8824	30	126		448
GE Aero Energy Products	LM6000 (PD) 60 Hz	42300	8763	30	126		452
GE Aero Energy Products	LM6000 (PC) 50 Hz	43000	9006	30	129		419
GE Aero Energy Products	LM6000 (PC) 60 Hz	43500	8950	30	129		422
GE Aero Energy Products	LM6000 (PC)	44742	8401	29.1	127.8		440
GE Aero Energy Products	LM6000 (PD) Sprint 60 Hz	46800	8686	30	132		447
GE Aero Energy Products	LM6000 (PD) Sprint 50 Hz	46900	8715	30	132		446
GE Aero Energy Products	LM6000 (PC) Sprint 50 Hz	49500	8935	30	135		438
GE Aero Energy Products	LM6000 (PC) Sprint 60 Hz	49500	8914	30	136		441
Rolls-Royce	TRENT 50	51918	8536	35	152.7		444
Rolls-Royce	TRENT	52032	8408	35	150.9		443
Rolls-Royce	TRENT 60	58207	8815	35	166		424

13

NOMENCLATURE

The nomenclature of the symbols used in the work is listed here.

A lot of symbols have been used in this work, and not all are listed here. In some instances a formula is described in detail in the surrounding text, and if it is not part of a larger model, it has been seen most appropriate to leave out the symbols here.

Symbol	Description	Unit
a	Specific area pr. unit volume of reactor Activity coefficient for reactor	m^2/m^3 (-)
A	Area	m^2
A_c	Cross section	m^2
AF	Air-to-Fuel ratio	(-)
C	Grassroot cost Constant Concentration	€ (-) $(kmole/m^3)$
c_p	Constant pressure specific heat capacity	kJ/kg-K
c_v	Constant volume specific heat capacity	kJ/kg-K
e	Specific exergy	kJ/kg
F	Heat capacity flow Molar flow rate	kW/K kmole/s
f_m	Material correction factor in cost function	(-)
f_p	Pressure correction factor in cost function	(-)
h	Specific enthalpy	kJ/kg
H_{rx}	Heat of reaction	kJ/kmole
k	Rate constants	
$\dot{m}$	Massflow	kg/s

Symbol	Description	Unit
N	Number of trays	
p	Pressure	bar or kPa
$\dot{Q}$	Heat	kW
r	Rate of reaction	kmole/kg-s
$\tilde{r}$	Actual rate of reaction, i.e. rate compensated for efficiency	kmole/kg-s
R	Reflux ratio	
R_u	Ideal gas constant = 8.314	kJ/kmole-K
t	Time	(s)
T	Temperature	K or °C
U	Overall heat transfer number Flooding velocity	kW/m²-K m/s
V	Volume	(m^3)
W	Catalyst weight	kg
$\dot{W}$	Work	kW
x	Mole fraction in liquid phase Conversion in reactor	(-) (-)
Y	Boolean variable	(-)
y	Mole fraction in vapour phase	(-)

Greek letters

Symbol	Description	Unit
γ	$\gamma = c_p / c_v$	(-)
η	Efficiency	
λ	Excess air	(-)
ρ	Density	kg/m3
τ	Time	(s)
ξ	Split fraction	(-)

Subscripts

A number of subscripts are self-explaining in the context they are used and will not be listed here.

Symbol	Description
in	Inlet to control volume
out	Outlet control volume
F	Fuel
0	Reference state
sat	Saturation condition
f	Saturated water
g	Saturated steam
fg	Difference between saturated water and steam
sh	Superheat
GR	Grassroot cost
CEPCI	
min	Minimum
s	Isentropic condition
c	Catalyst

14

REFERENCES

Here all the references used in the thesis is listed, sorted by primary author's last name.

Aaltola, J. (2002) Simultaneous synthesis of flexible heat exchanger networks *Applied Thermal Engineering*, *22*, 907-918

Aasberg-Petersen, K., Christensen, T. S., Nielsen, C. S., and Dybkjær, I. (2003) Recent developments in autothermal reforming and pre-reforming for synthesis gas production in GTL applications *Fuel Processing Technology*, *83*, 253-261

Alstom (2003) Alstom www.power.alstom.com

Askgaard, T. S., Nørskov, J. K., Ovesen, C. V., and Stoltze, P. (1995) A kinetic model of methanol synthesis *Journal of Catalysis*, *156*, 229-242

Balakrishna, S. and Biegler, L. T. (1992a) Constructive targeting approaches for the synthesis of chemical reactor networks *Industrial and Engineering Chemistry Research*, *31*(1), 300-312

Balakrishna, S. and Biegler, L. T. (1992b) Targeting strategies for the synthesis and energy integration of nonisothermal reactor networks *Industrial and Engineering Chemistry Research*, *31*(9), 2152-2164

Balakrishna, S. and Biegler, L. T. (1993) A unified approach for the simultaneous synthesis of reaction, energy, and separation systems *Industrial and Engineering Chemistry Research*, *32*(7), 1372-1382

Bathie, W. W. (1996) Fundamentals of gas turbines 2nd ed.ed., John Wiley & Son, ISBN: 0471311227

Bedenik, N. I., Pahor, B., and Kravanja, Z. (2004) An integrated strategy for the hierarchical multilevel MINLP synthesis of overall process flowsheets using the combined synthesis/analysis approach *Computers & Chemical Engineering*, *28*, 693-706

Bejan, A., Tsatsaronis, G., and Moran, M. (1996) Thermal design & optimization 1.ed., Wiley-Interscience, ISBN: 0-471-58467-3

Bianchi, M. and Uctas, R (2003) Aromatics remain volatile *Chemical Market Reporter*, *263*(12), 26-27

Biegler, L. T., Cervantes, A. M., and Wächter, A. (2002) Advances in simultaneous strategies for dynamic process optimization *Chemical Engineering Science*, *57*, 575-593

Biegler, L. T. and Grossmann, I. E. (2004) Retrospective on optimisation *Computers & Chemical Engineering*, *28*, 1169-1192

Biegler, L. T., Grossmann, I. E., and Westerberg, A. W. (1997) Systematic methods of chemical process design 1.ed., Prentice Hall, ISBN: 0-13-492422-3

Björk, K. M., Lindberg, P. O., and Westerlund, T. (2003) Some convexifications in global optimization of problems containing signomial terms *Computers & Chemical Engineering*, *27*, 669-679

Björk, K. M. and Westerlund, T. (2002) Global optimization of heat exchanger network synthesis problems with and without the isothermal mixing assumption *Computers & Chemical Engineering*, *26*, 1581-1593

Brandrup, J. and Immergut, E. H. (1975) Polymer handbook 2nd edition.ed., John Wiley & Sons, ISBN: 0-471-09804-3

Briones, V. and Kokossis, A. C. (1999) Hypertargets: a conceptual programming approach for the optimisation of industrial heat exchanger networks - I. grassroots design and network complexity *Chemical Engineering Science*, *54*, 519-539

Brooke, A., Kendrick, D., Meeraus, A., and Raman, R. (1998) *GAMS* © GAMS Development Corporation www.gams.com

Brown, R. (2003) Benzene and Styrene prices skyrocket on soaring feedstock costs *Chemical Market Reporter*, *263*(3), 7-7

Bruno, J. C., Fernandez, F., Castells, F., and Grossmann, I. E. (1998) A rigorous MINLP model for the optimal synthesis and operation of utility plants *Chemical Engineering Research and Design*, *76*(A), 246-257

Caballero, J. A. and Grossmann, I. E. (2004) Design of distillation sequences: from conventional to fully thermal coupled distillation systems *Computers & Chemical Engineering*, *28*, 2307-2329

Chemical Engineering (2005) Chemical Engineering www.che.com

Chou, C. C. and Shih, Y. S. (1987) A thermodynamic approach to the design and synthesis of plant utility systems *Industrial and Engineering Chemistry Research*, *26*, 1100-1108

Conn, A. R., Gould, N. I. M., and Toint, P. L. (2000) Trust-region methods 1st.ed., SIAM (Society for Industrial and Applied Mathematics), ISBN: 0-89871-460-5

Daichendt, M. M. and Grossmann, I. E. (1997) Integration of hierarchical decomposition and mathematical programming for the synthesis of process flowsheets *Computers & Chemical Engineering*, *22*(1-2), 147-175

DeGroote, A. M. and Froment, G. F. (1996) Simulation of the catalytic partial oxidation of methane to synthesis gas *Applied Catalysis*, *138*, 245-264

Douglas, J. M. (1988) Conceptual design of chemical processes 1.ed., McGraw-Hill, ISBN: 0-07017762-7

Drud, A. S. (2002) SIAM optimisation meeting 2002

Duran, M. A. and Grossmann, I. E. (1986a) A Mixed Integer Nonlinear Programming Algorithm for Process Systems Synthesis *AIChE Journal*, *32*(4), 592-601

Duran, M. A. and Grossmann, I. E. (1986b) Simultaneous Optimization and Heat Integration of Chemical Processes *AIChE Journal*, *32*(1), 123-137

Edgar, T. F., Himmelblau, D. M., and Lasdon, L. S. (2001) Optimization of chemical processes , McGraw-Hill, ISBN: 0-07-039359-1

Elsam (2003) Energy Together www.energytogether.org; www.elsam.com

European Union (2003) Restructuring of the community framework for the taxation of energy products and electricity *Official Journal of the European Union*, *L283*, 51-70

Eurostat (2000) Labour cost, wages and salaries, direct remuneration http://epp.eurostat.cec.eu.int/portal/page?_pageid=1090,30070682,1090_30298591&_dad=portal&_schema=PORTAL

Fausto-Hernández, S., Rice-Ramírez, V., Jiménez-Gutiérrez, A., and Hernández-Castro, S. (2003) MINLP synthesis of heat exchanger networks considering pressure drop effects *Computers & Chemical Engineering*, *27*, 1143-1152

Feng, X. and Zhu, X. X. (1997) Combining pinch and exergy analysis for process modifications *Applied Thermal Engineering*, *17*(3), 249-261

Fogler, H. S. (1999) Elements of Chemical Reaction Engineering 3.ed., Prentice-Hall, ISBN: 0139737855

Franck, P. Å., Gundersen, T., Johansson, M., and Petterson, F. (1998) Procesintegration i industrien - kursuskompendium , Nordisk Energiforskningsprogram

Froment, G. F. and Bischoff, K. B. (1990) Chemical Reactor Analysis and Design 2nd.ed., John Wiley & Sons, ISBN: 0-471-51044-0

GE (2003) General Electric www.gepower.com

GE Enter (2003) *GateCycle* © GE Enter Software www.geenter.com

Gorsek, A. and Glavic, P. (2003) Process integration of a steam turbine *Applied Thermal Engineering*, *23*, 1227-1234

Graaf, G. H., Sijtsema, P. J. J. M, Stamhuis, E. J., and Joosten, G. E. H. (1986) Chemical equilibria in methanol synthesis *Chemical Engineering Science*, *41*(11), 2883-2890

Graaf, G. H., Stamhuis, E. J., and Beenackers, A. A. C. M. (1988) Kinetics of low-pressure methanol synthesis *Chemical Engineering Science*, *43*(12), 3185-3195

Greeff, I. L., Visser, J. A., Ptasinski, K. J., and Janssen, F. J. J. G. (2002) Utilisation of reactor heat in methanol synthesis to reduce compressor duty - application of power cycle principles and simulation tools *Applied Thermal Engineering*, *22*, 1549-1558

Greeff, I. L., Visser, J. A., Ptasinski, K. J., and Janssen, F. J. J. G. (2004) Using turbine expanders to recover exothermic reaction heat - flow sheet development for typical chemical processes *Energy*, *29*, 2045-2060

Grossmann, I. E. and Biegler, L. T. (2004) Part II: Future of optimisation *Computers & Chemical Engineering*, *28*, 1193-1218

Grossmann, I. E. and Kravanja, Z. (1995) Mixed-integer nonlinear programming techniques for process systems engineering *Computers & Chemical Engineering*, *19*(Suppl.), S189-S204

Grossmann, I. E., Yeomans, H., and Kravanja, Z. (1998) A Rigorous Disjunctive Optimization Model for Simultaneous Flowsheet Optimization and Heat Integration *Computers & Chemical Engineering*, *22S*, S157-S164

Grue, J and Bach, I. (2000) Simulation of absorption heat pumps in energy supply systems *Proc.of the 41st Scandinavian Conference on Simulation and Modelling*

Grue, J and Bendtsen, J. (2003a) Simultaneous process optimisation, heat integration and utility system design *Presented at PRES '03*

Grue, J and Bendtsen, J. (2003b) Synthesis and optimisation of a methanol proces *Proc.of the 44th Scandinavian Conference on Simulation and Modelling*

Grue, J and Bendtsen, J. (2005) Simultaneous Process Integration of Processes and Utility Systems *Computers & Chemical Engineering*, *Submitted for review*

Gundersen, T. (1997) A worldwide catalogue on process integration

Hellmann, H. M. and Grossman, G. (1996) Improved Property Data Correlations of Absorption Fluids for Computer Simulation of Heat Pump Cycles *ASHRAE Transaction*, *102*(1), 980-997

Hillestad, M. (2004) A systematic generation of reactor designs I: Isothermal conditions *Computers & Chemical Engineering*, *28*, 2717-2726

Hillestad, M. (2005) A systematic generation of reactor designs II: Non-isothermal conditions *Computers & Chemical Engineering*, *29*, 1101-1112

Hoffman, J. (2003) High natural gas costs pose protracted problems for the north american plastic industry *Chemical Market Reporter*, *264*(8), 1-16

Hohmann, E. (1971) Optimum networks for heat exchange *Ph.D. Thesis thesis University of Southern California, LA, USA*

Hostrup, M. (2002) Integrated approach to computer aided process synthesis *Ph.D. thesis Technical University of Denmark, Department of Chemical Engineering*

IEA (2003) Oil Market Report - Annual statistical supplement 2002

IEA (2005) End user petroleum product prices and average crude oil import costs - september 2005

Invensys (2003) *Pro/II* © Invensys SimSci-Esscor www.simsci.com

Jaksland, C. A., Gani, R., and Lien, K. M. (1995) Separation process design and synthesis based on thermodynamic insights *Chemical Engineering Science*, *50*(3), 511-530

Kirschner, M. (2003a) Chemical profile Hydrogen *Chemical Market Reporter*, *263*(8), 43-43

Kirschner, M. (2003b) Chemical profile Toluene *Chemical Market Reporter*, *263*(18), 27-27

Kocis, G. R. and Grossmann, I. E. (1989) A modelling and decomposition strategy for the MINLP optimization of process flowsheets *Computers & Chemical Engineering*, *13*(7), 797-819

Kokossis, A. C. and Floudas, C. A. (1990) Optimization of complex reactor networks I. Isothermal operation *Chemical Engineering Science*, *45*(3), 595-614

Kokossis, A. C. and Floudas, C. A. (1991) Synthesis of isothermal reactor-spearator-recycle systems *Chemical Engineering Science*, *46*(5-6), 1361-1383

Kokossis, A. C. and Floudas, C. A. (1994) Optimization of complex reactor networks II. Nonisothermal operation *Chemical Engineering Science*, *49*(7), 1037-1051

Kovac, A. and Glavic, P. (1995) Retrofit of complex and energy intensive processes - I *Computers & Chemical Engineering*, *19*(12), 1255-1270

Kravanja, Z. and Grossmann, I. E. (1990) PROSYN - An MINLP process synthesizer *Computers & Chemical Engineering*, *14*(12), 1363-1378

Lakshmanan, A. and Biegler, L. T. (1996) Synthesis of optimal chemical reactor networks *Industrial and Engineering Chemistry Research*, *35*, 1344-1353

Lavric, V., Plesu, V., and Ruyck, J. (2005) Chemical reactors energy integration through virtual heat exchangers - benefits and drawbacks *Applied Thermal Engineering*, *25*, 1033-1044

Leboreiro, J. and Acevedo, J. (2004) Processes synthesis and design of distillation sequences using modular simulators: a genetic algorithm framework *Computers & Chemical Engineering*, *28*, 1223-1236

Lee, S. and Grossmann, I. E. (2000) New algorithms for nonlinear generalized disjunctive programming *Computers & Chemical Engineering*, *24*(9-10), 2125-2141

Levenspiel, O. (1999) Chemical Reaction Engineering 3rd.ed., John Wiley & Sons, Inc, ISBN: 0-471-25424-X

Li, X. and Kraslawski, A. (2004) Conceptual process synthesis: Past and current trends *Chemical Engineering and Processing*, *43*, 589-600

Linderoth, J. T. and Savelsbergh, M. W. P. (1999) A computational study of search strategies for mixed integer programming *INFORMS Journal on Computing*, *11*(2), 173-187

Linnhoff, B., Townsend, D. W., Boland, D., Hewitt, G. F., Thomas, B. E. A., Guy, A. R., and Marsland, R. H. (1982) User Guide on process integration for the efficient use of energy 1st.ed., Institution of Chemical Engineers, ISBN: 0852953437

Linstrom, P. J. and Mallard, W. G (2001) NIST Chemistry WebBook, NIST Standard Reference Database Number 69

Løvik, I. (2001) Modelling, Estimation and Optimization of the Methanol Synthesis with Catalyst Deactivation *ph.d.thesis thesis Norwegian University of Science and Technology, Department of Chemical Engineering*

Lurgi Chemie (2005) Integrated Low Pressure Methanol Process

Manninen, J. (1999) Flowsheet synthesis and optimisation of power plants *Ph.D. thesis University of Manchester Institute of Science and Technology*

Manninen, J. and Zhu, X. X. (1999a) Optimal flowsheeting synthesis for power station design considering overall integration *Energy*, *24*, 451-478

Manninen, J. and Zhu, X. X. (1999b) Optimal gas turbine integration to the process industries *Industrial and Engineering Chemistry Research*, *38*, 4317-4329

Maréchal, F. and Kalitventzeff, B. (1998) Process Integration: Selection of the optimal utility system *Computers & Chemical Engineering*, *22*(Suppl), S149-S156

Mashproekt (2003) Mashproekt www.mashproekt.nikolaev.ua

Mavromatis, S. P. and Kokossis, A. C. (1998a) A logic based model for the analysis and optimisation of steam turbine networks *Computers in industry*, *36*, 165-179

Mavromatis, S. P. and Kokossis, A. C. (1998b) Conceptual optimisation of utility networks for operational variations - I. targets and level optimisation *Chemical Engineering Science*, *53*(8), 1585-1608

Mavromatis, S. P. and Kokossis, A. C. (1998c) Hardware composites: A new conceptual tool for the analysis and optimisation of steam turbine networks in chemical process industries: Part 1, principles and construction procedure *Chemical Engineering Science*, *53*(7), 1405-1434

McBride, B. J. (1984) *CEA - Chemical Equilibrium with Application* © http://www.grc.nasa.gov/WWW/CEAWeb/

Methanex (2005) Methanex www.methanex.com

Mitsubishi (2003) Mitsubishi Heavy Industries www.mbhi.co.jp

Moulijn, J. A., Makkee, M., and Diepen, A. (2001) Chemical Process Technology 1st.ed., John Wiley & Sons Ltd, ISBN: 0-471-63009-8

Najjar, Y. S. H. (2001) Efficient use of energy by utilizing gas turbine combined systems *Applied Thermal Engineering*, *21*, 407-438

Papoulias, S. A. and Grossmann, I. E. (1983a) A structural optimization approach in process synthesis - I - Utility Systems *Computers & Chemical Engineering*, *7*(6), 695-706

Papoulias, S. A. and Grossmann, I. E. (1983b) A structural optimization approach in process synthesis - II - Heat recovery networks *Computers & Chemical Engineering*, *7*(6), 707-721

Papoulias, S. A. and Grossmann, I. E. (1983c) A structural optimization approach in process synthesis - III - Total processing systems *Computers & Chemical Engineering*, *7*(6), 723-734

Perry, R. H. (1997) Perry's Chemical Engineer's Handbook 7th.ed., McGraw-Hill

Peters, M. S., Timmerhaus, K. D., and West, R. E. (2003) Plant Design and Economics for Chemical Engineers 5th.ed., McGraw-Hill, ISBN: 0-07-119872-5

Petterson, F. (2005) Synthesis of large scale heat exchanger networks using a sequential match reduction approach *Computers & Chemical Engineering*, *29*, 993-1007

Pörn, R, Harjunkoski, I, and Westerlund, T. (1999) Convexification of different classes of non-convex MINLP problems *Computers & Chemical Engineering*, *23*, 439-448

Pratt and Whitney (2003) P&W www.pratt-whitney.com

Rice, R. G. and Do, D. D. (1995) Applied mathematics and modelling for chemical engineers , John Wiley & Sons, ISBN: 0471303771

Rolls Royce (2003) Rolls Royce www.rollsroyce.com

Rostrup-Nielsen, J. R. M (2000) New aspects of syngas production and use *Catalysis today*, *63*, 159-164

Schweiger, C. A. and Floudas, C. A. (1999) Optimization framework for the synthesis of chemical reactor networks *Industrial and Engineering Chemistry Research*, *38*, 744-766

Seuranen, T., Hurme, M., and Pajula, E. (2005) Synthesis of separation processes by case-based reasoning *Computers & Chemical Engineering*, *29*, 1473-1482

Shang, Z. and Kokossis, A. C. (2004) A transhipment model for the optimisation of steam levels of total site utility system for multiperiod operation *Computers & Chemical Engineering*, *28*, 1673-1688

Skatteministeriet (2000) Effektiv selskabsbeskatning i international sammenligning *Skat*

Smet, C. R. H. de, Croon, M. H. J. M. de, Berger, R. J., Marin, G. B., and Schouten, J. C. (2001) Design of adiabatic fixed-bed reactors for the partial oxidation of methane to synthesis gas. Application to production of methanol and hydrogen-for-fuel-cells *Chemical Engineering Science*, *56*, 4849-4861

Smith, E. M. B and Pantelides, C. C. (1995) Design of reaction/separation networks using detailed models *Computers & Chemical Engineering*, *19*(Suppl), S83-S88

Solar Turbines (2005) Solar Turbines http://mysolar.cat.com/

Sondreal, E. A., Benson, S. A., Hurley, J. P., Mann, M. D., Pavlish, J. H., Swanson, M. L., Weber, G. F., and Zygarlicke, J. (2001) Review of advances in combustion technology and biomass cofiring *Fuel Processing Technology*, *71*, 7-38

Spencer, R. C., Cotton, K. C., and Cannon, C. N. (1963) A method for predicting the performance of stream turbine-generators *Journal of Engineering for Power*

Thermoflow (2000) *GT Pro Demo* © www.thermoflow.com

Thermoflow (2001) Design of gas turbine combined cycle and cogeneration systems - course notes

Thong, D. Y. C., Liu, G., Jobson, M., and Smith, R. (2004) Synthesis of distillation sequences for separating multicomponent azeotropic mixtures *Chemical Engineering and Processing*, *43*, 239-250

Tijm, P. J. A., Waller, F. J., and Brown, D. M. (2001) Methanol technology developments for the new millenium *Applied Energy*, *221*, 275-282

Türkay, M. and Grossmann, I. E. (1996) Logic-based MINLP algorithms for the overall optimal synthesis of process networks *Computers & Chemical Engineering*, *20*(8), 959-978

Turkay, M. and Grossmann, I. E. (1998) Structural flowsheet optimization with complex investment cost functions *Computers & Chemical Engineering*, *22*(4/5), 673-686

Turton, R., Bailie, R. C., Whiting, W. B., and Shaeiwitz, J. A. (1998) Analysis, synthesis, and design of chemical processes 1.ed., Prentice Hall, ISBN: 0-13-570565-7

Tveit, T. M. (2005) Experimental design methods and flowsheet synthesis of energy systems *Applied Thermal Engineering*, *25*, 283-293

Vanden Bussche, K. M. and Froment, G. F. (1996) A steady-state kinetic model for methanol synthesis and the water gas shift reaction on a commercial Cu/ZnO/Al2O3 catalyst *Journal of Catalysis*, *161*, 1-10

Varbanov, P., Perry, S., Klemes, J., and Smith, R. (2005) Synthesis of industrial utility systems: cost-effective de-carbonisation *Applied Thermal Engineering*, *25*, 985-1001

Vasantharajan, S. and Biegler, L. T. (1990) Simulatneous strategies for optimization of differential-algebraic systems with enforcement of error criteria *Computers & Chemical Engineering*, *14*(10), 1083-1100

Vasnetsov, S. (2003) Strategic Implications: Natural gas fever for US chemicals *Chemical Market Reporter*, *263*(15), 16-19

Vericor (2003) Vericor Power Systems www.vericor.com

Wagner, W. (2000) The IAPWS Industrial Formulation 1997 for the Thermodynamic Properties of Water and Steam *Journal of Engineering for Gas turbines and Power*, *122*, 150-182

Westerlund, T., Skrifvars, H., Harjunkoski, I, and Pörn, R (1998) An extended cutting plane method for a class of non-convex MINLP problems *Computers & Chemical Engineering*, *22*(3), 357-365

Xu, J. and Froment, G. F. (1989) Methane steam reforming, methanation and water-gas shift: I. intrinsic kinetics *AIChE Journal*, *35*(1), 88-96

Yee, T. F., Grossmann, I. E., and Kravanja, Z. (1990a) Simultaneous optimization models for heat integration - II. Heat exchanger network synthesis *Computers & Chemical Engineering*, *14*(10), 1165-1184

Yee, T. F., Grossmann, I. E., and Kravanja, Z. (1990b) Simultaneous optimization models for heat integration - III. Process and heat exchanger network optimization *Computers & Chemical Engineering*, *14*(11), 1185-1200

Zamora, J. M. and Grossmann, I. E. (1998) A global MINLP optimization algorithm for the synthesis of heat exchanger networks with no stream splits *Computers & Chemical Engineering*, *22*(3), 367-384

Zhu, X. X. and Nie, X. R. (2002) Pressure drop considerations for heat exchanger network grassroot design *Computers & Chemical Engineering*, *26*, 1661-1676

Zhu, X. X., O'Neill, B. K., Roach, J. R., and Wood, R. M. (1995) Area-targeting methods for direct synthesis of heat exchanger networks with unequal film coefficients *Computers & Chemical Engineering*, *19*(2), 223-239